Role of Insulin-like Growth Factors in Granulosa Cell Differentiation and Ovarian Follicle Maturation

BY

SARAH C. BAUMGARTEN
B.A., Vanderbilt University, 2009

THESIS

Submitted as partial fulfillment of the requirements
for the degree of Doctor of Philosophy in Physiology and Biophysics
in the Graduate College of the
University of Illinois at Chicago, 2017

Chicago, IL

Defense Committee:

Carlos Stocco, Advisor
Mrinalini Rao, Chair
Joanna Burdette, Department of Medicinal Chemistry and Pharmacognosy
Ahlke Heydemann
Terry Unterman, Department of Medicine

ACKNOWLEDGEMENTS:

I would like to thank all of those that I have worked with in the Department of Physiology and Biophysics over the last 4 years, particularly my advisor Dr. Carlos Stocco. He took me into his lab essentially sight unseen and allowed me to conduct research that I am truly passionate about. He gave me the independence to pursue questions, make mistakes, and grow as a scientist. He gave me the guidance I needed to conduct productive and meaningful research and constantly reminded me of how fun science can be. To Carlos, I will forever be grateful for your generosity, your patience, and your persistence in helping me become the best that I can be.

I would also like to thank our collaborators on the Reproductive Endocrinology & Infertility team at the University of Illinois Hospital. Without their willingness to give us cells from IVF patients, this project would not have been possible. In particular, I would like to thank Nicola Winston, who was always willing to lend her expertise to guide and enhance the scientific and clinical relevance of my work.

Thank you to the members of my thesis committee—Dr. Mrinalini Rao, Dr. Terry Unterman, Dr. Joanna Burdette, and Dr. Ahlke Heydemann—for always having an open door and for providing valuable advice for my thesis project as well as my future pursuits.

I would like to thank the MSTP program at UIC for believing in me and supporting me without hesitation throughout my PhD journey, including Roberta Bernstein, Larry Tobacman, and Nancy Freitag.

I would be remiss if I did not give great thanks to Mrs. Theresa (Short) Clark, my 6th grade science teacher. She believed in me like no one else and motivated me to

work hard and achieve great things. Without her influence, it is highly unlikely that I would be here today. Even today, 16 years later, she inspires me to be the best that I can be.

Lastly, I would like to thank my friends and family for always being there for me, and Becca for her constant and unwavering support throughout my pursuit of a PhD and her willingness to stand by me in my future endeavors.

In loving memory of Dr. James A. Baumgarten, Sr., Dorothy Kirchner Baumgarten, and Mary Ann Armstrong Bauer.

SCB

TABLE OF CONTENTS

CHAPTER PAGE

TABLE OF CONTENTS (continued)

CHAPTER PAGE

TABLE OF CONTENTS (continued)

CHAPTER PAGE

LIST OF TABLES

TABLE PAGE

LIST OF FIGURES

FIGURE PAGE

LIST OF FIGURES (continued)

FIGURE PAGE

LIST OF ABBREVIATIONS

17βHSD	17-beta hydroxysteroid dehydrogenase
3βHSD	3-beta hydroxysteroid dehydrogenase
ACTB	β-actin
Adeno-cre	adenoviral cre-recombinase
AKT	v-akt murine thymoma viral oncogene homolog 2
AMH	anti-Müllerian hormone
ART	assisted reproductive technologies
AEW	NVP-AEW451, an IGF1R inhibitor
CA-AKT	constitutively active AKT
cAMP	cyclic adenosine monophosphate
COC	cumulus-oocyte-complex
Cre	causes recombination
CREB	cAMP response element-binding protein
CYP11A1	cholesterol side-chain cleavage enzyme
CYP19A1	aromatase
DMSO	Dimethyl sulfoxide
DOR	diminished ovarian reserve
E2	17β-estradiol
ECM	extracellular matrix
ERK	extracellular signal-regulated kinases
FDR	false discovery rate
FGF	fibroblast growth factor

FOXO3	forkhead box O3
FSH	follicle stimulating hormone
FSHR	follicle stimulating hormone receptor
GCs	granulosa cells
GDF9	growth differentiation factor 9
GFP	green fluorescent protein
GH	growth hormone
GnRH	gonadotropin-releasing hormone
H&E	Hematoxylin and Eosin
hCG	human chorionic gonadotropin
HDL	high-density lipoprotein
HPO axis	hypothalamic-pituitary-ovarian axis
HSP60	heat shock protein 60
IGF1	insulin-like growth factor 1
IGF1R	type 1 insulin-like growth factor receptor
IGF2	insulin-like growth factor 2
IGF2R	type 2 insulin-like growth factor receptor
IGFBP	insulin-like growth factor binding protein
INSR	insulin receptor (gene)
IR	insuin receptor (protein)
IRS	insulin receptor substrate
IVF	*in vitro* fertilization

JNK	c-Jun N-terminal kinases
LDL	low-density lipoprotein
LDLR	low-density lipoprotein receptor
LH	luteinizing hormone
LHR	luteinizing hormone receptor
MAPK	Mitogen-activated protein kinase
mRNA	messenger ribonucleic acid
OHSS	ovarian hyperstimulation syndrome
OSFs	oocyte secreted factors
PAPP-A	pregnancy-associated plasma protein A
PCR	polymerase chain reaction
PKA	protein kinase A
PMSG	Pregnant mare's serum gonadotropin
qPCR	quantitative real-time polymerase chain reaction
RIPA	Radioimmunoprecipitation Assay
RPL19	60S ribosomal protein L19
SCARB1	scavenger receptor class B member 1
SCP2	sterol carrier protein 2
SH2	Src Homology 2
STAR	steroidogenic acute regulatory protein,
VEGF	Vascular endothelial growth factor
ZP3	zona pellucida glycoprotein 3

SUMMARY

Infertility affects more than 7% of couples in the United States. Approximately 40% of these infertility cases can be attributed to ovarian dysfunction, where a woman is unable to produce and/or ovulate mature oocytes for fertilization. For those who seek assisted reproductive technologies such as *in vitro* fertilization (IVF), anovulation is often overcome by the administration of follicle stimulating hormone (FSH) to induce the development of the oocyte-containing ovarian follicles. During follicle development to the preovulatory stage, undifferentiated granulosa cells proliferate and differentiate into two distinct populations: mural granulosa cells that line the wall of the follicle and cumulus granulosa cells that surround the oocyte. These cells work together to foster steroid hormone synthesis and oocyte development, respectively, both of which are required for normal fertility.

In humans, little is understood about the process of granulosa cell differentiation because access to undifferentiated granulosa cells is extremely rare. However, cumulus and mural granulosa cells can be collected from the follicular aspirates of women undergoing IVF. Studies in rodents have revealed that the cumulus granulosa cells are protected from FSH-induced differentiation by factors secreted from the oocyte. Thus, we hypothesized that cumulus cells obtained from patients undergoing *in vitro* fertilization (IVF) treatment could be cultured to study human granulosa cell differentiation, once separated from the oocyte and its influence. In a novel approach, cumulus and mural granulosa cells were collected from the follicular aspirates of IVF patients and cultured in serum-free, phenol red-free media. Gene expression analysis revealed that cumulus granulosa cells expressed significantly lower levels of

differentiation genes including the *luteinizing hormone receptor* (LHR) and steroidogenic genes such as *CYP19A1* (aromatase), *CYP11A1* (P450 side chain cleavage), and *STAR* (steroidogenic acute regulatory protein) than the mural granulosa cells. Additionally, in cumulus, but not in mural, cells, treatment with FSH stimulated the expression of key differentiation genes including CYP19A1, CYP11A1, and StAR at both the mRNA and protein level. The fact that cumulus cells are less differentiated than mural cells in culture and differentiate in response to FSH treatment indicate the cultured cumulus granulosa cells can be used as an experimental approach to study human granulosa cell differentiation.

Using cultured cumulus granulosa cells, we sought to understand the role of locally produced ovarian factors, such as insulin-like growth factors (IGFs), in granulosa cell differentiation and follicle maturation. Previous studies demonstrated that IGFs enhance FSH-induced granulosa cell differentiation. We found that FSH upregulated IGF2 at both the RNA and protein level, and that this stimulation was driven specifically by the P3-promoter of *IGF2.* We then showed that IGF2 enhanced FSH-induced CYP19A1 expression and synergized with FSH to stimulate granulosa cell proliferation. Because IGF2 is produced by the granulosa cells and constantly present, we inhibited IGF1 receptor (IGF1R) activity to eliminate IGF2 action, and study mechanisms by which FSH promotes granulosa cell differentiation. The FSH-induced expression of steroidogenic genes was inhibited at both the mRNA and protein level and, accordingly, the stimulation of estradiol production by FSH was eliminated. Further inspection revealed that FSH and IGF2 cooperatively enhance AKT and ERK simulation, and that IGF1R activity is required for FSH to stimulate AKT phosphorylation. Without this

activation of AKT, FSH is not able to stimulate the expression of aromatase or enhance estradiol production. Additionally, FSH is not able to stimulate IGF2 expression when AKT activation is inhibited, demonstrating that by activating the IGF1R and allowing for FSH-induced AKT activation, IGF2 is an auto-regulator in human granulosa cells. Taken together, our results suggest that granulosa cells establish a niche environment within the follicle in which locally produced IGF2 stimulates AKT activation through the IGF1R to allow FSH to simulate human granulosa cell differentiation.

I. INTRODUCTION: OVARIAN PHYSIOLOGY AND HUMAN FERTILITY

A. Infertility

In the United States, 15.5% of women who desire to have children suffer from infertility (1, 2). The reasons for female infertility vary, but age is a strong contributing factor (3). The current trend among women is to wait until an older age to have their first child (4, 5), and thus more women are seeking out services and treatments for infertility. In fact, the number of *in vitro* fertilization (IVF) cycles performed each year has increased by over 50% in the US over the last 10 years (6). Unfortunately, the chance of achieving a pregnancy from IVF services has not made significant improvements during this same time (Figure 1A). The success rate of IVF is approximately 40% in patients less than 35 years of age, and this sharply declines to less than 10% after age 40 (6) (Figure 1B).

Infertility can impose significant emotional, physical, and financial stresses on affected couples. IVF costs $12,000 per attempt on average (7), and with the current IVF success rates it is common for couples to undergo multiple cycles of IVF to become pregnant. Additionally, weeks of hormone treatments for IVF can have adverse health effects. For example, a common complication of the hormone treatments for IVF is ovarian hyperstimulation syndrome (OHSS), where the ovaries enlarge and fluid can accumulate in the abdomen causing severe pain and shortness of breath that in some cases necessitates hospitalization. In extreme cases, OHSS can be life threatening. It is, therefore, essential to gain an understanding of mechanisms underlying infertility, so that more effective treatments can be developed and administered to improve the success rates and minimize the health risks for women undergoing IVF.

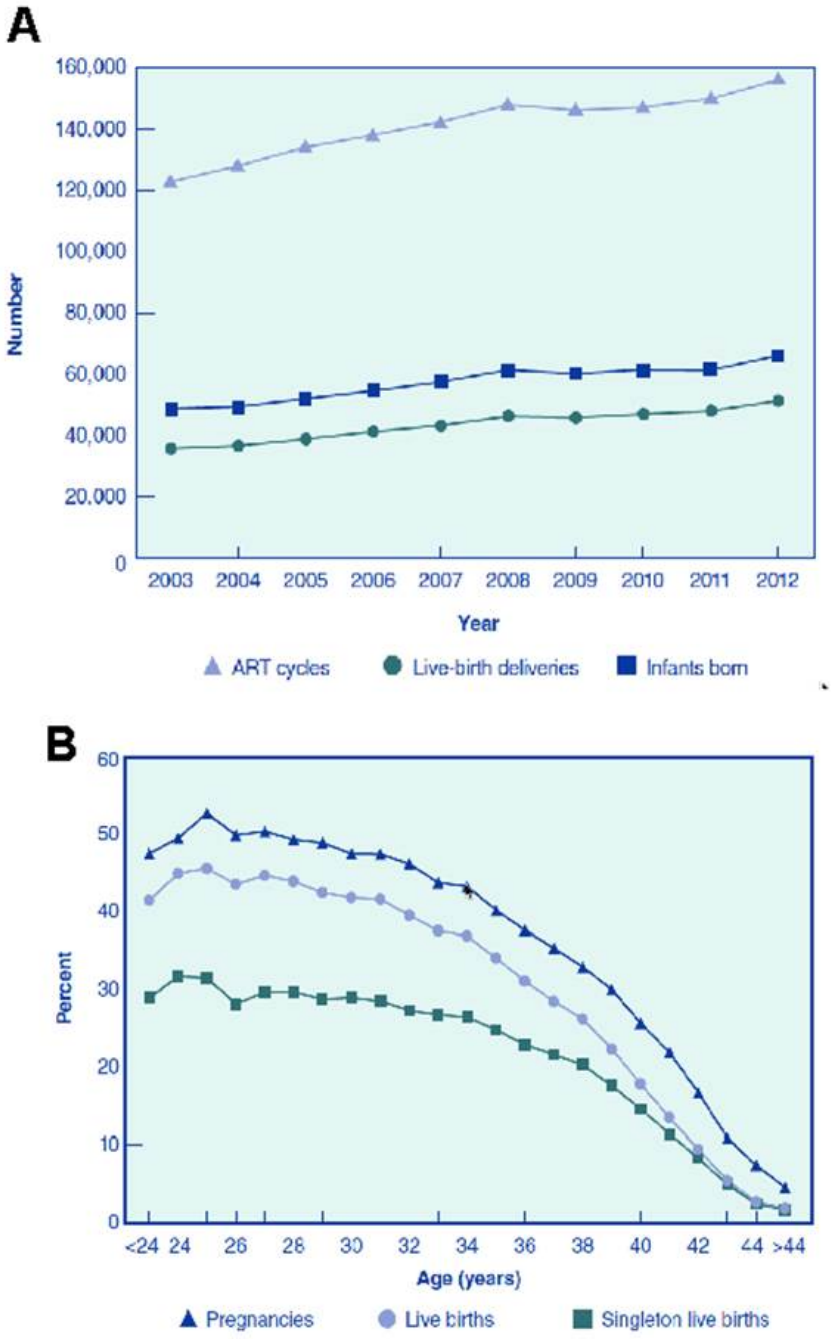

Figure 1: *Summary report of assisted reproductive technologies (ART) in the United States in 2012.*

(**A**) Numbers of ART cycles performed, live-birth deliveries, and infants born using ART from 2003-2012 (6).
(**B**) Percentages of IVF Cycles that result in pregnancies, live births, and singleton live births by age of woman (6).

B. Ovary

The ovary is the female gonad that fosters the development and maturation of the female gametes, the oocytes, and produces the hormones, including estrogen and progesterone, needed to coordinate the reproductive process. The ovary has three main regions: the hilum, the medulla, and the cortex. The ovarian ligament is attached to the ovary at the hilum, and blood vessels and nerves enter/exit the ovary in this region. The medulla is the central region of the ovary, and it consists of highly vascularized and innervated stromal tissue. The outermost region of the ovary is the cortex, which is comprised of ovarian follicles that contain oocytes and the stroma that lies between the follicles.

Follicles are the functional units of the ovary. Each follicle consists of an oocyte surrounded by one or several layers of specialized somatic cells called granulosa cells. Initially, follicles consist of an oocyte surrounded by a single layer of flattened granulosa cells, which is known as a primordial follicle. Women are born with approximately 2 million primordial follicles, and by the initiation of puberty this number has decreased to nearly 200,000 (8). During folliculogenesis, groups of primordial follicles transition to become primary, preantral, and antral follicles. During each cycle, one antral follicle then becomes dominant over others in the same cohort, and this follicle develops to the preovulatory stage (Figure 2) poised to release a mature oocyte for fertilization. This process, known as folliculogenesis, is a continuous, dynamic process and ovarian follicles at various stages of maturation are present in the ovary at any given time during a woman’s reproductive period.

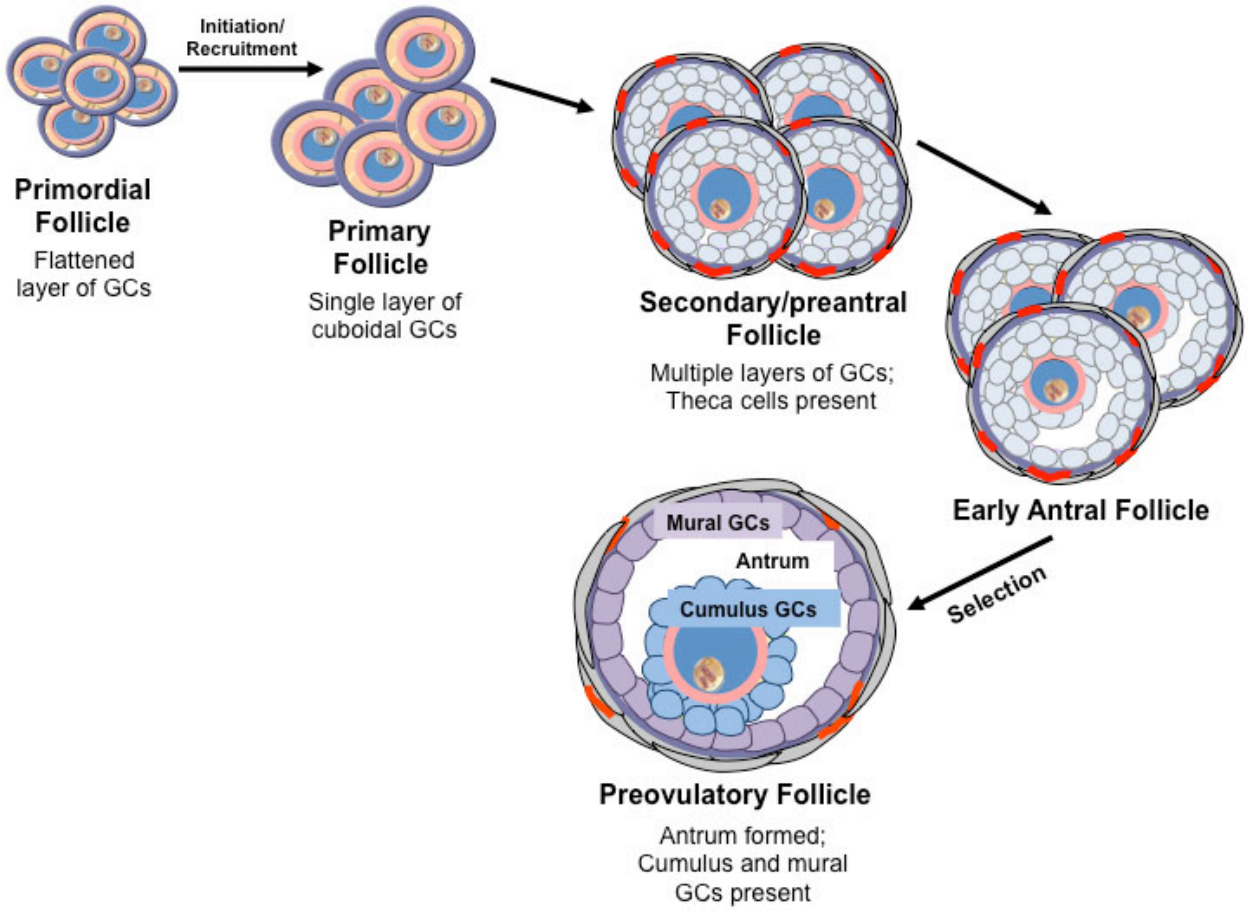

Figure 2: *Follicle development.*

During follicle maturation in the ovary, the oocyte is initially surrounded by a flattened layer of granulosa cells in the primordial follicle. As the follicle progresses to the primary stage, the granulosa cells change morphology to become a single layer of cuboidal cells surrounding the oocyte. These granulosa cells proliferate to form multiple layers in the secondary/preantral follicle. A fluid filled cavity then begins to form within the granulosa cells, known as the antrum. A single developing follicle becomes dominant over others in the growing cohort, and this follicle progresses to the preovulatory stage. The antrum grows and the granulosa cells differentiate into the mural granulosa cells lining the wall of the follicle and the cumulus granulosa cells that immediately surround the oocyte. (GCs=granulosa cells)

As ovarian follicles mature, granulosa cells change morphology, proliferate and differentiate. At the same time an additional layer of somatic cells—theca cells—are recruited and surround the follicle. As follicles progress from the preantral to the preovulatory stage, granulosa cells lining the wall of the follicle differentiate to form mural granulosa cells. These cells are steroidogenic and, together with the theca cells, produce increasing levels of estradiol throughout follicle development. In contrast, the cumulus granulosa cells that immediately surround the oocyte are protected from differentiation and have minimal steroidogenic capacity. The mural and cumulus cells in the preovulatory follicle create a niche environment within the follicle that maintains oocyte arrest in the meiotic phase and prevents premature maturation of the oocyte prior to ovulation (9).

1. **Hypothalamic-pituitary-ovarian axis**

Ovarian folliculogenesis and steroid hormone synthesis are regulated by the ovary itself, as well as the hypothalamus and anterior pituitary. The hypothalamic-pituitary-ovarian (HPO) axis coordinates a dynamic fluctuation of gonadotropins and sex steroid hormones to regulate ovarian function (10, 11). The hypothalamus produces and releases gonadotropin releasing hormone (GnRH) in a pulsatile fashion (12). GnRH then acts on gonadotropes in the anterior pituitary, where it stimulates both the expression and the secretion of follicle stimulating hormone (FSH) and luteinizing hormone (LH) (13). These hormones enter the circulation and act on distinct target cells in the ovary.

In the ovary, the FSH receptor (FSHR) is expressed in the granulosa cells of developing follicles (14). FSH simulates follicle growth, specifically granulosa cell

differentiation and estradiol production. The LH receptor (LHR) is expressed in the theca cells of developing follicles, and LH stimulates steroidogenesis in these cells.

As the follicles mature in response to gonadotropins, the follicles produce steroid hormones, estradiol and progesterone. These hormones, in turn, regulate the secretion of gonadotropins from the anterior pituitary throughout folliculogenesis. The increase in estradiol during follicle maturation first exerts negative feedback to reduce FSH and LH levels in the circulation. This decrease in gonadotropins is thought to play a role in the establishment of a single dominant follicle that matures to the preovulatory stage. This maturing dominant follicle produces high levels of estradiol, and once circulating levels of estradiol surpass a critical level, approximately 200pg/ml, estradiol exerts a positive feedback to increase circulating levels of FSH and LH (15) to promote ovulation and subsequent luteinization.

2. Folliculogenesis

a) Activation/recruitment of primordial follicles

As primordial follicles are recruited and transition to primary follicles, the morphology of granulosa cells changes from a single layer of flattened, squamous cells to a single layer of cuboidal granulosa cells. Primordial follicle recruitment occurs independently of gonadotropins. Instead, it is regulated locally by ovarian factors, and crosstalk between the oocyte and granulosa cells is crucial for primordial follicle activation. For example, KIT ligand produced by the granulosa cells activates KIT, a tyrosine kinase receptor expressed in the oocyte, to promote follicle activation. Newborn mice that received peritoneal injections of an antibody blocking the KIT/KIT ligand interaction showed follicles paused at the primordial stage and few, if any, follicles that

had transitioned to become primary follicles (16). On the other hand, when cultured rat ovaries were treated with KIT ligand, there was a significant increase in the percentage of follicles that had undergone recruitment from the primordial stage to the growing follicle pool (17).

While the KIT/KIT ligand interaction promotes follicle activation/recruitment, another set of factors is present to prohibit this process. For example, the transcription factor forkhead box O3 (FOXO3) prevents oocyte activation and subsequent follicle progression from the primordial to primary stage. FOXO3 knockout mice have a drastic increase in follicle recruitment compared to control animals, and by 2 weeks of age no primordial follicles remain in FOXO3 knockout ovaries. At 9 weeks of age, there is evidence of follicle death, or atresia, and the animals are ultimately sterile by 15 weeks of age (18). Thus, primordial follicle activation/recruitment is tightly regulated locally within the ovary by factors such as KIT and FOXO3.

b) Preantral follicle growth

During growth of the primary follicle to the preantral stage, the single layer of cuboidal granulosa cells surrounding the oocyte proliferate to form multiple layers. Like the initial follicle recruitment, preantral follicle growth is gonadotropin independent and crosstalk between the oocyte and granulosa cells regulate the process. Growth differentiation factor 9 (GDF9) is one example of a factor mediating oocyte-granulosa cell communication during preantral follicle growth. GDF9 is expressed in the oocyte beginning at the primary follicle stage (19). Primordial and primary follicles are present in the ovaries of GDF9 null mice but there is an absence of follicles beyond the primary stage (20). There is also evidence of accelerated oocyte growth without concurrent

growth and development of follicular granulosa and theca cells, which results in oocyte degeneration (21).

Several studies exploring genetic associations in women with diminished ovarian reserve (DOR), characterized by a low number of remaining oocytes in the ovary, have identified a number of mutations in GDF9 in these women (22-24). One particular mutation renders GDF9 unable to stimulate human granulosa cell proliferation (25). This could potentially lead to a pause in follicle development at this stage or death of the oocyte without appropriate proliferation of granulosa cells, both of which could be underlying mechanisms of DOR. Thus, GDF9 is essential for growth of preantral follicles in rodents, and it appears to have an important role in human follicle growth as well; however, more research is needed to gain insight into the exact role of GDF9 in human preantral follicle development.

At the preantral stage an additional layer of somatic cells—theca cells—are recruited and surround the follicle. Theca cells are steroidogenic cells that produce high levels of androgens throughout follicle development, and they cooperate with granulosa cells to produce estradiol.

c) Antral follicle to preovulatory follicle growth

During the transition from the preantral to antral follicle stage, a fluid-filled cavity called the antrum forms within the follicle. The fluid-filled cavity physically separates regions of granulosa cells, which become two functionally distinct populations. The mural granulosa cells, which line the wall of the ovarian follicle, are the primary site of steroidogenesis and produce estradiol as the follicle matures. On the other hand, cumulus cells that immediately surround the oocyte primarily function to promote the

growth and maturation of the oocyte (Figure 2). The differentiation of the undifferentiated preantral granulosa cells into mural and cumulus types is crucial for steroid hormone production as well as oocyte maturation.

During the preantral to the preovulatory follicle transition, FSH stimulates the differentiation of preantral granulosa cells to the mural granulosa cell type. This includes the upregulation of steroidogenic enzymes, such as aromatase, and the consequent increase in steroid hormone synthesis, in particular estradiol. In contrast, the cumulus cells surrounding the oocyte are protected from FSH induced differentiation by the oocyte and oocyte-secreted factors (OSFs) (26-28). For example, GDF9 and bone morphogenetic protein 15 (BMP15), which belong to the transforming growth factor pathway, are OSFs that activate SMAD2/3 signaling in the granulosa cells in close proximity to the oocyte. Activation of SMAD2/3 in these granulosa cells prevents FSH from stimulating the expression of key mural granulosa cell genes, including enzymes necessary for steroidogenesis (26); however, when SMAD2/3 activation is inhibited in cumulus cells, FSH is able to stimulate the differentiation of these cumulus granulosa cells into the mural granulosa cell type. Overall, a gradient of FSH signaling and SMAD2/3 activation establishes the fate of preantral granulosa cells as either mural or cumulus in the preovulatory follicle (26, 28).

(1) Steroidogenesis

During follicle maturation from the early antral to the preovulatory stage, the follicles begin producing increasing levels of steroid sex hormones including progestins, estrogens, and androgens. In developing follicles, the mural granulosa cells and adjacent theca cells surrounding the ovarian follicles are the primary sites of

steroidogenesis. Together, they produce estradiol, which is critical for granulosa cell proliferation (29), follicle development, and the regulation of circulating gonadotropins throughout folliculogenesis.

Theca cells express the enzymes necessary to convert cholesterol to the androgens androstenedione and testosterone. This includes expression of steroid acute regulatory protein (StAR), which transports cholesterol into the mitochondria, and P450 side chain cleavage (P450scc, CYP11A1) in the mitochondria, which catalyzes the first step of steroidogenesis. The mural granulosa cells lack the enzymes necessary for androgen synthesis; however they express aromatase (CYP19A1), the enzyme that converts androgens to estradiol (30). According to the “two cell” theory of steroidogenesis, the theca cells produce androgens, which are converted to estradiol in the mural granulosa cells by aromatase (31). In mural granulosa cells, testosterone is directly converted to estradiol by aromatase, while the conversion of androstenedione to estradiol requires an additional enzyme: 17β-hydroxysteroid dehydrogenase (17β-HSD).

The level of aromatase expression in granulosa cells, and therefore estradiol synthesis, increases throughout follicle maturation. FSH is a potent stimulator of aromatase expression in both humans and rodents (32, 33), and aromatase is critical for fertility. In aromatase knockout animals antral follicles are present, but they are arrested before ovulation (34). Additionally, without estradiol and its feedback on the HPO axis, gonadotropins levels are dysregulated, and FSH and LH are both higher than normal. This demonstrates how critical aromatase and estradiol are for ovulation and fertility.

(2) Selection

In humans, only one follicle is selected to complete its development to the preovulatory stage each cycle. The processes and mechanisms that are involved in the selection of this dominant follicle are not well understood, but FSH is thought to play a role in follicle selection. A cohort of follicles grows simultaneously and progresses to the early antral follicle stage. Within this cohort only a single follicle becomes dominant and the rest stop growing and become atretic. The “FSH Threshold/Window/Gate Concept” postulates that changes in FSH levels drive the deviation between the dominant follicle and subordinate follicles (35-38). According to this concept, increasing levels of FSH during the follicular phase drive the maturation of a cohort of preantral follicles to the antral stage. These antral follicles begin producing estrogen, which exerts a negative feedback on the hypothalamus and anterior pituitary to inhibit FSH synthesis and secretion. For a brief time, FSH levels are above a threshold to support the growth of one follicle in particular so that when FSH levels decline after negative feedback from estradiol, it can survive while the other follicles regress. It is thought that the dominant follicle may initially be larger with more granulosa cells and more FSHR, predisposing it to be more responsive to FSH than other follicles of the same developing cohort (39, 40). This follicle grows to become a preovulatory follicle that is poised to release a mature oocyte at the time of ovulation. The results of this thesis provide new information that may contribute to a better understanding of the mechanisms that drive follicle selection.

d) Ovulation and luteinization

The high level of estradiol produced by the developing dominant follicle exerts a positive feedback on the anterior pituitary resulting in a surge of FSH and LH production and release into the circulation (11, 15). Ultimately, this LH surge leads to the rupture of the preovulatory follicle and the release of a mature oocyte from the ovary for fertilization. Following ovulation, the remaining follicular cells in the ovary differentiate under the influence of LH to form the endocrine structure known as the corpus luteum. The mural granulosa and theca cells luteinize into large and small luteal cells of the corpus luteum, respectively. Both cell types produce progesterone, which stimulates blood vessel growth and nutrient secretion in the endometrium of the uterus to support implantation of the embryo. If a fertilized embryo implants into the uterus, the corpus luteum function is maintained by human chorionic gonadotropin (hCG) in most mammals and produces progesterone throughout the first trimester of the pregnancy. If implantation does not occur within 9 days, the corpus luteum regresses and forms the corpus albicans, and menses ensues.

C. Endocrine and local regulation of preovulatory follicle formation

1. Follicle Stimulating Hormone

a) Hormone and receptor

FSH is a glycoprotein hormone produced by the gonadotropes in the anterior pituitary. It is a heterodimer consisting of an α and β subunit. The α subunit of FSH is identical to that of several glycoprotein hormones, including LH. The β subunit of FSH (FSHβ) imparts its specific interaction with the FSHR and downstream biological actions unique from other glycoproteins that share the same alpha subunit. Upon stimulation by

GnRH, gonadotropes increase the expression of FSHβ and the secretion of FSH into the circulation. In the ovarian follicle, FSHR expression, and therefore FSH action, is limited to granulosa cells (41).

b) Actions in preovulatory follicle development

FSH plays a critical role in follicle maturation from the preantral to the preovulatory stage. This is evidenced by the infertility of female FSH knockout mice. Inspection of ovarian histology revealed that folliculogenesis stops at the preantral stage in the FSH knockout animals, and no antral or preovulatory follicles are formed (42). Mice in which the FSHR was knocked out are also infertile with a similar ovarian phenotype (43, 44). In agreement with these findings in rodents, genetic studies have identified mutations in both FSH and the FSHR in women suffering from infertility (45-47). Together, these studies in humans and rodents establish that FSH is required for the formation of preovulatory follicles and, therefore, fertility.

During the transition from the preantral to the preovulatory stage, FSH stimulates granulosa cell proliferation and differentiation. It regulates the transcription of over 100 genes in granulosa cells (48), including aromatase, and enhances estradiol production in human and rodent granulosa cells. FSH also regulates the expression of LHR in granulosa cells. LHR expression in mural granulosa cells of mature follicles is critical in order for LH to stimulate ovulation and luteinization. Studies in rodent granulosa cells have shed light on mechanisms by which FSH regulates gene expression and the differentiation of preantral granulosa cells to the mural granulosa cell type through activation of the FSHR (48).

The FSHR is a G-protein coupled receptor that stimulates adenylyl cyclase activity in granulosa cells (49); consequently, FSH-induced activation of the FSHR results in an increase of intracellular cyclic AMP (cAMP) and subsequent activation of protein kinase A (PKA). One well-known target of PKA in granulosa cells is cAMP response element-binding protein (CREB), a transcription factor. PKA phosphorylates CREB, which is then recruited to cAMP response elements in the promoter of specific genes to upregulate transcription of a subset of FSH-regulated genes, including steroidogenic genes such as aromatase (50). PKA can also mediate the activation of extracellular signal-regulated kinases (ERK) (51), whose proposed target SF-1 is necessary for the activation of aromatase (50) and other FSH-target genes. In addition to these better-understood targets, PKA is also found to mediate the FSH-induced activation of the PI3K/AKT pathway in granulosa cells, which is essential for granulosa cell differentiation (52). Mechanisms by which PKA activates this latter pathway are not fully understood (53); however, it is clear that the PI3K/AKT pathway is essential for the activation of steroidogenic gene expression by FSH (32). In sum, FSH stimulates the activation of PKA, ERK, and PI3K/AKT in rodent granulosa cells in order to alter the transcription of over 100 genes in granulosa cells (48). The intracellular signaling pathways activated by FSH in human granulosa cells have not yet been defined.

2. Insulin-like Growth Factors

a) Growth factors and receptors

The two insulin-like growth factors (IGFs), IGF1 and IGF2, are single-chain polypeptide hormones that share 70% sequence homology. The expression of *IGF1*, also known as somatomedin C, is driven by 2 promoters in a tissue-specific manner

(54). Transcription driven by each promoter results in a variety of *IGF1* transcripts; however, after processing, all transcripts yield the same 70-amino acid IGF1 peptide. IGF1 is expressed in most tissues (55), supporting the role of paracrine and autocrine activity in a variety of tissues. The liver is the primary source of circulating IGF1, and growth hormone (GH) is a potent stimulator of IGF1 expression and release in the liver (56). In target tissues, IGF1 activates the type 1 IGF receptor (IGF1R) to promote growth and mediate cellular events such as cell proliferation, differentiation, and survival (54, 57).

IGF2 is considered the major growth factor of fetal development; however, IGF2 is expressed in a variety of adult tissues, including the liver (58). *IGF2* is an imprinted gene that is expressed primarily from the paternal allele in normal tissues (59). The *IGF2* gene consists of 9 exons and gene expression is driven by 4 different promoters that each result in a unique *IGF2* transcript (60). Similar to IGF1, after processing the various *IGF2* transcripts all yield the same 67-amino acid peptide hormone. IGF2 is produced in the liver in response to GH and released into the circulation, but its actions in adult target tissues are largely unknown (58, 61). Like IGF1, IGF2 has been demonstrated to activate the IGF1R to elicit changes in intracellular signaling to regulate gene expression and alter cellular physiology.

The IGF1R consists of two α subunits, which serve as the site of ligand binding for IGF1 and IGF2, and two intracellular β subunits that possess intrinsic tyrosine kinase activity necessary for signal transduction. When IGF1R is activated following ligand binding, tyrosine residues within the catalytic loop of the beta subunits are phosphorylated (reviewed in (62)). This phosphorylation enhances the tyrosine kinase

activity of the receptor and, additionally, serves as docking sites for intracellular proteins containing SH2 (src homology 2) domains. In particular, insulin receptor substrate (IRS) proteins are recruited to the receptor and serve as scaffolds to recruit proteins necessary for the activation of MAPK (mitogen-activated protein kinase) and AKT pathways in IGF-stimulated cells. Once activated, these pathways can lead to changes in expression of essential genes for granulosa cell function, including steroidogenic genes such as aromatase (32). Both IGF1 and IGF2 actions are mediated primarily by the IGF1R (63).

The type 2 IGF receptor (IGF2R) is a single-chain polypeptide with large extracellular domains that have high affinity for binding IGF2 (64). The primary role of the IGF2R is to mediate the internalization of IGF2 upon binding to the receptor. Additionally, the IGF2R can be released from the cell membrane into the extracellular space and bind IGF2 at high affinity (65), which suggests it could regulate IGF2 action locally in tissues. It is largely accepted that the IGF2R does not propagate intracellular signaling or pathway activation within cells, and the majority of evidence indicates that IGF2 signaling is primarily mediated by the IGF1R (63).

In addition to the IGF receptors, hybrid receptors consisting of one α/β subunit of the IGF1R and one α/β subunit of the insulin receptor (IR) can form (66, 67). IGF1 binds with 50-fold higher affinity that insulin, and IGF2 affinity is intermediate to these two ligands (68, 69). These hybrid receptors have been detected in a variety of tissues (70). Currently, there is no direct evidence that these hybrid receptors are present in the ovary; however, granulosa cells, for example, express both the IR and the IGF1R, so hybrid receptors could be possible.

b) Regulators of IGF system

IGF binding proteins (IGFBPs) and IGFBP-specific proteases regulate the bioavailability of both IGF1 and IGF2 to act in target cells and tissues. There are six known IGFBPs (IGFBP1-6), which share 50% homology and function to bind and alter the interactions of IGFs with the IGF1R and IGF2R. Studies IGFBP-IGF interaction have revealed that IGFBP1 and IGFBP4 bind IGF1 and IGF2 with similar affinity, while IGFBP2 and IGFBP3 show a higher affinity for binding IGF2 (71). There is also evidence that IGFBPs can have effects independent of IGF regulation. For example, in human granulosa cells IGFBP4 can inhibit estradiol and progesterone synthesis (72). Additionally, IGFBP1 and IGFBP3 have been shown to have IGF-independent effects on cell motility and proliferation in other cell types (73).

In addition to IGFBPs that directly bind and regulate IGF action, a variety of IGFBP proteases exist to degrade IGFBPs and alter the bioavailability of IGFs. Pregnancy-associated plasma protein-A (PAPP-A) is a specific protease for IGFBP4 (74, 75). It decreases the affinity of IGFBP4 to IGFs, thereby increasing the amount of IGF available to act on surrounding cells in the environment. Together, IGFBPs and IGFBP proteases intricately regulate IGF action in the ovary, as well as other tissues.

c) Expression in the Ovary

In mice and rats, IGF1 is the predominant IGF in the ovary. It is detected at both the mRNA and protein level in granulosa cells of healthy antral follicles, and is absent in granulosa cells of preantral or atretic follicles (76-78). In contrast, *IGF1* expression is absent in the granulosa cells of follicles of all stages of development in the human ovary (79-81). Instead, IGF2 is the predominant IGF in the human ovary. *IGF2* is present in

both the granulosa and theca cells of small follicles and is abundant in the granulosa cells of large, preovulatory follicles (79). The IGF1R is present in the granulosa cells of follicles of all stages in both the human and rodent ovaries (78, 82). In humans, *IGF1R* expression becomes more abundant in the granulosa cell compartment as follicles mature (79, 81). *IGF2R* is also expressed in granulosa cells, with higher levels in large dominant follicles compared to small antral follicles (79). The increase in the expression of IGFs and the IGFRs during human follicle growth suggest that IGF action has a role in the process of follicle maturation.

The IGFs and their regulators are also found in the follicular fluid of antral follicles, and their levels have been measured in studies of human follicles. While circulating levels of both IGF1 and IGF2 do not change according to the menstrual cycle, levels in the follicular fluid change during follicle maturation (83). Changes in IGF1 levels in the follicular fluid do not correlate with follicular size or follicle dominance. In contrast, IGF2 levels are positively correlated with follicle size and are found to be higher in dominant follicles (83). IGFBP1-5 are expressed in the human ovary (81, 84) and present at high levels in the follicular fluid in small antral as opposed to large dominant follicles (85). These findings support the idea that IGF2 levels are dynamic during human follicle maturation, and autocrine IGF2 action plays a role in the growth of the dominant follicle in the ovary.

3. Role of insulin-like growth factors and FSH in the ovary

IGFs are critical for fertility. *Igf1* null mice are infertile with follicle maturation arrested at the early antral stage (86); however, it is unclear if the infertility in these animals is due to absence of IGF1 action in the ovarian cells or if it is the consequence

of additional phenotypes observed in *Igf1* null mice. For example, IGF1 acts at several levels in the HPO axis and is known to regulate the secretion of GnRH and LH from the hypothalamus and pituitary gland, respectively (87, 88). Therefore, the infertile phenotype in *Igf1* null mice could be a result of aberrant gonadotropin levels in the circulation.

In vitro studies in rodent granulosa cells have demonstrated that IGF1 has an important role in the process of granulosa cell differentiation. IGF1 alone does not appear to influence granulosa cell differentiation, but IGF1 has been shown to potentiate FSH-induced upregulation of LHR expression (89) and the expression of steroidogenic genes (32). Accordingly, FSH-induced progesterone biosynthesis (90), and aromatase activity (91) is enhanced by IGF1 in undifferentiated rodent granulosa cells.

The cooperation between FSH and IGF1 in rodent granulosa cell differentiation appears to be dependent on AKT signaling (32). Both FSH and IGF1 stimulate AKT phosphorylation and, together, they enhance AKT phosphorylation further. While mechanisms by which IGF1R activates AKT downstream have been established, it is less clear how FSH can stimulate AKT phosphorylation following activation of its G-protein coupled receptor. Careful studies in rodent granulosa cells have demonstrated that FSH stimulates AKT activation through PKA-dependent activation of insulin receptor substrate-1 (53). Additionally, the activity of the IGF1R is required for FSH to stimulate AKT phosphorylation (32). Because rodent granulosa cells produce IGF1, it appears that endogenous IGF1 activates the IGF1R, and this is required for FSH to stimulate AKT phosphorylation and granulosa cell differentiation *in vitro.*

In contrast to findings in rodent granulosa cells, IGF1 has effects on human granulosa cells. IGF1 treatment stimulates granulosa cell proliferation and steroid hormone synthesis in human granulosa-luteal cells collected from patients undergoing IVF (92, 93). Additionally, IGF1 enhances FSH-induced estradiol and progesterone production by these cells (93, 94). Similar to IGF1, IGF2 also stimulates human granulosa cell proliferation and steroid hormone synthesis likely by upregulating the expression of key steroidogenic enzymes like STAR (95, 96).

Studies exploring any interactions between FSH and IGF2 at the level of steroid hormone production, gene expression, or signaling have yet to be conducted in human granulosa cells. Based on the localization of the IGF system during human follicle maturation and from findings in rodent granulosa cells, this interaction is likely critical for FSH action and follicle development. This warrants studies of FSH and IGF2 action in human granulosa cells to enhance the understanding of folliculogenesis in humans, and potentially improve therapies for infertile patients with aberrant follicle development.

D. Clinical application of gonadotropin action: In vitro fertilization

Over 40% of female infertility cases are due to ovarian dysfunction, where a mature oocyte is not produced and/or ovulated for fertilization (6). To overcome this issue, patients undergo weeks of hormone treatments to promote the maturation of multiple ovarian follicles to collect as many mature oocytes as possible for fertilization *in vitro*. Two of the most common hormone protocols for *in vitro* fertilization (IVF) are the “agonist protocol” and the “antagonist protocol” (97). In the agonist protocol, women are administered a GnRH agonist which initially stimulates gonadotropin release but later

causes the desensitization of the pituitary leading to a block in the release of FSH and LH. FSH is then administered to the patient for 10-14 days to promote growth of a pool of follicles to the preovulatory stage, followed by hCG, which binds the LHR to trigger final oocyte maturation. Oocytes are collected before ovulation occurs by transvaginal aspiration approximately 35 hours after hCG administration. In the antagonist protocol, GnRH antagonists are administered to prevent endogenous GnRH from stimulating gonadotropin production and release from the anterior pituitary. Patients are then treated with exogenous FSH and hCG as in the agonist protocol to stimulate follicle growth and oocyte maturation respectively. In the case of the antagonist protocol, oocyte maturation can also be induced by the administration of a bolus of a GnRH agonist, which will stimulate the pituitary to release LH and FSH.

Unfortunately, up to 24% of women respond poorly to FSH stimulation and produce very few mature oocytes for collection and fertilization *in vitro (98)*. Inadequate egg production is the reason for over 80% of the cancelled IVF cycles each year (6). The mechanisms by which FSH promotes follicle maturation in the human ovary are poorly understood. Additionally, the extent to which growth factors such as IGFs play a role in FSH-induced follicle maturation are also unclear. This is largely because a robust model to study the process of human granulosa cell differentiation is not available. Access to preantral, undifferentiated human granulosa cells is extremely limited. To overcome this obstacle, researchers have used luteinized mural granulosa cells collected from patients undergoing oocyte retrieval for IVF. After 7 or more days in culture, the luteinized mural granulosa cells regain responsiveness to gonadotropin treatments (99); however, these cells are not ideal for mechanistic studies of human

granulosa cell differentiation because they have been exposed to high levels of exogenous gonadotropins *in vivo* during the IVF hormonal treatment regimen. Therefore, it is unclear how accurately the cultured luteinized mural granulosa cells that have already undergone differentiation represent the response of undifferentiated human granulosa cells to FSH. A better understanding of the process of granulosa cell differentiation and follicle development in response to FSH treatment could aid in identifying new targets and therapies that improve the number of oocytes retrieved and the success rate for infertile women undergoing IVF while minimizing the risks, such as OHSS, of the procedure.

E. Statement of Hypothesis and Aims

Aspects of human ovarian follicle development are poorly understood, including the role of FSH in granulosa cells during follicle development. Compelling data from our laboratory has demonstrated that in rodents FSH requires IGF1R activity in order to stimulate granulosa cell differentiation, a crucial process in follicle development. This finding has yet to be pursued in humans, as a robust approach to study human granulosa cell differentiation is not currently available. *The central hypothesis of this thesis is that IGFs are essential for folliculogenesis and fertility by facilitating FSH-induced activation of genes necessary for granulosa cell proliferation, steroidogenesis, and differentiation*. To test this central hypothesis the following aims were pursued:

Specific Aim 1: Develop and characterize a model for human granulosa cell differentiation using granulosa cells collected from patients undergoing *in vitro* fertilization. Our working hypothesis was that the *human cumulus granulosa cells*

remain in an undifferentiated-like state and, when separated from the oocyte, are able to differentiate into mural cells by action of FSH, as it has been observed in mice. A protocol for culturing human cumulus and mural cells was developed and tested. The cultured cumulus and mural granulosa cells were then characterized by gene expression analysis and hormone production assays.

Specific Aim 2: Identify the role of FSH and IGFs in the process of human granulosa cell differentiation. We hypothesized that *in human granulosa cells FSH-induced differentiation will be lost when IGF signaling or the activity IGF1R is absent*. Using cultured cumulus granulosa cells, the roles of FSH and IGFs in gene expression and hormone synthesis were explored.

Specific Aim 3: Investigate the role of IGFs during ovarian follicle progression to the preovulatory stage *in vivo*. Our working hypothesis was that *animals lacking IGF1R, and therefore IGF1 signaling, in granulosa cells during follicle development would be infertile with abnormalities in follicular maturation*. To accomplish this aim, animals with granulosa cell-specific knockout of the IGF1R were generated and changes in fertility, gene expression, and steroid hormone production were evaluated.

II. MATERIALS AND METHODS

A. Human granulosa cell isolation and culture:

Primary cumulus and mural granulosa cells were collected from the follicular aspirates of 186 women undergoing IVF at the University of Illinois under an Institute Review Board-exempt protocol. No clinical information about patients can be provided under this protocol. Patients underwent controlled ovarian hyperstimulation, and transvaginal oocyte retrieval was performed 35 h after hCG administration, at which point cumulus cells are still in contact with the oocyte (100) and mural cells have initiated the luteinization process (33), as previously described (101). Cumulus oocyte complexes (COCs) were removed from the follicular aspirates, placed in a separate dish, and cumulus granulosa cells were mechanically separated from the oocyte. Cumulus granulosa cells from all COCs of an individual patient were pooled, centrifuged at 1000xg for 5 min, re-suspended in phenol-red free DMEM/F12, and gently pipetted to break up clusters of cells to yield individual cells. At the same time, the remainder of the follicular aspirates containing mural granulosa cells were collected and applied to a 50% percoll cushion (Sigma-Aldrich) and centrifuged to remove erythrocytes. The mural granulosa cell layer was resuspended in phenol-red free DMEM/F12, and gently pipetted to break up clusters of cells to yield individual cells. An aliquot of cumulus and mural cells was diluted in 0.4% Trypan and counted using a hemacytometer to estimate the cell number and the percentage of viability. An average of 80% viability was found for both cumulus and mural cells. Cumulus and mural cells were seeded on tissue culture plates pre-coated with BD Matrigel (BD Biosciences) at a density of approximately $1x10^5$ cells/ml in serum-free, phenol-red free DMEM/F12 media

supplemented with penicillin (50 IU/ml, Mediatech), streptomycin (50 µg/ml, Mediatech), sodium bicarbonate (1.2g/L; Sigma-Aldrich), and BSA (0.25w/v; Sigma-Aldrich). Cumulus and mural granulosa cells were cultured for 24 hours before treatments were administered as indicated in the figure legends. Cells from different patients were cultured separately; therefore, each independent experiment represents results from cumulus or mural cells from a single patient.

B. Treatments and inhibitors

Cumulus and mural granulosa cells were cultured for 24h before treatments with recombinant FSH (Serono), estradiol (Sigma-Aldrich), activin-A (Sigma-Aldrich), fibroblast growth factor (FGF, Sigma-Aldrich) human recombinant IGF2 (Sigma-Aldrich), human recombinant IGFBP-4 (Sigma-Aldrich), NVP-AEW451 (AEW, a specific inhibitor of IGF1R, Cayman Chemical Co), MK2206 (an inhibitor if AKT, Selleck Chemicals), U0126 (an inhibitor of ERK1/2 activation, Calbiochem) or dimethyl sulfoxide (DMSO).

C. Polymerase chain reaction

Total RNA was isolated using TRIzol reagent (Invitrogen) as stated in the manufacturer's protocol. Total RNA was reverse transcribed at 42°C for 1h using Moloney murine leukemia virus reverse transcriptase (Invitrogen). The resulting cDNA was diluted to 10ng/µl in H_2O. Quantitative real-time PCR (qPCR) was carried out using 50ng of sample for each reaction. The number of transcripts of the target gene in each sample was quantified using a standard curve generated using purified target gene-specific cDNA diluted to concentrations ranging from 6×10^6 to 9.6×10^3 copies per reaction. The qPCR results are reported as relative expression of the target gene to ribosomal protein L19 (*RPL19)*, an internal control, unless otherwise noted. Real-time

quantification of the PCR product in each cycle was carried out in an iQcycler Real Time PCR machine (Bio-Rad) with the following cycling conditions: pre-incubation at 95°C for 2 min, followed by 40 cycles of denaturation at 95°C for 5 sec, annealing at 60°C for 10 sec, and extension at 72°C for 40 sec. The melting peak of each sample was routinely determined by melting curve analysis to ensure that multiple or unintended products were not being amplified. The qPCR results are expressed as the ratio of copies of the target gene transcript to that of *RPL19* unless otherwise noted. For Figure 13 and Figure 24, PCR was performed using the same cycling parameters as for qPCR, and 1% agarose gel electrophoresis was carried out to visualize the reaction product. All designed primer pairs are intron spanning (Table I).

D. Western Blotting

Cultured cumulus cells were harvested in Lysis Buffer 6 (R&D systems) supplemented with protease inhibitor cocktail (Sigma) and Halt phosphatase inhibitor cocktail (Thermo Scientific). Primary mouse granulosa cells were harvested in ice-cold RIPA (Radioimmunoprecipitation Assay) buffer (50 mM Tris-HCl, pH 7.4; 150 mM NaCl; 1% Nonidet P-40; 0.25% sodium deoxycholate; 1 mM phenylmethylsulfonyl fluoride; 1 mM EDTA; 1X protease inhibitor cocktail (Sigma); 1 mM NaF; and 1 mM Na_3VO_4). Protein was quantified using Pierce BCA Protein Assay Kit (Thermo Scientific) using a BSA standard. Approximately 12µg total protein was separated on 12% bis-Tris- PAGE gels in 50mM 3[*N*-morpholino]propanesulfonic acid, 50mM Tris, 1mM EDTA, 5mM sodium bisulfite, and 0.1% sodium dodecyl sulfate buffer.

TABLE I:

QUANTITATIVE REAL-TIME PCR PRIMERS.

Species	Gene	Forward (5)	Reverse (3)
Human	RPL19	GCT GTG GCA AGA AGA AGG TCT GG	TGT TTT TCC GGC ATC GAG CCC
Human	CYP19A1	GCT GGA CAC CTC TAA CAC GCT	CAG GTC ACC ACG TTT CTC TGC T
Human	StAR	GGC TCA GGA AGG ACG AAG AAC C	ATC ACA GCC TGT TGC CTC AGC
Human	CYP11A1	GTG ATG ACC TGT TCC GCT TTG C	AAG GTT GAG CAT GGG GAC GC
Human	LHR	CTA ATT GCC ACG TCA TCC	CAG TTC ACT CTC AGC AAG C
Human	FSHR	AGC CAT TGC TGT GCC TTT GC	ATG CAT CTG GCT TAG GGG AGC
Human	AMH	ATA GGC TGC CAG GGA CAG AAA GG	TGC CTT AAG TGA GCC GAG TGG
Human	IGF1	CAT CTA CCA ACA AGA ACA CG	AAC AGC AAT CTA CCA ACT CC
Human	IGF2	AGT CCG AGA GGG ACG TGT	TGG ACT GCT TCC AGG TGT
Human	IGF1R	GAC AAC TGT CCT GAC ATG C	CGC TGT AGT AGA AGG AGA CC
Human	IGF2R	TGC ATC ATA GAG AGC AGG GCG	ACT GAA GAC TTG TGG CCT CCC
Human	IGF2 Promoter 1	TAC AGG GGC CGA AGA GTC ACC	ACA GAC GAA CTG GAG GGT GTC C
Human	IGF2 Promoter 2	CCT GCC ACA GAG CGT TCG	GTC TCA CTG GGG CGG TAA GC
Human	IGF2 Promoter 3	CTG TTC GGT TTG CGA CAC GC	GTC TCA CTG GGG CGG TAA GC
Human	IGF2 Promoter 4	TTC TCC TGT GAA AGA GAC TTC CAG C	ACG TCC CTC TCG GAC TTG GC
Mouse	RPL19	CAA TGA GAC CAA TGA AAT CG	GCA GTA CCC TTC CTC TTC C
Mouse	CYP19A1	ATT GCA GCC CCT GAC ACC AT	TGG CGA TGT ACT TCC CAG CA
Mouse	CYP11A1	GAT GTT CCA CAC CAG TGT CCC	AGG GTA CTG GCT GAA GTC TCG C
Mouse	StAR	TTT TGG GGA GAT GCC GGA GC	GCG AAC TCT ATC TGG GTC TGC G
Mouse	IGF1R Ex 2-3	GGA CAT TGG AGG AGA AGC	CAG CAC TCG TTG TTC TCG

Protein was then transferred to nitrocellulose membranes in transfer buffer (25mM Tris, 0.19M glycine, 20% methanol). Membranes were then blocked in 5% nonfat dry milk in TBS-T (2mM Tris, 15mM NaCl, 0.1% Tween-20, pH 7.6).

The primary antibodies were diluted in 5% nonfat dry milk in TBST, and membranes were probed overnight at 4°C. Primary antibodies used for Western blotting were β-actin (ACTB): (1:5000, Abcam), AKT (1:2000, Cell Signaling), phospho-AKT(Ser473) (1:2000, Cell Signaling), ERK1/2 (1:2000, Cell Signaling), phospho-ERK1/2(Thr202/Tyr204) (1:1000, Cell Signaling), IGF1R (1:1000, Cell Signaling), or phospho-IGF1R (1:1000, Cell Signaling), phospho-CREB(Ser133) (1:1000, Cell Signaling), CREB (1:1000, Cell Signaling), phospho-JNK (1:1000,Cell Signaling), JNK (1:1000, Cell Signaling), IGF1R-β (1:1000, Cell Signaling), and heat shock protein 60 (HSP60;1:2000, Cell Signaling). Antibodies used for steroidogenic enzymes were CYP19A1 (1:1000, Epitomics), CYP11A1 (1:1000, Millipore), and StAR (1:1000) kindly donated by Dr. B. Hales (102). After washing in TBS-T, membranes were incubated with goat anti-rabbit secondary antibody (1:15,000) diluted in 5% nonfat dry milk in TBS-T for 2h at room temperature. Protein-antibody complexes were visualized using Supersignal Westfento Maximum Senstitivity Substrate (Thermo Scientific). The band intensities were quantified using Image Lab software (Bio-Rad Laboratories) and adjusted relative to ACTB or HSP60 (loading controls), as specified in figure legends.

E. Steroid sex hormone measurement

1. 17β-Estradiol measurement in media from human granulosa cell cultures

Cumulus and mural granulosa cells were cultured in media supplemented with ATS (androstenedione 1μM, transferrin 5μg/ml, and selenium 2μg/ml) throughout the

duration of the experiment in Figure 7. In all other instances of estradiol measurements, testosterone (50nM) was added to the media 4h prior to the experimental endpoint. Cell culture medium from the wells of cultured human cumulus or mural granulosa cells was collected at the experimental endpoint. Medium samples were diluted 1:150, and 17β-estradiol levels were determined using the Estradiol ELISA kit (DRG Instruments GmbH) following the manufacturer's protocol.

2. 17β-Estradiol measurement in media from mouse granulosa cell cultures

Primary mouse granulosa cells were cultured for experiments, and testosterone (50nM) was added to the media 4h prior to the experimental endpoint. Media was then collected from each well, and the 17β-estradiol levels were determined in undiluted media using the Estradiol ELISA kit (DRG Instruments GmbH) following the manufacturer's protocol.

3. 17β-Estradiol and progesterone measurement in mouse serum

Truncal blood from control and experimental mice was centrifuged, and the serum fraction was collected for hormone measurements. Serum levels of estradiol and progesterone were measured using the estradiol and progesterone ELISA kits (DRG Instruments GmbH) following the manufacturer's protocol. Undiluted serum was used to measure estradiol levels, and serum diluted 1:5 in the provided dilution buffer was used to measure progesterone levels.

F. Microarray

For each of three patients (Table II), cumulus granulosa cells were cultured in serum-free media for 24h, followed by treatment with or without FSH (50ng/ml) for 48h. RNA was isolated from control and FSH-treated cells of the three patients using Direct-zol™

RNA MiniPrep (Zymo Research) following the manufacturer's instructions. DNA was eliminated from each sample using DNase I digestion during the procedure. Prior to microarray analysis, RNA quality was assessed on an Agilent 2200 TapeStation, and all samples had an RNA integrity number (RIN) of 5.1-8. Total RNA samples were then labeled and hybridized according to standard 3' IVT target labeling protocol recommended by Affymetrix. After hybridization each image was analyzed for the following quality metrics: average signal present, signal intensity of species-specific house-keeping genes, relative signal intensities of labeling controls, and absolute signal intensities of hybridization controls. All hybridizations passed according to indicated labeling and hybridization controls. For each sample, the signal intensity of a particular probe was normalized the intensity of *RPL*19 probe for that particular sample, and only probes that met a minimum intensity of 50 were considered. Using BRB Array Tools, gene probes in which less than 25% of the samples had at least 1.5 fold change and those with a variance in the bottom 80th percentile were filtered. A class comparison analysis was executed on control and FSH treated samples paired by patient, and gene probes significantly regulated by FSH were reported (univariate test, significance threshold= 0.005) along with the false discovery rate (FDR). If multiple probes for a single gene were significantly regulated, only the most highly regulated probe was considered in order to determine the number of unique genes regulated by FSH treatment. Heatmaps representing changes in gene expression were generated using Microsoft Excel. The average intensity for a particular gene in control and FSH treated cells was determined for each patient, and the intensity of color for control and FSH treatments corresponds to their difference from the average intensity.

TABLE II:

PATIENT CHARACTERISTICS OF MICROARRAY SAMPLE

Patient	Age	Etiology	Protocol	FSH Dose (Units)	LH Dose (Units)	Peak Estradiol	Day of Ovarian Stimulation	Oocytes Retrieved
1	32	Male Factor	GnRH Antagonist	1175	675	3633	10	25
2	37	Male Factor	GnRH Antagonist	900	1200	7307	9	34
3	32	N/A	GnRH Antagonist	1200	975	3136	11	16
Mean	**33.7 ± 1.7**			**1091.7 ± 96.1**	**950 ± 152.1**	**4692 ± 1315.3**	**10 ± 0.6**	**25 ± 5.2**

G. Human Phospho-Kinase Antibody Array

Cumulus granulosa cells were cultured in serum-free media for 24h, followed by treatment with or without FSH (50ng/ml) for 1h. The phosphorylation status of 43 kinase phosphorylation sites was assessed simultaneously in 170µg of whole cell lysates of control and FSH-treated cells using the Proteome Profiler™ Array: Human Phospho-Kinase Array Kit (R&D Systems, Inc.) following the manufacturer's protocol. The spot intensities were quantified using ImageJ software. The intensities of duplicate spots were averaged and corrected to the intensity of the total protein controls on the array. The ratio of the adjusted intensities between control and FSH-treated cells was calculated for each of the 43 unique kinase phosphorylation sites (Table VI, Appendix A).

H. Lentivirus induction

A lentivirus construct containing a constitutively activated AKT (CA-AKT) was kindly provided by Michael Robinson, Children's Hospital of Philadelphia, Philadelphia, Pennsylvania (24). The construct was sub-cloned into the pTY-CMV lentivirus transfer plasmid and the virus was generated in HEK (human embryonic kidney)-293 cells. For experiments, CA-AKT or green fluorescent protein (GFP)-expressing (control) lentivirus was added to human cumulus granulosa cells 2h after plating. After 36h, cells were treated for 1h with AEW or DMSO vehicle followed by 48h treatment with FSH.

I. Proliferation Assay

Cumulus granulosa cells were cultured in 96-well plates at a density of $8x10^3$ cells per well. After culture for 24h, triplicate wells were treated as indicated in the figure legends for 96h. At 96h, 10µl of MTT (3-(4, 5-dimethylthiazol-2-yl)-2, 5-

diphenyltetrazolium bromide) 5 mg/ml stock solution was added to each well. The plates were incubated at 37°C for 2.5h. Wells were carefully aspirated, and formazan crystals were dissolved in 100µl of DMSO. The absorbance of each well was measured at 562 nm.

J. Animals

Animals were treated in accordance with the NIH Guide for Care and Use of Laboratory Animals, and all protocols were approved by the University of Illinois at Chicago Animal Care Committee. Mice of the following strains were used: IGF1R F/F mice (B6;129-Igf1rtm2Arge/J) and ZP3-Cre mice (C57BL/6-Tg(Zp3-cre)93Knw/J) were obtained from The Jackson Laboratory (Bar Harbor, ME), and Cyp19-Cre mice (103) were kindly provided by Dr. Joanne Richards (Baylor College of Medicine).

K. Genotyping

The genotype of animals for this study was determined using PCR on DNA isolated from tail snips of 16d old animals. For each genotyping reaction, 1µg total DNA was used. The reactions were carried out in PCR buffer with a 1.5mM final Mg concentration. Final concentrations of all components were 0.2µM primer mix (Table III), 0.2mM dNTPs, 0.12µl Taq polymerase. To detect IGF1R floxed and IGF1RKO (null allele), reactions were incubated at 95°C for 2min followed by 35 cycles of 95°C 10sec, 57°C 30sec, 72°C 60sec and a final 3min incubation at 72°C. To detect Cyp19-cre, reactions were incubated at 95°C for 2min followed by 35 cycles of 92°C 20sec, 63°C 20sec, 72°C 45sec and a final 3min incubation at 72°C. To detect ZP3-cre, reactions were incubated at 95°C for 2min followed by 35 cycles of 94°C 30sec, 53°C 30sec, 72°C 60sec and a final 3min incubation at 72°C.

PCR products were visualized by 3% agarose gel electrophoresis. After staining with ethidium bromide, products were visualized by UV light. The molecular weights of the reaction products are: IGF1R WT is 215bp, IGF1R Floxed is 315bp, IGF1R null (IGF1R-KO) is 250bp, Cyp19-Cre is 500bp and Zp3-Cre is 250bp. The molecular weight of the PCR product is used to determine if mice carry floxed (F/F), wildtype (+/+), or both (F/+) IGF1R alleles. The presence of a band in the IGF1R null reaction denotes a null allele. The presence of a band in the Cyp19-cre and ZP3-cre reactions indicates that the animals carry that promoter-driven cre-recombinase (Figure 3).

L. Granulosa cell isolation:

Immature female mice between 21-25 days old were injected subcutaneously with 7.5 IU pregnant mare serum gonadotropin (PMSG) (Sigma-Aldrich) and the ovaries were collected after 48h. For ovary collection, mice were anesthetized using isofluorane followed by cervical dislocation prior to ovary removal. Mature ovarian follicles were ruptured, and the granulosa cells were collected and re-suspended in TRIzol Reagent (Invitrogen) for RNA analysis or in ice-cold radioimmunoprecipitation assay (RIPA) lysis buffer for protein analysis by Western blot.

M. Hematoxylin and eosin staining:

Immature female mice between 21-25 days old were injected subcutaneously with 7.5 IU pregnant mare serum gonadotropin (PMSG) (Sigma-Aldrich) and the ovaries were collected after 48h. Ovaries were fixed in formalin before paraffin embedding. Dewaxed and rehydrated tissue sections were stained with Harris Hemotoxylin (Fisher Scientific) and counterstained with Eosin-Y and Phloxine (Thermo Scientific).

TABLE III:

PRIMER SEQUENCES FOR ANIMAL GENOTYPING REACTIONS.

Reaction	Forward (5)	Reverse (3)
***Cyp19*-cre**	TAC AGC ACC CTC TGA AGC AA	ACT TGG TCA AAG TCA GTG CG
***ZP3*-cre**	GTG AAA CAG CAT TGC TGT CAC TT	GGA CAT GTT CAG GGA TCG CCA GGC G
IGF1R F/WT	CGG TGG AGA CTT TAA CTA CA	TTA GAG AAA GGA GGT TCT GG
IGF1R KO	CAT GGA ACA GTA ATG TGT GG	TTA GAG AAA GGA GGT TCT GG

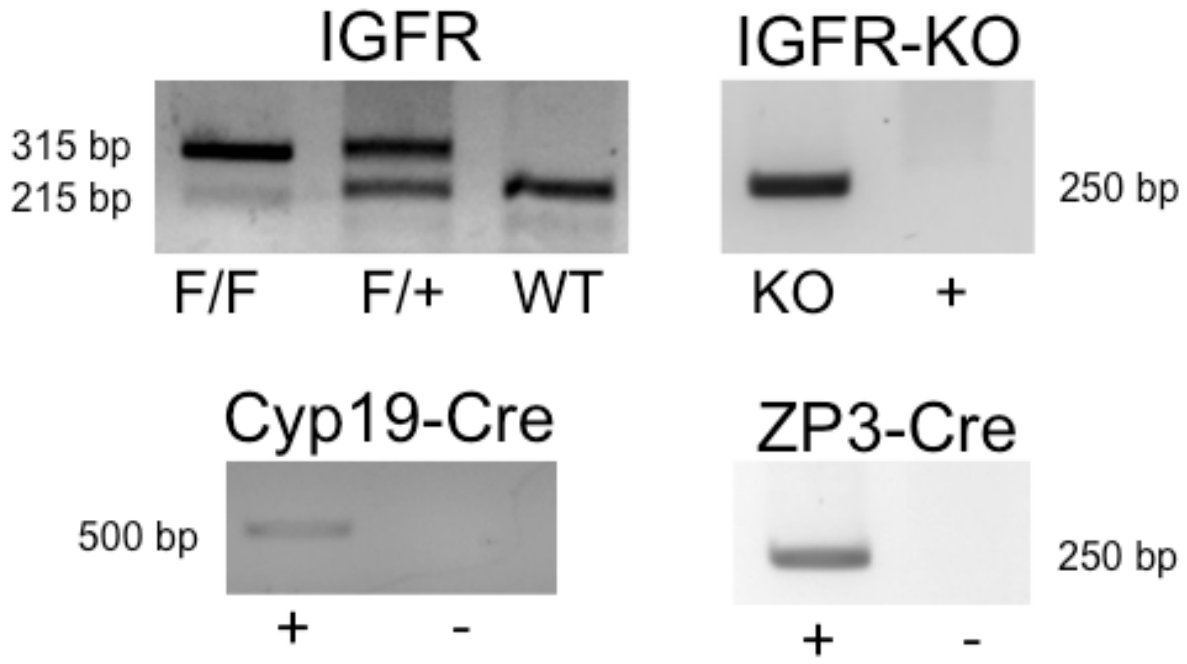

Figure 3: *Mouse genotyping reaction products*.

PCR products from IGF1R floxed, IGF1RKO (null), Cyp19-cre, and ZP3-cre genotyping reactions were run on 3% agarose gels and detected by UV light. Differences in the molecular weight of the PCR product were used to determine if mice carried floxed (F/F), wildtype (+/+), or both (F/+) IGF1R alleles. The presence of a band in the IGF1RKO (null) reaction denotes a null allele. The presence of a band in the Cyp19-cre and ZP3-cre reactions indicates that the animals carry cre-recombinase driven by that promoter.

N. Estrous cycling

In female mice of reproductive age, PBS was injected into the vagina, collected, and the stage of the estrous cycle was determined by vaginal cytology for 12 consecutive days. The samples were classified into 4 stages—proestrus, estrus, metaestrus, and diestrus—based on the presence or absence of leukocytes and the appearance of epithelial cells (104).

O. Ovulation Assay

Immature female mice between 21-15 days old were injected subcutaneously with 7.5 IU PMSG (Sigma-Aldrich) followed by 7.5 IU human chorionic gonadotropin (hCG Sigma-Aldrich) 48h later. After 17h, animals were sacrificed and oviducts were collected. The mass of cumulus-oocyte-complexes was extruded from the oviduct, and hyaluronic acid was added to disperse cells from the oocytes. The denuded oocytes were then counted.

P. Mouse primary granulosa cell culture

Immature female IGF1R F/F mice between 21-25 days old were injected subcutaneously with 1mg β-Estradiol (Sigma-Aldrich) in sesame oil daily for 3 days. 24h after the final injection, the ovaries were collected and undifferentiated granulosa cells were extruded from visible follicles. The primary granulosa cells were cultured on BD Matrigel (BD Biosciences)-coated plates at a density of $5.0x10^5$/ml in phenol-red free DMEM/F12 supplemented with penicillin (50 IU/mL), streptomycin (50 µg/mL), sodium bicarbonate (1.2g/L; Sigma-Aldrich), and BSA (0.25w/v; Sigma-Aldrich). After cells attached to the plate, adenoviral Cre-recombinase (adeno-cre; University of Iowa Gene Vector Transfer Core) was added at a multiplicity of infection (MOI) of 10 to each well.

After 24h, cells were treated with FSH (50ng/ml) (Serono) for 48h and RNA was isolated from the cells using TRIzol Reagent (Invitrogen) as specified in the manufacturer's protocol.

Q. Fluorescent Immunocytochemistry

Human cumulus granulosa cells were plated on ECM-coated 8 chamber tissue culture slides in phenol red-free and serum-free media at a density of 15,000 cells/well. After 24h of culture, cells were treated with FSH for 48h or left untreated (control). Cells were then fixed with 4% paraformaldehyde for 10 minutes, washed with PBS, and permeabilized with 0.5% Triton-X in PBS for 10 minutes. The cells were blocked with 2% BSA and incubated with anti-IGF2 antibody (Santa Cruz) diluted 1:100 in 2% BSA overnight at 4C. The next day, cells were washed with PBS and incubated with goat anti-rabbit Alexa Fluor® 488 secondary antibody (Invitrogen) and rhodamine-phalloidin in 2% BSA for 1h. Slides were then washed with PBS and coverslips were mounted using ProLong® Gold antifade reagent with DAPI. Slide images were taken on a Zeiss LSM 710 confocal microscope with a Plan-Apochromat 63x/1.40 oil DIC M27 objective.

R. Statistical Analyses

Each experiment was conducted at least three times and data for continuous variables are presented as mean values ± standard error of the mean (SEM). Statistical comparisons of mean values between groups were performed with t-tests and multiple comparisons were performed with one-way or two-way analysis of variance (ANOVA). Differences were considered to be statistically significant if the P-value was <0.05.

III. HUMAN CUMULUS GRANULOSA CELLS ARE LESS DIFFERENTIATED THAN MURAL GRANULOSA CELLS

A. Introduction

Currently, a robust approach to study human granulosa cell differentiation is lacking largely due to the paucity of preantral undifferentiated granulosa cells available for study. Although preantral follicles can be isolated from ovarian cortical biopsies (105), access to this tissue is rare. In contrast, cumulus and mural granulosa cells are readily available from the follicular aspirates of IVF patients. Our current understanding of the actions of FSH and other factors in human granulosa cells has been deduced from studies in cultured mural granulosa cells that have undergone luteinization. Breckwoldt *et al.* (99) demonstrate that these cells regain response to gonadotropins after long periods of hormone-free culture; however, luteinization is irreversible. Consequently, mural cells are not an ideal model to study preantral to preovulatory granulosa cell differentiation.

Previous studies have demonstrated that the oocyte plays a dominant role in establishing the heterogeneity of the granulosa cells found in preovulatory follicles by preventing the differentiation of the surrounding cumulus granulosa cells (106). Specifically, it has been shown that the oocyte suppresses FSH-induced luteinizing hormone receptor (*LHR*), *CYP19A1* (aromatase), and *CYP11A1* (P450scc) mRNA expression (26, 107), which are well-known markers of differentiation. This influence of the oocyte on cumulus cells appears to be mediated primarily by oocyte-secreted factors, such as GDF9 and BMPs, and is not dependent on continued close contact between them (108). Based on these findings, we hypothesized that culturing cumulus

cells from preovulatory follicles is a suitable approach to study granulosa cell differentiation as they are no longer under the influence of oocyte secreted factors. Here, we tested this idea and demonstrated that cumulus cells obtained from IVF patients respond to FSH by expressing several markers of differentiation.

B. Results

1. Mural granulosa cells express higher levels of differentiation genes than cumulus granulosa cells

To determine whether cumulus cells are protected from the differentiating effect of FSH during follicle maturation in humans, we evaluated the expression of differentiation and luteinization markers in human cumulus and mural cells obtained from preovulatory follicles. The results demonstrated that, despite the down regulation of *LHR* expression that occurs in mural cells during luteinization (109), cumulus cells expressed significantly lower levels of *LHR* when compared with mural cells (Figure 4). In contrast, the expression of *CYP19A1* and *FSHR* remain highly expressed in cumulus cells compared to mural cells. In addition, the expression of *CYP11A1* and *STAR*, which are required for progesterone production in luteal cells, was higher in mural than in cumulus cells. Finally, the expression of anti-Müllerian hormone (*AMH*), whose expression decreases toward the preovulatory stage, was 4-fold higher in cumulus than in mural cells. The fact that cumulus cells express low levels of *LHR* but retain *CYP19A1*, *FSHR* and *AMH* expression suggests that they do not undergo luteinization even after hCG administration; in contrast, their gene expression pattern resembles that of granulosa cells undergoing preantral to preovulatory differentiation.

2. Cumulus granulosa cells maintain features of undifferentiated granulosa cells during culture.

Next, we examined whether cumulus cells maintain an undifferentiated phenotype in culture. As shown in Figure 5, cumulus cells cultured for 72 h in serum-free media expressed significantly lower levels of *LHR*, *CYP19A1*, *CYP11A1*, and *STAR* than mural cells. Moreover, the relative expression of *CYP19A1*, a marker of preovulatory differentiation, was decreased in cultured cumulus cells when compared to freshly isolated cells. *AMH* mRNA expression was similar in cultured cumulus and mural cells. Furthermore, the steady-state levels of the *FSHR* mRNA in cumulus cells cultured in serum-free media increased at 48h and remained highly expressed at 96 h (Figure 6A). Together, these findings suggest that cultured cumulus cells resemble undifferentiated granulosa cells from early antral follicles.

3. FSH stimulates the differentiation of cultured cumulus granulosa cells

We next assessed whether FSH is able to stimulate the expression of differentiation markers in cultured cumulus cells. Treatment of cumulus cells with FSH for 48h significantly increased the expression of *CYP19A1*, *CYP11A1* and *STAR* mRNA (Figure 6B). In contrast, FSH had no effect on the expression of these genes in mural cells. Treatment of cumulus cells with FSH for 48h also led to an increase in the protein levels of CYP19A1, CYP11A1, and StAR (Figure 6C). In conjunction with the significant increase in CYP19A1 expression, 17β-estradiol levels in the culture medium of cumulus cells treated with FSH was significantly higher than in the culture medium of control cells (Figure 6D).

These findings indicate that freshly isolated cumulus granulosa cells express lower levels of differentiation genes compared to mural granulosa cells and that incubation of these cells in serum-free media leads to further de-differentiation. De-differentiated cumulus cells respond to FSH by up regulating the expression of several mural granulosa cell markers, supporting the idea that cultured cumulus granulosa cells behave as granulosa cells from preantral or early antral follicles. Thus, we propose that cultured cumulus cells can be used to explore the mechanisms by which FSH stimulates human granulosa cell differentiation.

4. Cumulus granulosa cells do not proliferate in culture

The number of cumulus granulosa cells obtained from each IVF patient typically ranges from 80,000 – 600,000 cells. This low cell number can limit the types of experiments that can be conducted to explore mechanisms of human granulosa cell differentiation. Therefore, we aimed to stimulate proliferation of the cumulus granulosa cells from IVF patients to increase the number of cells and, consequently, the types of experiments that could be conducted. We treated cells with hormones and growth factors, alone or in combination, that have been shown to stimulate granulosa cell proliferation, including FSH (29), activin (110), estradiol (29), and fibroblast growth factor (FGF) (111). After 96h of treatment, none of the tested hormones or growth factors significantly stimulated cumulus granulosa cell proliferation (Figure 7). Thus, the techniques used to explore human granulosa cell differentiation using cultured cumulus granulosa cells are limited by the number of cumulus cells obtained from IVF patients.

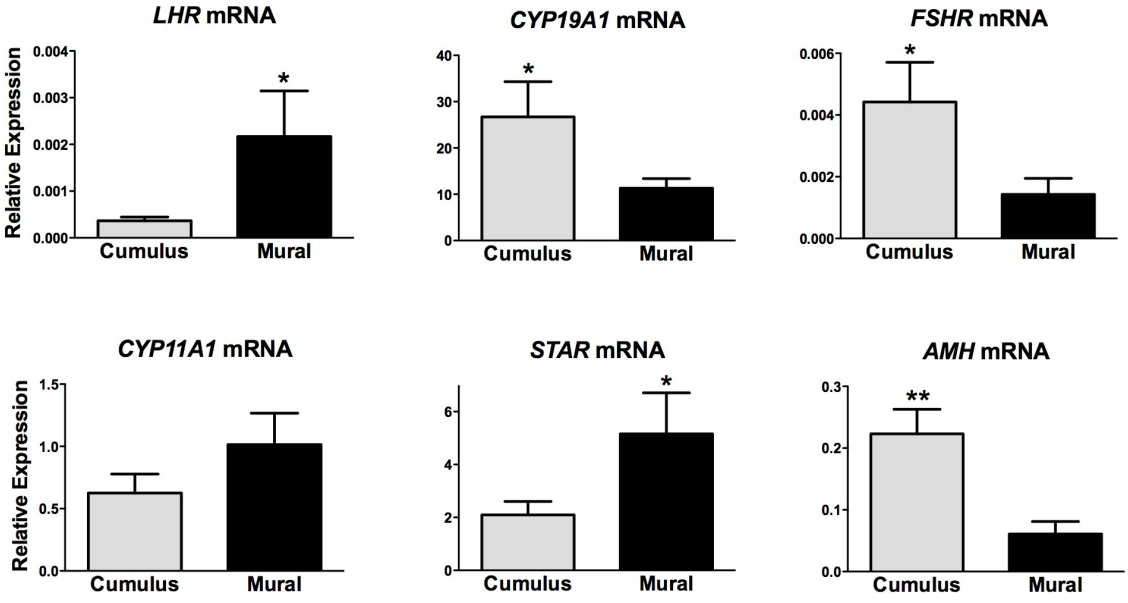

Figure 4: *Freshly isolated cumulus and mural cells have distinct gene expression profiles*.

RNA was isolated from freshly isolated, uncultured cumulus and mural cells collected from patients undergoing IVF. The expression of key gene markers of granulosa cell differentiation and luteinization, including *LHR*, *CYP19A1*, *FSHR*, *CYP11A1*, *STAR*, and *AMH*, were measured by qPCR. Columns represent the mean ± SEM for 6 independent experiments representing 6 different patients. (*p<0.05; **p<0.01; t-test)

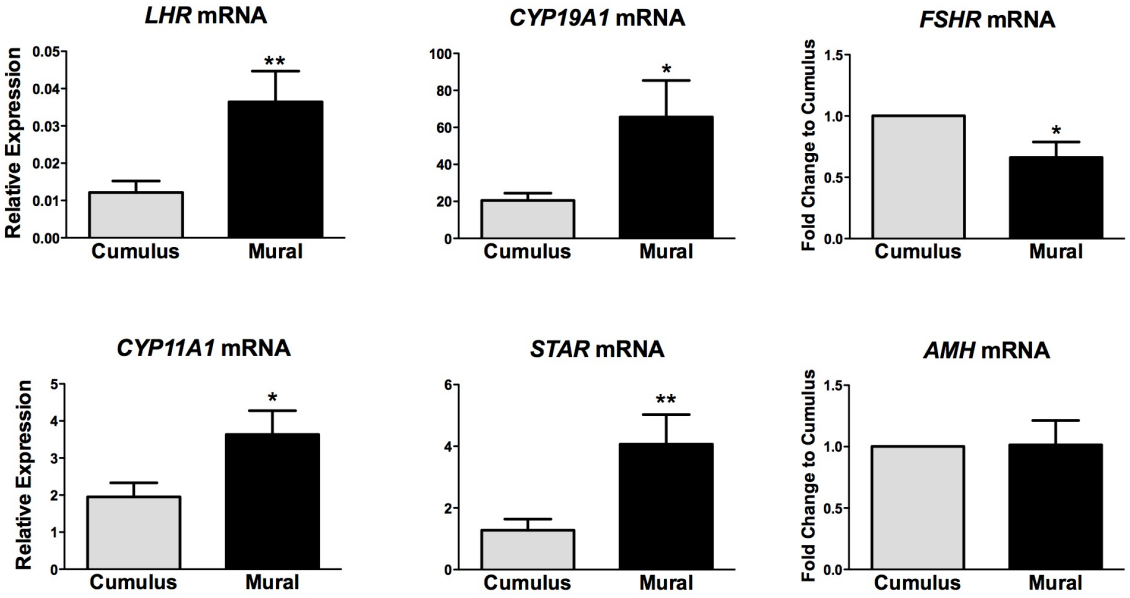

Figure 5: *Cultured cumulus cells are less differentiated than mural granulosa cells*.

RNA was isolated from cumulus and mural granulosa cells after culture in serum-free media for 72h and the expression of key gene markers of granulosa cell differentiation and luteinization, including *LHR*, *CYP19A1*, *FSHR*, *CYP11A1*, *STAR*, and *AMH*, were measured by qPCR. Columns represent the mean gene expression relative to *RPL19* or cumulus cell expression ± SEM for 14 independent experiments representing 14 different patients. (*p<0.05; **p<0.01; t-test)

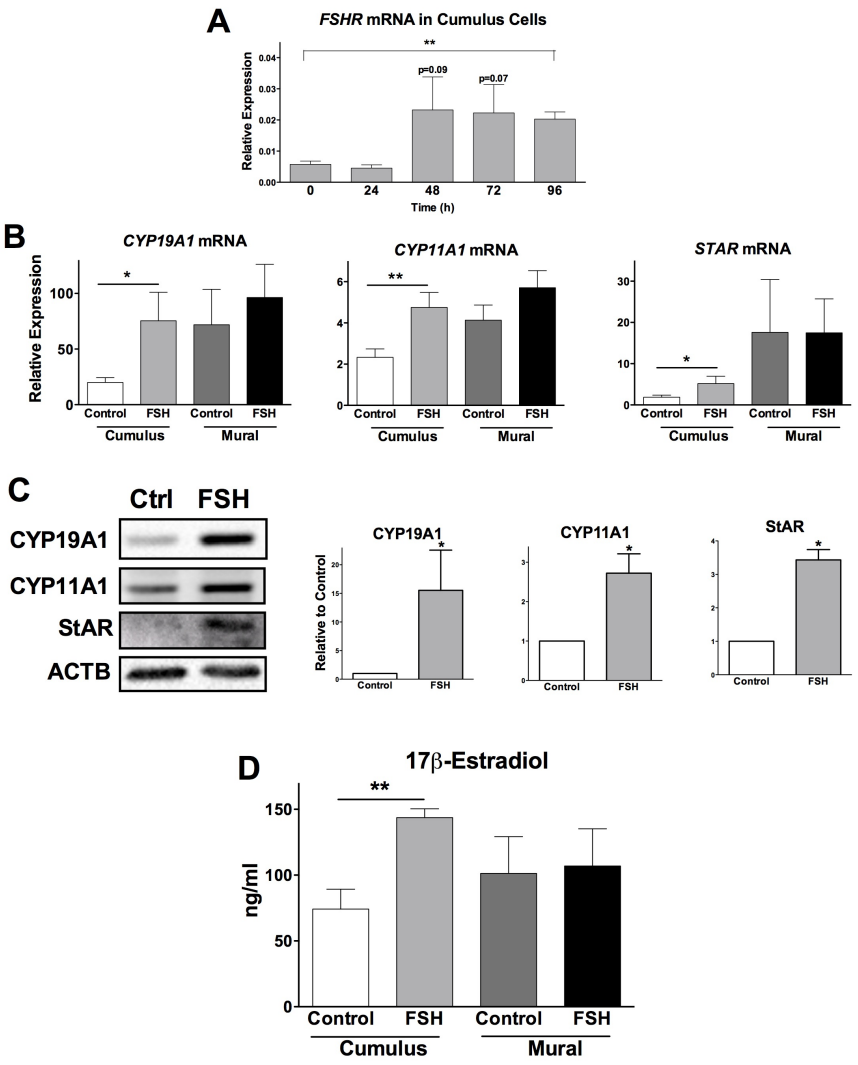

Figure 6: *Cumulus cells differentiate in response to FSH*.

(**A**) *FSHR* expression was measured in cumulus cells cultured for increasing periods of time (0-96h) by qPCR. Columns represent the mean ± SEM for 3 independent experiments.
(**B**) Cumulus and mural cells were cultured in serum-free media for 24h, then treated with FSH (50ng/ml) or left untreated (control) for 48h. RNA was isolated from the cells, and the expression of *CYP19A1*, *CYP11A1*, and *STAR* was measured by qPCR. Columns represent the mean ± SEM for 10 independent experiments.
(**C**) Cumulus cells were cultured in serum-free media for 24h then treated with FSH (50ng/ml) or left untreated (Ctrl) for 48h. Total protein was isolated from these cells and CYP19A1, CYP11A1, StAR and β-Actin (ACTB) protein levels were assessed by Western blot. Columns represent the mean ± SEM for 3 independent experiments.
(**D**) 17β-estradiol levels were measured in media collected from cultures of cumulus and mural cells that received FSH treatment (50ng/ml) or no treatment (control) for 48h. Columns represent the mean ± SEM for 3 independent experiments. (*p<0.05; **p<0.01; t-test)

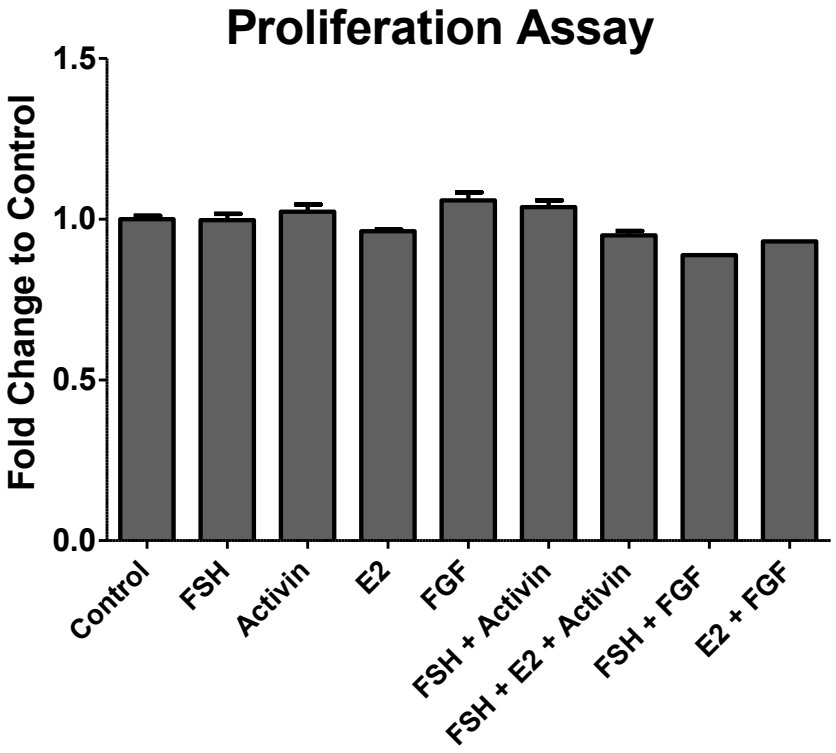

Figure 7: *Cumulus cells do not proliferate in culture.*

Cumulus cells were cultured in serum-free and phenol red-free media for 24h. Cells were treated with FSH (50ng/ml), activin (50ng/ml), estradiol (E2, 30nM), FGF (100ng/ml), or their combination for 96h in triplicate wells. Cell proliferation was measured by MTT assay. For each patient graph, the columns represent the mean absorbance of triplicate wells ± SEM for each treatment in cumulus cells of that patient. (*p<0.05, ***p<0.001 relative to control; one-way ANOVA).

C. Discussion

Our findings suggest that human cumulus cells are protected from FSH-induced differentiation and subsequent hCG-induced luteinization in humans. Gene expression studies in freshly isolated cumulus and mural cells revealed that cumulus cells expressed lower levels of *LHR* as well as key genes necessary for progesterone synthesis, indicating that they had not begun the luteinization process. In fact, we speculate that cumulus cells are not able to luteinize because of the low expression of *LHR*. Moreover, our findings suggest that cumulus cells have not undergone full differentiation to the preovulatory stage as *AMH* expression, which is strongest in preantral and small antral follicles but wanes in preovulatory follicles (112), is maintained in cumulus cells at significantly higher levels than in mural cells. This finding suggests that cumulus cells resemble granulosa cells from early antral follicles.

We also present evidence suggesting that when cultured free of the influence of the oocyte, cumulus cells further de-differentiate while mural cells maintain a luteinized phenotype. Thus, cumulus cells maintained in culture for 72h expressed low levels of the differentiation markers *CYP19A1*, *CYP11A1*, *STAR*, and *LHR*. Additionally, we demonstrated that the expression of these genes is significantly stimulated by FSH only in cumulus cells. Taken together, the fact that cumulus granulosa cells are protected from the influence of gonadotropins *in vivo*, further de-differentiate in culture, and differentiate in response to FSH suggest that cultured cumulus cells from preovulatory follicles are an adequate and physiologically relevant approach to gain insight into the process of human granulosa cell differentiation.

IV. FSH REGULATES THE EXPRESSION OF GENES IMPORTANT FOR STEROID HORMONE SYNTHESIS, CYTOSKELETAL STRUCTURE, AND THE IGF SYSTEM ACTIVITY IN HUMAN GRANULOSA CELLS

A. Introduction

Many aspects of follicular development and the process of mural granulosa cell differentiation are poorly understood, especially in humans. Several reports have examined the effect of FSH on the function of human granulosa cells (93, 94, 99, 113) recovered from follicular aspirates during IVF; however, these studies were conducted in luteinized mural granulosa cells, which may not accurately recapitulate the physiologic response of undifferentiated preantral granulosa cells to FSH. The previous chapter demonstrated that human cumulus granulosa cells from IVF patients are protected from FSH-induced differentiation and subsequent luteinization *in vivo.* Primary cultures of cumulus granulosa cells express markers of differentiated, preovulatory granulosa cells in response to FSH treatment, which resembles the FSH induced differentiation of preantral granulosa cells *in vivo.* For this reason, we conducted a microarray analysis in primary cultures of cumulus granulosa cells following treatment with FSH to gain insight into global gene expression changes during FSH-induced human granulosa cell differentiation.

B. Results

1. FSH differentially regulates the expression of 863 genes in cultured cumulus granulosa cells

For microarray analysis, cumulus granulosa cells from women that lack ovarian causes of infertility, either egg donors or women undergoing IVF for male-factor

infertility, were collected (Table II). The cumulus cells were cultured in serum-free and phenol-red free media for 24h followed by treatment with or without FSH (50ng/ml) for 48h. Analysis of differentially expressed genes between human cumulus granulosa cells treated with or without FSH for 48h revealed that 863 genes were significantly regulated by FSH treatment (Table VII, Appendix B). A majority of genes were upregulated (477) rather than downregulated (386) following treatment with FSH (Figure 8A). A heatmap of the 50 most upregulated genes and the 50 most downregulated genes shows the response to FSH treatment was conserved among the 3 patients (Figure 8B).

Within the list of the 20 most upregulated genes (Table IV) are several genes belonging to steroid hormone synthesis, including *CYP19A1* and *STAR*. These are classic genes stimulated by FSH treatment in undifferentiated, preantral granulosa cells in response to FSH. This supports the idea that findings in cultured human cumulus granulosa cells treated with FSH could be physiologically representative of the events occurring in FSH-induced preantral granulosa cell differentiation. Interestingly, *IGF2* expression is upregulated more than 4-fold after FSH treatment. FSH and IGFs have been shown to cooperate in granulosa cell differentiation in rodent granulosa cells, suggesting that enhanced IGF2 expression could be a mechanism by which FSH promotes granulosa cell differentiation in humans.

2. FSH upregulates steroidogenic genes in cultured cumulus granulosa cells

Steroid hormone synthesis is an essential function of differentiated mural granulosa cells throughout antral follicle maturation to the preovulatory stage. The mural cells convert androgens from the theca cells surrounding the follicle to produce

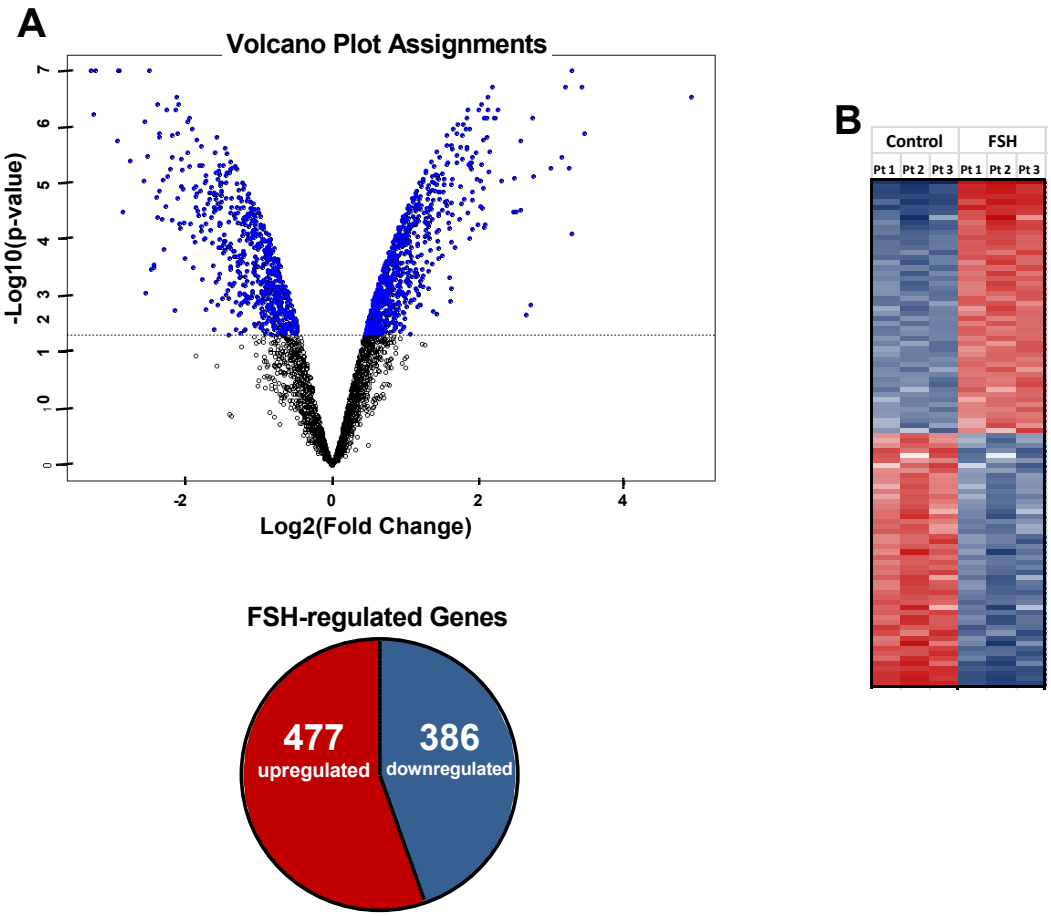

Figure 8: *FSH regulates the expression of over 850 genes human granulosa cells.*

Human cumulus granulosa cells were cultured in serum-free media for 24h then treated with FSH or no treatment (control) for 48h. Total RNA was isolated from cells, and gene expression in control and FSH-treated cells was assessed by mRNA microarray.
(**A, upper**) Volcano plot depicting the fold change (x-axis) vs. p-value (y-axis) of each unique probe set following treatment with FSH for 48h compared to untreated, control cumulus granulosa cells. Probe sets that are significantly regulated by FSH ($p<0.05$) are indicated in blue, and black dots represent probe sets that are not significantly regulated by FSH in human cumulus granulosa cells.
(**A, lower**) Numbers represent the number of unique genes that were significantly upregulated (red) and downregulated (blue) in cumulus granulosa cells after 48h FSH treatment.
(**B**) Heatmap of the top 50 upregulated genes and the top 50 downregulated genes following FSH treatment for 48h. Red indicates a high level of expression and blue indicates a lower level of expression. Each column represents an individual patient, and each row represents a single gene.

TABLE IV:

TOP 20 UPREGULATED GENES IN HUMAN CUMULUS GRANULOSA CELLS FOLLOWING 48H FSH TREATMENT

EntrezID	Symbol	Name	Geometric mean of intensities (FSH/Control)	P-value	FDR
83876	MRO	maestro	**30.30**	3.00E-07	6.97E-05
64131	XYLT1	xylosyltransferase I	**10.87**	1.30E-06	9.50E-05
374 /// 727738	AREG /// AREGB	amphiregulin /// amphiregulin B	**10.64**	2.00E-07	6.82E-05
85329	LGALS12	lectin, galactoside-binding, soluble, 12	**10.00**	< 1e-07	< 1e-07
1588	CYP19A1	cytochrome P450, family 19, subfamily A, polypeptide 1	**9.09**	2.00E-07	6.82E-05
3290	HSD11B1	hydroxysteroid (11-beta) dehydrogenase 1	**9.09**	3.50E-06	1.49E-04
3284	HSD3B2	hydroxy-delta-5-steroid dehydrogenase, 3 beta- and steroid delta-isomerase 2	**6.67**	1.45E-03	4.20E-03
3623	INHA	inhibin, alpha	**6.67**	7.00E-07	7.16E-05
6263	RYR3	ryanodine receptor 3	**5.88**	1.80E-06	1.06E-04
6770	STAR	steroidogenic acute regulatory protein	**5.88**	2.94E-05	3.51E-04
3949	LDLR	low density lipoprotein receptor	**4.76**	5.00E-07	6.97E-05
2869	GRK5	G protein-coupled receptor kinase 5	**4.55**	7.00E-07	7.16E-05
3156	HMGCR	3-hydroxy-3-methylglutaryl-CoA reductase	**4.55**	2.00E-07	6.82E-05
4504	MT3	metallothionein 3	**4.35**	6.30E-06	1.85E-04
4883	NPR3	natriuretic peptide receptor C/guanylate cyclase C (atrionatriuretic peptide receptor	**4.35**	3.00E-07	6.97E-05
56548	CHST7	carbohydrate (N-acetylglucosamine 6-O) sulfotransferase 7	**4.17**	2.82E-05	3.47E-04
2036	EPB41L1	erythrocyte membrane protein band 4.1-like 1	**4.17**	1.70E-06	1.04E-04
3481 /// 723961	IGF2 /// INS-IGF2	insulin-like growth factor 2 (somatomedin A) /// INS-IGF2 readthrough	**4.17**	5.44E-05	4.84E-04
151393	RMDN2	regulator of microtubule dynamics 2	**4.17**	4.00E-07	6.97E-05
13	AADAC	arylacetamide deacetylase	**4.00**	9.00E-06	2.14E-04

estradiol. As the follicle progresses to the preovulatory stage, FSH stimulates the expression of key steroidogenic enzymes that catalyze all steps of steroid hormone synthesis so that they are then able to convert cholesterol to estradiol themselves. Our microarray revealed that key receptors, proteins, and enzymes required for the conversion of cholesterol to estradiol are significantly upregulated in response to FSH treatment (Figure 9A).

Cholesterol, the common precursor to all steroid sex hormones, can be taken up into mural granulosa cells from circulating high- and low-density lipoproteins (HDL and LDL) via their specific receptors SCARB1 (scavenger receptor class B, member 1) and LDL receptor (LDLR) or synthesized *de novo* from lipid stores within the cell (Figure 10). The cholesterol is then shuttled to the mitochondria by sterol carrier protein 2 (SCP2) and transported into the mitochondria by steroidogenic acute regulatory protein (StAR). The conversion of cholesterol to pregnenolone by P450 side-chain cleavage (CYP11A1) is the initial step, and also the rate-limiting step, in steroidogenesis (114)**.** Pregnenolone is then converted to progesterone by the action of 3β-hydroxysteroid dehydrogenase (3β-HSD). Progesterone is converted to androstenedione and estradiol by 17β-hydroxysteroid dehydrogenase (17β-HSD) and aromatase (CYP19A1), respectively.

The receptors that foster cholesterol uptake by the mural granulosa cells and enzymes that convert cholesterol to steroid sex hormones are significantly upregulated in cultured human cumulus granulosa cells following FSH treatment (Figure 10, yellow arrows). To confirm the microarray findings, we measured the expression of *CYP19A1,*

A

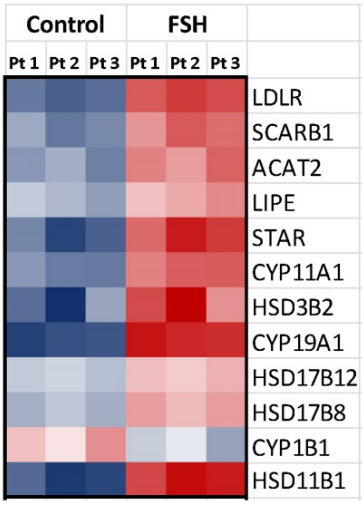

Symbol	Geometric mean of intensities (FSH/Control)	P-value	FDR
LDLR	**4.76**	5.00E-07	6.97E-05
SCARB1	**2.78**	1.95E-05	2.96E-04
ACAT2	**2.78**	1.41E-05	2.56E-04
STAR	**5.88**	2.94E-05	3.51E-04
CYP11A1	**3.45**	3.70E-06	1.53E-04
HSD3B2	**6.67**	1.45E-03	4.20E-03
CYP19A1	**9.09**	2.00E-07	6.82E-05
HSD17B12	**1.61**	5.16E-04	2.04E-03
HSD17B8	**1.96**	8.77E-05	6.49E-04
CYP1B1	**-1.52**	3.52E-03	8.44E-03
HSD11B1	**9.09**	3.50E-06	1.49E-04

B

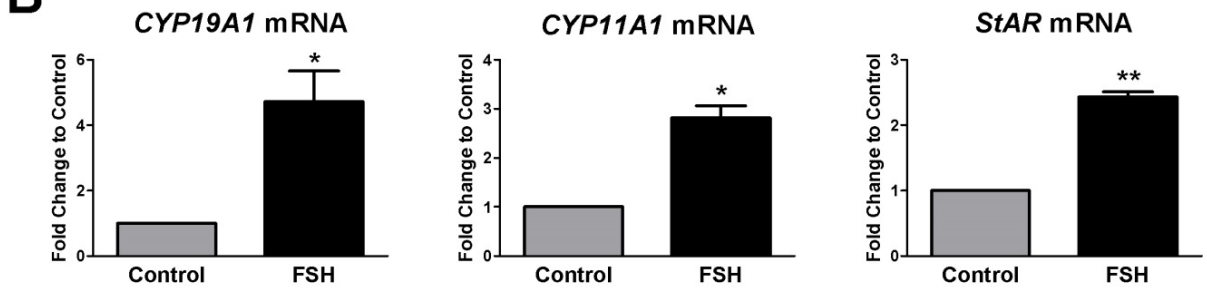

Figure 9: *FSH significantly upregulates the expression of steroidogenic genes in human granulosa cells.*

(**A, left**) Heatmap of the expression of FSH-regulated steroidogenic genes in control and FSH-treated cumulus granulosa cells from three patients. Red indicates a high level of expression and blue indicates a lower level of expression. Each column represents one patient, and each row represents a single gene.
(**A, right**) List of differentially-regulated steroidogenic genes indicating the fold change in expression following FSH treatment, and the p-value and false discovery rate (FDR) for each gene.
(**B**) Cumulus granulosa cells from three patients were cultured in serum-free media for 24h followed by treatment with FSH or no treatment for 48h. Total RNA was isolated, and the expression of *CYP19A1*, *CYP11A1*, and *StAR* was assessed by qPCR. (*p<0.05, **p<0.01 compared to control; t-test)

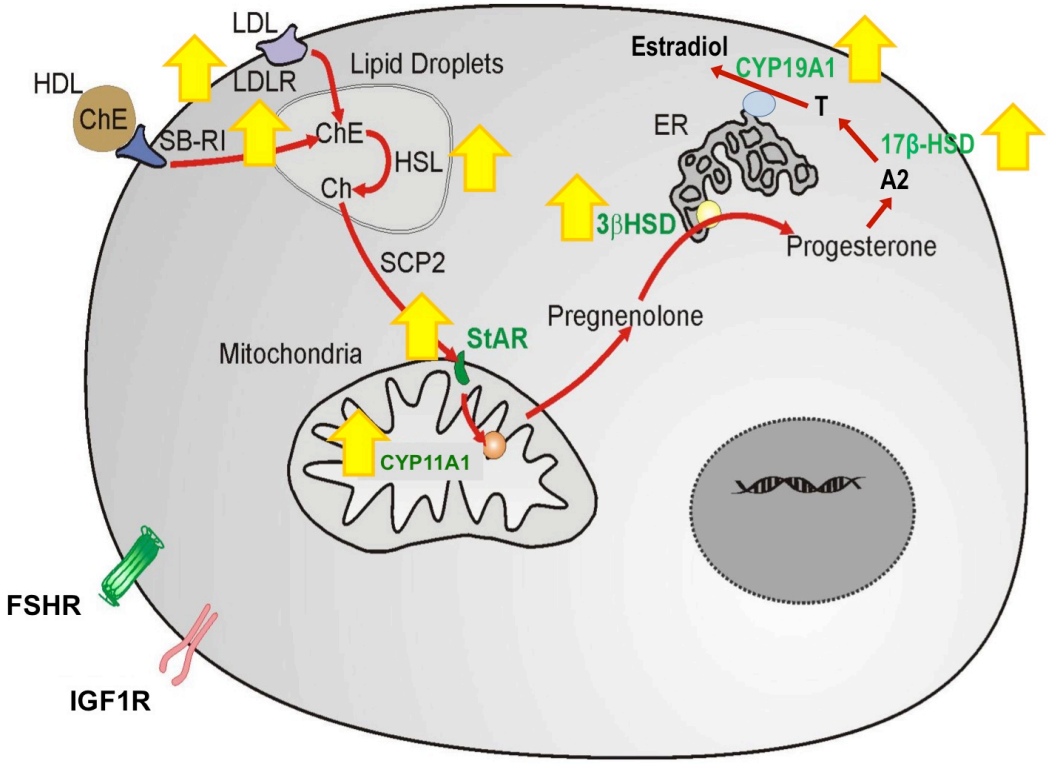

Figure 10: *FSH enhances steroidogenesis in human mural granulosa cells*.

Cholesterol can be taken up into cells from circulating HDL and LDL via their specific receptors (SCARB1 or SB-R1 and LDLR) as cholesterol esters (ChE) or synthesized *de novo* from lipid stores within the cell. Hormone sensitive lipase (HSL or LIPE) hydrolyzes ChE to cholesterol, which is then shuttled to the mitochondria by sterol carrier protein 2 (SCP2) and transported into the mitochondria by steroidogenic acute regulatory protein (STAR). The conversion of cholesterol to pregnenolone by P450 side-chain cleavage (P450scc, CYP11A1) is the initial step, and also the rate-limiting step, in steroidogenesis. Pregnenolone is then converted to progesterone by the action of 3β-hydroxysteroid dehydrogenase (3β-HSD). Pregnenolone is then converted to androstenedione (A2), which is converted to testosterone (T) by 17β-hydroxysteroid dehydrogenase (17β-HSD) and finally estradiol by CYP19A1. Yellow arrows indicate that the gene encoding the protein is upregulated upon FSH treatment.

CYP11A1, and *STAR* by qPCR in three additional patients (Figure 9B) and found that FSH significantly stimulated the expression of these enzymes.

3. FSH downregulates cytoskeletal genes in cultured cumulus granulosa cells

The cytoskeleton is a structural matrix within the cells that can influence the cell shape and function. It consists of 3 kinds of filaments: microfilaments, intermediate filaments, and microtubules. A number of genes encoding cytoskeletal proteins are within the 20 genes that are most downregulated in human cumulus granulosa cells following FSH treatment (Table V). Further inspection revealed that genes encoding proteins for all 3 cytoskeletal filament types are regulated by FSH treatment (Figure 11A). Tubulins, which make up microtubules, keratin 18, a key component of intermediate filaments, and actins, which make up microfilaments, are all significantly downregulated after 48h FSH treatment. Because intermediate filaments and microfilaments both have roles in cell morphology, we explored the effect of FSH treatment on cultured cumulus granulosa cell morphology. Actin filaments on FSH-treated and untreated granulosa cells were stained with phalloidin (Figure 11B). Untreated cumulus granulosa cells showed an organized series of parallel actin filaments. Upon FSH treatment, there was a clear change in actin filament morphology where the filaments were not uniformly parallel. Instead, the actin filaments in FSH-treated cells were clustered in bundles within the cell.

TABLE V:

TOP 20 DOWNREGULATED GENES IN HUMAN CUMULUS GRANULOSA CELLS FOLLOWING 48H FSH TREATMENT

EntrezID	Symbol	Name	Geometric mean of intensities (FSH/Control)	P-value	FDR
1278	COL1A2	collagen, type I, alpha 2	**-4.17**	1.13E-05	2.30E-04
2878	GPX3	glutathione peroxidase 3 (plasma)	**-4.34**	1.30E-06	9.50E-05
167681	PRSS35	protease, serine, 35	**-4.36**	3.00E-07	6.97E-05
467	ATF3	activating transcription factor 3	**-4.42**	5.00E-07	6.97E-05
1303	COL12A1	collagen, type XII, alpha 1	**-4.43**	1.78E-03	4.95E-03
4133	MAP2	microtubule-associated protein 2	**-4.82**	5.00E-07	6.97E-05
152007	GLIPR2	GLI pathogenesis-related 2	**-5.03**	4.32E-05	4.33E-04
388115	C15orf52	chromosome 15 open reading frame 52	**-5.14**	1.38E-05	2.56E-04
72	ACTG2	actin, gamma 2, smooth muscle, enteric	**-5.16**	1.30E-06	9.50E-05
642938	FAM196A	family with sequence similarity 196, member A	**-5.22**	4.02E-05	4.15E-04
285016	FAM150B	family with sequence similarity 150, member B	**-5.26**	1.80E-05	2.92E-04
1490	CTGF	connective tissue growth factor	**-5.41**	2.79E-04	1.35E-03
27063	ANKRD1	ankyrin repeat domain 1 (cardiac muscle)	**-5.65**	< 1e-07	5.11E-05
4638	MYLK	myosin light chain kinase	**-5.77**	3.30E-06	1.47E-04
8654	PDE5A	phosphodiesterase 5A, cGMP-specific	**-5.96**	9.20E-06	2.15E-04
4879	NPPB	natriuretic peptide B	**-7.27**	3.25E-05	3.73E-04
6424	SFRP4	secreted frizzled-related protein 4	**-7.55**	< 1e-07	5.11E-05
6876	TAGLN	transgelin	**-7.57**	< 1e-07	< 1e-07
4982	TNFRSF11B	tumor necrosis factor receptor superfamily, member 11b	**-9.59**	6.00E-07	7.16E-05
1264	CNN1	calponin 1, basic, smooth muscle	**-9.85**	< 1e-07	5.11E-05

A

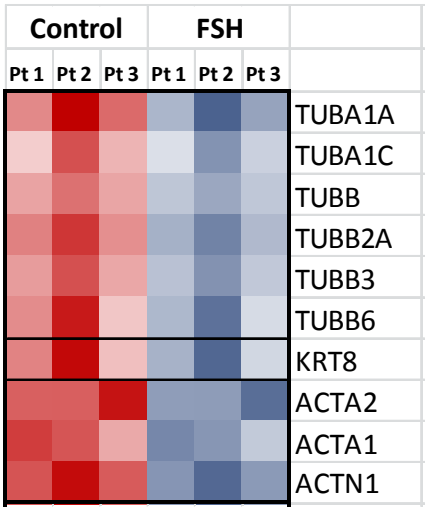

Symbol	Geometric mean of intensities (FSH/Control)	P-value	FDR
TUBA1A	**-3.00**	5.63E-04	2.16E-03
TUBA1C	**-1.79**	4.81E-03	1.07E-02
TUBB	**-1.83**	2.24E-04	1.17E-03
TUBB2A	**-2.40**	1.90E-04	1.06E-03
TUBB3	**-2.02**	5.44E-04	2.11E-03
TUBB6	**-1.93**	2.33E-03	6.07E-03
KRT18	**-2.38**	1.44E-03	4.19E-03
ACTA2	**-3.15**	4.04E-05	4.15E-04
ACTA1	**-1.79**	1.81E-04	1.03E-03
ACTN1	**-3.19**	1.93E-05	2.96E-04

B

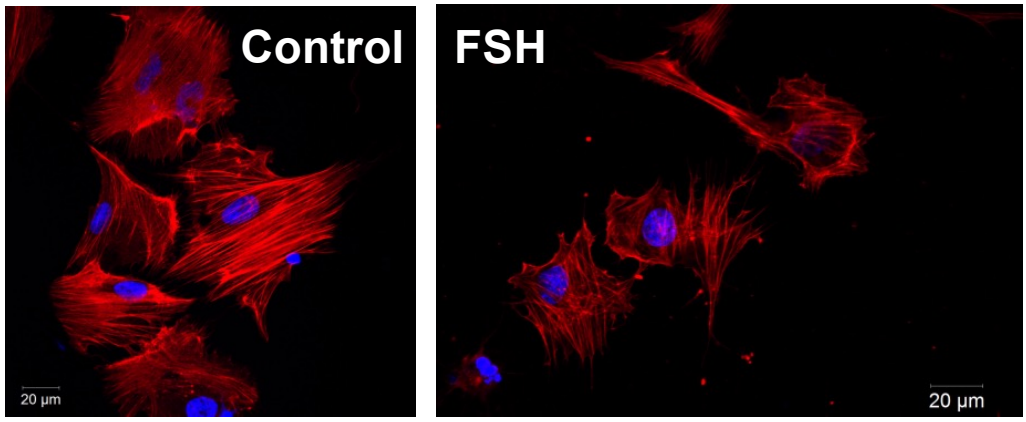

Figure 11: *FSH significantly downregulates the expression of cytoskeletal genes in human granulosa cells.*

(**A, left**) Heatmap of the expression of FSH-regulated cytoskeletal genes in control and FSH-treated cumulus granulosa cells from three patients. Red indicates a high level of expression and blue indicates a lower level of expression. Each column represents one patient, and each row represents a single gene.
(**A, right)** List of differentially-regulated cytoskeletal genes indicating the fold change in expression following FSH treatment, and the p-value and false discovery rate (FDR) for each gene.
(**B**) Cumulus granulosa cells were cultured in serum-free media for 24h followed by treatment with FSH for 48h. Cells were stained with rhodamine phalloidin and DAPI, and cell images were taken by confocal microscopy. Red indicates actin filaments within the cell, and blue indicates DAPI staining of the cell nucleus.

4. FSH differentially regulates the expression of the IGF system in human granulosa cells

Because IGF2 is highly upregulated in cultured cumulus granulosa cells following FSH treatment (TABLE IV), and IGF2 has been shown to stimulate human granulosa cell function (95, 96), we examined the expression of IGFs, the IGF receptors, and regulators of the IGF system (Figure 12A) in cultured human cumulus granulosa cells after FSH treatment. *IGF1* expression was not detected by microarray analysis; however, *IGF2* was expressed in cumulus granulosa cells and upregulated by FSH treatment. Both *IGF1R* and *IGF2R* mRNA were present, and their expression was not affected by FSH treatment. Interestingly, the expression of regulators of the IGF system (Figure 12B) was significantly altered upon FSH treatment such that IGF2 bioavailability would be increased. *IGFBP3*, which binds IGF2 and limits its interaction with IGF1R and IGF2R, is significantly downregulated. Additionally, *PAPP-A*, a protease that targets IGFBP4 and reduces its ability to bind IGFs, is increased. With an increase in the proteolysis of IGFBP4, more IGF2 is bioavailable to activate the IGF receptors and act on granulosa cells.

Although the levels of *IGF1R* and *IGF2R* do not change upon FSH treatment, the increase in *IGF2* expression and its bioavailability suggest that FSH enhances the activity of the IGF system. Additionally, FSH treatment increases the expression of *INSR,* the gene encoding insulin receptor (IR). IGF2 has been shown to activate the IR to activate downstream signaling cascades (115). Thus, increasing *INSR* expression may be another way by which FSH enhances the IGF system in human granulosa cells. Interestingly, IRS2, which interacts with IGF1R and IR and acts as a scaffold for

components of intracellular signaling, is downregulated by FSH. Activation of AKT, and consequent activation of FOXO1, has been shown to inhibit IRS expression (116). This downregulation could indicate that the IGF2 produced by the granulosa cells is acting in an autocrine manner to stimulate AKT activation and decrease IRS expression to alter signaling within the cell.

5. Cultured cumulus cells express IGF2 but not IGF1

To confirm the findings of our microarray analysis, we assessed the expression of key components of the IGF system in cumulus granulosa cells of additional IVF patients. Previous findings have demonstrated that human granulosa cells express exclusively *IGF2* (117) and that FSH stimulates *IGF2* expression in small antral (Class 2) human follicles (79). We confirmed our microarray findings that cultured cumulus granulosa cells express *IGF2* as well as *IGF1R* and *IGF2R*, but not *IGF1* (Figure 13A). Additionally, we demonstrated that these cells expressed significantly higher levels of *IGF1R* than *IGF2R*. Furthermore, we observed that FSH induced a 3-fold increase in *IGF2* expression, but it had no effect on the expression of either receptor (Figure 13B) suggesting that gonadotropins could modulate the IGF pathway in granulosa cells by up regulating *IGF2*. We confirmed that IGF2 protein was also increased following FSH treatment for 48h by Western blot (Figure 14A). Using immunocytochemistry, we observed an increase in IGF2 protein in the nucleus of cumulus granulosa cells after treatment with FSH for 48h (Figure 14B). Together, these results suggest that FSH is a potent stimulator of IGF2 expression at both the mRNA and protein level in human granulosa cells.

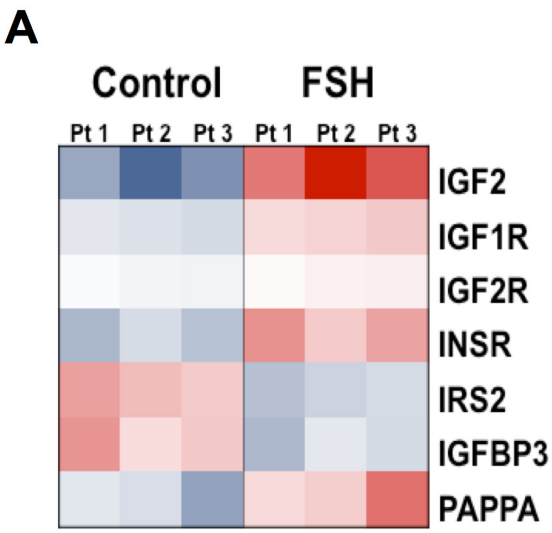

Symbol	Geometric mean of intensities (FSH/Control)	P-value	FDR
IGF2 /// INS-IGF2	4.17	5.44E-05	4.84E-04
INSR	1.89	3.64E-04	1.61E-03
IRS2	-1.73	1.14E-03	3.53E-03
IGFBP3	-1.64	3.21E-03	7.84E-03
PAPPA	1.59	1.49E-03	4.30E-03

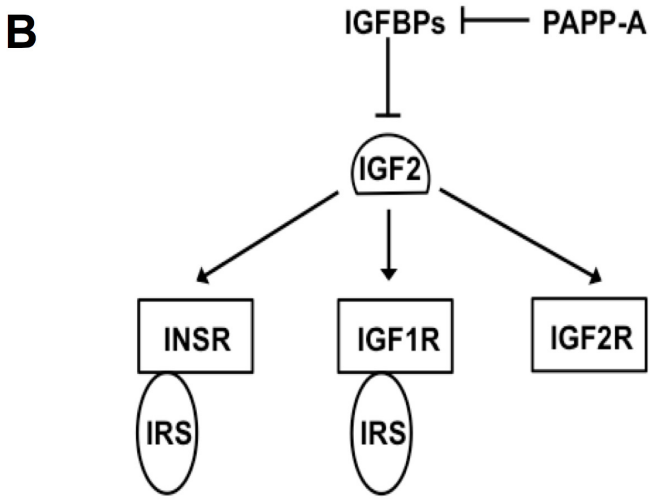

Figure 12: *FSH significantly regulates the expression of the IGF system in human granulosa cells.*

(**A, left**) Heatmap of the expression of FSH-regulated IGF system genes in control and FSH-treated cumulus granulosa cells from three patients. Red indicates a high level of expression and blue indicates a lower level of expression. Each column represents one patient, and each row represents a single gene.
(**A, right**) List of differentially-regulated genes in the IGF system indicating the fold change in expression following FSH treatment, and the p-value and false discovery rate (FDR) for each gene.
(**B**) Scheme depicting the IGF2 system including the ligand, receptors, and regulators of the system. IGF2 can activate the INSR, IGF1R, and IGF2R, and IRS associates with both the INSR and IGF1R to allow for activation of downstream signaling pathways. IGFBPs bind IGFs and limit their availability. PAPP-A can degrade IGFBPs, which lowers their affinity for IGFs and leads to an overall increase in IGF2 bioavailability.

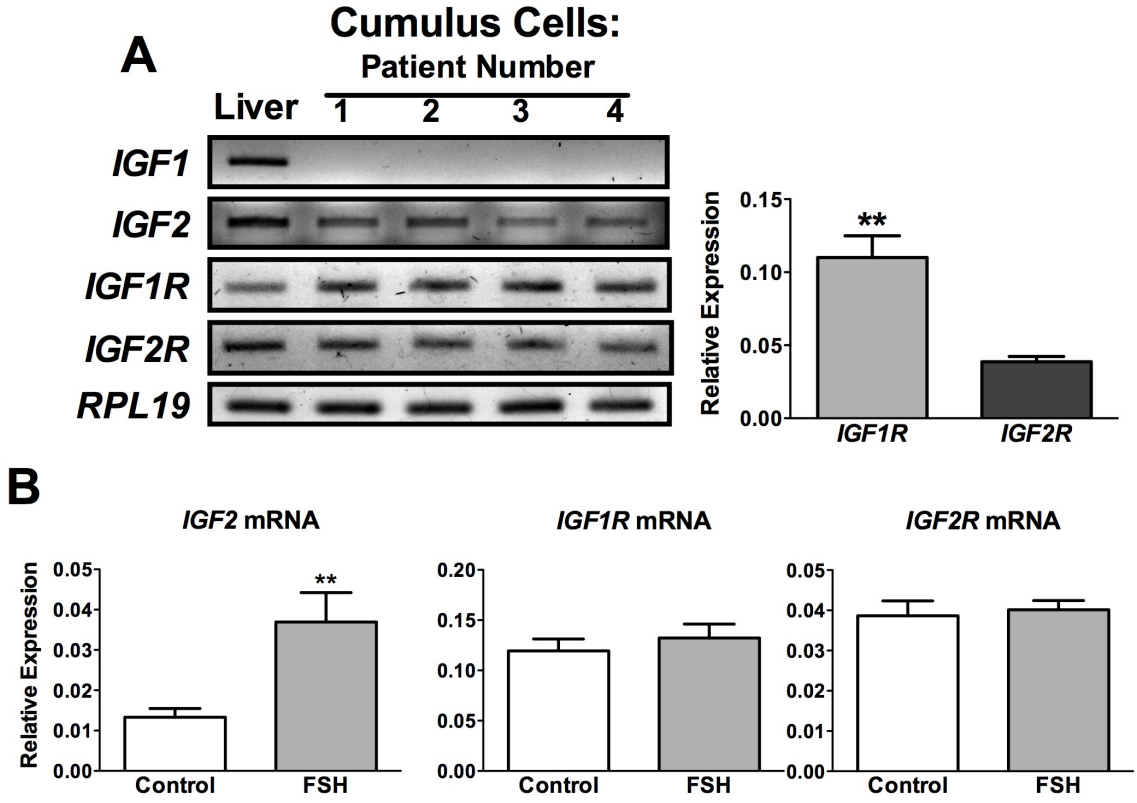

Figure 13: *Cumulus granulosa cells express IGF2 but not IGF1*.

Cumulus cells were cultured in serum-free media for 72h before RNA isolation.
(**A**) Cumulus cell RNA from 4 different patients as well as human liver RNA was reverse transcribed, and PCR was used to detect expression of *IGF1*, *IGF2*, *IGF1R*, *IGF2R* and the housekeeping gene *RPL19*. PCR products were visualized on agarose gels. *IGF1R* and *IGF2R* expression levels in cumulus cells were quantified by qPCR.
(**B**) Cumulus cells were cultured in serum-free media for 24h, then treated with FSH (50ng/ml) or left untreated for 48h. RNA was isolated from these cells, and the expression of *IGF2*, *IGF1R,* and *IGF2R* was measured by qPCR. For qPCR results, columns represent the mean ± SEM of at least 7 independent experiments. (**p<0.01; t-test)

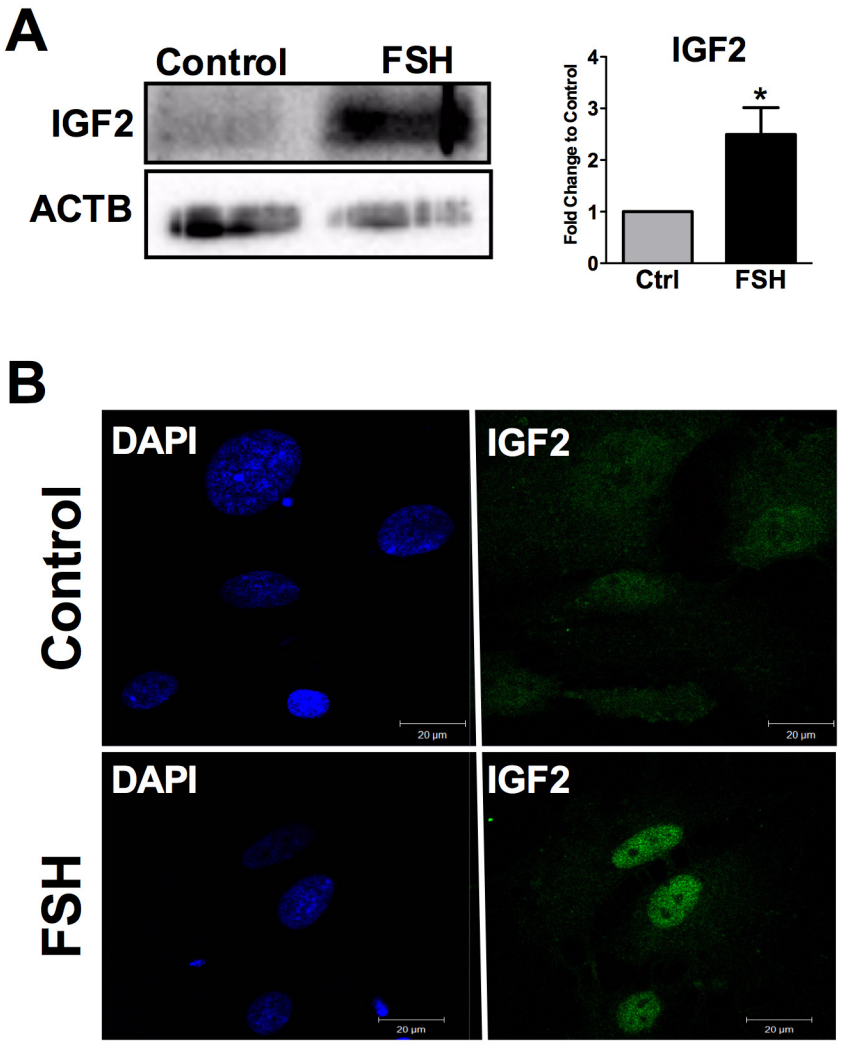

Figure 14: *FSH increases IGF2 protein expression in human granulosa cells*.

Cumulus cells cultured in serum-free and phenol red-free media for 24h were treated with FSH (50 ng/ml) or left untreated (Ctrl) for 48h.
(**A**) IGF2 and ACTB expression (loading control) was assessed by Western blot. The IGF2 band intensities were adjusted to band intensity of ACTB on the same blot, and the ratio of FSH-treated relative to untreated cells is reported on the right graph. Columns represent the mean ± SEM for three independent experiments (*$p<0.05$; t-test).
(**B**) Using immunocytochemistry, IGF2 protein (green, right column) was detected in cumulus granulosa cells with (bottom row) and without (top row) FSH treatment (50ng/ml) for 48h. Cell nuclei (blue, left column) were detected using DAPI. Representative image of 3 patients.

C. Discussion

We previously demonstrated that cultures of primary cumulus granulosa cells collected from IVF patients recapitulate many characteristics of preantral granulosa cells, including differentiating in response to FSH treatment. Using cultured cumulus granulosa cells from three IVF patients without ovarian dysfunction, we conducted a microarray to gain insight into the global changes in gene expression during human granulosa cell differentiation following FSH treatment. Here, we demonstrate that FSH significantly regulates the expression of 863 genes, including those with an important role for steroidogenesis, cytoskeletal structure, and IGF action.

It is well-known that FSH stimulates steroid hormone synthesis, which is a key function of differentiated granulosa cells (113, 118-120). We demonstrate that this is true in cultured primary cumulus granulosa cells as well. Essential receptors and enzymes that, together, mediate the production of estradiol and other steroid sex hormones from cholesterol were upregulated in response to FSH treatment. This included *SCARB1* and *LDLR*, which mediate the uptake of HDL and LDL as a source of cholesterol. The enzymes that mediate cholesterol uptake into the mitochondria and its conversion to estradiol, including *STAR*, *CYP11A1*, and *CYP19A1*, were also significantly upregulated. Overall, the upregulation of steroidogenic genes in cultured cumulus granulosa cells in response to FSH adds validity to our use of these cells to study mechanisms of FSH-induced granulosa cell differentiation.

FSH also significantly downregulated a large subset of genes, including genes that encode cytoskeletal proteins. Components of microfilaments, intermediate filaments, and microtubules all showed a decrease in expression following treatment

with FSH. This is similar to what has been observed in long-term cultures of luteinized mural granulosa cells (113, 121). Inspection of the actin microfilaments in cultured cumulus granulosa cells revealed that FSH elicits cytoskeletal changes. Rather than thin, parallel filaments dispersed throughout the cells, the filaments take on a web-like appearance. Previous studies have suggested that the cytoskeletal rearrangement upon FSH treatment is an essential part of granulosa cell differentiation that allows for changes in organelle size and number as the cells enhance their steroidogenic capacity (121, 122).

In this study, we observed that FSH differentially regulates genes encoding proteins in the IGF system in cultured cumulus granulosa cells. We determined that FSH could enhance IGF activity in human granulosa cells in a number of ways. FSH significantly upregulates IGF2 expression at both the mRNA and protein level. Interestingly, the increase in IGF2 in response to FSH was localized to the nucleus. To our knowledge, there is only one reported observation of nuclear IGF2, which was in osteosarcoma cells (123). The significance of nuclear IGF2 in either osteosarcoma cells or human granulosa cells is unknown, and additional studies are needed to confirm these findings. Additionally, FSH downregulates *IGFBP3* expression and enhances *PAPP-A* expression—both of which can result in an increase in IGF2 bioavailability. The intricate regulation of the IGF system by FSH in human granulosa cells suggests that IGFs may have an integral role in FSH-induced granulosa cell differentiation during follicle maturation.

V. FSH AND IGF2 COOPERATE TO REGULATE HUMAN GRANULOSA CELL FUNCTION

A. Introduction

Significant differences in the ovarian IGF system exist between rodents and humans. In rodents, granulosa cells produce mostly IGF1 (76). In contrast, *IGF2* mRNA levels are high in human granulosa cells and *IGF1* mRNA is not detectable (79, 124, 125). Consequently, the follicular fluid of human dominant follicles contains up to 10-fold more IGF2 than IGF1 (126, 127). Intrafollicular IGF2 also appears to be critical for follicle maturation in primates, as a 1.6-fold increase in intrafollicular IGF1 has no effect on follicle maturation (128). A central role of IGF2 in regulating follicle growth in humans is further supported by the positive association between intrafollicular IGF2 levels, follicle maturation, and oocyte maturation (83, 127, 129). Together, these observations suggest that IGF2 is the main player of the IGF system in human granulosa cells.

IGF2 has been shown to stimulate proliferation (96) and the production of estradiol and progesterone in human luteinized granulosa cells (95, 130-132). In primates, IGF2 increases steroidogenesis and promotes VEGF production in preovulatory follicles (63, 95, 133, 134). IGF2 stimulates estradiol and progesterone accumulation in granulosa cells of small (2 to 7 mm) follicles and preovulatory follicles, but it seems to have no effect on proliferation (63). Finally, the preferential gene expression and secretion of IGF2 by the granulosa cells of the human dominant follicle strongly suggests that IGF2 plays a critical role in follicular maturation by the way of autocrine actions (79). Despite this evidence, the interaction between FSH and IGF2

during human granulosa cell differentiation has not been examined. We hypothesize that granulosa cell-produced IGF2 acts in concert with FSH to regulate granulosa cell differentiation and follicle growth in humans.

B. Results

1. FSH and IGF2 enhance human granulosa cell differentiation

To determine the interplay between IGF2 and FSH on the regulation of granulosa cell differentiation, we quantified *CYP19A1* mRNA levels in cells treated with increasing concentration of IGF2 in the absence or presence of FSH. When cells were treated with 1 to 250 ng/ml of IGF2, a concentration-dependent increase in *CYP19A1* mRNA transcripts was observed in which maximal stimulation was reached at 50 ng/ml and remained at this level at higher concentrations of IGF2 (Figure 15A). Co-treatment with increasing concentration of IGF2 and FSH (50 ng/ml) synergistically increased *CYP19A1* transcript abundance. For example, IGF2 at 1 ng/ml did not stimulate *CYP19A1* expression alone but it synergized with FSH to enhance *CYP19A1* expression above levels induced by FSH alone. Two-way ANOVA analysis of these results indicated that IGF2 treatment has a significant effect on the stimulation of *CYP19A1* by FSH (p=0.0001). Reciprocally, this analysis demonstrated that FSH significantly affects the IGF2 stimulation of *CYP19A1* (p<0.001). Similarly, FSH and IGF2 synergized in stimulating the expression of CYP19A1 protein (Figure 15B) and estradiol accumulation (Figure 15C). These results suggest that IGF2, even at low concentrations, has a major impact on FSH-induced granulosa cell differentiation.

Because human granulosa cells produce IGF2, and IGF2 synergizes with FSH (Figure 15A), we next investigated the extent to which FSH action in granulosa cells

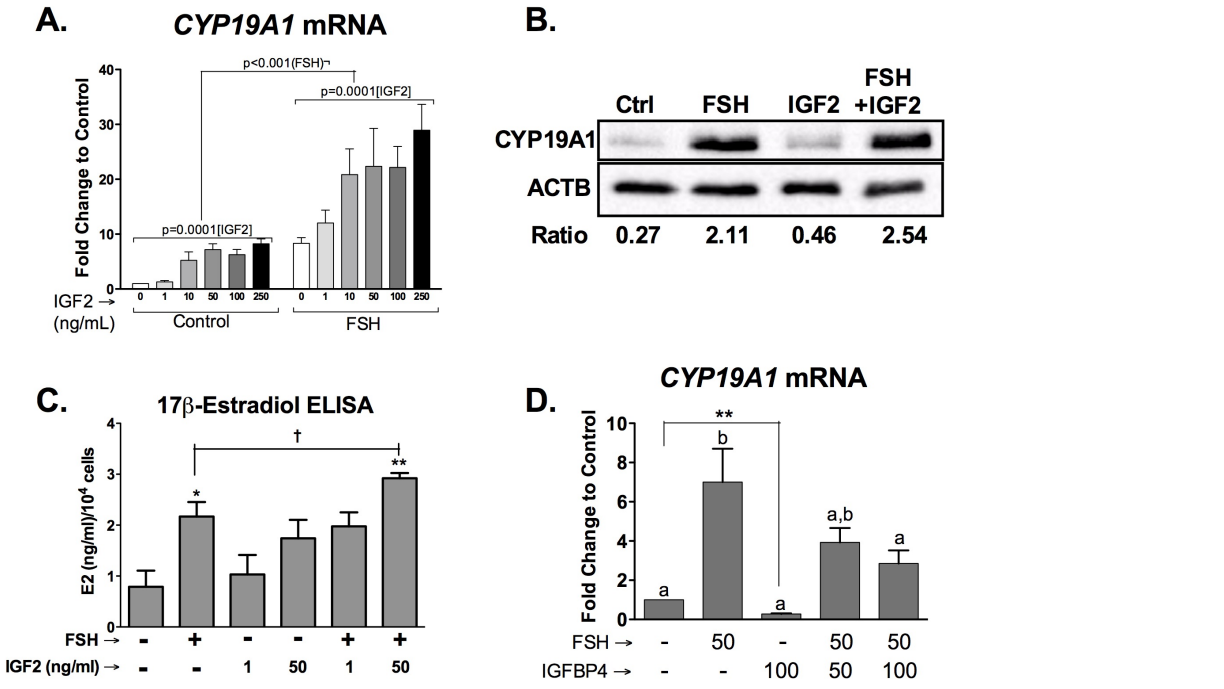

Figure 15: *IGF2 is essential for FSH-induced cumulus cell differentiation*

(**A**) Cumulus cells were cultured for 24h in serum-free and phenol red-free media then treated with FSH (50 ng/ml), IGF2 (1-250 ng/ml), or both for 48h. Two-way ANOVA analysis of these results indicated that IGF2 treatment has a significant effect on the stimulation of *CYP19A1* by FSH (p=0.0001) and that FSH significantly affects the IGF2 stimulation of *CYP19A1* (p<0.001).
(**B**) Cumulus cells from one patient were cultured in serum-free and phenol red-free media for 24h and treated with FSH (50 ng/ml), IGF2 (50 ng/ml), or their combination for 48h. Total protein was isolated from the cells, and the expression of CYP19A1 and ACTB (loading control) was assessed by Western blot. CYP19A1 band intensities were adjusted to band intensity of ACTB for the same sample, and the ratio is indicated below the Western blot images.
(**C**) Cumulus cells from three patients were cultured in serum-free and phenol red-free media for 24h and treated with FSH (50 ng/ml), IGF2 (1 or 50ng/ml), or their combination for 48h. Media was collected from the cells and 17β-Estradiol levels were measured by ELISA (intra-assay coefficient of variability = 3.5%). The E2 levels are reported per 10,000 cells. (*p<0.05 compared to control; one-way ANOVA; † p<0.05; t-test)
(**D**) Cumulus cells were cultured for 24h in serum-free and phenol red-free media then treated with FSH (50 ng/ml), insulin-like growth factor binding protein 4 (IGFBP4) (50-100 ng/ml), or both for 48h. RNA was isolated from the cumulus cells and *CYP19A1* mRNA levels were measured by qPCR. Columns represent the mean ± SEM of at least three independent experiments. Different letters denote a significant difference of at least p<0.05 (one-way ANOVA) between treatment groups. Control and IGFBP4-treated groups are significantly different when compared using a *t*-test (**p<0.01).

depends on locally produced IGF2. For this purpose, we treated cells with insulin-like growth factor binding protein 4 (IGFBP4). IGFBP4 binds IGFs and, consequently, blocks IGF1R activation. Co-treatment with IGFBP4 blunted the increase in *CYP19A1* induced by FSH (Figure 15D). The addition of IGFBP4 (100ng/ml) not only significantly decreased FSH-induced stimulation of *CYP19A1* but also diminished basal *CYP19A1* transcript levels by approximately 70%. The effect of IGFBP4 on basal *CYP19A1* mRNA abundance was statistically significant ($p<0.01$) when control and IGFBP4-treated groups were compared using a *t* Test. These results suggest that IGF2 actions are required for FSH-induced granulosa cell differentiation and for basal *CYP19A1* expression and are in agreement with our previous findings demonstrating that IGF signaling through IGF1R is required for FSH-induced granulosa cell differentiation in rodent granulosa cells (32).

2. FSH and IGF2 synergize to enhance human granulosa cell proliferation

Next, we evaluated the impact of IGF2 on granulosa cell proliferation, a crucial event in follicle progression towards the preovulatory state. For this purpose, cells were treated with FSH, increasing doses of IGF2, or both factors combined. Treatment with FSH or IGF2 alone had no effect on granulosa cell proliferation. However, when cells were co-treated with FSH and IGF2 a significant increase in cell proliferation was observed (Figure 16). The effect of IGF2 dosage varied from patient to patient. Thus, as shown in Figure 16, a concentration-dependent synergism was observed between IGF2 and FSH in patients #1 and #3; whereas, for patient #2, only the highest concentrations of IGF2 used were able to stimulate cell proliferation in the presence of FSH.

3. FSH stimulates ERK, AKT, and JNK Phosphorylation in human granulosa cells

In order to gain an understanding of how FSH and IGF2 may cooperate to enhance both *CYP19A1* expression and granulosa cell proliferation, we first had to identify the action of FSH in human granulosa cells. To assess which signaling pathways were activated upon FSH treatment, a human phospho-kinase array was used. This assay allowed for the measurement of phosphorylation of 43 different kinases in a verity of cellular signaling pathways simultaneously in a single protein sample. Cumulus granulosa cells were cultured for 24h in serum-free and phenol-red free media, then treated with or without FSH for 1h. An equal amount of total protein from either control of FSH treated cells was applied to the phospho-array membranes, and the phosphorylation of each target kinase was measured in duplicate, adjacent spots (Figure 17A). The intensity of duplicate spots was quantified and compared between untreated and FSH-treated samples (Table VI, Appendix A). In cultured cumulus granulosa cells, FSH treatment for 1h stimulated the phosphorylation of ERK, AKT, JNK, and CREB by at least 2-fold compared to the untreated cells (Figure 17B).

The phosphorylation of ERK, AKT, JNK, and CREB was then assessed by Western blot in cultured cumulus granulosa cells after treatment with FSH for 1h. The phosphorylation of ERK1/2 and AKT (S473) were strongly enhanced after FSH

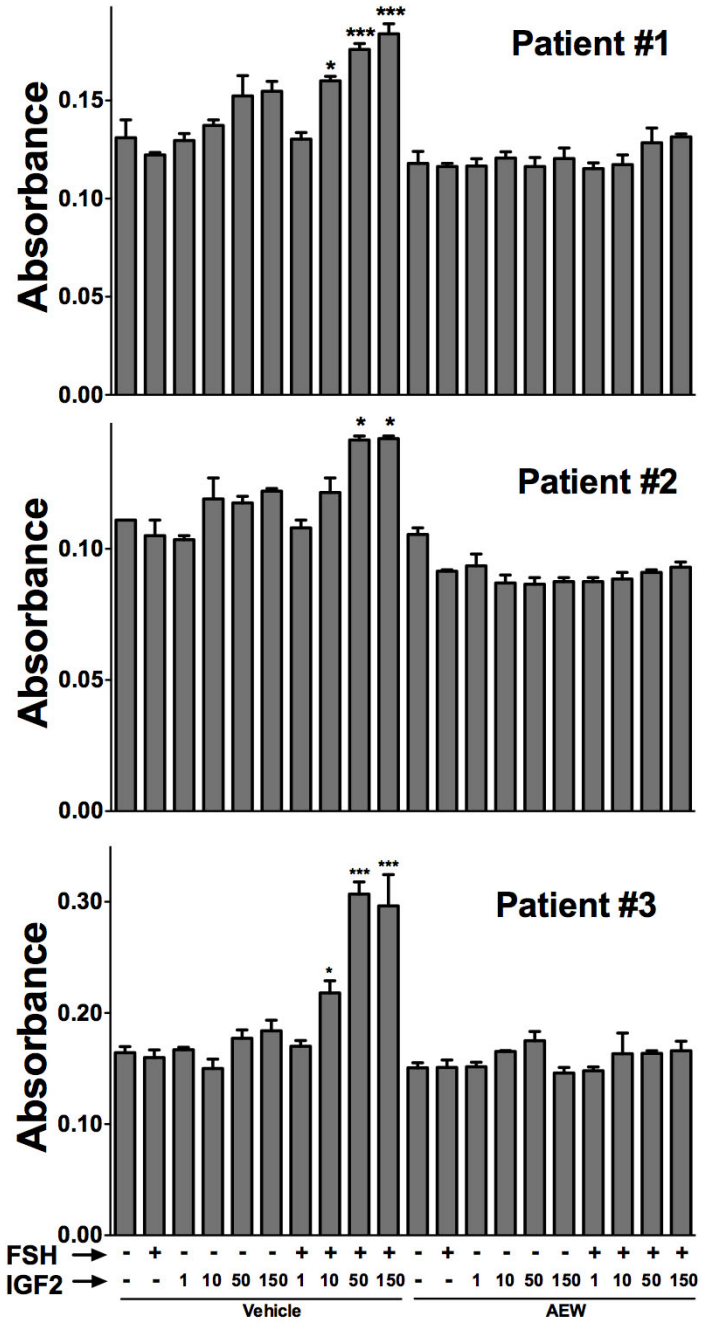

Figure 16: *FSH and IGF2 synergize to stimulate cumulus cell proliferation.*

Cumulus cells were cultured in serum-free and phenol red-free media for 24h. Cells were treated with AEW (0.5 μM) or vehicle (DMSO) for 1h, followed by treatment with FSH (50 ng/ml), IGF2 (1-150 ng/ml), or both for 96h in triplicate wells. Cell proliferation was measured by MTT assay. For each patient graph, the columns represent the mean absorbance of triplicate wells ± SEM for each treatment in cumulus cells of that patient. (*p<0.05, ***p<0.001 relative to control; one-way ANOVA).

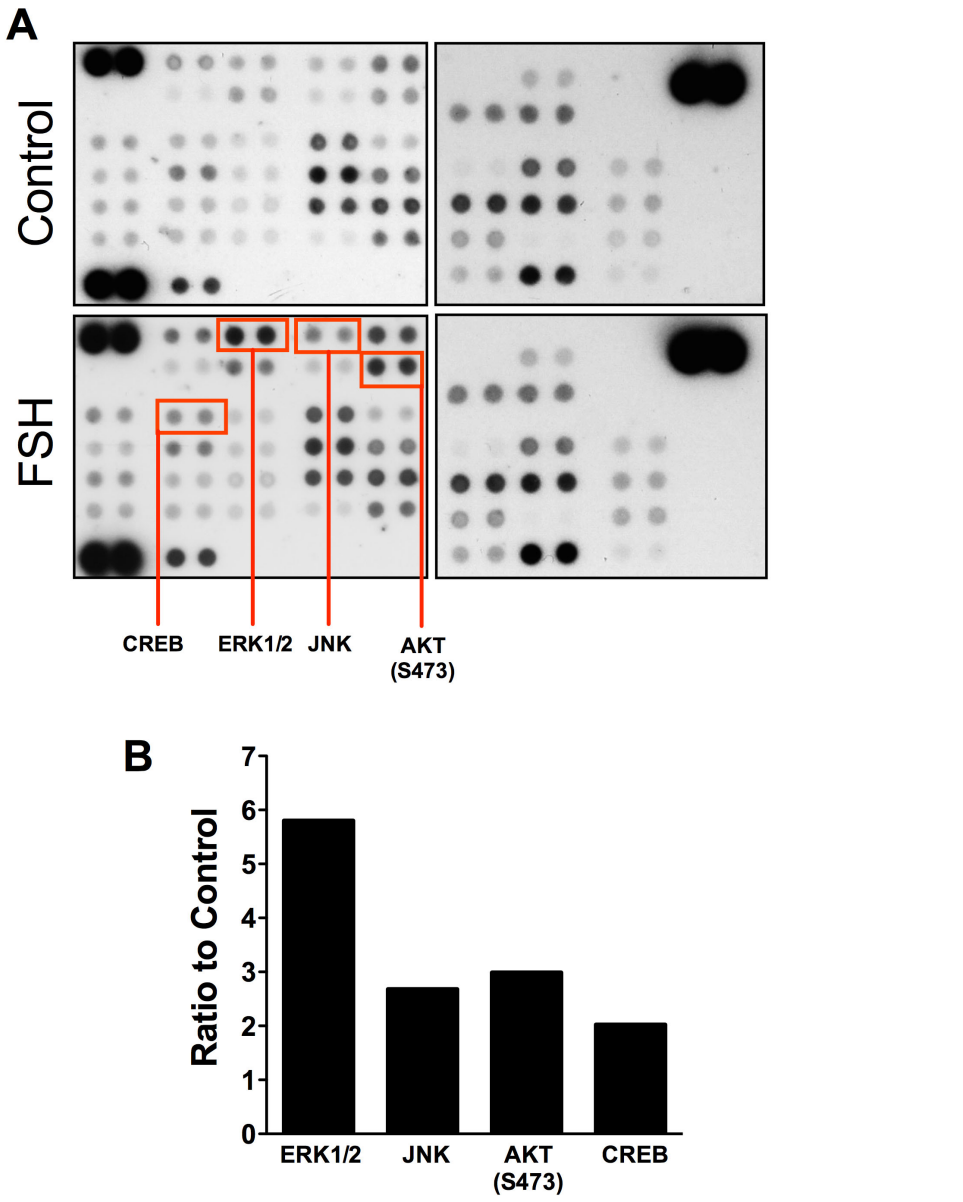

Figure 17: *FSH-induced cellular signaling pathways.*

(**A**) Cumulus granulosa cells from one patient were cultured in serum-free and phenol red-free media for 24h, followed by treatment with or without FSH (50ng/ml) for 1h. Total protein was isolated from the cells, and 170µg of whole cell lysates of control and FSH-treated cells was applied to the antibody-spotted membranes in the Human Phospho-kinase Array (R&D Systems). The phosphorylation status of 43 kinases was assessed in duplicate, adjacent spots.
(**B**) The intensity of each pair of kinase-specific spots was quantified using ImageJ and averaged. After correction to control spots on each membrane, the intensities were compared between FSH and control. The ratio of intensity (FSH:Control) is plotted for ERK1/2, JNK, AKT(S473), and CREB. The corresponding spots are labeled in (A).

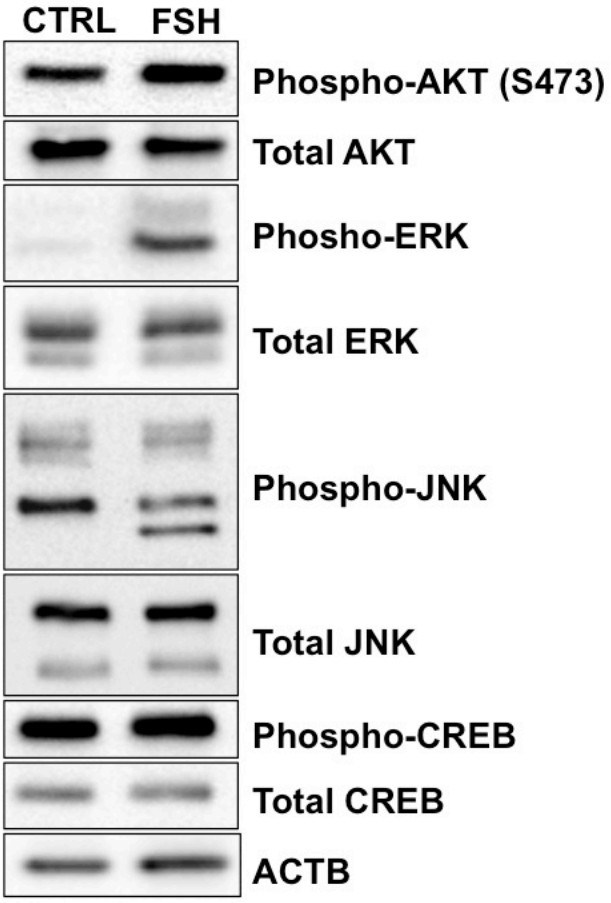

Figure 18: *FSH activates ERK1/2, AKT(S473), and JNK phosphorylation in cultured cumulus granulosa cells.*

Cumulus granulosa cells were cultured for in serum-free and phenol red-free media for 24h, followed by treatment with or without FSH (50ng/ml) for 1h. Total protein was isolated from the cells and the level of phosphorylated and total AKT, ERK1/2, JNK, and CREB were detected by Western blot. A representative blot of three patients is shown.

treatment (Figure 18). Little is known about JNK activation in granulosa cells, but AKT and ERK are well known targets of FSH action in rodent granulosa cells. Interestingly, CREB, which is thought to be the primary mediator of FSH action in granulosa cells, was not strongly or consistently phosphorylated in response to FSH treatment amongst the patients tested.

4. FSH and IGF2 cooperate to enhance AKT and ERK activation

To explore possible mechanisms by which FSH and IGF2 synergize to promote granulosa cell proliferation, we examined the AKT and ERK signaling pathways, which are known to regulate proliferation and are targets of FSH and IGF2 action. When cumulus cells were treated with FSH or IGF2, an increase in AKT and ERK phosphorylation was observed (Figure 19A). However, the results suggest that FSH stimulates ERK1/2 more strongly than IGF2; whereas IGF2 stimulates AKT more strongly than FSH. More importantly, the combination of FSH and IGF2 further stimulated the phosphorylation of both AKT and ERK above the level of either factor alone (Figure 19B). As the main effect of IGF2 is the stimulation of AKT, we next examined its contribution to cell proliferation. For this purpose, cumulus cells were treated with AEW, an inhibitor of IGF1R activity that inhibits AKT phosphorylation but has no effect on ERK signaling (32). When cumulus cells were treated with AEW, the stimulation of granulosa cell proliferation by the combination of IGF2 and FSH was abolished in all patients (Figure 16, right). This demonstrates that IGF1R activity is critical for granulosa cell proliferation.

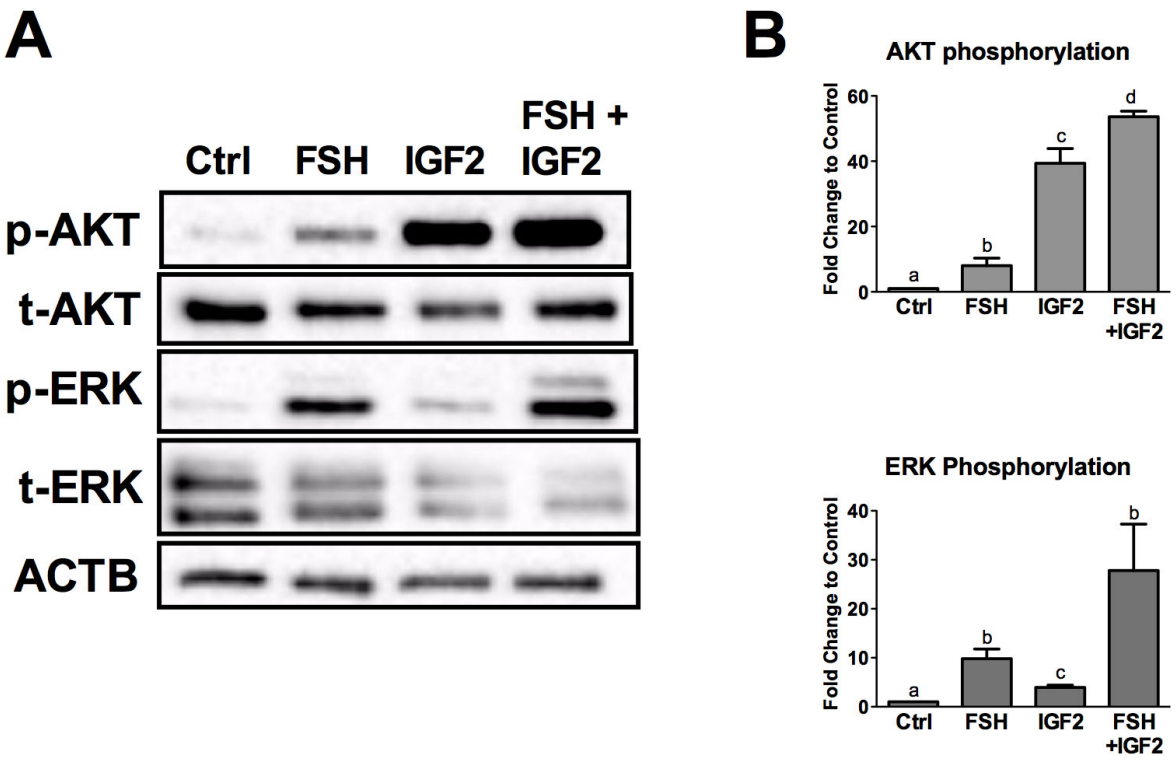

Figure 19: *FSH and IGF2 enhance AKT and ERK phosphorylation in cultured cumulus granulosa cells.*

(**A**) Cumulus cells from three patients were cultured in serum-free and phenol red-free media for 24h and treated with FSH (50 ng/ml), IGF2 (50 ng/ml), or their combination for 1h. Total protein was isolated from the cells and phosphorylated and total AKT and ERK was assessed by Western blot.
(**B**) Band intensities were quantified and normalized to ACTB (loading control), and the ratio of phosphorylated to total AKT and ERK is reported. Different letters denote groups that are significantly different from each other, $p<0.05$; one way-ANOVA.

C. Discussion

Herein, we contribute to the understanding of the interplay between FSH and IGF2 during the process of human granulosa cell differentiation. We demonstrate that IGF2 synergizes with FSH to stimulate human granulosa cell proliferation and enhances FSH-induced *CYP19A1* expression in a dose dependent manner. These findings agree with early evidence showing that IGF2 has a significant role in human ovarian follicle maturation and follicle selection (117). A high level of IGF2 in the follicular fluid of women undergoing IVF correlates with good prognosis for oocyte maturation and early embryo development (129). Interestingly, when IGF2 action is blunted by the addition of IGFBP4, FSH no longer fully stimulates *CYP19A1* expression in human granulosa cells. This suggests that the action of IGF2, produced locally by the granulosa cells, is necessary for FSH to stimulate *CYP19A1* expression.

We wanted to examine mechanisms by which FSH and IGF2 synergize to enhance granulosa cell proliferation; however, FSH-induced signaling pathway activation in human granulosa cells had not been established. We demonstrated that FSH significantly stimulates the phosphorylation of ERK, AKT, and JNK in human granulosa cells. FSH is known to stimulate CREB phosphorylation downstream of PKA activation in rodent granulosa cells (48); however, a significant increase in CREB phosphorylation was not detected in human granulosa cells following FSH treatment. This suggests that aspects of FSH-induced granulosa cell differentiation may be mediated by different mechanisms in rodents and humans.

To explore how FSH and IGF2 may be cooperating to regulate granulosa cell differentiation and proliferation, we examined ERK and AKT signaling pathway

activation by both factors. Both AKT and ERK activation enhances cell proliferation, and FSH and IGF2 each activate both pathways. We found that FSH enhanced the high level of AKT phosphorylation following IGF2 treatment, and that IGF2 enhanced the high level of ERK phosphorylation following FSH treatment. AEW, which only inhibits AKT activation, eliminated the synergism of FSH and IGF2 on granulosa cell proliferation. Thus, the IGF2-induced AKT activation through the IGF1R is necessary for FSH to enhance granulosa cell proliferation, which is critical in the process of ovarian follicle maturation.

VI. IGF1R SIGNALING IS NECESSARY FOR FSH-INDUCED ACTIVATION OF AKT AND DIFFERENTIATION OF HUMAN CUMULUS GRANULOSA CELLS

A. Introduction

Because human granulosa cells express IGF2, and this expression is enhanced in the presence of FSH, it is difficult to observe the role of FSH—independent of any IGF action—in granulosa cell differentiation. We recently demonstrated that FSH fails to stimulate *Cyp19a1* and *Cyp11a1* expression and 17β-estradiol production when the activity of the type I IGF receptor (IGF1R) is inhibited in rat granulosa cells (32). Here, we explore the relationship between FSH and IGF signaling during human granulosa cell differentiation using primary cumulus cell cultures. Our results suggest that IGF1R signaling is necessary for FSH-induced activation of AKT, a kinase shown to be essential for rat granulosa cell differentiation (52), and the subsequent differentiation of human granulosa cells to the mural/preovulatory stage.

B. Results

1. IGF1R activity is necessary for FSH-induced expression of steroidogenic genes in cumulus cells

As FSH strongly stimulates IGF2 expression in human cumulus cells, we investigated whether the activation of IGF1R by endogenous IGF2 plays a role in the regulation of differentiation genes by FSH. For this purpose, cells were stimulated with FSH in the presence or absence of AEW, a highly specific inhibitor of IGF1R activity (135). We found that the FSH-induced up regulation of *CYP19A1, CYP11A1,* and *STAR* mRNA levels was inhibited by co-treatment with AEW (Figure 20A). Further experiments demonstrated that AEW inhibits FSH-induced *CYP19A1* expression in a

dose-dependent (0.05-2 μM) manner (Figure 20B). In agreement with our findings at the level of mRNA expression, the stimulation of CYP19A1, CYP11A1, and StAR protein expression by FSH was significantly decreased by co-treatment with AEW (Figure 20C). Finally, inhibition of the IGF1R prevented the increase of 17β-estradiol production induced by FSH (Figure 20D). These findings suggest that IGF1R activity is required for the induction of well-known markers of granulosa cell differentiation and for the stimulation of 17β-estradiol synthesis by FSH in human cumulus granulosa cells.

2. FSH-induced AKT phosphorylation requires IGF1R activity

To investigate the mechanisms by which IGF1R may regulate FSH-induced granulosa cell differentiation, we first examined if FSH enhances the phosphorylation of the IGF1R itself. In good agreement with our previous report in rat granulosa cells (32), we found that FSH does not phosphorylate the IGF1R (Figure 21A), suggesting that the interaction between FSH and IGF1R signaling occurs downstream of this receptor. Therefore, we examined the effect of either FSH or AEW alone or combined on the activation of AKT, a well-known downstream target of IGF1R and an essential component of FSH-mediated rat granulosa cell differentiation (32, 52). Phospho-AKT (Ser473) was low in untreated cumulus cells but increased significantly after treatment with FSH for 1h (Figure 21B). Remarkably, inhibition of IGF1R activity by AEW not only prevented AKT activation by FSH but also reduced AKT phosphorylation to undetectable levels in cells treated with AEW alone. In marked contrast, lack of IGF1R activity had no effect on the phosphorylation of ERK1/2 by FSH (Figure 21B). These findings suggest that basal IGF1R and AKT activation are likely maintained by locally

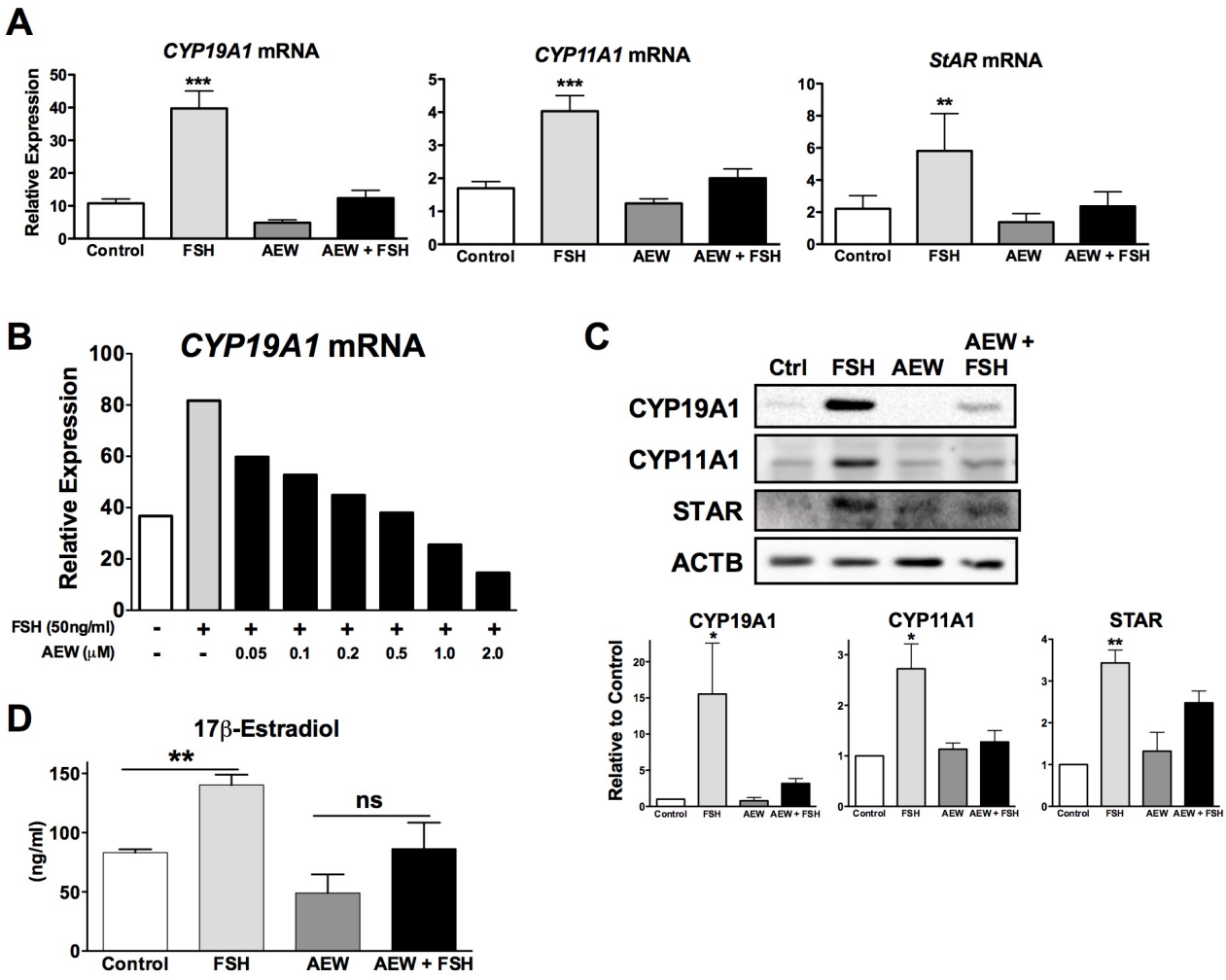

Figure 20: *FSH action in cumulus granulosa cells requires IGF1R activity*.

Cumulus cells were cultured in serum-free and phenol red-free media for 24h, then pre-treated with AEW (0.5μM) or vehicle (DMSO) for 1h before the addition of FSH (50ng/ml) for 48h.
(**A**) RNA and (**C**) total protein were isolated and the mRNA and protein levels of CYP19A1, CYP11A1, and StAR were measured by qPCR and Western blot. For mRNA quantification, columns represent the mean ± SEM for 5 independent experiments. For protein quantification, columns represent the mean ± SEM for 3 independent experiments.
(**B**) Cells were pre-treated with increasing doses of AEW (0.05-2.0μM) for 1h prior to treatment with FSH (50ng/ml) for 48h. RNA was isolated, and the expression of *CYP19A1* was assessed by qPCR. Results shown are for one representative patient.
(**D**) 17β-Estradiol levels were measured in media collected from cultures of cumulus cells by ELISA. Columns represent the mean ± SEM for 3 independent experiments.
(*p<0.05; **p<0.01; ***p<0.001; ns= not significant; one-way ANOVA)

produced IGF2 and that IGF1R activity is required for FSH-induced AKT phosphorylation.

Next, we compared the effect of AEW, the IGF1R inhibitor, with that of an AKT specific inhibitor, MK2206. As shown in Figure 22A, inhibition of either IGF1R or AKT activity prevented the stimulatory effect of FSH on *CYP19A1* mRNA accumulation as well as CYP19A1 activity, as indicated by the significantly suppressed production of 17β-estradiol in the presence of IGF1R and AKT inhibitors (Figure 22B). This finding suggests that AKT activation is required for the stimulation of granulosa cell differentiation by FSH in humans. To test this possibility, we overexpressed an active form of AKT to investigate whether it could overcome the inhibitory effect of AEW on FSH-induced *CYP19A1* expression. For this purpose, cumulus cells were infected with increasing concentrations of lentivirus carrying a construct encoding human constitutively active AKT (CA-AKT) (32). As shown in Figure 22C, in the presence of AEW, CA-AKT rescued the stimulatory effect of FSH on *CYP19A1* expression in a dose dependent manner.

The response to CA-AKT varied among patients such that in Patient A CA-AKT restored *CYP19A1* expression to the levels observed following FSH treatment alone, whereas in Patient B FSH plus CA-AKT increased *CYP19A1* expression to levels significantly higher than those stimulated by FSH alone. Despite these individual differences, CA-AKT was able to overcome the inhibitory effect of AEW in experiments conducted using cells from different patients (Figure 22C). Moreover, overexpression of CA-AKT also rescued 17β-estradiol production in the presence of AEW (Figure 22D).

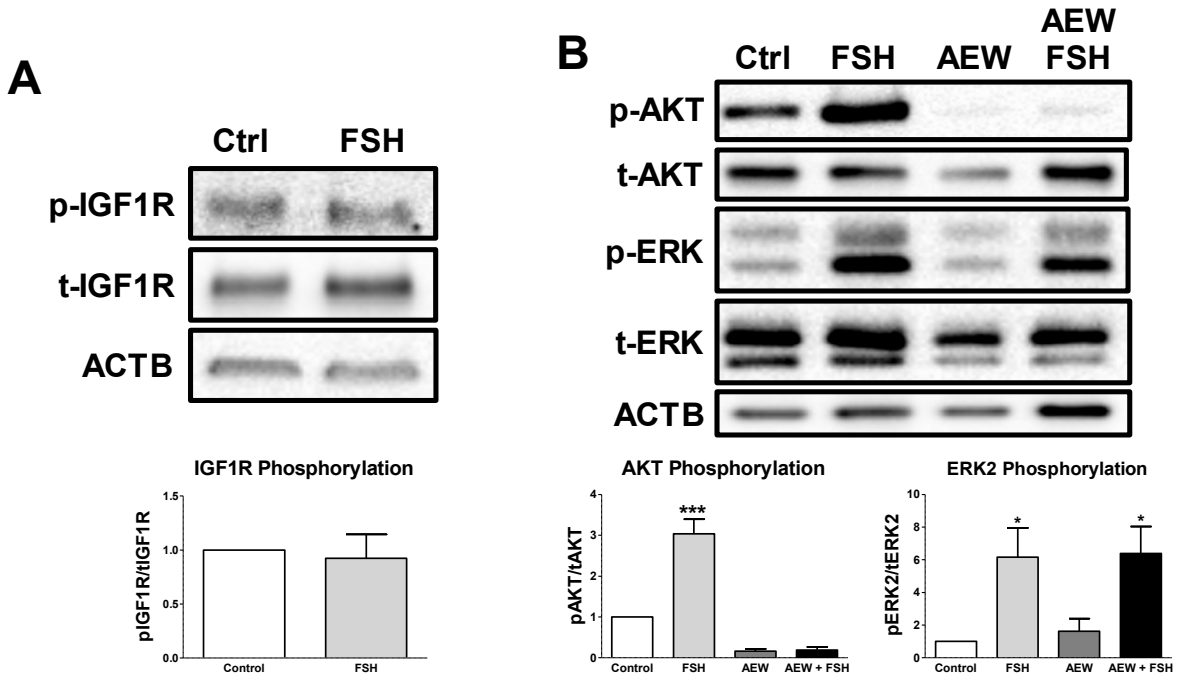

Figure 21: *FSH-induced AKT phosphorylation requires IGF1R activity*.

(**A**) Cumulus cells were cultured in serum-free media for 24h and then treated with FSH (50ng/ml) for 1h. Total protein was isolated from these cells, and phosphorylated and total IGF1R were detected by Western blot. Protein levels were normalized to β-actin (ACTB) and the ratio of phosphorylated to total IGF1R is reported. Columns represent the mean ± SEM for 3 independent experiments.

(**B**) Cumulus cells were cultured in serum-free media for 24h and pre-treated with AEW (0.5μM) or vehicle (DMSO) for 1h before the addition of FSH (50mg/ml) for 1h. Phosphorylated and total AKT and ERK were assessed by Western Blot of whole cell lysates. Protein levels were normalized to β-actin (ACTB) and the ratio of phosphorylated to total AKT and ERK are reported. Columns represent the mean ± SEM for 3 independent experiments. (*$p<0.05$; ***$p<0.001$; one-way ANOVA)

This effect of CA-AKT on 17β-estradiol production followed a similar pattern between patients to that observed for *CYP19A1* expression.

C. Discussion

We used cumulus cells to gain an understanding of the relationship between FSH and IGF action in the process of granulosa cell differentiation. Previous studies demonstrated that IGFs can synergize with FSH to stimulate CYP19A1 activity (93) and progesterone production (94) in humans; however mechanisms underlying this synergistic relationship were not explored. Here, we report that IGF1R activity is required for FSH-induced granulosa cell differentiation. In the presence of AEW, an inhibitor of IGF1R activity, FSH is unable to stimulate the expression of steroidogenic genes and 17β-estradiol production, which are essential for proper function of preovulatory mural granulosa cells. Our results provide a possible mechanism to explain the inhibitory effect of insulin-growth factor binding proteins or anti-IGF1R antibodies in FSH-induced steroidogenesis in humans (63, 117); however, the mechanisms involved in the integration of IGF1R and FSHR signaling are not known.

In this regard, our findings provide evidence suggesting that FSHR and IGF1R signaling synergistically activate AKT and that this cooperation is essential for human granulosa cell differentiation. Previous reports in rodents demonstrated that FSH also stimulates AKT (124) and that the activity of this kinase is essential for the induction of 3β-HSD and LHR by FSH (52, 136, 137). Here, we demonstrate that AKT activity is necessary for FSH-induced *CYP19A1* expression in humans, suggesting that AKT is a pivotal factor underlying the cooperation of FSH and the IGF system in human granulosa cell differentiation as well.

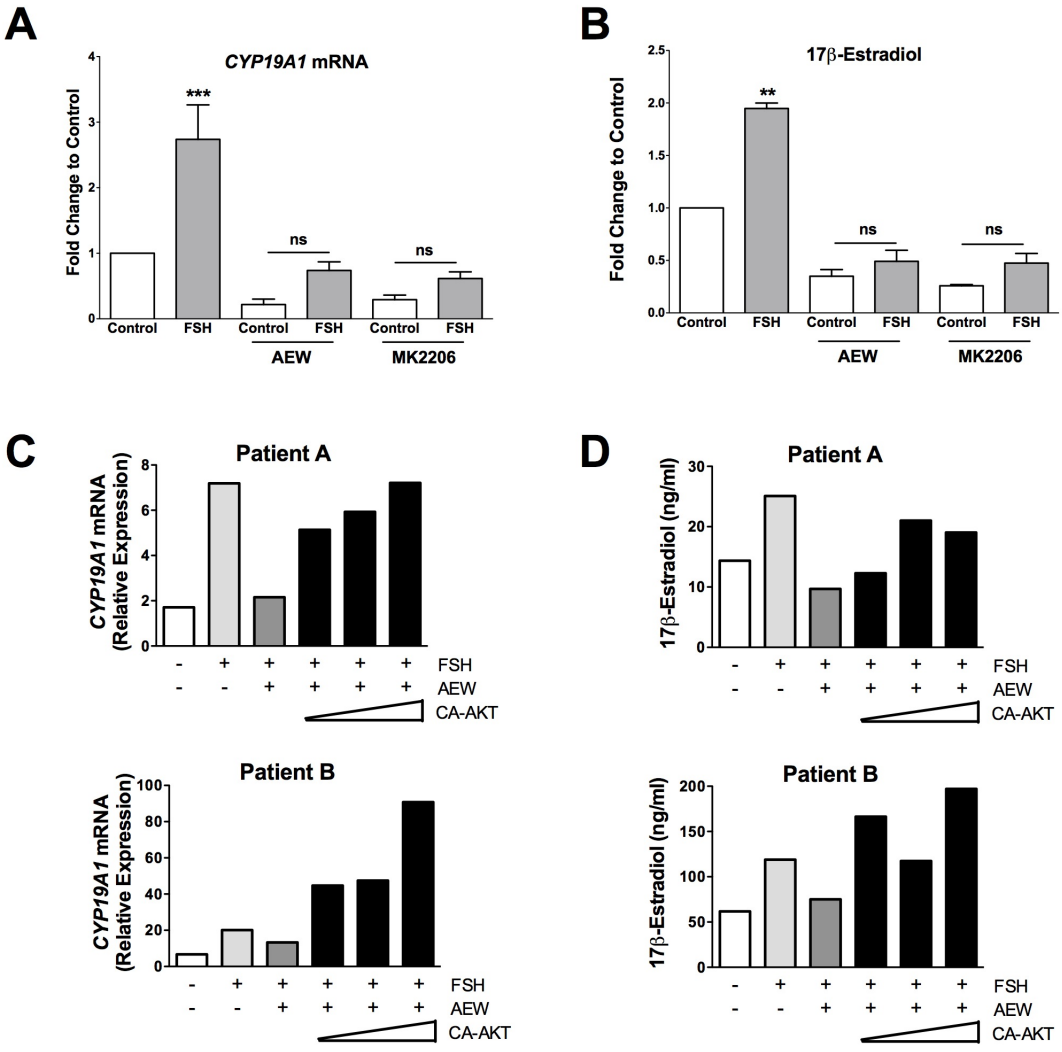

Figure 22: *AKT activation is critical for FSH-induced aromatase expression and activity.*

(**A**) Cumulus granulosa cells were cultured in serum-free media for 24h, then pre-treated with AEW (0.5μM), MK2206 (1μM) or vehicle (DMSO) for 1h followed by treatment with FSH (50ng/ml) for 48h. RNA was isolated from the cells, and the expression of *CYP19A1* was measured by qPCR. Columns represent the mean ± SEM for 5 independent experiments. (***p<0.001; ns= not significant; one-way ANOVA)

(**B**) 17β-estradiol was measured in media collected from treated cells, and columns represent the mean ± SEM for 3 patients. (**p<0.01; ns= not significant; one-way ANOVA)

(**C**) Cumulus granulosa cells were cultured in serum-free media for 24h, and then pre-treated with AEW (0.5μM) for 1h before addition of FSH (50ng/ml) for 48h in the presence of lentivirus expressing GFP or constitutively active AKT (CA-AKT). The expression of *CYP19A1* as well as the production of 17β-estradiol (**D**) is reported for 2 patients.

We demonstrate that FSH increases AKT phosphorylation in cultured cumulus granulosa cells, but the mechanisms by which FSH stimulates AKT are unclear. We observe AKT phosphorylation in untreated cumulus cells, which is eliminated by incubation with an IGF1R inhibitor, suggesting that endogenous IGF2 acts in an autocrine manner to stimulate the IGF1R and AKT. Strikingly, FSH is unable to stimulate AKT in the presence of the IGF1R inhibitor. This suggests that FSH does not phosphorylate AKT directly; rather it enhances IGF1R-mediated AKT activation in human granulosa cells. Studies in rodents suggest that FSH could enhance AKT activation by down regulating phosphatases that increase IGF1R phosphorylation and activity (118). Additionally, FSH could stimulate AKT phosphorylation by activating IRS-1 through a PKA-dependent mechanism (53). Further studies are warranted to determine the molecular crosstalk between FSH and IGF1R signaling that leads to AKT phosphorylation in both rodent and human granulosa cells.

These observations have critical implications for granulosa cell differentiation and represent a shift in the current understanding of how FSH promotes human follicle development. We have provided evidence demonstrating that the IGF system does not merely enhance FSH actions but that it is essential for FSH-induced granulosa cell differentiation. The activation of AKT by IGF2 through the IGF1R may prime granulosa cells to adequately respond to FSH resulting in granulosa cell differentiation and follicle development. We propose that FSH amplifies IGF1R signaling and/or removes inhibitory influences present in unstimulated cells. This hypothesis implies that only those follicles exposed to increasing levels of FSH can benefit from locally produced IGF2 and only follicles with high endogenous IGF2's production are able to fully respond to FSH. Thus,

the interaction between the endocrine effects of FSH and the autocrine actions of IGF2 might play an essential role in the establishment of selection and follicle dominance in humans.

VII. FSH REGULATES IGF2 EXPRESSION IN HUMAN GRANULOSA CELLS IN AN AKT-DEPENDENT MANNER

A. Introduction

Our findings have evidenced an interdependent relationship where FSH stimulates *IGF2* expression, and IGF2 is required and synergizes with FSH to stimulate human granulosa cell proliferation and differentiation. Therefore, it is critical to understand how FSH regulates *IGF2* expression in human granulosa cells. The aim of this study was to examine the mechanisms involved in the regulation of the *IGF2* gene by FSH in human granulosa cells. To explore this aim, we used an *in vitro* model of primary cultures of human cumulus granulosa cells, described previously in Chapter III. Our previous findings demonstrate that IGF2 and FSH synergize to promote the proliferation and differentiation of human granulosa cells and, furthermore, that IGF2 is required for FSH to stimulate granulosa cell differentiation. Here, we show that FSH exclusively activates promoter-3 driven expression of the *IGF2* gene, and demonstrate that AKT activity stimulated by endogenous IGF2 is critical for the FSH-induced *IGF2* expression in human granulosa cells.

B. Results

1. FSH stimulates IGF2 expression in human cumulus cells

To examine the mechanisms involved in the regulation of *IGF2* gene expression in human granulosa cells, we first explored the time and concentration dependent effects of FSH. Using 50 ng/ml of FSH, a concentration that maximally stimulates *CYP19A1* in human granulosa cells (125), we quantified *IGF2* mRNA transcript abundance from 2h to 72h after initiation of treatment (Figure 23A). After two and four

hours of treatment, a non-statistically significant increase in the relative amount of *IGF2* mRNA was observed. At 8h, FSH had significantly increased *IGF2* transcript levels to nearly 3-fold when compared to non-treated cells. *IGF2* mRNA abundance reached a maximum of 4-fold stimulation with respect to non-treated cells at 24h and remained at this level at 48 and 72h. Based on this result, dose-response experiments were conducted using 48h treatment. The average *IGF2* transcript abundance was increased more than 2.5-fold at all FSH concentrations, even at 1 ng/ml, the lowest concentration tested (Figure 23B). However, due to wide confidence intervals related to patient-to-patient variability, statistical significance was only reached at 1 and 50 ng/ml concentrations of FSH ($p<0.01$ vs. 0 ng/ml one-way ANOVA).

2. FSH regulates IGF2 expression via activation of the P3 promoter

IGF2 gene transcription is driven by four different promoters (60) (Figure 24A). Activity of each promoter generates *IGF2* mRNA with promoter-specific untranslated exons upstream of the protein-coding exons 7 to 9 that are common to all transcripts. To determine the activation status of *IGF2* alternative promoters in human granulosa cells, exon analysis of RNAs was performed using 5'-UTR-specific forward primers and reverse primers located in exon 7 or 8 (Figure 24A). The results demonstrated that P1-driven *IGF2* transcripts were absent in human cumulus cells and P2-driven transcripts were barely detectable after 40 cycles, even in human liver cDNA. This is consistent with previous reports of low P2-driven IGF2 expression in liver (61, 138). In contrast, P3 and P4-driven *IGF2* transcripts were abundant (Figure 24B).

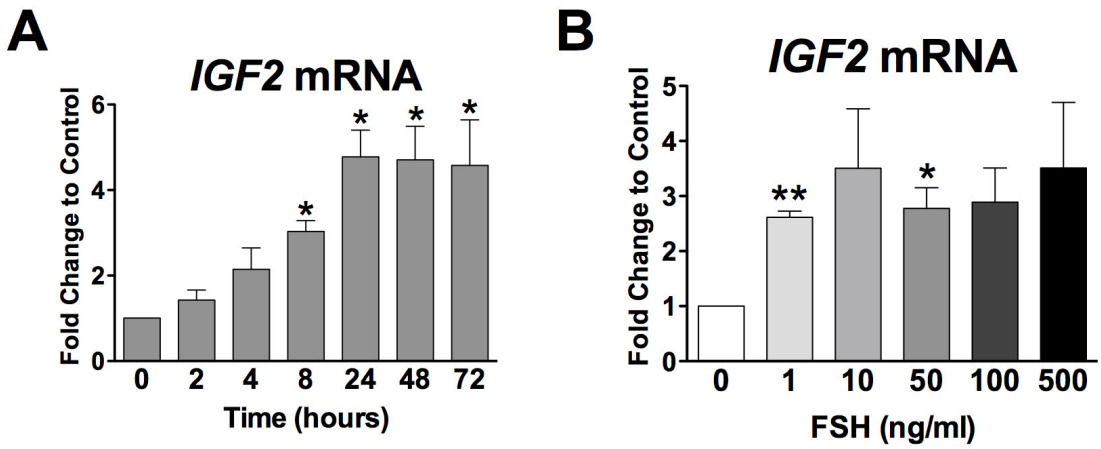

Figure 23: *FSH up-regulates* IGF2 *expression.*

Cumulus cells were cultured in serum-free and phenol red-free media for 24h, followed by treatment with (**A**) FSH (50 ng/ml) for increasing amounts of time (2h to 72h) or (**B**) increasing doses of FSH (1-500 ng/ml) for 48h. RNA was isolated and reverse transcribed and *IGF2* transcript abundance was quantified by qPCR. For A and B, columns represent the mean ± SEM for three independent experiments, **p*<0.05, ***p*<0.01 relative to control (one-way ANOVA).

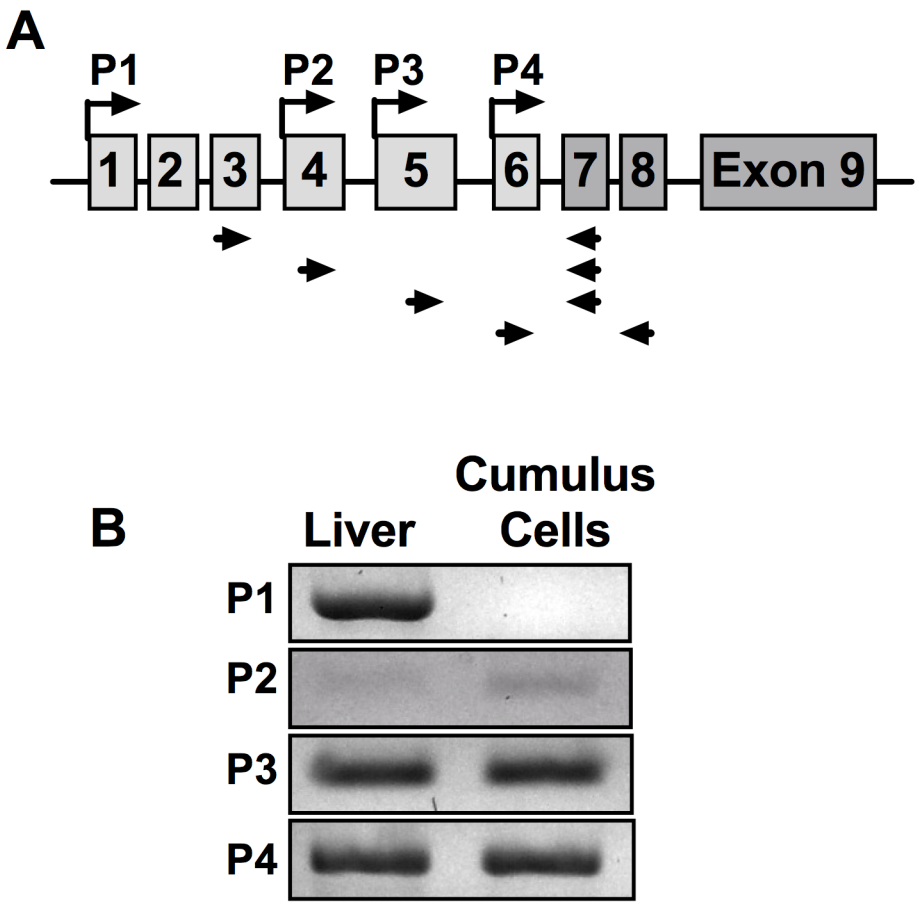

Figure 24: *Cumulus cells express P3 and P4 promoter-specific* IGF2 *transcripts.*

(**A**) Scheme of *IGF2* gene region indicating the promoter that drives the expression of specific exons. Arrows represent locations of primer pairs designed to detect promoter-specific *IGF2* transcripts.
(**B**) RNA was isolated from cumulus cells after culture in serum-free and phenol red-free media for 24h. Cumulus cell RNA and RNA from human liver was reverse transcribed and PCR with promoter-specific primers (indicated in A) was used to detect promoter-specific (P1-P4) *IGF2* transcripts. PCR products were visualized on an agarose gel.

To determine if the P3 or the P4 promoter was regulated by FSH, the mRNA abundance of the promoter-specific transcripts was quantified in cells treated with FSH (50 ng/ml) for up to 72h (Figure 25). Over this period, P3 specific transcript levels increased in a manner that resembles the changes observed for the *IGF2* coding region described in Figure 23. In contrast, P4-driven *IGF2* transcripts did not increase significantly over time. When cumulus cells were treated with increasing concentrations of FSH for 48h, P3-driven *IGF2* mRNA transcripts significantly increased in a concentration dependent manner whereas P4-specific *IGF2* mRNA abundance was not affected by any of the concentrations of FSH used. Taken together, these results suggest that the P3 and P4 promoters of the *IGF2* gene are active in human granulosa cells and, of these promoters, only P3 is activated by FSH.

3. FSH regulation of IGF2 expression is AKT-dependent

In cultured human cumulus cells, FSH activates both the AKT and ERK pathways (Figure 18). To investigate if FSH regulates *IGF2* expression in an AKT or ERK dependent manner, we treated cells with MK2206, an inhibitor of AKT, and U0126, an inhibitor of ERK activation, and measured the effect of FSH treatment on *IGF2* mRNA. In the presence of MK2206, FSH was no longer able to increase *IGF2* mRNA transcript abundance (Figure 26). In contrast, inhibition of ERK activation did not alter the ability of FSH to simulate *IGF2*, suggesting that FSH-induced *IGF2* expression depends on AKT, but not on ERK. Moreover, in the absence of FSH, MK2206 treatment significantly decreased *IGF2* transcript levels when compared with vehicle-treated cells. These results suggest that AKT activity is crucial for both basal and FSH-stimulated *IGF2* expression in human granulosa cells.

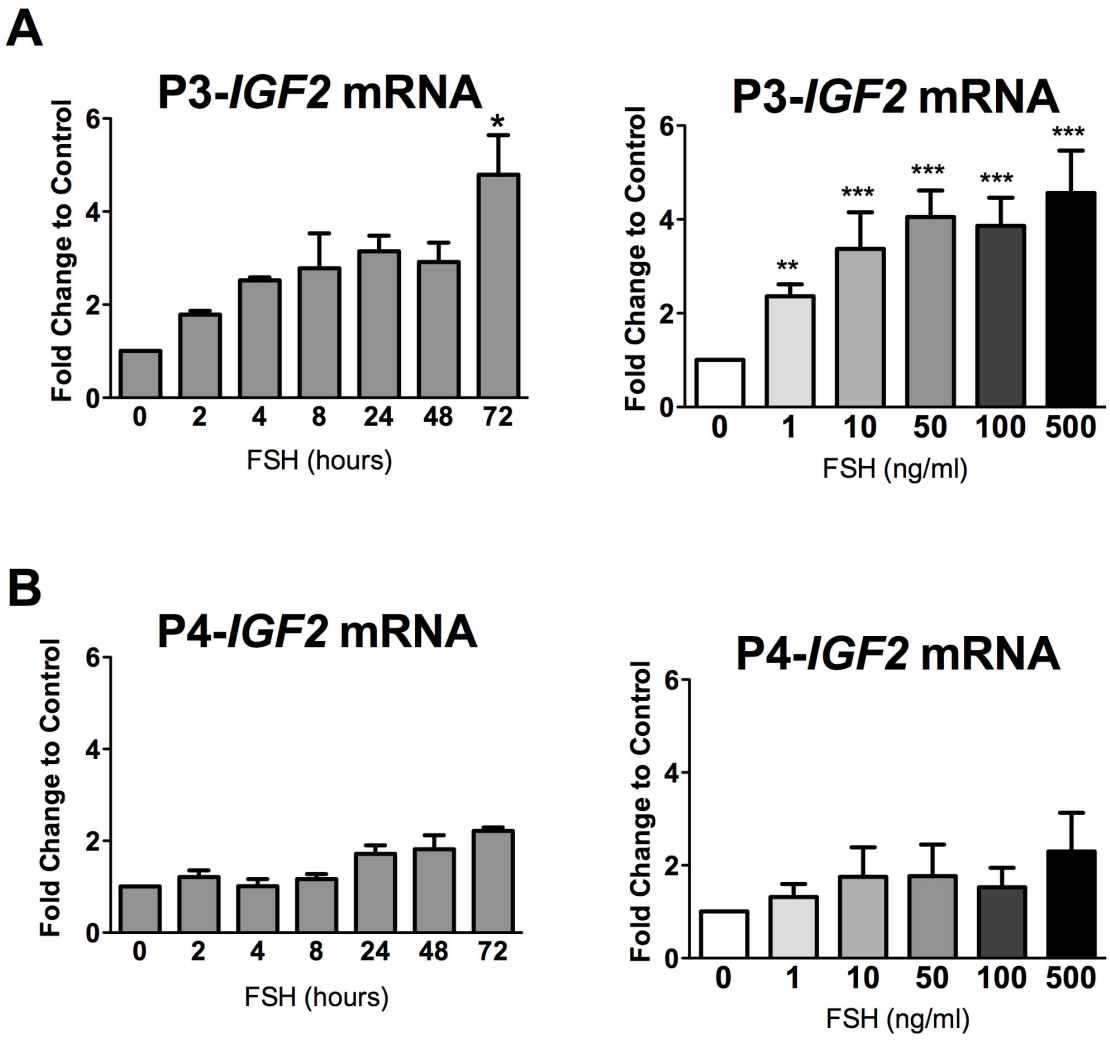

Figure 25: *FSH-induced up-regulation of IGF2 expression is driven by the P3 promoter.*

Expression of (**A**) P3 and (**B**) P4-promoter specific *IGF2* transcripts was measured in cumulus cells treated with increasing doses of FSH (1-500 ng/ml) for 48h or FSH (50 ng/ml) for increasing amounts of time (2h to 72h). Columns represent the mean ± SEM for 3 independent experiments (*p<0.05, **p<0.01, ***p<0.001 relative to control; one-way ANOVA).

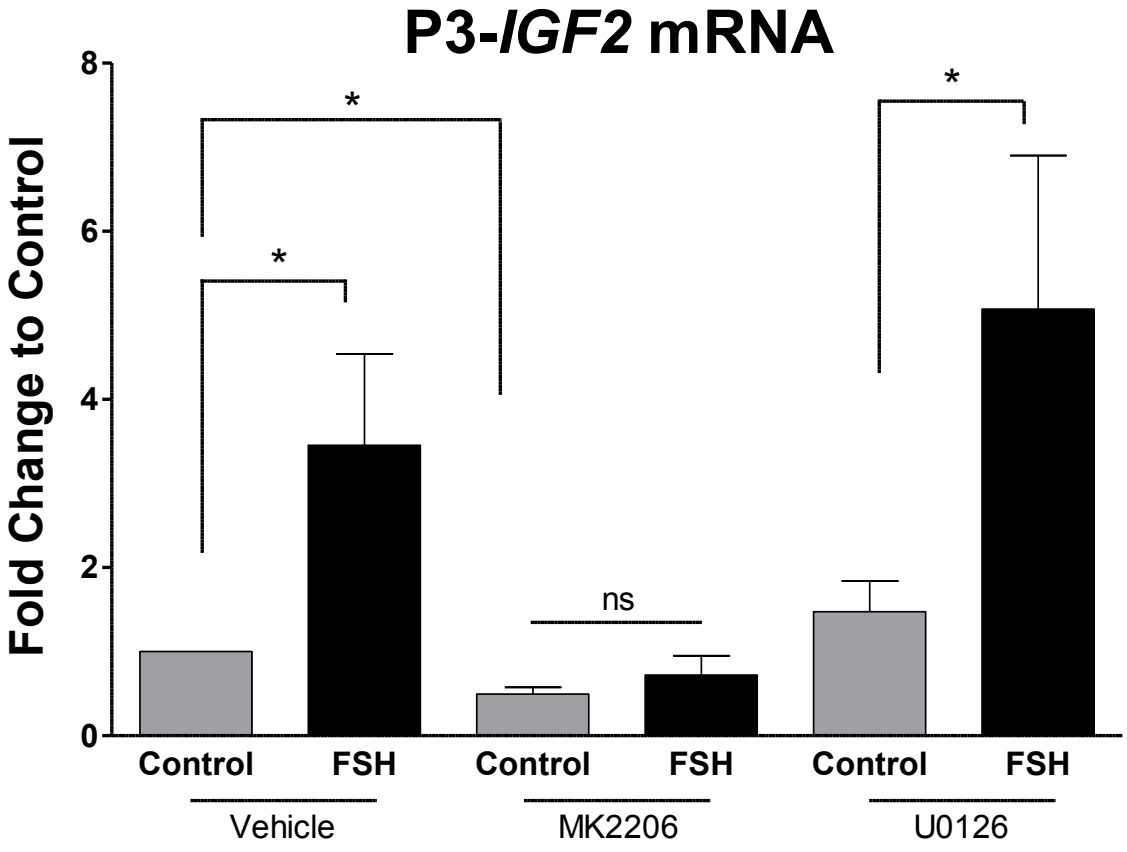

Figure 26: *FSH regulates P3 promoter-driven* IGF2 *expression in an AKT-dependent manner*.

Cumulus granulosa cells were cultured in serum-free and phenol red-free media for 24h, followed by treatment with MK2206 (1μM), U0126 (5μM), or vehicle (DMSO) for 1h. Cells were then treated with FSH (50 ng/ml) for 48h and RNA was isolated and reverse transcribed. P3 promoter-driven *IGF2* mRNA expression was measured by qPCR. Columns represent the mean ± SEM for at least 3 independent experiments (*p<0.05; t-test).

4. Endogenous IGF2 is essential for basal and FSH-stimulated IGF2 expression

Because IGF2 activates the IGF1R, which results in downstream AKT activation, we examined whether endogenous IGF2 contributes to *IGF2* expression by incubating cells with IGFBP4. Treatment of granulosa cells with IGFBP4 alone reduced promoter P3-driven *IGF2* transcripts by 50% (Figure 27A). This decrease was statistically significant when control and IGBP4 groups were compared using *t* test ($p<0.01$). In addition, co-treatment with IGFBP4 caused a 60% decrease in FSH-induced stimulation of *IGF2* mRNA accumulation, suggesting a positive auto-regulation of IGF2 in human granulosa cells.

To further support this idea, we examined whether IGF1R activity is required for basal and FSH-induced *IGF2* expression. For this purpose, cells were treated with AEW, a specific inhibitor of IGF1R activity (135, 139). As observed for IGFBP4 treatment, in the presence of the IGF1R inhibitor, basal *IGF2* mRNA transcript abundance was reduced nearly 50% and FSH was unable to increase *IGF2* transcript levels (Figure 27B). These data suggest that activation of the IGF1R by IGF2 is required for both basal and FSH-stimulated *IGF2* expression in human granulosa cells.

Inhibition of AKT activity prevented the stimulation of *IGF2* expression by FSH (Figure 26) and because previous reports demonstrated that AKT is downstream of the IGF1R in granulosa cells (32, 125), we next explored whether AKT mediates IGF2 auto stimulation. For this purpose, cells were treated with AEW, to eliminate basal AKT activation (125) and infected with lentivirus carrying expression constructs for GFP or constitutively active AKT (CA-AKT). In the presence of AEW and CA-AKT, FSH

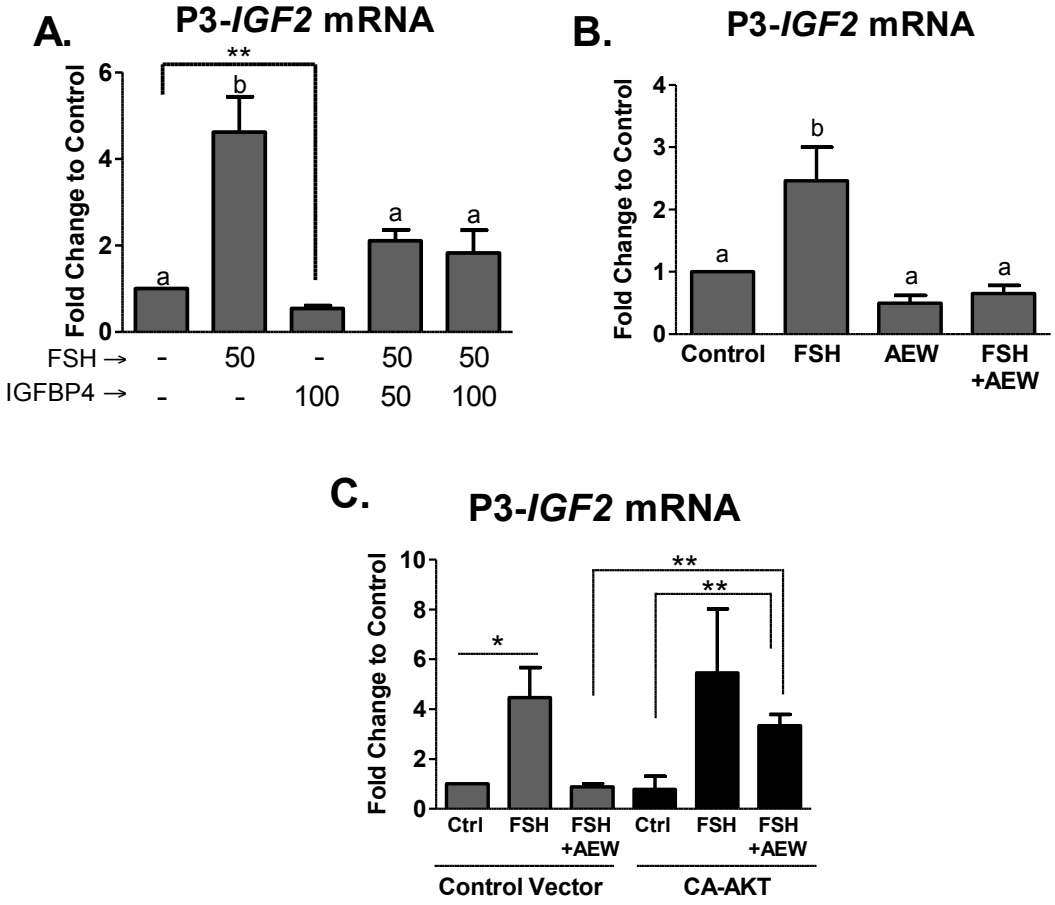

Figure 27: *Activation of the IGF1R is required for P3 promoter-driven* IGF2 *expression.*

Cumulus cells were cultured for 24h in serum-free and phenol red free media.
(**A**) Cumulus cells were treated with FSH (50 ng/ml), IGFBP4 (50-100 ng/ml), or both for 48h.
(**B**) Cumulus cells were treated with AEW (0.5 μM) or vehicle (DMSO) for 1h followed by treatment with FSH (50 ng/ml) for 48h.
(**C**) Cumulus cells were infected with a lentivirus expressing constitutively active AKT (CA-AKT) or an empty virus (control vector). These cells were then treated with AEW (0.5 μM) or vehicle (DMSO) for 1h followed by treatment with FSH (50 ng/ml) for 48h. RNA was isolated from cumulus cells at the end of each experiment and reverse transcribed. P3 promoter-driven *IGF2* mRNA expression was measured by qPCR.

Columns represent the mean ± SEM for at least 4 independent experiments in A and B and 3 independent experiments in C. Different letters denote significant difference of at least $p<0.05$ (one-way ANOVA) between treatment groups. In A, control and IGFBP4-treated groups are significantly different when compared using a *t*-test (**P<0.01). In C, indicated treatments are significantly different from each other (*p<0.05, **p<0.01) by one-way ANOVA.

treatment overcame the inhibitory effect of AEW and was able to stimulate *IGF2* mRNA transcript accumulation to the levels observed in cells treated with FSH alone (Figure 27C). These results suggest that AKT acts downstream of the IGF1R in the stimulation of *IGF2* expression. In addition, this finding demonstrates that in human granulosa cells, AKT activity is sufficient for FSH to stimulate *IGF2* expression.

C. Discussion

Here, we provide the first evidence of the mechanisms of IGF2 regulation in human granulosa cells. We demonstrate that FSH enhances *IGF2* expression in human granulosa cells by stimulating P3 promoter-driven *IGF2* transcription in an AKT-dependent manner. Furthermore, basal activation of AKT, possibly by endogenous IGF2, is necessary for FSH to stimulate *IGF2* expression in human granulosa cells. We carried out these studies in cultured human cumulus cells which, as demonstrated in Chapter III, share characteristics with undifferentiated, preantral granulosa cells and respond to FSH treatment within 24h of culture. Therefore, we believe our findings are indicative of FSH and IGF2 actions during the process of human granulosa cell differentiation and follicle maturation in the ovary.

Because IGF2 is critical during follicle maturation and in particular for FSH-induced granulosa cell proliferation and differentiation, we explored the mechanisms by which IGF2 expression is regulated in human cells. In the liver, growth hormone regulates *IGF2* expression, but this is not the case in granulosa cells (61, 140, 141). This suggests that mechanisms of *IGF2* expression are cell type-specific and a closer inspection of these mechanisms specifically in human granulosa cells is necessary to understand IGF2 regulation during follicle development. Here, we demonstrate that the

P3 promoter drives FSH stimulated *IGF2* expression. This promoter-specific increase in *IGF2* expression is dependent on FSH-stimulated AKT activation. These findings, together with our previous report that FSH-induced *CYP19A1* expression requires AKT activation by FSH (125), adds to the increasing evidence that FSH-induced AKT activation is crucial for human granulosa cell differentiation; however, the molecular mechanisms involved in FSH stimulation of AKT and *IGF2* P3-promoter activity are unknown and further research is warranted.

VIII. ANIMALS WITH REDUCED IGF1R IN GRANULOSA CELLS ARE SUBFERTILE

A. Introduction

It is well established that insulin-like growth factors (IGFs) play a critical role in ovarian granulosa cell function in both humans and rodents; however, the effect of the IGF system on female fertility is unclear. Rodent studies can offer insight into the role of IGFs in the ovary as well as fertility. In mice and rats, IGF1 is the predominant IGF in the ovary. In healthy antral follicles, IGF1 is present at both the mRNA and protein level in granulosa cells of healthy antral follicles, and is absent in granulosa cells of preantral or atretic follicles (76-78). IGF1 produced by the granulosa cells can act in an autocrine/paracrine manner to stimulate granulosa cell function (73).

IGF1 has been shown to stimulate granulosa cell proliferation and enhance granulosa cell survival by inhibiting apoptosis (142, 143). While IGF1 alone has no effect on the expression of steroidogenic genes, it can synergize with FSH to stimulate steroidogenic gene expression and steroid hormone production (32). Moreover, we recently demonstrated that the IGF1R activity is required for FSH to stimulate steroidogenic gene expression in both rodent and human granulosa cells (32). These findings suggest that the critical role of IGFs on granulosa cell function seems to be mediated by a close cross-talk interaction with FSH signaling.

In addition to *in vitro* evidence that IGF1 is critical for granulosa cell function, *in vivo* studies have evidenced a role of IGF1 in follicle maturation in the ovary. *Igf1* null mice are infertile with impaired follicle maturation (86), suggesting that IGF1 is necessary for the formation of preovulatory follicles. However, IGF1 knockout animals show a number of additional phenotypes that could confound these findings. For

example, IGF1 knockout mice show growth deficiency, females have infantile uteri and do not appear to undergo puberty (86), and, depending on the genetic background, a variable portion die soon after birth (144). Additionally, IGF1 acts at several levels in the hypothalamic-pituitary-gonadal axis and is known to regulate the secretion of gonadotropin releasing hormone (GnRH) and luteinizing hormone (LH) from the hypothalamus and pituitary gland, respectively (87, 88). Taken together, these findings suggest that the infertile phenotype of animals lacking IGF1 could be a result of defects in the secretion of pituitary hormones.

The aim of this study was to determine the role of IGF1 in ovarian follicle maturation during the transition from the preantral to the preovulatory stage. To accomplish this, mice with granulosa cell specific knockout of the *Igf1r* were generated. In these conditional knockout mice, IGF1R and IGF1 expression remain unchanged in other tissues, thereby eliminating confounding phenotypes that may otherwise affect their reproductive capacity. We hypothesized that mice lacking IGF1R in granulosa cells during the transition from the preantral to the preovulatory stage would have deficiencies in follicle maturation and function that ultimately affect the fertility of female mice.

B. Results

1. Knockdown of IGF1R in ovarian granulosa cells:

To target knockdown of *Igf1r* in ovarian granulosa cells, a cre-lox system was used. Mice carrying the exon 3 of the *Igf1r* flanked by lox-p sites (referred to as IGF1R floxed mice) were used. Exon 3 of the *Igf1r* contains the ligand binding domain of the receptor. The *Igf1r* floxed mice were bred with mice expressing cre-recombinase driven

by the *Cyp19a1* (aromatase) proximal promoter (referred to as Cyp19-cre). The *Cyp19a1* proximal promoter is active exclusively in the granulosa cells in the ovary in adult mice in follicles transitioning from the preantral to the preovulatory stage (103).

IGF1R mRNA and protein levels were examined in granulosa cells of control and experimental mice to determine the efficiency of the knockdown. Compared to control mice (wild-type and IGF1RF/F), IGF1R F/F Cyp19-cre mice had an approximately 50% knockdown of the receptor at the level of mRNA and a variable knockdown of the receptor at the protein level in granulosa cells (Figure 28). To maximize the recombination efficiency in *Igf1r* -floxed mice, mice with one floxed *Igf1r* allele and one null allele were generated using zona pellucida glycoprotein 3 (ZP3)-Cre mice (145). Following PMSG treatment to stimulate follicular maturation and maximize *Igf1r* knockdown, mice with one floxed and one null allele (IGF1R F/-) showed a 50% decrease in *Igf1r* expression, with only 10% knockdown of IGF1R at the protein level. IGF1R F/- mice with Cyp19-cre showed greater than 60% knockdown of *Igf1r* mRNA, and protein was decreased by over 85% when compared to control mice (Figure 28).

2. IGF1R in granulosa cells is critical for normal female fertility

The fertility of mice with granulosa-cell specific IGF1R knockdown was assessed by mating control, IGF1R F/F Cyp19-cre, or IGF1R F/- Cyp19-cre animals with males of proven fertility. The number of pups per litter and the total number of pups was recorded during 6 months of continuous breeding (Figure 29). Control animals averaged 6.9± 0.2 pups per litter and 43.3 ± 1.1 pups over 6 months. IGF1R F/F Cyp19-cre experimental mice showed normal fertility compared to control animals; however, IGF1R F/- Cyp-19cre animals were subfertile. The average litter size of IGF1R F/- Cyp-19cre mice was

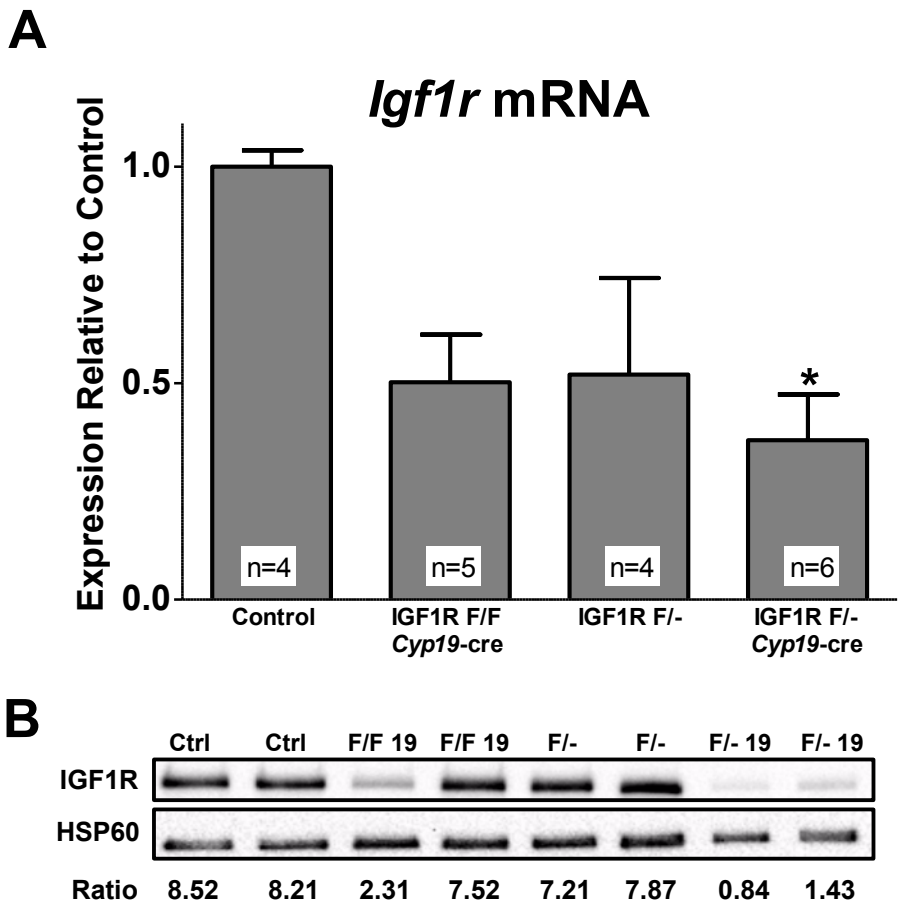

Figure 28: *Cyp19-cre driven IGF1R knockdown in ovarian granulosa cells.*

Mice were treated with PMSG for 48h before sacrifice and isolation of granulosa cells from ovaries.
(**A**) RNA was isolated from freshly isolated granulosa cells, reverse transcribed, and the level of *Igf1r* expression was assessed by qPCR. Columns represent the mean expression relative to control ± SEM, and the number of animals in each group is noted in each column. (*$p<0.05$ compared to WT mice; one-way ANOVA)
(**B**) Total protein was isolated from freshly isolated granulosa cells, and the expression of IGF1R and HSP60 (loading control) was assessed by Western blot. IGF1R band intensities were adjusted to the band intensity of HSP60 for the same sample, and the ratio is reported below the Western blot images.

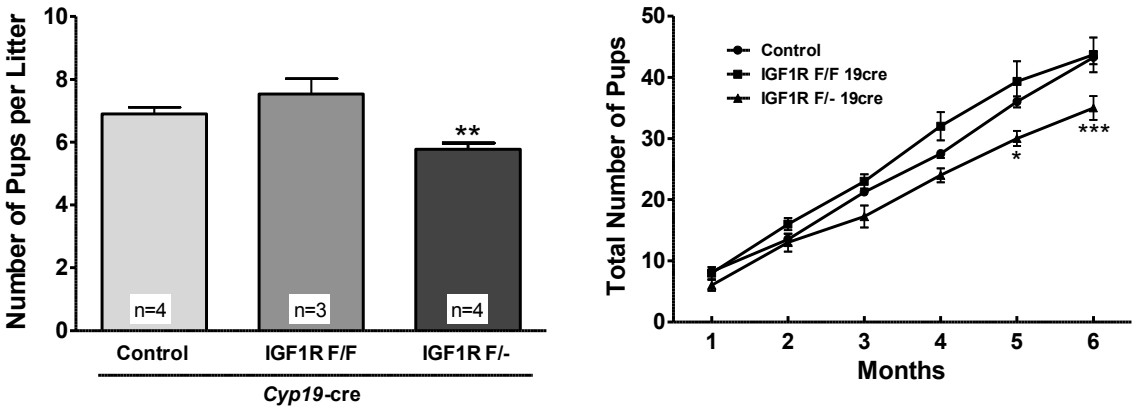

Figure 29: *Mice with reduced IGF1R in granulosa cells are sub-fertile.*

The number of pups per litter was recorded for control and experimental mice over a period of 6 months.
(**Left**) Columns represent the average number of pups per litter ± SEM for each genotype, and the number of mice per group is indicated in each column. (**p<0.01 compared to control mice; one-way ANOVA).
(**Right)** The cumulative total number of pups per mouse of each genotype is reported over a period of 6 months. (*p<0.05; ***p<0.001 compared to other mouse genotypes; two-way ANOVA).

5.8 ± 0.2 pups and the total number of pups per female over 6 months was 35 ± 1.9 both significantly lower compared to control animals.

3. Mice with reduced IGF1R in ovarian granulosa cells have impaired estradiol synthesis and ovulation

To identify changes that may contribute to the observed subfertility in IGF1R F/- Cyp19-cre mice, we traced the estrous cycle in adult females over a period of 12 days. On average, control and IGF1R F/- Cyp19-cre animals spent a similar number of days in proestrus, estrus, diestrus, and metaestrus stages as determined by vaginal cytology (Figure 30A). In addition, the histology of ovaries from control, IGF1R F/F Cyp19-cre, IGF1R F/-, and IGF1R F/- Cyp19-cre mice (Figure 30B-E) was examined after 48h PMSG treatment. Ovarian follicles at all stages of development were present in ovaries from mice of each genotype, suggesting no gross defects in folliculogenesis take place in IGF1R F/- Cyp19-cre mice.

As follicle structure and formation appears normal, we next examined whether the follicles function normally. Serum was collected from control and IGF1R F/- Cyp19-cre mice at the proestrus stage and the estradiol levels were measured by ELISA. The results revealed a significant decrease (>30%) in estradiol levels in IGF1R F/- Cyp19-cre mice compared to control mice (Figure 31A). Because estradiol is critical for ovulation, we next explored the ovulatory capacity of control and IGF1R F/- Cyp19-cre mice. Mice were injected with PMSG followed 48h later by hCG administration. The oviducts were collected from control and experimental mice 17h after hCG, and the number of oocytes in the oviducts were counted (Figure 31B). On average, IGF1R F/-

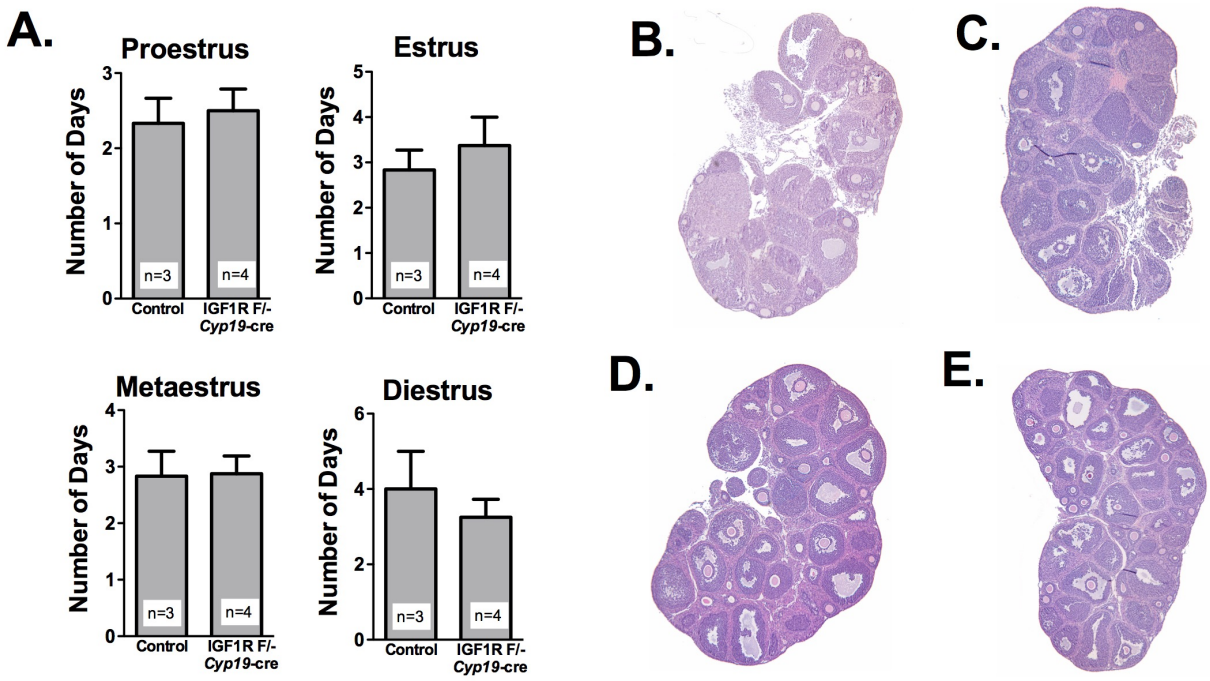

Figure 30: *Mice with reduced IGF1R in granulosa cells have a normal estrous cycle and folliculogenesis.*

(**A**) Vaginal smears were collected from control and experimental IGF1R F/- Cyp19-cre mice for 12 consecutive days. The estrous cycle stages were determined by vaginal cytology and classified as proestrus, estrus, metaestrus, and diestrus based on the presence or absence of leukocytes and the appearance of epithelial cells (104). Columns represent the mean number of days mice spent in that estrous stage over the 12 day period ± SEM. The number of animals in each group is noted in each column. (**B-E**) Representative Hematoxylin and eosin (H&E) staining of ovaries from 48h PMSG treated (B) wild-type, (C) IGF1R F/F Cyp19-cre, (D) IGF1R F/-, and (E) IGF1R F/- Cyp19-cre mice.

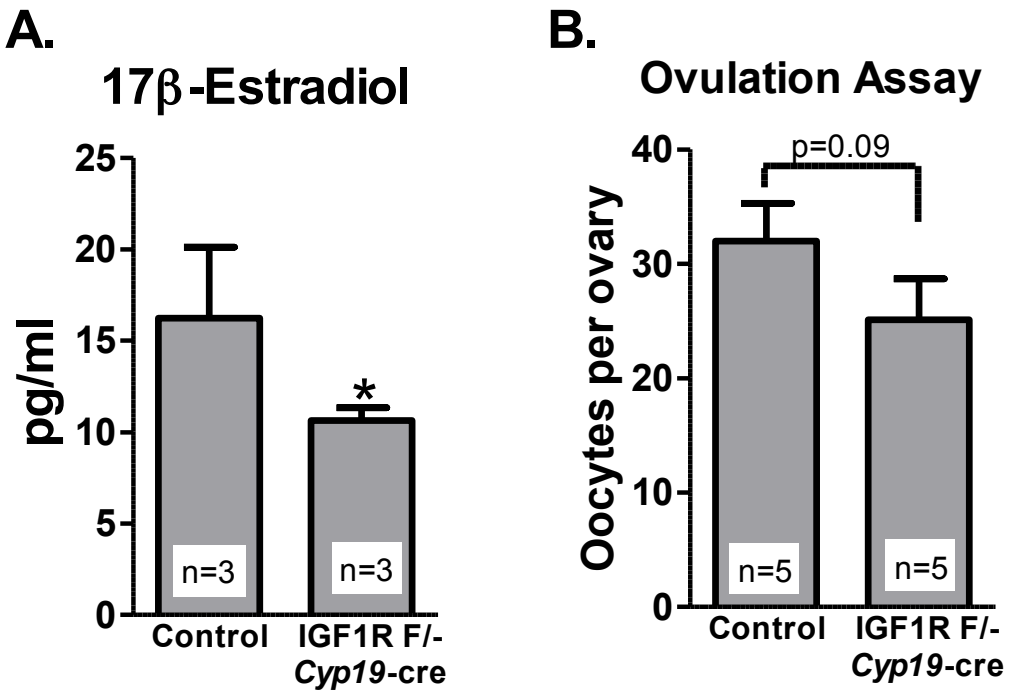

Figure 31: *Reduced IGF1R expression in granulosa cells impairs steroidogenesis and ovulation.*

(**A**) Estradiol levels were measured in serum collected from control and experimental female mice at proestrus. Columns represent the mean estradiol measurement ± SEM, and the number of animals in each group is noted in each column (*$p<0.05$ compared to control; t-test).
(**B**) Mice were treated with PMSG followed by hCG 48h later. Oviducts were dissected 17h after hCG administration and the number of oocytes per oviduct were counted. Columns represent the mean number of oocytes ± SEM, and the number of animals in each group is noted in each column.

Cyp19-cre mice tended to ovulate fewer oocytes than control animals (Control: 32 ± 3.3; IGF1R F/- Cyp19-cre 25.1± 3.5; p=0.09)

4. IGF1R is critical for FSH-induced steroidogenesis

The significant decrease on serum estradiol levels observed at proestrus in IGF1R F/- Cyp19-cre mice suggests that diminished IGF1R expression in granulosa cells impairs normal FSH-induced steroidogenesis. To confirm these findings and to further explore the role of the IGF1R on steroidogenesis *in vivo*, mice were super-stimulated with PMSG for 48h before granulosa cell isolation. Under this protocol, the knockdown of IGF1R is nearly 90% at the protein level (Figure 28). When IGF1R was maximally knocked down, the induction of steroidogenic genes by PMSG treatment was significantly decreased in the granulosa cells of IGF1R F/- Cyp19-cre animals when compared with control animals (Figure 32A). The expression of *Star*, *Cyp11a1*, and *Cyp19a1* were reduced by 5-fold, 2.5-fold, and 2-fold, respectively. Accordingly, the estradiol levels were reduced by 60% in IGF1R F/- Cyp19-cre mice in respect to control mice (Figure 32B). Together these findings demonstrate that IGF1R is critical for FSH-induced steroidogenesis.

Since the IGF1R was not completely knocked down in IGF1R F/- Cyp19-cre mice, we cultured primary granulosa cells from IGF1R F/F mice and infected the cells with a cre-recombinase expressing adenovirus (adeno-cre) to eliminate IGF1R in granulosa cells *in vitro*. Compared to cells infected with a GFP-expressing control virus, *Igf1r* expression in adeno-cre infected cells was reduced by 92% (Figure 33A). When cells were treated with FSH, the more than 3.5-fold increase in *Cyp19a1* expression was abolished when IGF1R was absent

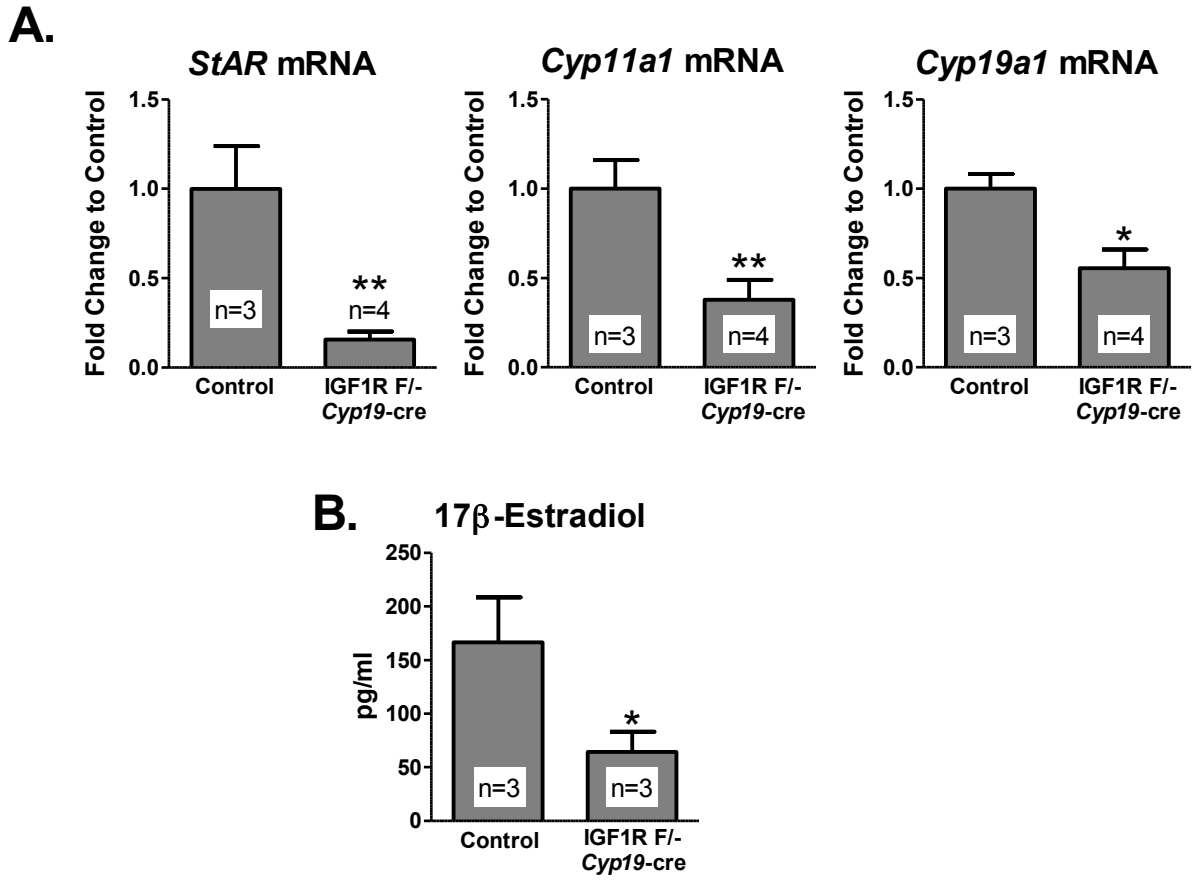

Figure 32: *Super-stimulated IGF1R F/- Cyp19-cre mice have deficient steroidogenic gene expression and estradiol production*.

Mice were treated with PMSG for 48h before sacrifice and isolation of granulosa cells from ovaries.

(**A**) RNA was isolated from granulosa cells, reverse transcribed, and the level of *StAR*, *Cyp11a1*, and *Cyp19a1* expression was assessed by qPCR. Columns represent the mean ± SEM, and the number of animals in each group is noted in each column. (*p<0.05, **p<0.01 compared to control mice; t-test)
(**B**) 17β-Estradiol was measured in blood collected from PMSG treated mice by ELISA. Columns represent the mean ± SEM, and the number of animals in each group is noted in each column. (*p<0.05 compared to control mice; t-test)

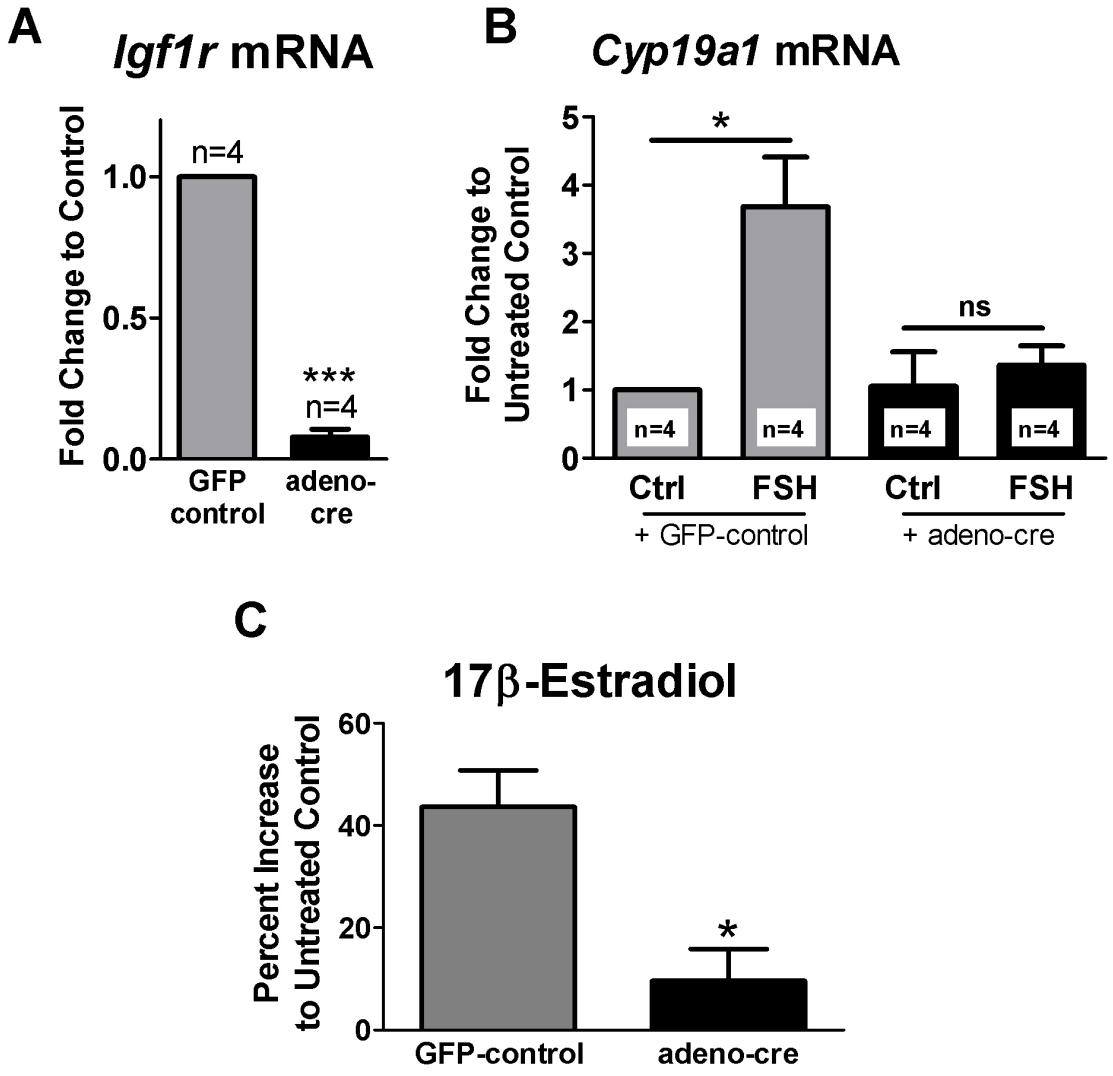

Figure 33: *IGF1R is required for FSH-induced aromatase expression and estradiol production in granulosa cells.*

(**A, B**) Immature IGF1R F/F mice were treated with estradiol for 72h to stimulate granulosa cell proliferation. Granulosa cells were isolated and cultured in serum-free media. Adeno-cre or a control, GFP expressing virus was added to cultured granulosa cells for 24h before cells were treated with or without FSH (50ng/ml) for 48h. RNA was isolated, reverse transcribed, and expression of *Igf1r* (**A**) and *Cyp19a1* (**B**) was assessed by qPCR. Columns represent the mean ± SEM of 4 experiments.
(**C**) Estradiol levels were measured in media collected from each well, and normalized to total RNA for each sample. Columns represent the mean percentage increase in estradiol levels in FSH-treated versus untreated samples for each virus ± SEM of 3 experiments (*$p<0.05$,***$p<0.001$; t-test).

(Figure 33B). Additionally, the increase in estradiol production in response to FSH treatment was significantly lower in cells lacking IGF1R (Figure 33C). These *in vitro* results emphasize the importance of IGF1R in FSH-stimulated steroidogenic function of granulosa cells.

C. Discussion

Previous studies in *Igf1* null mice have demonstrated that this growth factor is crucial for female fertility (86). Follicle maturation in the ovary is paused at the antral stage in *Igf1* null mice, and mature preovulatory follicles or corpora lutea, which indicate ovulation has occurred, are absent. However, infertility is not the only phenotype in total-body *Igf1* null animals. These animals weigh less than 30% of wildtype mice, and the lack of IGF1 could have consequences for gonadotropin production in the brain (86-88, 144). These confounding phenotypes make it difficult to assess the direct role of IGFs in the ovary during folliculogenesis.

In the present study, we used a cre-lox system to knockdown the *Igf1r* specifically in granulosa cells of ovarian follicles as they mature from the preantral to the preovulatory stage. Using this system, we were able to evaluate the necessity of IGF action in granulosa cell differentiation during follicle development without altering IGF action in other tissues throughout the body. We found that IGF1R F/- Cyp19-cre females with reduced IGF1R in granulosa cells were sub-fertile. While they had a normal estrous cycle, these animals had significantly less estradiol measured in their serum and a tendency to ovulate fewer oocytes than control animals. When these animals were injected with PMSG to stimulate folliculogenesis and maximize the Cyp19-cre driven knockdown of the *Igf1r*, the expression of steroidogenic genes was

significantly lower than control animals, and estradiol was reduced by more than 60% compared to control animals. This suggests that IGF1R activity is critical for granulosa cell function during follicle maturation from the preantral to the preovulatory stage.

We next isolated granulosa cells from IGF1R F/F mice, and cultured them *in vitro*. Upon treatment with adeno-cre, *Igf1r* mRNA was knocked down approximately 92% in the cells. Without *Igf1r* these cells were not able to respond to FSH treatment. Aromatase expression and activity, measured as estradiol production in the media, was significantly enhanced by FSH in GFP-control infected cells, but did not change in FSH-treated cells lacking *Igf1r*. This suggests that a complete knockdown of *Igf1r in vivo* would have more drastic effects on FSH- induced granulosa cell differentiation, specifically the increase in steroidogenesis, than the IGF1R F/- Cyp19-cre animals used in the study.

Previous studies *in vitro* cell culture models have demonstrated that even 7% of remaining IGF1R is sufficient to activate the AKT pathway in cells. Thus, in our IGF1R F/- Cyp19-cre animals, the nearly 60% knockdown of the *Igf1r* mRNA and 85% knockdown of IGF1R protein is likely not sufficient to eliminate IGF1R activity, and therefore IGF action, in the granulosa cells. Additionally, it is possible that the remaining IGF1R could form hybrid receptors with insulin receptor (IR) in granulosa cells to mediate IGF activity in granulosa cells. Overall, we demonstrate that a knockdown in IGF1R has impacts on granulosa cell function and female fertility; however, with the complete lack of response to FSH treatment in our *in vitro* experiments, we believe that a more efficient knockdown of the IGF1R *in vivo* would have drastic effects on the fertility of these animals.

IX. GENERAL CONCLUSIONS AND FUTURE DIRECTIONS

In 2010, over 25% of women having their first child were in their thirties, compared to only 5% in 1975 (5, 146). Age is a strong contributing factor to infertility, and as more women delay having children, the number of women needing assisted reproductive technologies, such as IVF, increases. Compounding this issue, the success of IVF itself is highly age dependent. A 35 year-old women undergoing IVF has a 35% chance of a pregnancy that results in a child, and this drops to 20% by age 40 and less than 5% by age 44. Unfortunately, the percentage of IVF cycles resulting in a live birth has not significantly improved over the last decade (6). Significant advances are needed in the IVF process to provide infertile patients with a greater chance of having a child. Unfortunately, the precise actions of FSH on follicle development, particularly in granulosa cell differentiation, are largely unknown. A better understanding of FSH-induced follicle maturation could provide insight into ways to optimize FSH-induced follicle maturation in IVF patients. Additionally, it could help to identify women who are not good candidates for IVF who may not respond to FSH therapy or those who respond too strongly and are at an increased risk of developing OHSS.

A major obstacle to researchers studying human granulosa cell differentiation is that a good model is not available. Human preantral, undifferentiated granulosa cells are essentially unavailable for studies, so researchers have used luteinized mural granulosa cells collected from IVF patients during the oocyte collection procedure. After 7 days in culture, the luteinized mural granulosa cells respond to FSH with increased expression of steroidogenic genes and estradiol production (99). However, the fact that

these cells have been exposed to hormone treatments, undergone luteinization *in vivo*, and are cultured for at least 7 days in the presence of serum raises questions about how closely their response to FSH resembles that of preantral granulosa cells.

Here, we have developed a new model for studying human granulosa cell differentiation that overcomes many of the deficits of cultured luteinized mural granulosa cells. We demonstrated that after 24h of culture in phenol red-free and serum-free media, cumulus granulosa cells from IVF patients recapitulate many features of preantral granulosa cells. Cumulus granulosa cells are less differentiated than mural, and they express lower levels of steroidogenic genes and LHR. This suggests that cumulus granulosa cells are protected from gonadotropin-induced differentiation *in vivo.* The expression of steroidogenic genes and steroidogenesis increases in cumulus granulosa cells following treatment with FSH, similar to what occurs in preantral granulosa cells during FSH-induced differentiation; however, these changes are not observed in mural granulosa cells. Together, these findings indicate that cultured cumulus granulosa cells are superior to luteinized mural granulosa cells to gain insight into the process of FSH-induced granulosa cell differentiation.

We then used the cultured cumulus granulosa cells to investigate the molecular mechanisms underlying human granulosa cell differentiation. Global gene expression analysis revealed that FSH upregulates proteins required for steroidogenesis, including receptors for cholesterol-containing lipoproteins and enzymes that catalyze reactions required to produce estradiol from cholesterol. At the same time, FSH downregulates genes encoding cytoskeletal proteins. Thus, FSH elicits structural changes needed to

support the enhanced steroidogenic function during human granulosa cell differentiation.

FSH also intricately regulates the IGF system in cultured cumulus granulosa cells. There was a significant increase in IGF2 in response to FSH treatment, which is consistent with the increase in *IGF2* observed in follicles as they progress from the preantral to the preovulatory stage (79). *IGF1*, which is the main IGF in rodent granulosa cells, was not expressed in the cultured human cumulus granulosa cells. Additionally, we observed that FSH downregulates *IGFBP3* and upregulates *PAPP-A* mRNA expression, which can both result in an increase in the bioavailability of IGF2. This increase in IGF2 expression as well as its bioavailability by FSH is critical because IGF2 can enhance FSH-induced aromatase expression and activity and synergize with FSH to stimulate granulosa cell proliferation.

Upon further inspection of the relationship between FSH and IGF2 during granulosa cell differentiation we demonstrated that IGF2 does not merely enhance FSH action in granulosa cells; IGF2 action through the IGF1R is required for FSH to stimulate the expression of steroidogenic genes and the production of estradiol. Specifically, IGF1R mediated AKT activation is required in order for FSH to stimulate AKT phosphorylation and subsequent steroidogenic gene expression. Steroidogenesis is a major function of differentiated granulosa cells, so these findings suggest that IGF1R activity is critical for FSH-induced human granulosa cell differentiation during follicle maturation in the ovary.

Because IGF2 is so critical for FSH action in human granulosa cells, we aimed to understand the mechanisms by which *IGF2* expression is regulated in human granulosa

cells. In human tissues, *IGF2* expression is driven by four promoters. We show that the P3 and P4 promoters are the main drivers of *IGF2* expression in human granulosa cells. FSH is a potent stimulator specifically of P3 promoter-driven *IGF2* expression. We were able to demonstrate that AKT activation is necessary for FSH to stimulate P3 promoter-driven *IGF2* expression. Moreover, when we treated cells with IGFBP4 or AEW, FSH was unable to stimulate *IGF2* expression, suggesting that endogenous IGF2 produced by the granulosa cells is necessary for FSH to stimulate IGF2 expression. This demonstrates that IGF2 is an auto-regulator in human granulosa cells.

Interestingly, we observed that the increase in IGF2 protein levels after FSH treatment was localized to the nucleus. To our knowledge, there is only one other report of nuclear IGF2 (123) and nothing is known about the consequences of IGF2 localization to the nucleus. Several studies have detected IGF1R in the nucleus following activation by IGF1 and subsequent sumoylation (147-149). The nuclear IGF1R is then able to bind to the promoter of specific genes and regulate their expression (150). It is plausible that a similar phenomenon is occurring in human granulosa cells in response to IGF2, where upon IGF2 binding, the IGF1R and ligand are relocalized to the nucleus to alter gene transcription; however, this is purely speculative and further studies are needed to validate this proposed mechanism of IGF2 localization to the nucleus.

Knowing that IGF1R activity is crucial for human and rodent granulosa cell differentiation *in vitro,* we examined the importance of IGF1R activity during follicle maturation *in vivo*. We generated mice with IGF1R knockdown specifically in the granulosa cells during follicle maturation from the preantral to the preovulatory stage,

thereby eliminating IGF action in the granulosa cells in ovarian follicles during this time. We observed that female mice with a reduced level of IGF1R in granulosa cells were sub-fertile with reduced estradiol production. When animals were treated with PMSG to enhance the level of IGF1R knockdown, there was a greater reduction in the level of steroidogenic genes and estradiol production. Furthermore, when IGF1R was knocked down over 90% in granulosa cells *in vitro* FSH was not able to significantly enhance aromatase expression or estradiol production. Together, these results demonstrate how critical IGF1R activity is for granulosa cell function in follicles as they mature to the preovulatory stage. We speculate that if a complete knockdown of IGF1R were achieved in rodent granulosa cells *in vivo* there would be drastic consequences on the overall fertility of mice.

Here, we redefine our understanding of the process of granulosa cell differentiation that occurs during follicle maturation to the preovulatory stage. FSH is known to stimulate granulosa cell differentiation and follicle development and is administered to IVF patients to do so; however, we demonstrate that IGF1R activity is required in order for FSH to promote human granulosa cell differentiation. We also show that FSH and IGF2 action are coordinated during granulosa cell differentiation, where FSH stimulates IGF2 expression, and IGF2 is required for, and synergizes with, FSH to stimulate granulosa cell proliferation and differentiation. This relationship implies that only follicles that sufficiently respond to FSH will have enhanced *IGF2* expression, and follicles with this enhanced IGF2 action will fully respond and differentiate in response to FSH. Thus, the interdependence of FSH and IGF2 could be a driver in follicle selection that occurs during folliculogenesis. In support of this idea, dominant follicles have been

shown to express more PAPP-A than other follicles in the cohort that become atretic (151), suggesting that increased IGF2 bioavailability may be critical for follicle selection.

Our findings could lead to the identification of new targets and therapies to improve the success of IVF protocols. From our findings it is possible to speculate that intrafollicular IGF2 levels and/or IGF1R expression/activity could be predictors of a patient's response to FSH stimulation during controlled ovarian stimulation. High IGF2 levels in the follicular fluid of follicles retrieved for IVF are correlated with better oocyte maturation and early embryo development *in vitro* (129). Additionally, in *in vitro* follicle cultures, IGF2 can act as a survival factor and decrease follicle death in long-term culture (152). In women undergoing oocyte cryopreservation in anticipation of having children later in life, measurement of IGF2 in the follicular fluid could possibly be used an indicator of the quality of oocytes being cryopreserved to ensure that they are likely to fertilize and form embryos years later when the patient returns for IVF.

In agreement with the positive role of IGF2 in follicle maturation, a study of follicular cells from IVF patients with diminished ovarian reserve (DOR) found a significant decrease in components of the IGF system, including IGF2, in comparison to patients with normal ovarian reserve (153). Also, the follicular fluid of women with polycystic ovary syndrome (PCOS) has been shown to contain higher levels of IGFBPs, which can bind and sequester IGFs and blunt their normal activity in the follicle (154, 155). This suggests that insufficient IGF activity in ovarian follicles could contribute to the decreased reproductive capacity of women with DOR, PCOS, and other etiologies of impaired fertility. In these patients, it is possible that enhancing IGF2 action in developing follicles could promote normal follicle growth and oocyte maturation. Serum

IGF2 levels do not appear to influence IGF2 levels in the follicular fluid; however, regulators of IGF2 could be targeted to enhance IGF2 bioavailability in the ovary. For example, MicroRNA (miR)-615 targets IGF2 and leads to its degradation (156). An inhibitor of miR-615 could be targeted to the ovary to neutralize miR-615-mediated IGF2 degradation, thereby increasing the level of IGF2 available to enhance granulosa cell differentiation and function.

To conclude, cultures of human cumulus granulosa cells are a powerful model that can be used to gain an understanding of mechanisms of human granulosa cell differentiation. Our current study has revealed that IGFs are critical for FSH-induced granulosa cell differentiation, and suggest that the IGF system should be considered when evaluating the chances that a patient has to become pregnant through IVF. Cultured cumulus granulosa cells could be an optimal model to investigate and establish predictive markers of IVF success so that infertile patients can be directed to the most appropriate resources, such as using donor oocytes or adoption, and can save the patient both time and money during the emotionally-taxing process of having children.

X. APPENDICES

A. Appendix A

TABLE VI:

FOLD CHANGE IN THE PHOSPHORYLATION OF KEY INTRACELLULAR SIGNALING PROTEINS IN CULTURED CUMULUS GRANULOSA CELLS FOLLOWING 1H FSH IN RELATION TO UNTREATED CELLS

Kinase	Phosphorylation Site	Ratio FSH:Control
ERK1/2	T202/Y204, T185/Y187	5.8
AKT1/2/3	S473	3.0
JNK1/2/3	T183/Y185, T221/Y223	2.7
EGFR	Y1086	2.1
CREB	S133	2.0
MSK1/2	S376/S360	1.9
PLC-γ1	Y783	1.9
AMPKα1	T183	1.7
WNK1	T60	1.7
Fyn	Y420	1.6
p38α	T180/Y182	1.5
STAT3	S727	1.4
TOR	S2448	1.4
GSK-3α/β	S21/S9	1.4
PDGFRβ	Y751	1.3
Hck	Y411	1.3
FAK	Y397	1.3
HSP27	S78/S82	1.3
p70 S6 Kinase	T389	1.3
Fgr	Y412	1.2
Lck	Y394	1.2
Chk-2	T68	1.2
AKT1/2/3	T308	1.1
RSK1/2/3	S380/S386/S377	1.1
PYK2	Y402	1.1
eNOS	S1177	1.1
STAT3	Y705	1.1
p53	S392	1.0
p27	T198	1.0
p70 S6 Kinase	T421/S424	1.0
Src	Y419	1.0
Yes	Y426	1.0
STAT5a/b	Y694/Y699	0.9
AMPKα2	T172	0.9
c-Jun	S63	0.9
PRAS40	T246	0.9
p53	S46	0.9
Lyn	Y397	0.9
STAT5b	Y699	0.9
STAT5a	Y694	0.9
STAT6	Y641	0.8
p53	S15	0.7
STAT2	Y689	0.7

B. Appendix B

TABLE VII:
GENES DIFFERENTIALLY EXPRESSED IN CULTURED HUMAN CUMULUS GRANULOSA CELLS FOLLOWING FSH TREATMENT FOR 48H

EntrezID	Symbol	Name	Geometric mean of intensities (FSH/Control)	P-value	FDR
83876	MRO	maestro	**30.30**	3.00E-07	6.97E-05
64131	XYLT1	xylosyltransferase I	**10.87**	1.30E-06	9.50E-05
374 /// 727738	AREG /// AREGB	amphiregulin /// amphiregulin B	**10.64**	2.00E-07	6.82E-05
85329	LGALS12	lectin, galactoside-binding, soluble, 12	**10.00**	< 1e-07	< 1e-07
1588	CYP19A1	cytochrome P450, family 19, subfamily A, polypeptide 1	**9.09**	2.00E-07	6.82E-05
3290	HSD11B1	hydroxysteroid (11-beta) dehydrogenase 1	**9.09**	3.50E-06	1.49E-04
3284	HSD3B2	hydroxy-delta-5-steroid dehydrogenase, 3 beta- and steroid delta-isomerase 2	**6.67**	1.45E-03	4.20E-03
3623	INHA	inhibin, alpha	**6.67**	7.00E-07	7.16E-05
6263	RYR3	ryanodine receptor 3	**5.88**	1.80E-06	1.06E-04
6770	STAR	steroidogenic acute regulatory protein	**5.88**	2.94E-05	3.51E-04
3949	LDLR	low density lipoprotein receptor	**4.76**	5.00E-07	6.97E-05
2869	GRK5	G protein-coupled receptor kinase 5	**4.55**	7.00E-07	7.16E-05
3156	HMGCR	3-hydroxy-3-methylglutaryl-CoA reductase	**4.55**	2.00E-07	6.82E-05
4504	MT3	metallothionein 3	**4.35**	6.30E-06	1.85E-04
4883	NPR3	natriuretic peptide receptor C/guanylate cyclase C (atrionatriuretic peptide receptor C)	**4.35**	3.00E-07	6.97E-05
56548	CHST7	carbohydrate (N-acetylglucosamine 6-O) sulfotransferase 7	**4.17**	2.82E-05	3.47E-04
2036	EPB41L1	erythrocyte membrane protein band 4.1-like 1	**4.17**	1.70E-06	1.04E-04

Appendix B (continued)

TABLE VII:
GENES DIFFERENTIALLY EXPRESSED IN CULTURED HUMAN CUMULUS GRANULOSA CELLS FOLLOWING FSH TREATMENT FOR 48H

EntrezID	Symbol	Name	Geometric mean of intensities (FSH/Control)	P-value	FDR
3481 /// 723961	IGF2 /// INS-IGF2	insulin-like growth factor 2 (somatomedin A) /// INS-IGF2 readthrough	**4.17**	5.44E-05	4.84E-04
151393	RMDN2	regulator of microtubule dynamics 2	**4.17**	4.00E-07	6.97E-05
13	AADAC	arylacetamide deacetylase	**4.00**	9.00E-06	2.14E-04
57476	GRAMD1B	GRAM domain containing 1B	**4.00**	2.57E-05	3.45E-04
56246	MRAP	melanocortin 2 receptor accessory protein	**4.00**	5.00E-07	6.97E-05
84059	GPR98	G protein-coupled receptor 98	**3.85**	2.90E-06	1.37E-04
2947	GSTM3	glutathione S-transferase mu 3 (brain)	**3.85**	3.40E-06	1.47E-04
283551	C14orf182	chromosome 14 open reading frame 182	**3.70**	4.40E-06	1.67E-04
54541	DDIT4	DNA-damage-inducible transcript 4	**3.70**	5.20E-06	1.73E-04
3157	HMGCS1	3-hydroxy-3-methylglutaryl-CoA synthase 1 (soluble)	**3.70**	5.70E-06	1.75E-04
9536	PTGES	prostaglandin E synthase	**3.70**	9.60E-05	6.82E-04
23554	TSPAN12	tetraspanin 12	**3.70**	1.40E-05	2.56E-04
2230	FDX1	ferredoxin 1	**3.57**	2.30E-06	1.24E-04
117245	HRASLS5	HRAS-like suppressor family, member 5	**3.57**	7.00E-07	7.16E-05
10673	TNFSF13B	tumor necrosis factor (ligand) superfamily, member 13b	**3.57**	2.50E-06	1.28E-04
54996	41700	mitochondrial amidoxime reducing component 2	**3.45**	1.40E-06	9.54E-05
60370	AVPI1	arginine vasopressin-induced 1	**3.45**	9.00E-07	8.12E-05
1583	CYP11A1	cytochrome P450, family 11, subfamily A, polypeptide 1	**3.45**	3.70E-06	1.53E-04
94031	HTRA3	HtrA serine peptidase 3	**3.45**	1.92E-05	2.96E-04

Appendix B (continued)

TABLE VII:
GENES DIFFERENTIALLY EXPRESSED IN CULTURED HUMAN CUMULUS GRANULOSA CELLS FOLLOWING FSH TREATMENT FOR 48H

EntrezID	Symbol	Name	Geometric mean of intensities (FSH/Control)	P-value	FDR
6676	SPAG4	sperm associated antigen 4	**3.45**	2.28E-05	3.22E-04
4023	LPL	lipoprotein lipase	**3.33**	2.30E-06	1.24E-04
6307	MSMO1	methylsterol monooxygenase 1	**3.33**	9.00E-07	8.12E-05
4885	NPTX2	neuronal pentraxin II	**3.33**	4.37E-05	4.34E-04
3638	INSIG1	insulin induced gene 1	**3.23**	1.30E-06	9.50E-05
5210	PFKFB4	6-phosphofructo-2-kinase/fructose-2,6-biphosphatase 4	**3.23**	1.39E-04	8.63E-04
6542	SLC7A2	solute carrier family 7 (cationic amino acid transporter, y+ system), member 2	**3.23**	3.20E-06	1.47E-04
1717	DHCR7	7-dehydrocholesterol reductase	**3.13**	2.10E-06	1.19E-04
10682	EBP	emopamil binding protein (sterol isomerase)	**3.13**	8.40E-06	2.09E-04
284611	FAM102B	family with sequence similarity 102, member B	**3.13**	2.50E-06	1.28E-04
4502	MT2A	metallothionein 2A	**3.13**	1.12E-04	7.49E-04
887	CCKBR	cholecystokinin B receptor	**3.03**	4.97E-05	4.68E-04
10570	DPYSL4	dihydropyrimidinase-like 4	**3.03**	1.22E-03	3.73E-03
9518	GDF15	growth differentiation factor 15	**3.03**	4.69E-04	1.92E-03
4489	MT1A	metallothionein 1A	**3.03**	6.26E-05	5.23E-04
8553	BHLHE40	basic helix-loop-helix family, member e40	**2.94**	2.50E-05	3.42E-04
3422	IDI1	isopentenyl-diphosphate delta isomerase 1	**2.94**	1.40E-06	9.54E-05
3590	IL11RA	interleukin 11 receptor, alpha	**2.94**	4.40E-06	1.67E-04

Appendix B (continued)

TABLE VII:
GENES DIFFERENTIALLY EXPRESSED IN CULTURED HUMAN CUMULUS GRANULOSA CELLS FOLLOWING FSH TREATMENT FOR 48H

EntrezID	Symbol	Name	Geometric mean of intensities (FSH/Control)	P-value	FDR
151556	GPR155	G protein-coupled receptor 155	**2.86**	1.96E-04	1.07E-03
64078	SLC28A3	solute carrier family 28 (sodium-coupled nucleoside transporter), member 3	**2.86**	2.98E-05	3.54E-04
10140	TOB1	transducer of ERBB2, 1	**2.86**	8.30E-06	2.09E-04
39	ACAT2	acetyl-CoA acetyltransferase 2	**2.78**	1.41E-05	2.56E-04
9077	DIRAS3	DIRAS family, GTP-binding RAS-like 3	**2.78**	3.40E-06	1.47E-04
2592	GALT	galactose-1-phosphate uridylyltransferase	**2.78**	1.43E-05	2.56E-04
949	SCARB1	scavenger receptor class B, member 1	**2.78**	1.95E-05	2.96E-04
1831	TSC22D3	TSC22 domain family, member 3	**2.78**	3.69E-05	3.97E-04
230	ALDOC	aldolase C, fructose-bisphosphate	**2.70**	8.10E-06	2.09E-04
3400	ID4	inhibitor of DNA binding 4, dominant negative helix-loop-helix protein	**2.70**	6.74E-05	5.48E-04
80856	KIAA1715	KIAA1715	**2.70**	1.07E-04	7.30E-04
4217	MAP3K5	mitogen-activated protein kinase kinase kinase 5	**2.70**	1.05E-05	2.24E-04
4501	MT1X	metallothionein 1X	**2.70**	2.12E-04	1.13E-03
388121	TNFAIP8L3	tumor necrosis factor, alpha-induced protein 8-like 3	**2.70**	7.10E-06	1.96E-04
79956	ERMP1	endoplasmic reticulum metallopeptidase 1	**2.63**	1.99E-05	2.98E-04
6319	SCD	stearoyl-CoA desaturase (delta-9-desaturase)	**2.63**	5.10E-06	1.72E-04
27346	TMEM97	transmembrane protein 97	**2.63**	9.80E-06	2.17E-04
79656	BEND5	BEN domain containing 5	**2.56**	1.88E-03	5.15E-03

Appendix B (continued)

TABLE VII:
GENES DIFFERENTIALLY EXPRESSED IN CULTURED HUMAN CUMULUS GRANULOSA CELLS FOLLOWING FSH TREATMENT FOR 48H

EntrezID	Symbol	Name	Geometric mean of intensities (FSH/Control)	P-value	FDR
25966	C2CD2	C2 calcium-dependent domain containing 2	**2.56**	7.60E-06	1.99E-04
5046 /// 100507472	LOC100507472 /// PCSK6	uncharacterized LOC100507472 /// proprotein convertase subtilisin/kexin type 6	**2.56**	2.68E-04	1.32E-03
9971	NR1H4	nuclear receptor subfamily 1, group H, member 4	**2.56**	1.31E-05	2.53E-04
7275	TUB	tubby homolog (mouse)	**2.56**	4.10E-06	1.63E-04
7422	VEGFA	vascular endothelial growth factor A	**2.56**	9.30E-06	2.16E-04
23461	ABCA5	ATP-binding cassette, sub-family A (ABC1), member 5	**2.50**	5.94E-05	5.10E-04
685	BTC	betacellulin	**2.50**	3.18E-05	3.70E-04
147015	DHRS13	dehydrogenase/reductase (SDR family) member 13	**2.50**	5.09E-05	4.72E-04
50506	DUOX2	dual oxidase 2	**2.50**	3.83E-05	4.05E-04
29923	HILPDA	hypoxia inducible lipid droplet-associated	**2.50**	7.28E-04	2.60E-03
23531	MMD	monocyte to macrophage differentiation-associated	**2.50**	7.86E-05	6.10E-04
55647	RAB20	RAB20, member RAS oncogene family	**2.50**	1.52E-05	2.63E-04
57556	SEMA6A	sema domain, transmembrane domain (TM), and cytoplasmic domain, (semaphorin) 6A	**2.50**	3.62E-04	1.61E-03
9469	CHST3	carbohydrate (chondroitin 6) sulfotransferase 3	**2.44**	2.48E-04	1.26E-03
3992 /// 100302263	FADS1 /// MIR1908	fatty acid desaturase 1 /// microRNA 1908	**2.44**	1.24E-05	2.44E-04
4047	LSS	lanosterol synthase (2,3-oxidosqualene-lanosterol cyclase)	**2.44**	8.51E-05	6.35E-04

Appendix B (continued)

TABLE VII:
GENES DIFFERENTIALLY EXPRESSED IN CULTURED HUMAN CUMULUS GRANULOSA CELLS FOLLOWING FSH TREATMENT FOR 48H

EntrezID	Symbol	Name	Geometric mean of intensities (FSH/Control)	P-value	FDR
9104	RGN	regucalcin (senescence marker protein-30)	**2.44**	6.40E-06	1.85E-04
7448 /// 645832	SEBOX /// VTN	SEBOX homeobox /// vitronectin	**2.44**	5.25E-05	4.76E-04
55244	SLC47A1	solute carrier family 47, member 1	**2.44**	8.87E-05	6.51E-04
83862	TMEM120A	transmembrane protein 120A	**2.44**	4.81E-05	4.58E-04
59272	ACE2	angiotensin I converting enzyme 2	**2.38**	9.50E-06	2.17E-04
51205 /// 101060704	ACP6 /// LOC101060704	acid phosphatase 6, lysophosphatidic /// lysophosphatidic acid phosphatase type 6-like	**2.38**	8.40E-06	2.09E-04
2256	FGF11	fibroblast growth factor 11	**2.38**	1.10E-04	7.46E-04
51141	INSIG2	insulin induced gene 2	**2.38**	3.38E-05	3.78E-04
10200	MPHOSPH6	M-phase phosphoprotein 6	**2.38**	8.60E-06	2.09E-04
22822	PHLDA1	pleckstrin homology-like domain, family A, member 1	**2.38**	6.95E-04	2.50E-03
80315	CPEB4	cytoplasmic polyadenylation element binding protein 4	**2.33**	1.12E-05	2.30E-04
10561	IFI44	interferon-induced protein 44	**2.33**	3.43E-04	1.55E-03
4597	MVD	mevalonate (diphospho) decarboxylase	**2.33**	2.45E-05	3.39E-04
5997	RGS2	regulator of G-protein signaling 2, 24kDa	**2.33**	5.38E-04	2.10E-03
7295	TXN	thioredoxin	**2.33**	4.82E-04	1.96E-03
405753	DUOXA2	dual oxidase maturation factor 2	**2.27**	1.30E-04	8.28E-04
2224	FDPS	farnesyl diphosphate synthase	**2.27**	2.79E-05	3.46E-04
23421	ITGB3BP	integrin beta 3 binding protein (beta3-endonexin)	**2.27**	2.59E-05	3.45E-04

Appendix B (continued)

TABLE VII:
GENES DIFFERENTIALLY EXPRESSED IN CULTURED HUMAN CUMULUS GRANULOSA CELLS FOLLOWING FSH TREATMENT FOR 48H

EntrezID	Symbol	Name	Geometric mean of intensities (FSH/Control)	P-value	FDR
25840	METTL7A	methyltransferase like 7A	**2.27**	4.64E-05	4.50E-04
5251	PHEX	phosphate regulating endopeptidase homolog, X-linked	**2.27**	3.87E-05	4.05E-04
144195	SLC2A14	solute carrier family 2 (facilitated glucose transporter), member 14	**2.27**	1.90E-05	2.94E-04
6515 /// 144195	SLC2A14 /// SLC2A3	solute carrier family 2 (facilitated glucose transporter), member 14 /// solute carrier family 2 (facilitated glucose transporter), member 3	**2.27**	1.72E-05	2.84E-04
6533	SLC6A6	solute carrier family 6 (neurotransmitter transporter, taurine), member 6	**2.27**	1.43E-03	4.18E-03
8869	ST3GAL5	ST3 beta-galactoside alpha-2,3-sialyltransferase 5	**2.27**	9.80E-06	2.17E-04
4189	DNAJB9	DnaJ (Hsp40) homolog, subfamily B, member 9	**2.22**	1.45E-05	2.56E-04
3309	HSPA5	heat shock 70kDa protein 5 (glucose-regulated protein, 78kDa)	**2.22**	3.85E-04	1.68E-03
4495	MT1G	metallothionein 1G	**2.22**	4.52E-04	1.87E-03
5621	PRNP	prion protein	**2.22**	1.39E-05	2.56E-04
58480	RHOU	ras homolog family member U	**2.22**	8.98E-05	6.55E-04
6713	SQLE	squalene epoxidase	**2.22**	1.88E-05	2.94E-04
27010	TPK1	thiamin pyrophosphokinase 1	**2.22**	2.71E-05	3.45E-04
64225	ATL2	atlastin GTPase 2	**2.17**	3.88E-05	4.05E-04
152189	CMTM8	CKLF-like MARVEL transmembrane domain containing 8	**2.17**	5.00E-05	4.69E-04

Appendix B (continued)

TABLE VII:
GENES DIFFERENTIALLY EXPRESSED IN CULTURED HUMAN CUMULUS GRANULOSA CELLS FOLLOWING FSH TREATMENT FOR 48H

EntrezID	Symbol	Name	Geometric mean of intensities (FSH/Control)	P-value	FDR
23052	ENDOD1	endonuclease domain containing 1	**2.17**	4.35E-05	4.34E-04
10082	GPC6	glypican 6	**2.17**	1.64E-05	2.73E-04
6303	SAT1	spermidine/spermine N1-acetyltransferase 1	**2.17**	1.14E-03	3.53E-03
6309	SC5D	sterol-C5-desaturase	**2.17**	1.77E-05	2.90E-04
658	BMPR1B	bone morphogenetic protein receptor, type IB	**2.13**	1.40E-04	8.65E-04
117248	GALNT15	UDP-N-acetyl-alpha-D-galactosamine:polypeptide N-acetylgalactosaminyltransferase 15	**2.13**	4.49E-04	1.86E-03
5178	PEG3	paternally expressed 3	**2.13**	1.87E-05	2.94E-04
23475	QPRT	quinolinate phosphoribosyltransferase	**2.13**	5.86E-05	5.06E-04
7049	TGFBR3	transforming growth factor, beta receptor III	**2.13**	1.18E-03	3.63E-03
360200	TMPRSS9	transmembrane protease, serine 9	**2.13**	2.68E-05	3.45E-04
26007	DAK	dihydroxyacetone kinase 2 homolog (S. cerevisiae)	**2.08**	5.83E-05	5.06E-04
1852	DUSP9	dual specificity phosphatase 9	**2.08**	3.25E-05	3.73E-04
2053	EPHX2	epoxide hydrolase 2, cytoplasmic	**2.08**	6.38E-05	5.29E-04
9415	FADS2	fatty acid desaturase 2	**2.08**	1.70E-04	9.89E-04
2729	GCLC	glutamate-cysteine ligase, catalytic subunit	**2.08**	6.54E-05	5.39E-04
9380	GRHPR	glyoxylate reductase/hydroxypyruvate reductase	**2.08**	6.51E-04	2.40E-03
5648	MASP1	mannan-binding lectin serine peptidase 1 (C4/C2 activating component of Ra-reactive factor)	**2.08**	2.75E-05	3.45E-04

Appendix B (continued)

TABLE VII:
GENES DIFFERENTIALLY EXPRESSED IN CULTURED HUMAN CUMULUS GRANULOSA CELLS FOLLOWING FSH TREATMENT FOR 48H

EntrezID	Symbol	Name	Geometric mean of intensities (FSH/Control)	P-value	FDR
201595	STT3B	STT3B, subunit of the oligosaccharyltransferase complex (catalytic)	**2.08**	2.71E-05	3.45E-04
23321	TRIM2	tripartite motif containing 2	**2.08**	2.75E-05	3.45E-04
375567	VWC2	von Willebrand factor C domain containing 2	**2.08**	1.65E-04	9.73E-04
7474	WNT5A	wingless-type MMTV integration site family, member 5A	**2.08**	1.28E-03	3.88E-03
63934	ZNF667	zinc finger protein 667	**2.08**	8.79E-05	6.49E-04
10058 /// 79065	ABCB6 /// ATG9A	ATP-binding cassette, sub-family B (MDR/TAP), member 6 /// autophagy related 9A	**2.04**	5.66E-04	2.16E-03
224	ALDH3A2	aldehyde dehydrogenase 3 family, member A2	**2.04**	4.85E-04	1.97E-03
353322	ANKRD37	ankyrin repeat domain 37	**2.04**	1.64E-04	9.68E-04
341	APOC1	apolipoprotein C-I	**2.04**	4.22E-05	4.26E-04
2683	B4GALT1	UDP-Gal:betaGlcNAc beta 1,4- galactosyltransferase, polypeptide 1	**2.04**	2.49E-05	3.42E-04
441168	FAM26F	family with sequence similarity 26, member F	**2.04**	2.52E-04	1.28E-03
10578	GNLY	granulysin	**2.04**	8.43E-04	2.88E-03
8337 /// 723790	HIST2H2AA3 /// HIST2H2AA4	histone cluster 2, H2aa3 /// histone cluster 2, H2aa4	**2.04**	1.62E-04	9.67E-04
3998	LMAN1	lectin, mannose-binding, 1	**2.04**	4.76E-05	4.57E-04
51537	MTFP1	mitochondrial fission process 1	**2.04**	3.12E-04	1.46E-03
4547	MTTP	microsomal triglyceride transfer protein	**2.04**	7.46E-05	5.90E-04

Appendix B (continued)

TABLE VII:
GENES DIFFERENTIALLY EXPRESSED IN CULTURED HUMAN CUMULUS GRANULOSA CELLS FOLLOWING FSH TREATMENT FOR 48H

EntrezID	Symbol	Name	Geometric mean of intensities (FSH/Control)	P-value	FDR
126969	SLC44A3	solute carrier family 44, member 3	**2.04**	3.91E-04	1.69E-03
6907	TBL1X	transducin (beta)-like 1X-linked	**2.04**	5.87E-04	2.22E-03
26608	TBL2	transducin (beta)-like 2	**2.04**	2.76E-05	3.45E-04
148534	TMEM56	transmembrane protein 56	**2.04**	8.38E-05	6.30E-04
131540	ZDHHC19	zinc finger, DHHC-type containing 19	**2.04**	5.50E-04	2.13E-03
11041	B3GNT1	UDP-GlcNAc:betaGal beta-1,3-N-acetylglucosaminyltransferase 1	**2.00**	3.84E-05	4.05E-04
3417	IDH1	isocitrate dehydrogenase 1 (NADP+), soluble	**2.00**	1.14E-03	3.53E-03
66004	LYNX1	Ly6/neurotoxin 1	**2.00**	3.65E-05	3.96E-04
84709	MGARP	mitochondria-localized glutamic acid-rich protein	**2.00**	1.76E-04	1.01E-03
27030	MLH3	mutL homolog 3 (E. coli)	**2.00**	8.92E-05	6.53E-04
25849	PARM1	prostate androgen-regulated mucin-like protein 1	**2.00**	4.38E-05	4.34E-04
26499	PLEK2	pleckstrin 2	**2.00**	1.77E-04	1.02E-03
55974	SLC50A1	solute carrier family 50 (sugar transporter), member 1	**2.00**	1.25E-04	8.05E-04
171546	SPTSSA	serine palmitoyltransferase, small subunit A	**2.00**	6.91E-05	5.56E-04
1282	COL4A1	collagen, type IV, alpha 1	**1.96**	8.76E-04	2.97E-03
1909	EDNRA	endothelin receptor type A	**1.96**	2.00E-03	5.40E-03
2026	ENO2	enolase 2 (gamma, neuronal)	**1.96**	3.38E-04	1.54E-03
10144	FAM13A	family with sequence similarity 13, member A	**1.96**	5.23E-05	4.76E-04

Appendix B (continued)

TABLE VII:
GENES DIFFERENTIALLY EXPRESSED IN CULTURED HUMAN CUMULUS GRANULOSA CELLS FOLLOWING FSH TREATMENT FOR 48H

EntrezID	Symbol	Name	Geometric mean of intensities (FSH/Control)	P-value	FDR
2222	FDFT1	farnesyl-diphosphate farnesyltransferase 1	**1.96**	8.26E-05	6.29E-04
2626	GATA4	GATA binding protein 4	**1.96**	9.80E-04	3.18E-03
7923	HSD17B8	hydroxysteroid (17-beta) dehydrogenase 8	**1.96**	8.77E-05	6.49E-04
3655	ITGA6	integrin, alpha 6	**1.96**	3.97E-05	4.11E-04
1955	MEGF9	multiple EGF-like-domains 9	**1.96**	5.86E-05	5.06E-04
56675	NRIP3	nuclear receptor interacting protein 3	**1.96**	4.64E-05	4.50E-04
11145	PLA2G16	phospholipase A2, group XVI	**1.96**	8.40E-04	2.88E-03
6457	SH3GL3	SH3-domain GRB2-like 3	**1.96**	1.01E-04	7.07E-04
5552	SRGN	serglycin	**1.96**	3.46E-03	8.32E-03
7076	TIMP1	TIMP metallopeptidase inhibitor 1	**1.96**	9.25E-05	6.66E-04
26036	ZNF451	zinc finger protein 451	**1.96**	3.89E-04	1.69E-03
55907	CMAS	cytidine monophosphate N-acetylneuraminic acid synthetase	**1.92**	6.32E-05	5.25E-04
58487	CREBZF	CREB/ATF bZIP transcription factor	**1.92**	1.31E-04	8.32E-04
30001	ERO1L	ERO1-like (S. cerevisiae)	**1.92**	2.59E-04	1.29E-03
9289	GPR56	G protein-coupled receptor 56	**1.92**	9.11E-04	3.03E-03
326625	MMAB	methylmalonic aciduria (cobalamin deficiency) cblB type	**1.92**	4.44E-05	4.37E-04
79770	TXNDC15	thioredoxin domain containing 15	**1.92**	4.26E-04	1.79E-03
10349	ABCA10	ATP-binding cassette, sub-family A (ABC1), member 10	**1.89**	6.41E-04	2.37E-03

Appendix B (continued)

TABLE VII:
GENES DIFFERENTIALLY EXPRESSED IN CULTURED HUMAN CUMULUS GRANULOSA CELLS FOLLOWING FSH TREATMENT FOR 48H

EntrezID	Symbol	Name	Geometric mean of intensities (FSH/Control)	P-value	FDR
64283	ARHGEF28	Rho guanine nucleotide exchange factor (GEF) 28	**1.89**	6.23E-04	2.32E-03
91947	ARRDC4	arrestin domain containing 4	**1.89**	6.92E-05	5.56E-04
26033	ATRNL1	attractin-like 1	**1.89**	6.62E-05	5.43E-04
126731	CCSAP	centriole, cilia and spindle-associated protein	**1.89**	5.72E-04	2.19E-03
1139 /// 89832	CHRFAM7A /// CHRNA7	CHRNA7 (cholinergic receptor, nicotinic, alpha 7, exons 5-10) and FAM7A (family with sequence similarity 7A, exons A-E) fusion /// cholinergic receptor, nicotinic, alpha 7 (neuronal)	**1.89**	6.02E-05	5.15E-04
84649	DGAT2	diacylglycerol O-acyltransferase 2	**1.89**	6.06E-05	5.16E-04
54566	EPB41L4B	erythrocyte membrane protein band 4.1 like 4B	**1.89**	2.58E-04	1.29E-03
202134 /// 285596 /// 653316 /// 100507387	FAM153A /// FAM153B /// FAM153C /// LOC100507387	family with sequence similarity 153, member A /// family with sequence similarity 153, member B /// family with sequence similarity 153, member C, pseudogene /// uncharacterized LOC100507387	**1.89**	4.40E-04	1.84E-03
26355	FAM162A	family with sequence similarity 162, member A	**1.89**	3.09E-03	7.63E-03
2897	GRIK1	glutamate receptor, ionotropic, kainate 1	**1.89**	7.06E-04	2.53E-03
3643	INSR	insulin receptor	**1.89**	3.64E-04	1.61E-03
8930	MBD4	methyl-CpG binding domain protein 4	**1.89**	2.81E-04	1.35E-03
23616 /// 57026	PDXP /// SH3BP1	pyridoxal (pyridoxine, vitamin B6) phosphatase /// SH3-domain binding protein 1	**1.89**	5.52E-04	2.13E-03

Appendix B (continued)

TABLE VII:
GENES DIFFERENTIALLY EXPRESSED IN CULTURED HUMAN CUMULUS GRANULOSA CELLS FOLLOWING FSH TREATMENT FOR 48H

EntrezID	Symbol	Name	Geometric mean of intensities (FSH/Control)	P-value	FDR
81579	PLA2G12A	phospholipase A2, group XIIA	**1.89**	8.01E-05	6.16E-04
59339	PLEKHA2	pleckstrin homology domain containing, family A (phosphoinositide binding specific) member 2	**1.89**	1.41E-03	4.15E-03
9050	PSTPIP2	proline-serine-threonine phosphatase interacting protein 2	**1.89**	1.96E-04	1.07E-03
5737	PTGFR	prostaglandin F receptor (FP)	**1.89**	1.38E-04	8.62E-04
22937	SCAP	SREBF chaperone	**1.89**	2.83E-04	1.36E-03
254428	SLC41A1	solute carrier family 41, member 1	**1.89**	6.16E-05	5.18E-04
7763	ZFAND5	zinc finger, AN1-type domain 5	**1.89**	1.29E-03	3.88E-03
83451	ABHD11	abhydrolase domain containing 11	**1.85**	2.71E-04	1.33E-03
55198	APPL2	adaptor protein, phosphotyrosine interaction, PH domain and leucine zipper containing 2	**1.85**	1.92E-04	1.06E-03
1051	CEBPB	CCAAT/enhancer binding protein (C/EBP), beta	**1.85**	9.45E-04	3.12E-03
130106	CIB4	calcium and integrin binding family member 4	**1.85**	1.90E-03	5.19E-03
51016	EMC9	ER membrane protein complex subunit 9	**1.85**	3.77E-04	1.65E-03
22875	ENPP4	ectonucleotide pyrophosphatase/phosphodiesterase 4 (putative)	**1.85**	1.42E-04	8.72E-04
55733	HHAT	hedgehog acyltransferase	**1.85**	6.63E-04	2.43E-03
3622	ING2	inhibitor of growth family, member 2	**1.85**	1.07E-04	7.30E-04
4208	MEF2C	myocyte enhancer factor 2C	**1.85**	8.20E-05	6.27E-04

Appendix B (continued)

TABLE VII:
GENES DIFFERENTIALLY EXPRESSED IN CULTURED HUMAN CUMULUS GRANULOSA CELLS FOLLOWING FSH TREATMENT FOR 48H

EntrezID	Symbol	Name	Geometric mean of intensities (FSH/Control)	P-value	FDR
4351	MPI	mannose phosphate isomerase	**1.85**	3.90E-04	1.69E-03
8497	PPFIA4	protein tyrosine phosphatase, receptor type, f polypeptide (PTPRF), interacting protein (liprin), alpha 4	**1.85**	3.03E-03	7.52E-03
9779	TBC1D5	TBC1 domain family, member 5	**1.85**	3.50E-04	1.58E-03
80194	TMEM134	transmembrane protein 134	**1.85**	9.17E-05	6.64E-04
1032	CDKN2D	cyclin-dependent kinase inhibitor 2D (p19, inhibits CDK4)	**1.82**	2.61E-03	6.67E-03
79586	CHPF	chondroitin polymerizing factor	**1.82**	3.40E-03	8.21E-03
51428	DDX41	DEAD (Asp-Glu-Ala-Asp) box polypeptide 41	**1.82**	5.00E-04	2.01E-03
2135	EXTL2	exostosin-like glycosyltransferase 2	**1.82**	3.08E-04	1.45E-03
2146	EZH2	enhancer of zeste homolog 2 (Drosophila)	**1.82**	8.57E-05	6.37E-04
54985	HCFC1R1	host cell factor C1 regulator 1 (XPO1 dependent)	**1.82**	2.64E-04	1.30E-03
10525	HYOU1	hypoxia up-regulated 1	**1.82**	1.35E-04	8.48E-04
9110	MTMR4	myotubularin related protein 4	**1.82**	2.37E-04	1.22E-03
266812	NAP1L5	nucleosome assembly protein 1-like 5	**1.82**	4.97E-04	2.00E-03
23037	PDZD2	PDZ domain containing 2	**1.82**	4.39E-04	1.83E-03
8544	PIR	pirin (iron-binding nuclear protein)	**1.82**	4.35E-04	1.82E-03
57580	PREX1	phosphatidylinositol-3,4,5-trisphosphate-dependent Rac exchange factor 1	**1.82**	2.63E-04	1.30E-03
84153	RNASEH2C	ribonuclease H2, subunit C	**1.82**	9.87E-05	6.93E-04

Appendix B (continued)

TABLE VII:
GENES DIFFERENTIALLY EXPRESSED IN CULTURED HUMAN CUMULUS GRANULOSA CELLS FOLLOWING FSH TREATMENT FOR 48H

EntrezID	Symbol	Name	Geometric mean of intensities (FSH/Control)	P-value	FDR
6448	SGSH	N-sulfoglucosamine sulfohydrolase	**1.82**	2.72E-04	1.33E-03
56935	SMCO4	single-pass membrane protein with coiled-coil domains 4	**1.82**	2.48E-04	1.26E-03
6745	SSR1	signal sequence receptor, alpha	**1.82**	1.11E-04	7.46E-04
353088	ZNF429	zinc finger protein 429	**1.82**	3.17E-03	7.77E-03
205 /// 100507855	AK4 /// LOC100507855	adenylate kinase 4 /// adenylate kinase isoenzyme 4, mitochondrial-like	**1.79**	2.07E-03	5.53E-03
342	APOC1P1	apolipoprotein C-I pseudogene 1	**1.79**	1.31E-04	8.32E-04
51008	ASCC1	activating signal cointegrator 1 complex subunit 1	**1.79**	2.00E-04	1.09E-03
444	ASPH	aspartate beta-hydroxylase	**1.79**	3.99E-04	1.72E-03
664	BNIP3	BCL2/adenovirus E1B 19kDa interacting protein 3	**1.79**	1.44E-03	4.19E-03
10384	BTN3A3	butyrophilin, subfamily 3, member A3	**1.79**	1.85E-04	1.04E-03
1026	CDKN1A	cyclin-dependent kinase inhibitor 1A (p21, Cip1)	**1.79**	1.78E-04	1.02E-03
29904 /// 101060570	EEF2K /// LOC101060570	eukaryotic elongation factor-2 kinase /// eukaryotic elongation factor 2 kinase-like	**1.79**	1.90E-04	1.06E-03
1948	EFNB2	ephrin-B2	**1.79**	4.10E-03	9.44E-03
2232	FDXR	ferredoxin reductase	**1.79**	1.38E-04	8.62E-04
5096	PCCB	propionyl CoA carboxylase, beta polypeptide	**1.79**	1.66E-04	9.73E-04
11099	PTPN21	protein tyrosine phosphatase, non-receptor type 21	**1.79**	2.47E-03	6.35E-03
57414	RHBDD2	rhomboid domain containing 2	**1.79**	5.01E-04	2.01E-03

Appendix B (continued)

TABLE VII:
GENES DIFFERENTIALLY EXPRESSED IN CULTURED HUMAN CUMULUS GRANULOSA CELLS FOLLOWING FSH TREATMENT FOR 48H

EntrezID	Symbol	Name	Geometric mean of intensities (FSH/Control)	P-value	FDR
6095	RORA	RAR-related orphan receptor A	**1.79**	1.90E-04	1.06E-03
60592	SCOC	short coiled-coil protein	**1.79**	1.12E-04	7.49E-04
84912	SLC35B4	solute carrier family 35, member B4	**1.79**	1.86E-04	1.04E-03
79939	SLC35E1	solute carrier family 35, member E1	**1.79**	4.17E-04	1.77E-03
7108	TM7SF2	transmembrane 7 superfamily member 2	**1.79**	3.93E-04	1.69E-03
65084	TMEM135	transmembrane protein 135	**1.79**	2.18E-04	1.15E-03
26118	WSB1	WD repeat and SOCS box containing 1	**1.79**	2.69E-04	1.32E-03
359	AQP2	aquaporin 2 (collecting duct)	**1.75**	4.73E-04	1.93E-03
26112	CCDC69	coiled-coil domain containing 69	**1.75**	1.78E-04	1.02E-03
22856	CHSY1	chondroitin sulfate synthase 1	**1.75**	1.84E-04	1.04E-03
1628	DBP	D site of albumin promoter (albumin D-box) binding protein	**1.75**	1.56E-03	4.44E-03
84293	FAM213A	family with sequence similarity 213, member A	**1.75**	5.20E-04	2.05E-03
2590	GALNT2	UDP-N-acetyl-alpha-D-galactosamine:polypeptide N-acetylgalactosaminyltransferase 2 (GalNAc-T2)	**1.75**	1.35E-04	8.51E-04
9563	H6PD	hexose-6-phosphate dehydrogenase (glucose 1-dehydrogenase)	**1.75**	2.54E-04	1.28E-03
3077	HFE	hemochromatosis	**1.75**	2.82E-04	1.36E-03
79143	MBOAT7	membrane bound O-acyltransferase domain containing 7	**1.75**	5.19E-04	2.05E-03

Appendix B (continued)

TABLE VII:
GENES DIFFERENTIALLY EXPRESSED IN CULTURED HUMAN CUMULUS GRANULOSA CELLS FOLLOWING FSH TREATMENT FOR 48H

EntrezID	Symbol	Name	Geometric mean of intensities (FSH/Control)	P-value	FDR
2494	NR5A2	nuclear receptor subfamily 5, group A, member 2	**1.75**	2.65E-04	1.31E-03
54502	RBM47	RNA binding motif protein 47	**1.75**	1.80E-04	1.02E-03
58528	RRAGD	Ras-related GTP binding D	**1.75**	5.22E-04	2.05E-03
8819	SAP30	Sin3A-associated protein, 30kDa	**1.75**	1.95E-03	5.31E-03
6484	ST3GAL4	ST3 beta-galactoside alpha-2,3-sialyltransferase 4	**1.75**	4.41E-03	9.99E-03
55578	SUPT20H	suppressor of Ty 20 homolog (S. cerevisiae)	**1.75**	1.70E-04	9.90E-04
9976	CLEC2B	C-type lectin domain family 2, member B	**1.72**	5.63E-04	2.16E-03
220002	CYB561A3	cytochrome b561 family, member A3	**1.72**	1.49E-03	4.30E-03
130589	GALM	galactose mutarotase (aldose 1-epimerase)	**1.72**	1.33E-03	3.98E-03
3708	ITPR1	inositol 1,4,5-trisphosphate receptor, type 1	**1.72**	2.97E-03	7.43E-03
3777	KCNK3	potassium channel, subfamily K, member 3	**1.72**	8.01E-04	2.80E-03
84918	LRP11	low density lipoprotein receptor-related protein 11	**1.72**	1.76E-04	1.01E-03
25895	METTL21B	methyltransferase like 21B	**1.72**	5.73E-04	2.19E-03
9761	MLEC	malectin	**1.72**	2.37E-04	1.22E-03
8613	PPAP2B	phosphatidic acid phosphatase type 2B	**1.72**	6.28E-04	2.34E-03
84513	PPAPDC1B	phosphatidic acid phosphatase type 2 domain containing 1B	**1.72**	1.63E-04	9.68E-04
6038	RNASE4	ribonuclease, RNase A family, 4	**1.72**	2.01E-03	5.41E-03
152503	SH3D19	SH3 domain containing 19	**1.72**	2.15E-03	5.69E-03

Appendix B (continued)

TABLE VII:
GENES DIFFERENTIALLY EXPRESSED IN CULTURED HUMAN CUMULUS GRANULOSA CELLS FOLLOWING FSH TREATMENT FOR 48H

EntrezID	Symbol	Name	Geometric mean of intensities (FSH/Control)	P-value	FDR
1317	SLC31A1	solute carrier family 31 (copper transporters), member 1	**1.72**	2.04E-04	1.10E-03
2542	SLC37A4	solute carrier family 37 (glucose-6-phosphate transporter), member 4	**1.72**	1.72E-04	9.97E-04
84314	TMEM107	transmembrane protein 107	**1.72**	8.17E-04	2.83E-03
7298	TYMS	thymidylate synthetase	**1.72**	1.72E-03	4.82E-03
84196	USP48	ubiquitin specific peptidase 48	**1.72**	5.99E-04	2.26E-03
5829	PXN	paxillin	**1.72**	5.32E-04	2.09E-03
29071	C1GALT1C1	C1GALT1-specific chaperone 1	**1.69**	3.27E-03	7.95E-03
441150	C6orf226	chromosome 6 open reading frame 226	**1.69**	3.33E-04	1.53E-03
4179	CD46	CD46 molecule, complement regulatory protein	**1.69**	2.80E-04	1.35E-03
9653	HS2ST1	heparan sulfate 2-O-sulfotransferase 1	**1.69**	2.50E-04	1.27E-03
57613	KIAA1467	KIAA1467	**1.69**	2.38E-04	1.22E-03
57631	LRCH2	leucine-rich repeats and calponin homology (CH) domain containing 2	**1.69**	1.74E-04	1.00E-03
4054	LTBP3	latent transforming growth factor beta binding protein 3	**1.69**	6.56E-04	2.42E-03
11237	RNF24	ring finger protein 24	**1.69**	2.13E-03	5.64E-03
6535	SLC6A8	solute carrier family 6 (neurotransmitter transporter, creatine), member 8	**1.69**	8.43E-04	2.88E-03
57620	STIM2	stromal interaction molecule 2	**1.69**	9.53E-04	3.12E-03
55080	TAPBPL	TAP binding protein-like	**1.69**	2.04E-03	5.45E-03

Appendix B (continued)

TABLE VII:
GENES DIFFERENTIALLY EXPRESSED IN CULTURED HUMAN CUMULUS GRANULOSA CELLS FOLLOWING FSH TREATMENT FOR 48H

EntrezID	Symbol	Name	Geometric mean of intensities (FSH/Control)	P-value	FDR
7769	ZNF226	zinc finger protein 226	**1.69**	2.43E-04	1.24E-03
196394	AMN1	antagonist of mitotic exit network 1 homolog (S. cerevisiae)	**1.67**	8.31E-04	2.86E-03
8542 /// 23780	APOL1 /// APOL2	apolipoprotein L, 1 /// apolipoprotein L, 2	**1.67**	8.47E-04	2.89E-03
79135	APOO	apolipoprotein O	**1.67**	1.16E-03	3.58E-03
387763	C11orf96	chromosome 11 open reading frame 96	**1.67**	2.57E-04	1.29E-03
1605	DAG1	dystroglycan 1 (dystrophin-associated glycoprotein 1)	**1.67**	3.36E-04	1.54E-03
9201	DCLK1	doublecortin-like kinase 1	**1.67**	4.45E-04	1.85E-03
5611	DNAJC3	DnaJ (Hsp40) homolog, subfamily C, member 3	**1.67**	6.46E-04	2.39E-03
55816	DOK5	docking protein 5	**1.67**	5.40E-04	2.10E-03
202134 /// 100507387	FAM153B /// LOC100507387	family with sequence similarity 153, member B /// uncharacterized LOC100507387	**1.67**	4.17E-03	9.55E-03
668	FOXL2	forkhead box L2	**1.67**	3.39E-04	1.54E-03
2537	IFI6	interferon, alpha-inducible protein 6	**1.67**	2.90E-04	1.39E-03
6535 /// 386757 /// 653562	LOC653562 /// SLC6A10P /// SLC6A8	sodium- and chloride-dependent creatine transporter 1-like /// solute carrier family 6 (neurotransmitter transporter, creatine), member 10, pseudogene /// solute carrier family 6 (neurotransmitter transporter, creatine), member 8	**1.67**	1.77E-03	4.92E-03
10529	NEBL	nebulette	**1.67**	2.40E-04	1.23E-03
51701	NLK	nemo-like kinase	**1.67**	2.19E-03	5.75E-03
54681	P4HTM	prolyl 4-hydroxylase, transmembrane (endoplasmic reticulum)	**1.67**	4.07E-04	1.74E-03

Appendix B (continued)

TABLE VII:
GENES DIFFERENTIALLY EXPRESSED IN CULTURED HUMAN CUMULUS GRANULOSA CELLS FOLLOWING FSH TREATMENT FOR 48H

EntrezID	Symbol	Name	Geometric mean of intensities (FSH/Control)	P-value	FDR
25797	QPCT	glutaminyl-peptide cyclotransferase	**1.67**	3.77E-04	1.65E-03
375287	RBM43	RNA binding motif protein 43	**1.67**	1.03E-03	3.31E-03
114134	SLC2A13	solute carrier family 2 (facilitated glucose transporter), member 13	**1.67**	2.80E-03	7.08E-03
113235	SLC46A1	solute carrier family 46 (folate transporter), member 1	**1.67**	1.11E-03	3.48E-03
6536	SLC6A9	solute carrier family 6 (neurotransmitter transporter, glycine), member 9	**1.67**	2.60E-03	6.66E-03
9806	SPOCK2	sparc/osteonectin, cwcv and kazal-like domains proteoglycan (testican) 2	**1.67**	5.60E-04	2.16E-03
161742	SPRED1	sprouty-related, EVH1 domain containing 1	**1.67**	1.09E-03	3.44E-03
84620	ST6GAL2	ST6 beta-galactosamide alpha-2,6-sialyltranferase 2	**1.67**	1.33E-03	3.98E-03
54885	TBC1D8B	TBC1 domain family, member 8B (with GRAM domain)	**1.67**	4.11E-04	1.75E-03
9524	TECR	trans-2,3-enoyl-CoA reductase	**1.67**	8.07E-04	2.81E-03
100113407	TMEM170B	transmembrane protein 170B	**1.67**	1.33E-03	3.98E-03
57695	USP37	ubiquitin specific peptidase 37	**1.67**	3.37E-04	1.54E-03
55326	AGPAT5	1-acylglycerol-3-phosphate O-acyltransferase 5	**1.64**	4.02E-04	1.72E-03
204	AK2	adenylate kinase 2	**1.64**	3.04E-03	7.54E-03
269	AMHR2	anti-Mullerian hormone receptor, type II	**1.64**	2.95E-04	1.40E-03
401152	C4orf3	chromosome 4 open reading frame 3	**1.64**	1.15E-03	3.55E-03
93058	COQ10A	coenzyme Q10 homolog A (S. cerevisiae)	**1.64**	3.55E-04	1.59E-03

Appendix B (continued)

TABLE VII:
GENES DIFFERENTIALLY EXPRESSED IN CULTURED HUMAN CUMULUS GRANULOSA CELLS FOLLOWING FSH TREATMENT FOR 48H

EntrezID	Symbol	Name	Geometric mean of intensities (FSH/Control)	P-value	FDR
285527	FRYL	FRY-like	**1.64**	1.12E-03	3.50E-03
55568	GALNT10	UDP-N-acetyl-alpha-D-galactosamine:polypeptide N-acetylgalactosaminyltransferase 10 (GalNAc-T10)	**1.64**	5.63E-04	2.16E-03
442245	GSTM2P1	glutathione S-transferase mu 2 (muscle) pseudogene 1	**1.64**	8.31E-04	2.86E-03
4817	NIT1	nitrilase 1	**1.64**	2.84E-04	1.36E-03
4940	OAS3	2'-5'-oligoadenylate synthetase 3, 100kDa	**1.64**	3.76E-03	8.86E-03
6041	RNASEL	ribonuclease L (2',5'-oligoisoadenylate synthetase-dependent)	**1.64**	3.42E-04	1.55E-03
5104	SERPINA5	serpin peptidase inhibitor, clade A (alpha-1 antiproteinase, antitrypsin), member 5	**1.64**	2.79E-03	7.05E-03
114132	SIGLEC11	sialic acid binding Ig-like lectin 11	**1.64**	3.10E-04	1.46E-03
10280	SIGMAR1	sigma non-opioid intracellular receptor 1	**1.64**	5.07E-04	2.02E-03
55186	SLC25A36	solute carrier family 25 (pyrimidine nucleotide carrier), member 36	**1.64**	9.49E-04	3.12E-03
23635	SSBP2	single-stranded DNA binding protein 2	**1.64**	4.24E-04	1.79E-03
11257	TP53TG1	TP53 target 1 (non-protein coding)	**1.64**	5.30E-04	2.08E-03
155382	VPS37D	vacuolar protein sorting 37 homolog D (S. cerevisiae)	**1.64**	8.11E-04	2.82E-03
205428	C3orf58	chromosome 3 open reading frame 58	**1.61**	1.98E-03	5.36E-03
51144	HSD17B12	hydroxysteroid (17-beta) dehydrogenase 12	**1.61**	5.16E-04	2.04E-03
9452	ITM2A	integral membrane protein 2A	**1.61**	3.46E-04	1.57E-03

Appendix B (continued)

TABLE VII:
GENES DIFFERENTIALLY EXPRESSED IN CULTURED HUMAN CUMULUS GRANULOSA CELLS FOLLOWING FSH TREATMENT FOR 48H

EntrezID	Symbol	Name	Geometric mean of intensities (FSH/Control)	P-value	FDR
11228 /// 100996477	LOC100996477 /// RASSF8	uncharacterized LOC100996477 /// Ras association (RalGDS/AF-6) domain family (N-terminal) member 8	**1.61**	5.06E-04	2.02E-03
4354	MPP1	membrane protein, palmitoylated 1, 55kDa	**1.61**	8.59E-04	2.92E-03
5359	PLSCR1	phospholipid scramblase 1	**1.61**	1.50E-03	4.31E-03
11228	RASSF8	Ras association (RalGDS/AF-6) domain family (N-terminal) member 8	**1.61**	1.51E-03	4.32E-03
55652	SLC48A1	solute carrier family 48 (heme transporter), member 1	**1.61**	4.91E-04	1.99E-03
801 /// 805 /// 808	CALM1 /// CALM2 /// CALM3	calmodulin 1 (phosphorylase kinase, delta) /// calmodulin 2 (phosphorylase kinase, delta) /// calmodulin 3 (phosphorylase kinase, delta)	**1.59**	4.72E-04	1.92E-03
55755	CDK5RAP2	CDK5 regulatory subunit associated protein 2	**1.59**	4.43E-04	1.84E-03
84064	HDHD2	haloacid dehalogenase-like hydrolase domain containing 2	**1.59**	1.23E-03	3.75E-03
25994	HIGD1A	HIG1 hypoxia inducible domain family, member 1A	**1.59**	2.64E-03	6.74E-03
3017	HIST1H2BD	histone cluster 1, H2bd	**1.59**	6.02E-04	2.26E-03
3652	IPP	intracisternal A particle-promoted polypeptide	**1.59**	5.38E-04	2.10E-03
10609	LEPREL4	leprecan-like 4	**1.59**	7.85E-04	2.75E-03
727764 /// 100132288 /// 100233156	LOC100233156 /// MAFIP /// TEKT4P2	tektin 4 pseudogene /// MAFF interacting protein (pseudogene) /// tektin 4 pseudogene 2	**1.59**	9.58E-04	3.13E-03

Appendix B (continued)

TABLE VII:
GENES DIFFERENTIALLY EXPRESSED IN CULTURED HUMAN CUMULUS GRANULOSA CELLS FOLLOWING FSH TREATMENT FOR 48H

EntrezID	Symbol	Name	Geometric mean of intensities (FSH/Control)	P-value	FDR
9227	LRAT	lecithin retinol acyltransferase (phosphatidylcholine--retinol O-acyltransferase)	**1.59**	7.74E-04	2.72E-03
100507436	MICA	MHC class I polypeptide-related sequence A	**1.59**	9.64E-04	3.14E-03
54681	P4HTM	prolyl 4-hydroxylase, transmembrane (endoplasmic reticulum)	**1.59**	3.24E-03	7.90E-03
5069	PAPPA	pregnancy-associated plasma protein A, pappalysin 1	**1.59**	1.49E-03	4.30E-03
51449	PCYOX1	prenylcysteine oxidase 1	**1.59**	3.63E-03	8.65E-03
2923	PDIA3	protein disulfide isomerase family A, member 3	**1.59**	7.10E-04	2.54E-03
5230	PGK1	phosphoglycerate kinase 1	**1.59**	3.67E-03	8.70E-03
114825	PWWP2A	PWWP domain containing 2A	**1.59**	8.77E-04	2.97E-03
92840	REEP6	receptor accessory protein 6	**1.59**	9.50E-04	3.12E-03
55316	RSAD1	radical S-adenosyl methionine domain containing 1	**1.59**	7.46E-04	2.65E-03
51092	SIDT2	SID1 transmembrane family, member 2	**1.59**	5.01E-04	2.01E-03
10413	YAP1	Yes-associated protein 1	**1.59**	4.72E-04	1.92E-03
			1.59	2.72E-03	6.90E-03
249	ALPL	alkaline phosphatase, liver/bone/kidney	**1.56**	2.21E-03	5.80E-03
11118	BTN3A2	butyrophilin, subfamily 3, member A2	**1.56**	7.55E-04	2.67E-03
28970	C11orf54	chromosome 11 open reading frame 54	**1.56**	7.46E-04	2.65E-03
387882	C12orf75	chromosome 12 open reading frame 75	**1.56**	8.85E-04	2.98E-03

Appendix B (continued)

TABLE VII:
GENES DIFFERENTIALLY EXPRESSED IN CULTURED HUMAN CUMULUS GRANULOSA CELLS FOLLOWING FSH TREATMENT FOR 48H

EntrezID	Symbol	Name	Geometric mean of intensities (FSH/Control)	P-value	FDR
55297	CCDC91	coiled-coil domain containing 91	**1.56**	4.11E-03	9.44E-03
79132	DHX58	DEXH (Asp-Glu-X-His) box polypeptide 58	**1.56**	6.07E-04	2.27E-03
55268	ECHDC2	enoyl CoA hydratase domain containing 2	**1.56**	6.28E-04	2.34E-03
54583	EGLN1	egl nine homolog 1 (C. elegans)	**1.56**	1.10E-03	3.47E-03
23065	EMC1	ER membrane protein complex subunit 1	**1.56**	1.45E-03	4.20E-03
80020	FOXRED2	FAD-dependent oxidoreductase domain containing 2	**1.56**	1.56E-03	4.44E-03
56261	GPCPD1	glycerophosphocholine phosphodiesterase GDE1 homolog (S. cerevisiae)	**1.56**	1.19E-03	3.66E-03
3977	LIFR	leukemia inhibitory factor receptor alpha	**1.56**	1.14E-03	3.53E-03
4061	LY6E	lymphocyte antigen 6 complex, locus E	**1.56**	3.80E-03	8.93E-03
23252	OTUD3	OTU domain containing 3	**1.56**	1.98E-03	5.35E-03
5034	P4HB	prolyl 4-hydroxylase, beta polypeptide	**1.56**	1.50E-03	4.30E-03
375484	SIMC1	SUMO-interacting motifs containing 1	**1.56**	6.69E-04	2.45E-03
6619	SNAPC3	small nuclear RNA activating complex, polypeptide 3, 50kDa	**1.56**	6.88E-04	2.49E-03
85014	TMEM141	transmembrane protein 141	**1.56**	9.31E-04	3.08E-03
7128	TNFAIP3	tumor necrosis factor, alpha-induced protein 3	**1.56**	1.98E-03	5.36E-03
376940	ZC3H6	zinc finger CCCH-type containing 6	**1.56**	4.87E-03	1.08E-02
155054	ZNF425	zinc finger protein 425	**1.56**	3.86E-03	9.02E-03
23204	ARL6IP1	ADP-ribosylation factor-like 6 interacting protein 1	**1.54**	4.34E-03	9.86E-03

Appendix B (continued)

TABLE VII:
GENES DIFFERENTIALLY EXPRESSED IN CULTURED HUMAN CUMULUS GRANULOSA CELLS FOLLOWING FSH TREATMENT FOR 48H

EntrezID	Symbol	Name	Geometric mean of intensities (FSH/Control)	P-value	FDR
400757	C1orf141	chromosome 1 open reading frame 141	**1.54**	1.87E-03	5.15E-03
794	CALB2	calbindin 2	**1.54**	1.35E-03	4.02E-03
1727	CYB5R3	cytochrome b5 reductase 3	**1.54**	1.46E-03	4.22E-03
2052	EPHX1	epoxide hydrolase 1, microsomal (xenobiotic)	**1.54**	9.10E-04	3.03E-03
2770	GNAI1	guanine nucleotide binding protein (G protein), alpha inhibiting activity polypeptide 1	**1.54**	8.40E-04	2.88E-03
23175	LPIN1	lipin 1	**1.54**	4.77E-03	1.06E-02
4669	NAGLU	N-acetylglucosaminidase, alpha	**1.54**	2.39E-03	6.20E-03
55228	PNMAL1	paraneoplastic Ma antigen family-like 1	**1.54**	7.65E-04	2.70E-03
7779	SLC30A1	solute carrier family 30 (zinc transporter), member 1	**1.54**	2.74E-03	6.95E-03
2040	STOM	stomatin	**1.54**	1.35E-03	4.02E-03
55959	SULF2	sulfatase 2	**1.54**	1.81E-03	5.01E-03
3268	AGFG2	ArfGAP with FG repeats 2	**1.52**	1.62E-03	4.57E-03
9459	ARHGEF6	Rac/Cdc42 guanine nucleotide exchange factor (GEF) 6	**1.52**	1.50E-03	4.30E-03
10396	ATP8A1	ATPase, aminophospholipid transporter (APLT), class I, type 8A, member 1	**1.52**	3.08E-03	7.61E-03
81617	CAB39L	calcium binding protein 39-like	**1.52**	2.24E-03	5.87E-03
961	CD47	CD47 molecule	**1.52**	1.11E-03	3.48E-03
1643	DDB2	damage-specific DNA binding protein 2, 48kDa	**1.52**	4.07E-03	9.37E-03

Appendix B (continued)

TABLE VII:
GENES DIFFERENTIALLY EXPRESSED IN CULTURED HUMAN CUMULUS GRANULOSA CELLS FOLLOWING FSH TREATMENT FOR 48H

EntrezID	Symbol	Name	Geometric mean of intensities (FSH/Control)	P-value	FDR
29904	EEF2K	eukaryotic elongation factor-2 kinase	**1.52**	3.94E-03	9.16E-03
3988	LIPA	lipase A, lysosomal acid, cholesterol esterase	**1.52**	8.90E-04	2.99E-03
84279	PRADC1	protease-associated domain containing 1	**1.52**	4.82E-03	1.07E-02
5962	RDX	radixin	**1.52**	2.09E-03	5.55E-03
51310	SLC22A17	solute carrier family 22, member 17	**1.52**	2.61E-03	6.68E-03
201895	SMIM14	small integral membrane protein 14	**1.52**	2.26E-03	5.91E-03
6609	SMPD1	sphingomyelin phosphodiesterase 1, acid lysosomal	**1.52**	1.47E-03	4.24E-03
6622	SNCA	synuclein, alpha (non A4 component of amyloid precursor)	**1.52**	1.01E-03	3.27E-03
64409	WBSCR17	Williams-Beuren syndrome chromosome region 17	**1.52**	1.41E-03	4.14E-03
10632	ATP5L	ATP synthase, H+ transporting, mitochondrial Fo complex, subunit G	**1.49**	4.54E-03	1.02E-02
1114	CHGB	chromogranin B (secretogranin 1)	**1.49**	2.26E-03	5.91E-03
150864	FAM117B	family with sequence similarity 117, member B	**1.49**	2.19E-03	5.76E-03
158405	KIAA1958	KIAA1958	**1.49**	1.96E-03	5.34E-03
5033	P4HA1	prolyl 4-hydroxylase, alpha polypeptide I	**1.49**	1.38E-03	4.06E-03
116987	AGAP1	ArfGAP with GTPase domain, ankyrin repeat and PH domain 1	**1.47**	5.00E-03	1.10E-02
9236	CCPG1	cell cycle progression 1	**1.47**	3.44E-03	8.28E-03
55790	CSGALNACT1	chondroitin sulfate N-acetylgalactosaminyltransferase 1	**1.47**	4.05E-03	9.34E-03

Appendix B (continued)

TABLE VII:
GENES DIFFERENTIALLY EXPRESSED IN CULTURED HUMAN CUMULUS GRANULOSA CELLS FOLLOWING FSH TREATMENT FOR 48H

EntrezID	Symbol	Name	Geometric mean of intensities (FSH/Control)	P-value	FDR
83641	FAM107B	family with sequence similarity 107, member B	**1.47**	1.96E-03	5.34E-03
2517	FUCA1	fucosidase, alpha-L- 1, tissue	**1.47**	2.02E-03	5.42E-03
51191	HERC5	HECT and RLD domain containing E3 ubiquitin protein ligase 5	**1.47**	1.20E-03	3.68E-03
51528	JKAMP	JNK1/MAPK8-associated membrane protein	**1.47**	2.99E-03	7.46E-03
9060	PAPSS2	3'-phosphoadenosine 5'-phosphosulfate synthase 2	**1.47**	1.38E-03	4.08E-03
5577	PRKAR2B	protein kinase, cAMP-dependent, regulatory, type II, beta	**1.47**	4.49E-03	1.01E-02
285368	PRRT3	proline-rich transmembrane protein 3	**1.47**	1.97E-03	5.35E-03
6646	SOAT1	sterol O-acyltransferase 1	**1.47**	1.44E-03	4.19E-03
7163	TPD52	tumor protein D52	**1.47**	4.78E-03	1.07E-02
54986	ULK4	unc-51-like kinase 4 (C. elegans)	**1.47**	3.02E-03	7.51E-03
23253	ANKRD12	ankyrin repeat domain 12	**1.45**	1.79E-03	4.97E-03
10159	ATP6AP2	ATPase, H+ transporting, lysosomal accessory protein 2	**1.45**	4.56E-03	1.03E-02
996	CDC27	cell division cycle 27	**1.45**	4.62E-03	1.04E-02
6720	SREBF1	sterol regulatory element binding transcription factor 1	**1.45**	2.95E-03	7.38E-03
51768	TM7SF3	transmembrane 7 superfamily member 3	**1.45**	4.25E-03	9.68E-03
27235	COQ2	coenzyme Q2 4-hydroxybenzoate polyprenyltransferase	**1.43**	2.44E-03	6.30E-03

Appendix B (continued)

TABLE VII:
GENES DIFFERENTIALLY EXPRESSED IN CULTURED HUMAN CUMULUS GRANULOSA CELLS FOLLOWING FSH TREATMENT FOR 48H

EntrezID	Symbol	Name	Geometric mean of intensities (FSH/Control)	P-value	FDR
53916 /// 100529262	MIA-RAB4B /// RAB4B	MIA-RAB4B readthrough (NMD candidate) /// RAB4B, member RAS oncogene family	**1.43**	4.80E-03	1.07E-02
23469	PHF3	PHD finger protein 3	**1.43**	4.81E-03	1.07E-02
57181	SLC39A10	solute carrier family 39 (zinc transporter), member 10	**1.43**	2.35E-03	6.09E-03
25917	THUMPD3	THUMP domain containing 3	**1.43**	3.40E-03	8.21E-03
51754	TMEM8B	transmembrane protein 8B	**1.43**	2.17E-03	5.74E-03
64756	ATPAF1	ATP synthase mitochondrial F1 complex assembly factor 1	**1.41**	2.32E-03	6.06E-03
8706	B3GALNT1	beta-1,3-N-acetylgalactosaminyltransferase 1 (globoside blood group)	**1.41**	3.09E-03	7.63E-03
3780	KCNN1	potassium intermediate/small conductance calcium-activated channel, subfamily N, member 1	**1.41**	3.95E-03	9.20E-03
55818	KDM3A	lysine (K)-specific demethylase 3A	**1.41**	4.02E-03	9.31E-03
10628 /// 101060503	LOC101060503 /// TXNIP	thioredoxin-interacting protein-like /// thioredoxin interacting protein	**1.41**	3.28E-03	7.96E-03
9500	MAGED1	melanoma antigen family D, 1	**1.41**	2.87E-03	7.22E-03
79646	PANK3	pantothenate kinase 3	**1.41**	4.16E-03	9.54E-03
118672	PSTK	phosphoseryl-tRNA kinase	**1.41**	2.72E-03	6.90E-03
201266	SLC39A11	solute carrier family 39 (metal ion transporter), member 11	**1.41**	3.18E-03	7.78E-03
63826	SRR	serine racemase	**1.41**	3.14E-03	7.72E-03

Appendix B (continued)

TABLE VII:
GENES DIFFERENTIALLY EXPRESSED IN CULTURED HUMAN CUMULUS GRANULOSA CELLS FOLLOWING FSH TREATMENT FOR 48H

EntrezID	Symbol	Name	Geometric mean of intensities (FSH/Control)	P-value	FDR
255758	TCTEX1D2	Tctex1 domain containing 2	**1.41**	4.85E-03	1.07E-02
124936	CYB5D2	cytochrome b5 domain containing 2	**1.39**	4.34E-03	9.85E-03
2589	GALNT1	UDP-N-acetyl-alpha-D-galactosamine:polypeptide N-acetylgalactosaminyltransferase 1 (GalNAc-T1)	**1.39**	3.93E-03	9.15E-03
113263	GLCCI1	glucocorticoid induced transcript 1	**1.39**	4.20E-03	9.59E-03
2954	GSTZ1	glutathione S-transferase zeta 1	**1.39**	3.37E-03	8.14E-03
3480	IGF1R	insulin-like growth factor 1 receptor	**1.39**	3.36E-03	8.12E-03
28951	TRIB2	tribbles homolog 2 (Drosophila)	**1.39**	3.71E-03	8.78E-03
538	ATP7A	ATPase, Cu++ transporting, alpha polypeptide	**1.37**	4.57E-03	1.03E-02
4267	CD99	CD99 molecule	**1.37**	3.86E-03	9.02E-03
79022	TMEM106C	transmembrane protein 106C	**1.37**	4.85E-03	1.07E-02
125488	TTC39C	tetratricopeptide repeat domain 39C	**1.37**	4.68E-03	1.05E-02
51309	ARMCX1	armadillo repeat containing, X-linked 1	**-1.39**	3.85E-03	9.02E-03
51704	GPRC5B	G protein-coupled receptor, family C, group 5, member B	**-1.39**	3.75E-03	8.86E-03
51351	ZNF117	zinc finger protein 117	**-1.39**	3.40E-03	8.21E-03
1809	DPYSL3	dihydropyrimidinase-like 3	**-1.40**	4.20E-03	9.59E-03
1281	COL3A1	collagen, type III, alpha 1	**-1.41**	2.49E-03	6.41E-03
64754	SMYD3	SET and MYND domain containing 3	**-1.41**	2.73E-03	6.92E-03
7675	ZNF121	zinc finger protein 121	**-1.41**	4.80E-03	1.07E-02

Appendix B (continued)

TABLE VII:
GENES DIFFERENTIALLY EXPRESSED IN CULTURED HUMAN CUMULUS GRANULOSA CELLS FOLLOWING FSH TREATMENT FOR 48H

EntrezID	Symbol	Name	Geometric mean of intensities (FSH/Control)	P-value	FDR
8663 /// 728689	EIF3C /// EIF3CL	eukaryotic translation initiation factor 3, subunit C /// eukaryotic translation initiation factor 3, subunit C-like	**-1.44**	1.95E-03	5.32E-03
3340	NDST1	N-deacetylase/N-sulfotransferase (heparan glucosaminyl) 1	**-1.44**	4.46E-03	1.01E-02
6453	ITSN1	intersectin 1 (SH3 domain protein)	**-1.45**	3.17E-03	7.77E-03
58499	ZNF462	zinc finger protein 462	**-1.45**	2.41E-03	6.23E-03
65009	NDRG4	NDRG family member 4	**-1.46**	3.14E-03	7.73E-03
57606	SLAIN2	SLAIN motif family, member 2	**-1.46**	3.84E-03	9.02E-03
8540	AGPS	alkylglycerone phosphate synthase	**-1.47**	2.22E-03	5.81E-03
2938	GSTA1	glutathione S-transferase alpha 1	**-1.47**	2.12E-03	5.63E-03
55081	IFT57	intraflagellar transport 57 homolog (Chlamydomonas)	**-1.47**	3.70E-03	8.77E-03
57619 /// 100996628	LOC100996628 /// SHROOM3	uncharacterized LOC100996628 /// shroom family member 3	**-1.48**	1.44E-03	4.19E-03
9208	LRRFIP1	leucine rich repeat (in FLII) interacting protein 1	**-1.48**	1.97E-03	5.35E-03
2817	GPC1	glypican 1	**-1.50**	3.84E-03	9.02E-03
10528 /// 26792 /// 692201 /// 692213 /// 100302138	MIR1292 /// NOP56 /// SNORD110 /// SNORD57 /// SNORD86	microRNA 1292 /// NOP56 ribonucleoprotein /// small nucleolar RNA, C/D box 110 /// small nucleolar RNA, C/D box 57 /// small nucleolar RNA, C/D box 86	**-1.50**	2.44E-03	6.30E-03
154796	AMOT	angiomotin	**-1.51**	3.04E-03	7.55E-03
1627	DBN1	drebrin 1	**-1.51**	9.01E-04	3.02E-03

Appendix B (continued)

TABLE VII:
GENES DIFFERENTIALLY EXPRESSED IN CULTURED HUMAN CUMULUS GRANULOSA CELLS FOLLOWING FSH TREATMENT FOR 48H

EntrezID	Symbol	Name	Geometric mean of intensities (FSH/Control)	P-value	FDR
11275	KLHL2	kelch-like family member 2	**-1.51**	2.01E-03	5.40E-03
51474	LIMA1	LIM domain and actin binding 1	**-1.51**	2.18E-03	5.75E-03
54407	SLC38A2	solute carrier family 38, member 2	**-1.51**	3.09E-03	7.63E-03
1545	CYP1B1	cytochrome P450, family 1, subfamily B, polypeptide 1	**-1.52**	3.52E-03	8.44E-03
3925	STMN1	stathmin 1	**-1.52**	1.06E-03	3.38E-03
308	ANXA5	annexin A5	**-1.53**	1.52E-03	4.33E-03
3224	HOXC8	homeobox C8	**-1.53**	1.74E-03	4.84E-03
89796	NAV1	neuron navigator 1	**-1.53**	8.22E-04	2.85E-03
158471	PRUNE2	prune homolog 2 (Drosophila)	**-1.53**	1.30E-03	3.92E-03
10308	ZNF267	zinc finger protein 267	**-1.53**	2.56E-03	6.55E-03
10276	NET1	neuroepithelial cell transforming 1	**-1.54**	1.63E-03	4.60E-03
81831	NETO2	neuropilin (NRP) and tolloid (TLL)-like 2	**-1.54**	3.79E-03	8.92E-03
7088	TLE1	transducin-like enhancer of split 1 (E(sp1) homolog, Drosophila)	**-1.54**	1.08E-03	3.43E-03
115123	41701	membrane-associated ring finger (C3HC4) 3, E3 ubiquitin protein ligase	**-1.55**	3.15E-03	7.75E-03
1969	EPHA2	EPH receptor A2	**-1.55**	2.26E-03	5.91E-03
10516	FBLN5	fibulin 5	**-1.55**	9.53E-04	3.12E-03
204962	SLC44A5	solute carrier family 44, member 5	**-1.55**	3.88E-03	9.06E-03
55714	TENM3	teneurin transmembrane protein 3	**-1.55**	2.29E-03	5.98E-03

Appendix B (continued)

TABLE VII:
GENES DIFFERENTIALLY EXPRESSED IN CULTURED HUMAN CUMULUS GRANULOSA CELLS FOLLOWING FSH TREATMENT FOR 48H

EntrezID	Symbol	Name	Geometric mean of intensities (FSH/Control)	P-value	FDR
64084	CLSTN2	calsyntenin 2	**-1.56**	9.22E-04	3.06E-03
8577 /// 100526694	MSANTD3-TMEFF1 /// TMEFF1	MSANTD3-TMEFF1 readthrough /// transmembrane protein with EGF-like and two follistatin-like domains 1	**-1.56**	2.16E-03	5.70E-03
6282	S100A11	S100 calcium binding protein A11	**-1.56**	4.33E-03	9.85E-03
3315	HSPB1	heat shock 27kDa protein 1	**-1.57**	3.25E-03	7.92E-03
4129	MAOB	monoamine oxidase B	**-1.57**	4.82E-03	1.07E-02
4641	MYO1C	myosin IC	**-1.57**	1.96E-03	5.34E-03
65062	TMEM237	transmembrane protein 237	**-1.57**	1.82E-03	5.02E-03
79158	GNPTAB	N-acetylglucosamine-1-phosphate transferase, alpha and beta subunits	**-1.59**	8.98E-04	3.01E-03
3958	LGALS3	lectin, galactoside-binding, soluble, 3	**-1.59**	1.06E-03	3.39E-03
8463	TEAD2	TEA domain family member 2	**-1.59**	7.65E-04	2.70E-03
51199	NIN	ninein (GSK3B interacting protein)	**-1.60**	1.80E-03	4.99E-03
10085	EDIL3	EGF-like repeats and discoidin I-like domains 3	**-1.61**	1.31E-03	3.92E-03
56925	LXN	latexin	**-1.61**	4.48E-03	1.01E-02
64359	NXN	nucleoredoxin	**-1.61**	2.77E-03	7.00E-03
55240	STEAP3	STEAP family member 3, metalloreductase	**-1.61**	4.42E-03	1.00E-02
2633	GBP1	guanylate binding protein 1, interferon-inducible	**-1.62**	3.96E-03	9.20E-03
4094	MAF	v-maf musculoaponeurotic fibrosarcoma oncogene homolog (avian)	**-1.62**	4.14E-03	9.52E-03

Appendix B (continued)

TABLE VII:
GENES DIFFERENTIALLY EXPRESSED IN CULTURED HUMAN CUMULUS GRANULOSA CELLS FOLLOWING FSH TREATMENT FOR 48H

EntrezID	Symbol	Name	Geometric mean of intensities (FSH/Control)	P-value	FDR
4659	PPP1R12A	protein phosphatase 1, regulatory subunit 12A	**-1.62**	8.43E-04	2.88E-03
26278	SACS	spastic ataxia of Charlevoix-Saguenay (sacsin)	**-1.62**	1.99E-03	5.38E-03
7111	TMOD1	tropomodulin 1	**-1.62**	2.10E-03	5.58E-03
94241	TP53INP1	tumor protein p53 inducible nuclear protein 1	**-1.62**	1.48E-03	4.26E-03
131566	DCBLD2	discoidin, CUB and LCCL domain containing 2	**-1.63**	1.11E-03	3.48E-03
54433	GAR1	GAR1 ribonucleoprotein homolog (yeast)	**-1.63**	2.98E-04	1.41E-03
8870	IER3	immediate early response 3	**-1.63**	6.94E-04	2.50E-03
116092	DNTTIP1	deoxynucleotidyltransferase, terminal, interacting protein 1	**-1.64**	1.57E-03	4.44E-03
3486	IGFBP3	insulin-like growth factor binding protein 3	**-1.64**	3.21E-03	7.84E-03
84230	LRRC8C	leucine rich repeat containing 8 family, member C	**-1.64**	1.04E-03	3.32E-03
30851 /// 100533970	P2RX5-TAX1BP3 /// TAX1BP3	P2RX5-TAX1BP3 readthrough /// Tax1 (human T-cell leukemia virus type I) binding protein 3	**-1.64**	5.06E-04	2.02E-03
6414	SEPP1	selenoprotein P, plasma, 1	**-1.64**	2.98E-03	7.43E-03
6575	SLC20A2	solute carrier family 20 (phosphate transporter), member 2	**-1.64**	1.45E-03	4.20E-03
9948	WDR1	WD repeat domain 1	**-1.64**	1.82E-03	5.03E-03
222389	BEND7	BEN domain containing 7	**-1.65**	4.46E-04	1.85E-03
2059	EPS8	epidermal growth factor receptor pathway substrate 8	**-1.65**	4.70E-04	1.92E-03
59274	MESDC1	mesoderm development candidate 1	**-1.65**	7.80E-04	2.74E-03
7837	PXDN	peroxidasin homolog (Drosophila)	**-1.65**	5.00E-04	2.01E-03

Appendix B (continued)

TABLE VII:
GENES DIFFERENTIALLY EXPRESSED IN CULTURED HUMAN CUMULUS GRANULOSA CELLS FOLLOWING FSH TREATMENT FOR 48H

EntrezID	Symbol	Name	Geometric mean of intensities (FSH/Control)	P-value	FDR
301	ANXA1	annexin A1	**-1.66**	5.07E-04	2.02E-03
323	APBB2	amyloid beta (A4) precursor protein-binding, family B, member 2	**-1.66**	3.87E-04	1.68E-03
51491	NOP16	NOP16 nucleolar protein	**-1.66**	1.55E-03	4.40E-03
26137	ZBTB20	zinc finger and BTB domain containing 20	**-1.66**	8.80E-04	2.97E-03
9076	CLDN1	claudin 1	**-1.67**	4.01E-04	1.72E-03
26528	DAZAP1	DAZ associated protein 1	**-1.67**	6.87E-04	2.49E-03
2317	FLNB	filamin B, beta	**-1.67**	4.10E-04	1.75E-03
10272	FSTL3	follistatin-like 3 (secreted glycoprotein)	**-1.67**	1.13E-03	3.51E-03
9448	MAP4K4	mitogen-activated protein kinase kinase kinase kinase 4	**-1.67**	3.64E-04	1.61E-03
81671 /// 406991	MIR21 /// VMP1	microRNA 21 /// vacuole membrane protein 1	**-1.67**	1.36E-03	4.03E-03
9792	SERTAD2	SERTA domain containing 2	**-1.67**	1.92E-03	5.25E-03
7414	VCL	vinculin	**-1.67**	3.15E-04	1.48E-03
654	BMP6	bone morphogenetic protein 6	**-1.68**	4.89E-03	1.08E-02
51735 /// 96459	FNIP1 /// RAPGEF6	folliculin interacting protein 1 /// Rap guanine nucleotide exchange factor (GEF) 6	**-1.68**	7.48E-04	2.65E-03
3554	IL1R1	interleukin 1 receptor, type I	**-1.68**	1.41E-03	4.13E-03
57486	NLN	neurolysin (metallopeptidase M3 family)	**-1.68**	3.30E-04	1.52E-03
88455	ANKRD13A	ankyrin repeat domain 13A	**-1.69**	1.00E-03	3.24E-03
9933	KIAA0020	KIAA0020	**-1.69**	2.08E-03	5.54E-03

Appendix B (continued)

TABLE VII:
GENES DIFFERENTIALLY EXPRESSED IN CULTURED HUMAN CUMULUS GRANULOSA CELLS FOLLOWING FSH TREATMENT FOR 48H

EntrezID	Symbol	Name	Geometric mean of intensities (FSH/Control)	P-value	FDR
1290	COL5A2	collagen, type V, alpha 2	**-1.70**	1.14E-03	3.53E-03
28996	HIPK2	homeodomain interacting protein kinase 2	**-1.70**	3.26E-04	1.51E-03
83857	TMTC1	transmembrane and tetratricopeptide repeat containing 1	**-1.70**	3.62E-03	8.63E-03
3976	LIF	leukemia inhibitory factor	**-1.71**	9.29E-04	3.08E-03
4121	MAN1A1	mannosidase, alpha, class 1A, member 1	**-1.71**	3.18E-04	1.49E-03
5358	PLS3	plastin 3	**-1.71**	4.20E-04	1.77E-03
2938 /// 2939	GSTA1 /// GSTA2	glutathione S-transferase alpha 1 /// glutathione S-transferase alpha 2	**-1.72**	2.71E-03	6.90E-03
4134	MAP4	microtubule-associated protein 4	**-1.72**	5.54E-04	2.14E-03
6383	SDC2	syndecan 2	**-1.72**	3.22E-04	1.50E-03
7114	TMSB4X	thymosin beta 4, X-linked	**-1.72**	1.08E-03	3.44E-03
8660	IRS2	insulin receptor substrate 2	**-1.73**	1.14E-03	3.53E-03
5295	PIK3R1	phosphoinositide-3-kinase, regulatory subunit 1 (alpha)	**-1.73**	3.27E-03	7.95E-03
7533	YWHAH	tyrosine 3-monooxygenase/tryptophan 5-monooxygenase activation protein, eta polypeptide	**-1.73**	7.16E-04	2.56E-03
10979	FERMT2	fermitin family member 2	**-1.74**	2.19E-04	1.15E-03
114294	LACTB	lactamase, beta	**-1.74**	3.25E-04	1.51E-03
9397	NMT2	N-myristoyltransferase 2	**-1.74**	1.43E-04	8.74E-04
4907	NT5E	5'-nucleotidase, ecto (CD73)	**-1.74**	2.54E-03	6.51E-03

Appendix B (continued)

TABLE VII:
GENES DIFFERENTIALLY EXPRESSED IN CULTURED HUMAN CUMULUS GRANULOSA CELLS FOLLOWING FSH TREATMENT FOR 48H

EntrezID	Symbol	Name	Geometric mean of intensities (FSH/Control)	P-value	FDR
24147	FJX1	four jointed box 1 (Drosophila)	**-1.75**	3.18E-03	7.78E-03
64780	MICAL1	microtubule associated monooxygenase, calponin and LIM domain containing 1	**-1.75**	2.32E-04	1.20E-03
8458	TTF2	transcription termination factor, RNA polymerase II	**-1.75**	3.22E-04	1.50E-03
60468	BACH2	BTB and CNC homology 1, basic leucine zipper transcription factor 2	**-1.76**	1.97E-03	5.35E-03
2744	GLS	glutaminase	**-1.76**	5.78E-04	2.20E-03
5806	PTX3	pentraxin 3, long	**-1.76**	1.90E-03	5.19E-03
196740	VSTM4	V-set and transmembrane domain containing 4	**-1.77**	1.56E-04	9.35E-04
84942	WDR73	WD repeat domain 73	**-1.77**	4.01E-04	1.72E-03
54764	ZRANB1	zinc finger, RAN-binding domain containing 1	**-1.77**	2.80E-04	1.35E-03
929	CD14	CD14 molecule	**-1.78**	2.77E-03	7.00E-03
79633	FAT4	FAT atypical cadherin 4	**-1.78**	6.31E-04	2.34E-03
2316	FLNA	filamin A, alpha	**-1.78**	1.52E-04	9.20E-04
4646	MYO6	myosin VI	**-1.78**	3.60E-04	1.61E-03
58	ACTA1	actin, alpha 1, skeletal muscle	**-1.79**	1.81E-04	1.03E-03
91663	MYADM	myeloid-associated differentiation marker	**-1.79**	1.39E-03	4.09E-03
5634	PRPS2	phosphoribosyl pyrophosphate synthetase 2	**-1.79**	9.81E-05	6.92E-04
84790	TUBA1C	tubulin, alpha 1c	**-1.79**	4.81E-03	1.07E-02
11174	ADAMTS6	ADAM metallopeptidase with thrombospondin type 1 motif, 6	**-1.80**	1.53E-03	4.36E-03

Appendix B (continued)

TABLE VII:
GENES DIFFERENTIALLY EXPRESSED IN CULTURED HUMAN CUMULUS GRANULOSA CELLS FOLLOWING FSH TREATMENT FOR 48H

EntrezID	Symbol	Name	Geometric mean of intensities (FSH/Control)	P-value	FDR
123920	CMTM3	CKLF-like MARVEL transmembrane domain containing 3	**-1.80**	6.95E-04	2.50E-03
57120	GOPC	golgi-associated PDZ and coiled-coil motif containing	**-1.80**	2.12E-04	1.13E-03
6273	S100A2	S100 calcium binding protein A2	**-1.80**	1.17E-04	7.69E-04
171024	SYNPO2	synaptopodin 2	**-1.80**	1.52E-04	9.20E-04
60312	AFAP1	actin filament associated protein 1	**-1.81**	7.97E-04	2.79E-03
84886	C1orf198	chromosome 1 open reading frame 198	**-1.81**	3.75E-04	1.65E-03
29775	CARD10	caspase recruitment domain family, member 10	**-1.81**	8.27E-04	2.85E-03
81578	COL21A1	collagen, type XXI, alpha 1	**-1.81**	2.22E-04	1.16E-03
5732	PTGER2	prostaglandin E receptor 2 (subtype EP2), 53kDa	**-1.81**	5.09E-04	2.02E-03
5898	RALA	v-ral simian leukemia viral oncogene homolog A (ras related)	**-1.81**	1.49E-04	9.09E-04
9780	PIEZO1	piezo-type mechanosensitive ion channel component 1	**-1.82**	2.00E-04	1.09E-03
56937	PMEPA1	prostate transmembrane protein, androgen induced 1	**-1.82**	6.18E-04	2.31E-03
25759	SHC2	SHC (Src homology 2 domain containing) transforming protein 2	**-1.82**	8.33E-05	6.29E-04
9435	CHST2	carbohydrate (N-acetylglucosamine-6-O) sulfotransferase 2	**-1.83**	1.82E-03	5.03E-03
5654	HTRA1	HtrA serine peptidase 1	**-1.83**	8.82E-04	2.98E-03
4060	LUM	lumican	**-1.83**	1.44E-03	4.19E-03
203068	TUBB	tubulin, beta class I	**-1.83**	2.24E-04	1.17E-03

Appendix B (continued)

TABLE VII:
GENES DIFFERENTIALLY EXPRESSED IN CULTURED HUMAN CUMULUS GRANULOSA CELLS FOLLOWING FSH TREATMENT FOR 48H

EntrezID	Symbol	Name	Geometric mean of intensities (FSH/Control)	P-value	FDR
7408	VASP	vasodilator-stimulated phosphoprotein	**-1.83**	1.82E-04	1.03E-03
4753	NELL2	NEL-like 2 (chicken)	**-1.84**	1.63E-03	4.59E-03
51177	PLEKHO1	pleckstrin homology domain containing, family O member 1	**-1.84**	8.65E-04	2.94E-03
11177	BAZ1A	bromodomain adjacent to zinc finger domain, 1A	**-1.85**	1.67E-04	9.77E-04
652	BMP4	bone morphogenetic protein 4	**-1.85**	4.03E-03	9.31E-03
11245	GPR176	G protein-coupled receptor 176	**-1.86**	1.08E-04	7.31E-04
11069	RAPGEF4	Rap guanine nucleotide exchange factor (GEF) 4	**-1.86**	1.43E-04	8.74E-04
6385	SDC4	syndecan 4	**-1.86**	6.75E-04	2.46E-03
23677	SH3BP4	SH3-domain binding protein 4	**-1.86**	1.40E-04	8.63E-04
23670	TMEM2	transmembrane protein 2	**-1.86**	1.96E-04	1.07E-03
7424	VEGFC	vascular endothelial growth factor C	**-1.86**	2.35E-04	1.21E-03
84962	AJUBA	ajuba LIM protein	**-1.87**	7.82E-04	2.74E-03
1277	COL1A1	collagen, type I, alpha 1	**-1.87**	2.72E-04	1.33E-03
22885	ABLIM3	actin binding LIM protein family, member 3	**-1.89**	1.99E-04	1.09E-03
340719	NANOS1	nanos homolog 1 (Drosophila)	**-1.89**	2.17E-03	5.72E-03
27303	RBMS3	RNA binding motif, single stranded interacting protein 3	**-1.89**	4.76E-03	1.06E-02
26509	MYOF	myoferlin	**-1.91**	1.08E-04	7.31E-04
23075	SWAP70	SWAP switching B-cell complex 70kDa subunit	**-1.91**	2.39E-03	6.19E-03
3371	TNC	tenascin C	**-1.91**	5.68E-05	4.98E-04

Appendix B (continued)

TABLE VII:
GENES DIFFERENTIALLY EXPRESSED IN CULTURED HUMAN CUMULUS GRANULOSA CELLS FOLLOWING FSH TREATMENT FOR 48H

EntrezID	Symbol	Name	Geometric mean of intensities (FSH/Control)	P-value	FDR
51421	AMOTL2	angiomotin like 2	**-1.92**	5.22E-04	2.05E-03
2170	FABP3	fatty acid binding protein 3, muscle and heart (mammary-derived growth inhibitor)	**-1.92**	2.68E-04	1.32E-03
7026	NR2F2	nuclear receptor subfamily 2, group F, member 2	**-1.92**	3.14E-03	7.73E-03
5783	PTPN13	protein tyrosine phosphatase, non-receptor type 13 (APO-1/CD95 (Fas)-associated phosphatase)	**-1.92**	6.65E-05	5.44E-04
23012	STK38L	serine/threonine kinase 38 like	**-1.92**	9.80E-05	6.92E-04
9315	NREP	neuronal regeneration related protein	**-1.93**	6.10E-05	5.18E-04
4919	ROR1	receptor tyrosine kinase-like orphan receptor 1	**-1.93**	5.51E-04	2.13E-03
84617	TUBB6	tubulin, beta 6 class V	**-1.93**	2.33E-03	6.07E-03
151126	ZNF385B	zinc finger protein 385B	**-1.93**	3.17E-04	1.49E-03
58489	ABHD17C	abhydrolase domain containing 17C	**-1.94**	1.36E-03	4.03E-03
6662	SOX9	SRY (sex determining region Y)-box 9	**-1.94**	6.03E-05	5.15E-04
7465	WEE1	WEE1 homolog (S. pombe)	**-1.94**	2.16E-04	1.14E-03
9235	IL32	interleukin 32	**-1.95**	1.26E-04	8.08E-04
5669 /// 440533	PSG1 /// PSG8	pregnancy specific beta-1-glycoprotein 1 /// pregnancy specific beta-1-glycoprotein 8	**-1.95**	1.12E-04	7.49E-04
10079	ATP9A	ATPase, class II, type 9A	**-1.96**	5.86E-04	2.22E-03
100131726	FAM83A-AS1	FAM83A antisense RNA 1	**-1.96**	1.19E-03	3.66E-03
81539	SLC38A1	solute carrier family 38, member 1	**-1.96**	8.75E-04	2.97E-03

Appendix B (continued)

TABLE VII:
GENES DIFFERENTIALLY EXPRESSED IN CULTURED HUMAN CUMULUS GRANULOSA CELLS FOLLOWING FSH TREATMENT FOR 48H

EntrezID	Symbol	Name	Geometric mean of intensities (FSH/Control)	P-value	FDR
7286	TUFT1	tuftelin 1	**-1.96**	1.68E-03	4.72E-03
79026	AHNAK	AHNAK nucleoprotein	**-1.97**	5.42E-05	4.83E-04
79572	ATP13A3	ATPase type 13A3	**-1.97**	1.24E-04	7.96E-04
1410	CRYAB	crystallin, alpha B	**-1.97**	6.15E-05	5.18E-04
650	BMP2	bone morphogenetic protein 2	**-1.98**	8.34E-05	6.29E-04
121512	FGD4	FYVE, RhoGEF and PH domain containing 4	**-1.98**	8.02E-05	6.16E-04
169611	OLFML2A	olfactomedin-like 2A	**-1.99**	1.23E-04	7.96E-04
63898	SH2D4A	SH2 domain containing 4A	**-1.99**	1.21E-04	7.89E-04
1030	CDKN2B	cyclin-dependent kinase inhibitor 2B (p15, inhibits CDK4)	**-2.01**	1.39E-04	8.63E-04
144347 /// 100533183	FAM101A /// ZNF664-FAM101A	family with sequence similarity 101, member A /// protein FAM101A	**-2.01**	3.39E-05	3.78E-04
9052	GPRC5A	G protein-coupled receptor, family C, group 5, member A	**-2.01**	1.24E-03	3.77E-03
84627	ZNF469	zinc finger protein 469	**-2.01**	2.87E-05	3.47E-04
4478	MSN	moesin	**-2.02**	3.35E-05	3.76E-04
10381	TUBB3	tubulin, beta 3 class III	**-2.02**	5.44E-04	2.11E-03
25932	CLIC4	chloride intracellular channel 4	**-2.03**	1.20E-04	7.82E-04
59277	NTN4	netrin 4	**-2.03**	1.51E-04	9.16E-04
9886	RHOBTB1	Rho-related BTB domain containing 1	**-2.03**	1.02E-03	3.29E-03
22800	RRAS2	related RAS viral (r-ras) oncogene homolog 2	**-2.04**	2.25E-04	1.17E-03

Appendix B (continued)

TABLE VII:
GENES DIFFERENTIALLY EXPRESSED IN CULTURED HUMAN CUMULUS GRANULOSA CELLS FOLLOWING FSH TREATMENT FOR 48H

EntrezID	Symbol	Name	Geometric mean of intensities (FSH/Control)	P-value	FDR
4609	MYC	v-myc myelocytomatosis viral oncogene homolog (avian)	**-2.05**	6.74E-05	5.48E-04
4627	MYH9	myosin, heavy chain 9, non-muscle	**-2.05**	8.53E-05	6.35E-04
11001	SLC27A2	solute carrier family 27 (fatty acid transporter), member 2	**-2.06**	1.37E-03	4.05E-03
1465	CSRP1	cysteine and glycine-rich protein 1	**-2.07**	2.64E-04	1.30E-03
8291	DYSF	dysferlin, limb girdle muscular dystrophy 2B (autosomal recessive)	**-2.07**	4.04E-05	4.15E-04
4052	LTBP1	latent transforming growth factor beta binding protein 1	**-2.07**	4.82E-05	4.58E-04
2152	F3	coagulation factor III (thromboplastin, tissue factor)	**-2.08**	4.15E-04	1.76E-03
8459	TPST2	tyrosylprotein sulfotransferase 2	**-2.08**	2.04E-04	1.10E-03
3725	JUN	jun proto-oncogene	**-2.09**	9.08E-05	6.59E-04
253827	MSRB3	methionine sulfoxide reductase B3	**-2.09**	1.57E-03	4.45E-03
150465	TTL	tubulin tyrosine ligase	**-2.09**	3.28E-04	1.52E-03
8038	ADAM12	ADAM metallopeptidase domain 12	**-2.10**	3.77E-05	4.00E-04
23603	CORO1C	coronin, actin binding protein, 1C	**-2.10**	7.65E-05	6.01E-04
116496	FAM129A	family with sequence similarity 129, member A	**-2.10**	1.39E-04	8.63E-04
3625	INHBB	inhibin, beta B	**-2.10**	6.99E-05	5.60E-04
9369	NRXN3	neurexin 3	**-2.10**	3.62E-04	1.61E-03
51762	RAB8B	RAB8B, member RAS oncogene family	**-2.10**	2.90E-05	3.48E-04
7171	TPM4	tropomyosin 4	**-2.10**	4.78E-05	4.57E-04

Appendix B (continued)

TABLE VII:
GENES DIFFERENTIALLY EXPRESSED IN CULTURED HUMAN CUMULUS GRANULOSA CELLS FOLLOWING FSH TREATMENT FOR 48H

EntrezID	Symbol	Name	Geometric mean of intensities (FSH/Control)	P-value	FDR
80114	BICC1	bicaudal C homolog 1 (Drosophila)	**-2.11**	2.28E-05	3.22E-04
200424	TET3	tet methylcytosine dioxygenase 3	**-2.11**	8.24E-05	6.29E-04
11030	RBPMS	RNA binding protein with multiple splicing	**-2.12**	3.16E-05	3.70E-04
6769	STAC	SH3 and cysteine rich domain	**-2.13**	7.33E-05	5.81E-04
222166	C7orf41	chromosome 7 open reading frame 41	**-2.14**	5.06E-05	4.72E-04
100133941	CD24	CD24 molecule	**-2.14**	9.25E-05	6.66E-04
100967225	ADAM12-OT1	ADAM12 overlapping transcript 1 (non-protein coding)	**-2.15**	2.73E-05	3.45E-04
4216	MAP3K4	mitogen-activated protein kinase kinase kinase 4	**-2.15**	3.53E-05	3.87E-04
4332	MNDA	myeloid cell nuclear differentiation antigen	**-2.15**	1.09E-03	3.44E-03
1300	COL10A1	collagen, type X, alpha 1	**-2.16**	1.18E-04	7.73E-04
1837	DTNA	dystrobrevin, alpha	**-2.16**	2.13E-05	3.08E-04
29995	LMCD1	LIM and cysteine-rich domains 1	**-2.16**	1.16E-04	7.65E-04
7041	TGFB1I1	transforming growth factor beta 1 induced transcript 1	**-2.16**	3.09E-05	3.65E-04
7357	UGCG	UDP-glucose ceramide glucosyltransferase	**-2.16**	2.75E-05	3.45E-04
1316	KLF6	Kruppel-like factor 6	**-2.20**	1.55E-05	2.67E-04
1265	CNN2	calponin 2	**-2.21**	5.94E-05	5.10E-04
55118	CRTAC1	cartilage acidic protein 1	**-2.22**	3.43E-05	3.80E-04
83937	RASSF4	Ras association (RalGDS/AF-6) domain family member 4	**-2.22**	1.14E-03	3.54E-03

Appendix B (continued)

TABLE VII:
GENES DIFFERENTIALLY EXPRESSED IN CULTURED HUMAN CUMULUS GRANULOSA CELLS FOLLOWING FSH TREATMENT FOR 48H

EntrezID	Symbol	Name	Geometric mean of intensities (FSH/Control)	P-value	FDR
112574	SNX18	sorting nexin 18	**-2.22**	1.60E-05	2.71E-04
54751	FBLIM1	filamin binding LIM protein 1	**-2.23**	4.13E-05	4.20E-04
399664	MEX3D	mex-3 homolog D (C. elegans)	**-2.23**	1.84E-05	2.94E-04
54532	USP53	ubiquitin specific peptidase 53	**-2.23**	8.00E-05	6.16E-04
1462	VCAN	versican	**-2.23**	1.36E-03	4.03E-03
800	CALD1	caldesmon 1	**-2.24**	3.61E-04	1.61E-03
221981	THSD7A	thrombospondin, type I, domain containing 7A	**-2.24**	2.74E-04	1.33E-03
10046	MAMLD1	mastermind-like domain containing 1	**-2.25**	3.69E-05	3.97E-04
27242	TNFRSF21	tumor necrosis factor receptor superfamily, member 21	**-2.25**	1.02E-04	7.07E-04
2171 /// 220832 /// 101060453	FABP5 /// FABP5P3 /// LOC101060453	fatty acid binding protein 5 (psoriasis-associated) /// fatty acid binding protein 5 pseudogene 3 /// fatty acid-binding protein, epidermal-like	**-2.26**	4.26E-05	4.29E-04
1075	CTSC	cathepsin C	**-2.28**	1.21E-03	3.70E-03
2887	GRB10	growth factor receptor-bound protein 10	**-2.29**	5.52E-05	4.88E-04
144165	PRICKLE1	prickle homolog 1 (Drosophila)	**-2.29**	4.08E-05	4.17E-04
7204	TRIO	trio Rho guanine nucleotide exchange factor	**-2.29**	1.11E-05	2.30E-04
81624	DIAPH3	diaphanous homolog 3 (Drosophila)	**-2.30**	1.86E-04	1.04E-03
10982	MAPRE2	microtubule-associated protein, RP/EB family, member 2	**-2.30**	9.30E-04	3.08E-03

Appendix B (continued)

TABLE VII:
GENES DIFFERENTIALLY EXPRESSED IN CULTURED HUMAN CUMULUS GRANULOSA CELLS FOLLOWING FSH TREATMENT FOR 48H

EntrezID	Symbol	Name	Geometric mean of intensities (FSH/Control)	P-value	FDR
10580	SORBS1	sorbin and SH3 domain containing 1	**-2.31**	1.80E-04	1.02E-03
8988	HSPB3	heat shock 27kDa protein 3	**-2.32**	1.27E-05	2.48E-04
7127	TNFAIP2	tumor necrosis factor, alpha-induced protein 2	**-2.32**	1.96E-04	1.07E-03
3983	ABLIM1	actin binding LIM protein 1	**-2.33**	7.15E-05	5.70E-04
84159	ARID5B	AT rich interactive domain 5B (MRF1-like)	**-2.33**	9.90E-06	2.17E-04
4053	LTBP2	latent transforming growth factor beta binding protein 2	**-2.33**	1.73E-04	9.97E-04
9645	MICAL2	microtubule associated monooxygenase, calponin and LIM domain containing 2	**-2.33**	4.41E-05	4.35E-04
10221	TRIB1	tribbles homolog 1 (Drosophila)	**-2.35**	2.54E-04	1.28E-03
11217 /// 445815	AKAP2 /// PALM2-AKAP2	A kinase (PRKA) anchor protein 2 /// PALM2-AKAP2 readthrough	**-2.36**	5.28E-05	4.76E-04
960	CD44	CD44 molecule (Indian blood group)	**-2.37**	4.53E-04	1.87E-03
7262	PHLDA2	pleckstrin homology-like domain, family A, member 2	**-2.37**	2.06E-05	3.04E-04
666	BOK	BCL2-related ovarian killer	**-2.38**	4.51E-03	1.02E-02
55740	ENAH	enabled homolog (Drosophila)	**-2.38**	2.57E-04	1.29E-03
3875	KRT18	keratin 18	**-2.38**	1.44E-03	4.19E-03
272	AMPD3	adenosine monophosphate deaminase 3	**-2.39**	2.21E-04	1.16E-03
219902	TMEM136	transmembrane protein 136	**-2.39**	1.84E-05	2.94E-04
8828	NRP2	neuropilin 2	**-2.40**	1.03E-04	7.15E-04
5734	PTGER4	prostaglandin E receptor 4 (subtype EP4)	**-2.40**	3.91E-04	1.69E-03

Appendix B (continued)

TABLE VII:
GENES DIFFERENTIALLY EXPRESSED IN CULTURED HUMAN CUMULUS GRANULOSA CELLS FOLLOWING FSH TREATMENT FOR 48H

EntrezID	Symbol	Name	Geometric mean of intensities (FSH/Control)	P-value	FDR
7280	TUBB2A	tubulin, beta 2A class IIa	**-2.40**	1.90E-04	1.06E-03
8572	PDLIM4	PDZ and LIM domain 4	**-2.41**	4.62E-04	1.90E-03
7078	TIMP3	TIMP metallopeptidase inhibitor 3	**-2.42**	1.80E-05	2.92E-04
28969	BZW2	basic leucine zipper and W2 domains 2	**-2.43**	1.33E-05	2.55E-04
85458	DIXDC1	DIX domain containing 1	**-2.44**	3.41E-05	3.79E-04
8434	RECK	reversion-inducing-cysteine-rich protein with kazal motifs	**-2.44**	3.66E-04	1.61E-03
3037	HAS2	hyaluronan synthase 2	**-2.46**	5.70E-06	1.75E-04
745	MYRF	myelin regulatory factor	**-2.46**	1.01E-05	2.18E-04
5292	PIM1	pim-1 oncogene	**-2.51**	4.11E-05	4.19E-04
3730	KAL1	Kallmann syndrome 1 sequence	**-2.53**	1.61E-04	9.65E-04
8490	RGS5	regulator of G-protein signaling 5	**-2.53**	2.03E-04	1.10E-03
142683	ITLN2	intelectin 2	**-2.54**	3.71E-05	3.97E-04
1901	S1PR1	sphingosine-1-phosphate receptor 1	**-2.54**	5.99E-04	2.26E-03
1368	CPM	carboxypeptidase M	**-2.57**	5.50E-06	1.75E-04
5021	OXTR	oxytocin receptor	**-2.57**	1.87E-03	5.13E-03
51339	DACT1	dishevelled-binding antagonist of beta-catenin 1	**-2.58**	6.60E-04	2.43E-03
57214	KIAA1199	KIAA1199	**-2.59**	2.65E-05	3.45E-04
84281	C2orf88	chromosome 2 open reading frame 88	**-2.62**	1.17E-04	7.67E-04
51621	KLF13	Kruppel-like factor 13	**-2.62**	4.10E-06	1.63E-04

Appendix B (continued)

TABLE VII:
GENES DIFFERENTIALLY EXPRESSED IN CULTURED HUMAN CUMULUS GRANULOSA CELLS FOLLOWING FSH TREATMENT FOR 48H

EntrezID	Symbol	Name	Geometric mean of intensities (FSH/Control)	P-value	FDR
4131	MAP1B	microtubule-associated protein 1B	**-2.62**	3.05E-04	1.44E-03
23089	PEG10	paternally expressed 10	**-2.62**	3.34E-04	1.53E-03
11259	FILIP1L	filamin A interacting protein 1-like	**-2.63**	3.33E-05	3.76E-04
7291	TWIST1	twist basic helix-loop-helix transcription factor 1	**-2.64**	2.12E-04	1.13E-03
29970 /// 100505385	IQCJ-SCHIP1 /// SCHIP1	IQCJ-SCHIP1 readthrough /// schwannomin interacting protein 1	**-2.66**	1.11E-03	3.48E-03
55450	CAMK2N1	calcium/calmodulin-dependent protein kinase II inhibitor 1	**-2.67**	4.90E-05	4.64E-04
3912	LAMB1	laminin, beta 1	**-2.68**	8.04E-04	2.80E-03
3936	LCP1	lymphocyte cytosolic protein 1 (L-plastin)	**-2.70**	1.34E-04	8.48E-04
11037	STON1	stonin 1	**-2.71**	3.00E-06	1.39E-04
26585	GREM1	gremlin 1, DAN family BMP antagonist	**-2.72**	6.50E-06	1.86E-04
5376	PMP22	peripheral myelin protein 22	**-2.74**	9.90E-06	2.17E-04
26353	HSPB8	heat shock 22kDa protein 8	**-2.75**	1.55E-04	9.31E-04
23022	PALLD	palladin, cytoskeletal associated protein	**-2.75**	2.40E-06	1.27E-04
51232	CRIM1	cysteine rich transmembrane BMP regulator 1 (chordin-like)	**-2.80**	1.71E-04	9.92E-04
11065	UBE2C	ubiquitin-conjugating enzyme E2C	**-2.81**	4.90E-06	1.71E-04
169792	GLIS3	GLIS family zinc finger 3	**-2.82**	1.09E-03	3.45E-03
84206	MEX3B	mex-3 homolog B (C. elegans)	**-2.82**	1.22E-04	7.89E-04
10602	CDC42EP3	CDC42 effector protein (Rho GTPase binding) 3	**-2.85**	2.14E-05	3.08E-04

Appendix B (continued)

TABLE VII:
GENES DIFFERENTIALLY EXPRESSED IN CULTURED HUMAN CUMULUS GRANULOSA CELLS FOLLOWING FSH TREATMENT FOR 48H

EntrezID	Symbol	Name	Geometric mean of intensities (FSH/Control)	P-value	FDR
23150	FRMD4B	FERM domain containing 4B	**-2.85**	1.43E-05	2.56E-04
8853	ASAP2	ArfGAP with SH3 domain, ankyrin repeat and PH domain 2	**-2.88**	2.64E-05	3.45E-04
51744	CD244	CD244 molecule, natural killer cell receptor 2B4	**-2.91**	6.90E-06	1.92E-04
55859	BEX1	brain expressed, X-linked 1	**-2.92**	4.11E-04	1.75E-03
4147 /// 100506558	LOC100506558 /// MATN2	uncharacterized LOC100506558 /// matrilin 2	**-2.92**	2.76E-05	3.45E-04
7169	TPM2	tropomyosin 2 (beta)	**-2.92**	4.90E-06	1.71E-04
2318	FLNC	filamin C, gamma	**-2.94**	1.38E-04	8.63E-04
5010	CLDN11	claudin 11	**-2.96**	8.60E-06	2.09E-04
90102	PHLDB2	pleckstrin homology-like domain, family B, member 2	**-2.97**	1.50E-06	9.59E-05
11096	ADAMTS5	ADAM metallopeptidase with thrombospondin type 1 motif, 5	**-2.98**	1.61E-05	2.71E-04
5074	PAWR	PRKC, apoptosis, WT1, regulator	**-2.99**	2.88E-05	3.47E-04
7846	TUBA1A	tubulin, alpha 1a	**-3.00**	5.63E-04	2.16E-03
928	CD9	CD9 molecule	**-3.02**	6.60E-06	1.87E-04
5054	SERPINE1	serpin peptidase inhibitor, clade E (nexin, plasminogen activator inhibitor type 1), member 1	**-3.04**	2.90E-06	1.37E-04
6347	CCL2	chemokine (C-C motif) ligand 2	**-3.06**	3.87E-03	9.03E-03
220213	OTUD1	OTU domain containing 1	**-3.07**	3.17E-05	3.70E-04
59	ACTA2	actin, alpha 2, smooth muscle, aorta	**-3.15**	4.04E-05	4.15E-04

Appendix B (continued)

TABLE VII:
GENES DIFFERENTIALLY EXPRESSED IN CULTURED HUMAN CUMULUS GRANULOSA CELLS FOLLOWING FSH TREATMENT FOR 48H

EntrezID	Symbol	Name	Geometric mean of intensities (FSH/Control)	P-value	FDR
84525	HOPX	HOP homeobox	**-3.15**	1.25E-03	3.80E-03
87	ACTN1	actinin, alpha 1	**-3.19**	1.93E-05	2.96E-04
23406	COTL1	coactosin-like 1 (Dictyostelium)	**-3.21**	1.47E-05	2.56E-04
5999	RGS4	regulator of G-protein signaling 4	**-3.24**	2.31E-05	3.25E-04
359845	FAM101B	family with sequence similarity 101, member B	**-3.30**	7.30E-06	1.98E-04
9915	ARNT2	aryl-hydrocarbon receptor nuclear translocator 2	**-3.35**	9.70E-06	2.17E-04
55089	SLC38A4	solute carrier family 38, member 4	**-3.35**	9.46E-05	6.77E-04
1647	GADD45A	growth arrest and DNA-damage-inducible, alpha	**-3.36**	2.86E-05	3.47E-04
4067	LYN	v-yes-1 Yamaguchi sarcoma viral related oncogene homolog	**-3.43**	5.10E-04	2.02E-03
91624	NEXN	nexilin (F actin binding protein)	**-3.43**	4.80E-06	1.71E-04
11067	C10orf10	chromosome 10 open reading frame 10	**-3.45**	2.20E-06	1.23E-04
153769	SH3RF2	SH3 domain containing ring finger 2	**-3.46**	5.75E-05	5.01E-04
5366	PMAIP1	phorbol-12-myristate-13-acetate-induced protein 1	**-3.60**	1.70E-06	1.04E-04
54898	ELOVL2	ELOVL fatty acid elongase 2	**-3.65**	1.13E-05	2.30E-04
3399	ID3	inhibitor of DNA binding 3, dominant negative helix-loop-helix protein	**-3.72**	1.24E-05	2.44E-04
2113	ETS1	v-ets erythroblastosis virus E26 oncogene homolog 1 (avian)	**-3.76**	1.10E-06	8.88E-05
7057	THBS1	thrombospondin 1	**-3.82**	5.19E-05	4.76E-04
3491	CYR61	cysteine-rich, angiogenic inducer, 61	**-3.86**	5.10E-06	1.72E-04

Appendix B (continued)

TABLE VII:
GENES DIFFERENTIALLY EXPRESSED IN CULTURED HUMAN CUMULUS GRANULOSA CELLS FOLLOWING FSH TREATMENT FOR 48H

EntrezID	Symbol	Name	Geometric mean of intensities (FSH/Control)	P-value	FDR
83481	EPPK1	epiplakin 1	**-3.86**	7.00E-07	7.16E-05
23034	SAMD4A	sterile alpha motif domain containing 4A	**-3.93**	8.00E-07	7.67E-05
6659	SOX4	SRY (sex determining region Y)-box 4	**-3.95**	2.90E-06	1.37E-04
157506	RDH10	retinol dehydrogenase 10 (all-trans)	**-4.04**	2.17E-04	1.14E-03
7168	TPM1	tropomyosin 1 (alpha)	**-4.13**	1.29E-05	2.50E-04
1278	COL1A2	collagen, type I, alpha 2	**-4.17**	1.13E-05	2.30E-04
2878	GPX3	glutathione peroxidase 3 (plasma)	**-4.34**	1.30E-06	9.50E-05
167681	PRSS35	protease, serine, 35	**-4.36**	3.00E-07	6.97E-05
467	ATF3	activating transcription factor 3	**-4.42**	5.00E-07	6.97E-05
1303	COL12A1	collagen, type XII, alpha 1	**-4.43**	1.78E-03	4.95E-03
4133	MAP2	microtubule-associated protein 2	**-4.82**	5.00E-07	6.97E-05
152007	GLIPR2	GLI pathogenesis-related 2	**-5.03**	4.32E-05	4.33E-04
388115	C15orf52	chromosome 15 open reading frame 52	**-5.14**	1.38E-05	2.56E-04
72	ACTG2	actin, gamma 2, smooth muscle, enteric	**-5.16**	1.30E-06	9.50E-05
642938	FAM196A	family with sequence similarity 196, member A	**-5.22**	4.02E-05	4.15E-04
285016	FAM150B	family with sequence similarity 150, member B	**-5.26**	1.80E-05	2.92E-04
1490	CTGF	connective tissue growth factor	**-5.41**	2.79E-04	1.35E-03
27063	ANKRD1	ankyrin repeat domain 1 (cardiac muscle)	**-5.65**	< 1e-07	5.11E-05
4638	MYLK	myosin light chain kinase	**-5.77**	3.30E-06	1.47E-04

Appendix B (continued)

TABLE VII:
GENES DIFFERENTIALLY EXPRESSED IN CULTURED HUMAN CUMULUS GRANULOSA CELLS FOLLOWING FSH TREATMENT FOR 48H

EntrezID	Symbol	Name	Geometric mean of intensities (FSH/Control)	P-value	FDR
8654	PDE5A	phosphodiesterase 5A, cGMP-specific	**-5.96**	9.20E-06	2.15E-04
4879	NPPB	natriuretic peptide B	**-7.27**	3.25E-05	3.73E-04
6424	SFRP4	secreted frizzled-related protein 4	**-7.55**	< 1e-07	5.11E-05
6876	TAGLN	transgelin	**-7.57**	< 1e-07	< 1e-07
4982	TNFRSF11B	tumor necrosis factor receptor superfamily, member 11b	**-9.59**	6.00E-07	7.16E-05
1264	CNN1	calponin 1, basic, smooth muscle	**-9.85**	< 1e-07	5.11E-05

C. Appendix C

UNIVERSITY OF ILLINOIS
AT CHICAGO

Office for the Protection of Research Subjects (OPRS)
Office of the Vice Chancellor for Research (MC 672)
203 Administrative Office Building
1737 West Polk Street
Chicago, Illinois 60612-7227

Approval Notice
Continuing Review

June 27, 2014

Carlos Stocco, PhD
Physiology and Biophysics
835 S. Wolcott Ave
M/C 901
Chicago, IL 60612
Phone: (312) 355-0150 / Fax: (312) 996-1414

RE: Protocol # 2013-0347
"Hormonal Regulation of Human Granulosa Cells"

According to OPRS records, the IRB training credit for Nicola Winston expired on March 23, 2014. Please inform this individual that they will not be able to participate in the conduct of the research until the continuing education requirement has been met. All UIC investigators and key research personnel involved in human subjects research must complete a minimum of two hours of continuing education in human subjects protection every two years. For further information, please see the OPRS website: http://tigger.uic.edu/depts/ovcr/research/protocolreview/irb/education/2-2-2/ce_requirements.shtml

Dear Dr. Stocco:

Your Continuing Review was reviewed and approved by the Expedited review process on June 26, 2014. You may now continue your research.

Please note the following information about your approved research protocol:

Protocol Approval Period: June 26, 2014 - June 26, 2015
Approved Subject Enrollment #: 500 (4 Enrolled to date)
Additional Determinations for Research Involving Minors: These determinations have not been made for this study since it has not been approved for enrollment of minors.
Performance Sites: UIC
Sponsor: Departmental
PAF#: Not Applicable
Research Protocol(s):

a) Hormonal Regulation of Human Granulosa Cells, Version #3, dated 12/09/2013

Recruitment Material(s):

Appendix C (continued)

a) None

Informed Consent/HIPAA Authorization:

a) Hormonal Regulation of Human Granulosa Cells, Version #4, 12/03/2013

Your research meets the criteria for expedited review as defined in 45 CFR 46.110(b)(1) under the following specific category:

(5) Research involving materials (data, documents, records, or specimens) that have been collected, or will be collected solely for nonresearch purposes (such as medical treatment or diagnosis).

Please note the Review History of this submission:

Receipt Date	Submission Type	Review Process	Review Date	Review Action
06/20/2014	Continuing Review	Expedited	06/26/2014	Approved

Please remember to:

→ Use your **research protocol number** (2013-0347) on any documents or correspondence with the IRB concerning your research protocol.

→ Review and comply with all requirements on the enclosure,
"UIC Investigator Responsibilities, Protection of Human Research Subjects"
(http://tigger.uic.edu/depts/ovcr/research/protocolreview/irb/policies/0924.pdf)

Please note that the UIC IRB has the prerogative and authority to ask further questions, seek additional information, require further modifications, or monitor the conduct of your research and the consent process.

Please be aware that if the scope of work in the grant/project changes, the protocol must be amended and approved by the UIC IRB before the initiation of the change.

We wish you the best as you conduct your research. If you have any questions or need further help, please contact OPRS at (312) 996-1711 or me at (312) 413-1835. Please send any correspondence about this protocol to OPRS at 203 AOB, M/C 672.

Sincerely,

Jonathan W. Leigh, MPH
IRB Coordinator, IRB # 1
Office for the Protection of Research Subjects

Enclosure(s):

1. **Informed Consent Document/HIPAA Authorization:**
   a) Hormonal Regulation of Human Granulosa Cells, Version #4, 12/03/2013

cc: John Solaro, Physiology and Biophysics, M/C 901

D. Appendix D

UIC UNIVERSITY OF ILLINOIS AT CHICAGO

Office of Animal Care and Institutional
Biosafety Committee (OACIB) (M/C 672)
Office of the Vice Chancellor for Research
206 Administrative Office Building
1737 West Polk Street
Chicago, Illinois 60612

4/17/2013

Carlos Stocco
Physiology & Biophysics
M/C 901

Dear Dr. Stocco:

The protocol indicated below was reviewed in accordance with the Animal Care Policies and Procedures of the University of Illinois at Chicago and **renewed on 4/17/2013.**

Title of Application: **Molecular Pathways Controlling Ovarian Gene Expression**
ACC NO: **12-057**
Original Protocol Approval: **5/22/2012 (3 year approval with annual continuation required).**
Current Approval Period: **4/17/2013 to 4/17/2014**

Funding: ***Portions of this protocol are supported by the funding sources indicated in the table below.***
Number of funding sources: 2

Funding Agency	**Funding Title**			**Portion of Funding Matched**
NIH	*Molecular Pathways Controlling Ovarian Gene Expression*			*All matched*
Funding Number	**Current Status**	**UIC PAF NO.**	**Performance Site**	**Funding PI**
RO1 HD057110	*Funded*	*2010-00093*	*UIC*	*Carlos Stocco*
Funding Agency	**Funding Title**			**Portion of Funding Matched**
NIH	*Regulation of Aromatase Expression in the Corpus Luteum*			*All matched*
Funding Number	**Current Status**	**UIC PAF NO.**	**Performance Site**	**Funding PI**
R21 HD066233	*Funded*	*2010-05141*	*UIC*	*Carlos Stocco*

This institution has Animal Welfare Assurance Number A3460.01 on file with the Office of Laboratory Animal Welfare, NIH. **This letter may only be provided as proof of IACUC approval for those specific funding sources listed above in which all portions of the grant are matched to this ACC protocol.**

Thank you for complying with the Animal Care Policies and Procedures of the UIC.

Sincerely,

Bradley Merrill, PhD
Chair, Animal Care Committee

BM/*kg*
cc: BRL, ACC File, Jill Bennett, Michael Bauschard, Yan Guang Wu

Phone (312) 996-1972 • Fax (312) 996-9088

E. Appendix E

Data in Figure 4, Figure 5, Figure 6, Figure 13, Figure 20, Figure 21, and Figure 22 as well as components of chapters III, IV, and VI were previously published (125) in the Journal of Clinical Endocrinology and Metabolism by ENDOCRINE SOCIETY Reproduced with permission of ENDOCRINE SOCIETY in the format Republish in a thesis/dissertation via Copyright Clearance Center. I collected material, conducted experiments, and wrote the manuscript. Dr. Bert Scoccia, Dr. Musa Zamah, Dr. Nicola Winson and Michelle Fierro provided materials for experiments and helped edit the manuscript. Scott Convissar helped to edit the manuscript. Dr. Carlos Stocco oversaw the project and helped write and edit the manuscript.

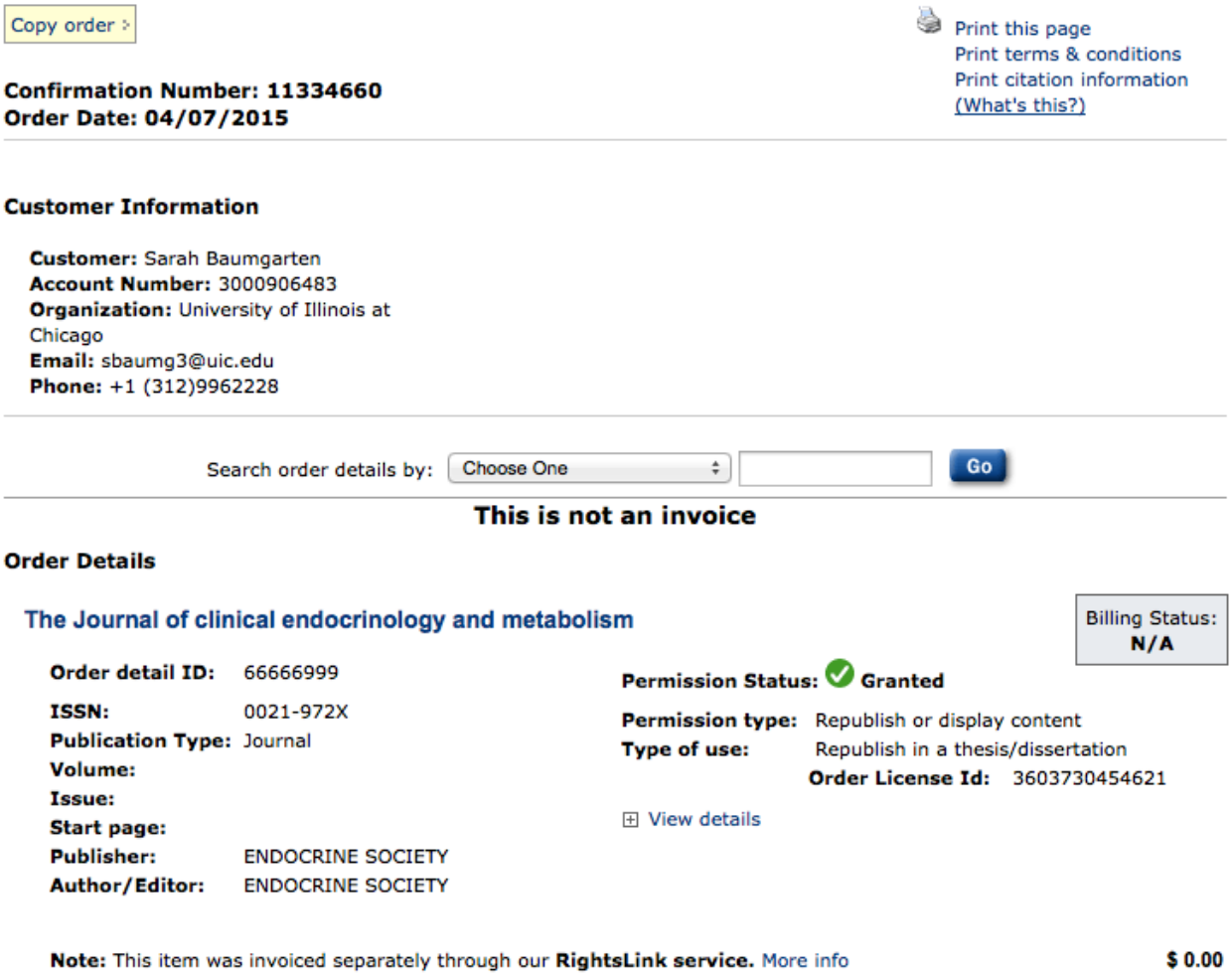

Copy order

Print this page
Print terms & conditions
Print citation information
(What's this?)

Confirmation Number: 11334660
Order Date: 04/07/2015

Customer Information

Customer: Sarah Baumgarten
Account Number: 3000906483
Organization: University of Illinois at Chicago
Email: sbaumg3@uic.edu
Phone: +1 (312)9962228

Search order details by: Choose One Go

This is not an invoice

Order Details

The Journal of clinical endocrinology and metabolism

Billing Status: **N/A**

Order detail ID: 66666999
ISSN: 0021-972X
Publication Type: Journal
Volume:
Issue:
Start page:
Publisher: ENDOCRINE SOCIETY
Author/Editor: ENDOCRINE SOCIETY

Permission Status: Granted
Permission type: Republish or display content
Type of use: Republish in a thesis/dissertation
Order License Id: 3603730454621

View details

Note: This item was invoiced separately through our **RightsLink service.** More info

$ 0.00

Appendix E (continued)

Data in Figure 14, Figure 15, Figure 16, Figure 19, Figure 23, Figure 24, Figure 25, Figure 26, and Figure 27 as well as components of chapters IV, V, and VII were previously published (157) in the Journal of Clinical Endocrinology and Metabolism by ENDOCRINE SOCIETY Reproduced with permission of ENDOCRINE SOCIETY in the format Republish in a thesis/dissertation via Copyright Clearance Center. I collected material, conducted experiments, and wrote the manuscript. Dr. Bert Scoccia, Dr. Musa Zamah, Dr. Nicola Winson and Michelle Fierro provided materials for experiments and helped edit the manuscript. Scott Convissar helped to edit the manuscript. Dr. Carlos Stocco oversaw the project and helped write and edit the manuscript.

OXFORD UNIVERSITY PRESS LICENSE TERMS AND CONDITIONS

Feb 14, 2017

This Agreement between University of Illinois at Chicago -- Sarah Baumgarten ("You") and Oxford University Press ("Oxford University Press") consists of your license details and the terms and conditions provided by Oxford University Press and Copyright Clearance Center.

License Number	4047691273482
License date	
Licensed content publisher	Oxford University Press
Licensed content publication	The Journal of Clinical Endocrinology & Metabolism
Licensed content title	FSH Regulates IGF-2 Expression in Human Granulosa Cells in an AKT-Dependent Manner
Licensed content author	Baumgarten, Sarah C.; Convissar, Scott M.
Licensed content date	2015-08-01
Type of Use	Thesis/Dissertation
Institution name	
Title of your work	Role of Insulin-like Growth Factors in Granulosa Cell Differentiation and Ovarian Follicle Maturation
Publisher of your work	n/a
Expected publication date	Mar 2017

XI. CITED LITERATURE

1. **Stanford JB** 2013 What is the true prevalence of infertility? Fertility and sterility 99:1201-1202
2. **Thoma ME, McLain AC, Louis JF, King RB, Trumble AC, Sundaram R, Buck Louis GM** 2013 Prevalence of infertility in the United States as estimated by the current duration approach and a traditional constructed approach. Fertility and sterility 99:1324-1331 e1321
3. **Chandra A, Copen CE, Stephen EH** 2013 Infertility and impaired fecundity in the United States, 1982-2010: data from the National Survey of Family Growth. Natl Health Stat Report:1-18, 11 p following 19
4. **Martin JA, Hamilton BE, Osterman MJ, Curtin SC, Matthews TJ** 2015 Births: final data for 2013. Natl Vital Stat Rep 64:1-65
5. **Ventura SJ** 1989 Trends and variations in first births to older women, United States, 1970-86. Vital Health Stat 21:1-27
6. **Centers for Disease Control and Prevention ASRM, Society for Assisted Reproductive Technology** 2014 2012 Assisted Reproductive Technology National Summary Report. In: Services UDoHaH ed. Atlanta (GA): US Dept of Health and Human Services
7. **Macaluso M, Wright-Schnapp TJ, Chandra A, Johnson R, Satterwhite CL, Pulver A, Berman SM, Wang RY, Farr SL, Pollack LA** 2010 A public health focus on infertility prevention, detection, and management. Fertility and sterility 93:16 e11-1

8. **Wallace WH, Kelsey TW** 2010 Human ovarian reserve from conception to the menopause. PloS one 5:e8772

9. **Wigglesworth K, Lee KB, O'Brien MJ, Peng J, Matzuk MM, Eppig JJ** 2013 Bidirectional communication between oocytes and ovarian follicular somatic cells is required for meiotic arrest of mammalian oocytes. Proceedings of the National Academy of Sciences of the United States of America 110:E3723-3729

10. **Christensen A, Bentley GE, Cabrera R, Ortega HH, Perfito N, Wu TJ, Micevych P** 2012 Hormonal regulation of female reproduction. Hormone and metabolic research = Hormon- und Stoffwechselforschung = Hormones et metabolisme 44:587-591

11. **Abraham GE, Odell WD, Swerdloff RS, Hopper K** 1972 Simultaneous radioimmunoassay of plasma FSH, LH, progesterone, 17-hydroxyprogesterone, and estradiol-17 beta during the menstrual cycle. The Journal of clinical endocrinology and metabolism 34:312-318

12. **Krsmanovic LZ, Stojilkovic SS, Merelli F, Dufour SM, Virmani MA, Catt KJ** 1992 Calcium signaling and episodic secretion of gonadotropin-releasing hormone in hypothalamic neurons. Proceedings of the National Academy of Sciences of the United States of America 89:8462-8466

13. **Shacham S, Harris D, Ben-Shlomo H, Cohen I, Bonfil D, Przedecki F, Lewy H, Ashkenazi IE, Seger R, Naor Z** 2001 Mechanism of GnRH receptor signaling on gonadotropin release and gene expression in pituitary gonadotrophs. Vitamins and hormones 63:63-90

14. **Hillier SG** 2001 Gonadotropic control of ovarian follicular growth and development. Molecular and cellular endocrinology 179:39-46

15. **Reiter EO, Kulin HE, Hamwood SM** 1974 The absence of positive feedback between estrogen and luteinizing hormone in sexually immature girls. Pediatr Res 8:740-745

16. **Yoshida H, Takakura N, Kataoka H, Kunisada T, Okamura H, Nishikawa SI** 1997 Stepwise requirement of c-kit tyrosine kinase in mouse ovarian follicle development. Developmental biology 184:122-137

17. **Parrott JA, Skinner MK** 1999 Kit-ligand/stem cell factor induces primordial follicle development and initiates folliculogenesis. Endocrinology 140:4262-4271

18. **Hosaka T, Biggs WH, 3rd, Tieu D, Boyer AD, Varki NM, Cavenee WK, Arden KC** 2004 Disruption of forkhead transcription factor (FOXO) family members in mice reveals their functional diversification. Proceedings of the National Academy of Sciences of the United States of America 101:2975-2980

19. **McGrath SA, Esquela AF, Lee SJ** 1995 Oocyte-specific expression of growth/differentiation factor-9. Mol Endocrinol 9:131-136

20. **Dong J, Albertini DF, Nishimori K, Kumar TR, Lu N, Matzuk MM** 1996 Growth differentiation factor-9 is required during early ovarian folliculogenesis. Nature 383:531-535

21. **Carabatsos MJ, Elvin J, Matzuk MM, Albertini DF** 1998 Characterization of oocyte and follicle development in growth differentiation factor-9-deficient mice. Developmental biology 204:373-384

22. **Greene AD, Patounakis G, Segars JH** 2014 Genetic associations with diminished ovarian reserve: a systematic review of the literature. J Assist Reprod Genet 31:935-946

23. **Kovanci E, Rohozinski J, Simpson JL, Heard MJ, Bishop CE, Carson SA** 2007 Growth differentiating factor-9 mutations may be associated with premature ovarian failure. Fertility and sterility 87:143-146

24. **Zhao H, Qin Y, Kovanci E, Simpson JL, Chen ZJ, Rajkovic A** 2007 Analyses of GDF9 mutation in 100 Chinese women with premature ovarian failure. Fertility and sterility 88:1474-1476

25. **Wang TT, Ke ZH, Song Y, Chen LT, Chen XJ, Feng C, Zhang D, Zhang RJ, Wu YT, Zhang Y, Sheng JZ, Huang HF** 2013 Identification of a mutation in GDF9 as a novel cause of diminished ovarian reserve in young women. Hum Reprod 28:2473-2481

26. **Diaz FJ, Wigglesworth K, Eppig JJ** 2007 Oocytes determine cumulus cell lineage in mouse ovarian follicles. Journal of cell science 120:1330-1340

27. **Diaz FJ, Wigglesworth K, Eppig JJ** 2007 Oocytes are required for the preantral granulosa cell to cumulus cell transition in mice. Developmental biology 305:300-311

28. **Gilchrist RB, Lane M, Thompson JG** 2008 Oocyte-secreted factors: regulators of cumulus cell function and oocyte quality. Hum Reprod Update 14:159-177

29. **Rao MC, Midgley AR, Jr., Richards JS** 1978 Hormonal regulation of ovarian cellular proliferation. Cell 14:71-78

30. **Stocco C** 2008 Aromatase expression in the ovary: hormonal and molecular regulation. Steroids 73:473-487

31. **Hillier SG, Whitelaw PF, Smyth CD** 1994 Follicular oestrogen synthesis: the 'two-cell, two-gonadotrophin' model revisited. Molecular and cellular endocrinology 100:51-54

32. **Zhou P, Baumgarten SC, Wu Y, Bennett J, Winston N, Hirshfeld-Cytron J, Stocco C** 2013 IGF-I signaling is essential for FSH stimulation of AKT and steroidogenic genes in granulosa cells. Mol Endocrinol 27:511-523

33. **Grondahl ML, Andersen CY, Bogstad J, Borgbo T, Boujida VH, Borup R** 2012 Specific genes are selectively expressed between cumulus and granulosa cells from individual human pre-ovulatory follicles. Molecular human reproduction 18:572-584

34. **Fisher CR, Graves KH, Parlow AF, Simpson ER** 1998 Characterization of mice deficient in aromatase (ArKO) because of targeted disruption of the cyp19 gene. Proceedings of the National Academy of Sciences of the United States of America 95:6965-6970

35. **Baerwald AR, Adams GP, Pierson RA** 2012 Ovarian antral folliculogenesis during the human menstrual cycle: a review. Hum Reprod Update 18:73-91

36. **Baird DT** 1987 A model for follicular selection and ovulation: lessons from superovulation. Journal of steroid biochemistry 27:15-23

37. **Brown JB** 1978 Pituitary control of ovarian function--concepts derived from gonadotrophin therapy. Aust N Z J Obstet Gynaecol 18:46-54

38. **Schipper I, Hop WC, Fauser BC** 1998 The follicle-stimulating hormone (FSH) threshold/window concept examined by different interventions with exogenous FSH during the follicular phase of the normal menstrual cycle: duration, rather than magnitude, of FSH increase affects follicle development. The Journal of clinical endocrinology and metabolism 83:1292-1298

39. **Fauser BC, Van Heusden AM** 1997 Manipulation of human ovarian function: physiological concepts and clinical consequences. Endocr Rev 18:71-106

40. **Ginther OJ, Gastal EL, Gastal MO, Bergfelt DR, Baerwald AR, Pierson RA** 2004 Comparative study of the dynamics of follicular waves in mares and women. Biology of reproduction 71:1195-1201

41. **George JW, Dille EA, Heckert LL** 2011 Current concepts of follicle-stimulating hormone receptor gene regulation. Biology of reproduction 84:7-17

42. **Kumar TR, Wang Y, Lu N, Matzuk MM** 1997 Follicle stimulating hormone is required for ovarian follicle maturation but not male fertility. Nature genetics 15:201-204

43. **Abel MH, Wootton AN, Wilkins V, Huhtaniemi I, Knight PG, Charlton HM** 2000 The effect of a null mutation in the follicle-stimulating hormone receptor gene on mouse reproduction. Endocrinology 141:1795-1803

44. **Dierich A, Sairam MR, Monaco L, Fimia GM, Gansmuller A, LeMeur M, Sassone-Corsi P** 1998 Impairing follicle-stimulating hormone (FSH) signaling in vivo: targeted disruption of the FSH receptor leads to aberrant gametogenesis and hormonal imbalance. Proceedings of the National Academy of Sciences of the United States of America 95:13612-13617

45. **Aittomaki K, Lucena JL, Pakarinen P, Sistonen P, Tapanainen J, Gromoll J, Kaskikari R, Sankila EM, Lehvaslaiho H, Engel AR, Nieschlag E, Huhtaniemi I, de la Chapelle A** 1995 Mutation in the follicle-stimulating hormone receptor gene causes hereditary hypergonadotropic ovarian failure. Cell 82:959-968

46. **Doherty E, Pakarinen P, Tiitinen A, Kiilavuori A, Huhtaniemi I, Forrest S, Aittomaki K** 2002 A Novel mutation in the FSH receptor inhibiting signal transduction and causing primary ovarian failure. The Journal of clinical endocrinology and metabolism 87:1151-1155

47. **Layman LC, Lee EJ, Peak DB, Namnoum AB, Vu KV, van Lingen BL, Gray MR, McDonough PG, Reindollar RH, Jameson JL** 1997 Delayed puberty and hypogonadism caused by mutations in the follicle-stimulating hormone beta-subunit gene. N Engl J Med 337:607-611

48. **Hunzicker-Dunn M, Maizels ET** 2006 FSH signaling pathways in immature granulosa cells that regulate target gene expression: branching out from protein kinase A. Cellular signalling 18:1351-1359

49. **Sprengel R, Braun T, Nikolics K, Segaloff DL, Seeburg PH** 1990 The testicular receptor for follicle stimulating hormone: structure and functional expression of cloned cDNA. Mol Endocrinol 4:525-530

50. **Carlone DL, Richards JS** 1997 Functional interactions, phosphorylation, and levels of 3',5'-cyclic adenosine monophosphate-regulatory element binding protein and steroidogenic factor-1 mediate hormone-regulated and constitutive expression of aromatase in gonadal cells. Mol Endocrinol 11:292-304

51. **Cottom J, Salvador LM, Maizels ET, Reierstad S, Park Y, Carr DW, Davare MA, Hell JW, Palmer SS, Dent P, Kawakatsu H, Ogata M, Hunzicker-Dunn M** 2003 Follicle-stimulating hormone activates extracellular signal-regulated kinase but not extracellular signal-regulated kinase kinase through a 100-kDa phosphotyrosine phosphatase. The Journal of biological chemistry 278:7167-7179

52. **Zeleznik AJ, Saxena D, Little-Ihrig L** 2003 Protein kinase B is obligatory for follicle-stimulating hormone-induced granulosa cell differentiation. Endocrinology 144:3985-3994

53. **Hunzicker-Dunn ME, Lopez-Biladeau B, Law NC, Fiedler SE, Carr DW, Maizels ET** 2012 PKA and GAB2 play central roles in the FSH signaling pathway to PI3K and AKT in ovarian granulosa cells. Proceedings of the National Academy of Sciences of the United States of America 109:E2979-2988

54. **Philippou A, Maridaki M, Pneumaticos S, Koutsilieris M** 2014 The complexity of the IGF1 gene splicing, posttranslational modification and bioactivity. Mol Med 20:202-214

55. **Daughaday WH, Rotwein P** 1989 Insulin-like growth factors I and II. Peptide, messenger ribonucleic acid and gene structures, serum, and tissue concentrations. Endocr Rev 10:68-91

56. **Chia DJ** 2014 Minireview: mechanisms of growth hormone-mediated gene regulation. Mol Endocrinol 28:1012-1025

57. **Jones JI, Clemmons DR** 1995 Insulin-like growth factors and their binding proteins: biological actions. Endocr Rev 16:3-34

58. **Livingstone C, Borai A** 2014 Insulin-like growth factor-II: its role in metabolic and endocrine disease. Clin Endocrinol (Oxf) 80:773-781

59. **Nordin M, Bergman D, Halje M, Engstrom W, Ward A** 2014 Epigenetic regulation of the Igf2/H19 gene cluster. Cell Prolif 47:189-199

60. **Sussenbach JS, Steenbergh PH, Jansen E, Holthuizen P, Meinsma D, van Dijk MA, Gloudemans T** 1991 Structural and regulatory aspects of the human genes encoding IGF-I and -II. Adv Exp Med Biol 293:1-14

61. **von Horn H, Ekstrom C, Ellis E, Olivecrona H, Einarsson C, Tally M, Ekstrom TJ** 2002 GH is a regulator of IGF2 promoter-specific transcription in human liver. J Endocrinol 172:457-465

62. **LeRoith D** 2000 Insulin-like growth factor I receptor signaling--overlapping or redundant pathways? Endocrinology 141:1287-1288

63. **Willis DS, Mason HD, Watson H, Franks S** 1998 Developmentally regulated responses of human granulosa cells to insulin-like growth factors (IGFs): IGF-I and IGF-II action mediated via the type-I IGF receptor. The Journal of clinical endocrinology and metabolism 83:1256-1259

64. **Schmidt B, Kiecke-Siemsen C, Waheed A, Braulke T, von Figura K** 1995 Localization of the insulin-like growth factor II binding site to amino acids 1508-1566 in repeat 11 of the mannose 6-phosphate/insulin-like growth factor II receptor. The Journal of biological chemistry 270:14975-14982

65. **Xu Y, Papageorgiou A, Polychronakos C** 1998 Developmental regulation of the soluble form of insulin-like growth factor-II/mannose 6-phosphate receptor in

human serum and amniotic fluid. The Journal of clinical endocrinology and metabolism 83:437-442

66. **Moxham CP, Duronio V, Jacobs S** 1989 Insulin-like growth factor I receptor beta-subunit heterogeneity. Evidence for hybrid tetramers composed of insulin-like growth factor I and insulin receptor heterodimers. The Journal of biological chemistry 264:13238-13244

67. **Soos MA, O'Brien RM, Brindle NP, Stigter JM, Okamoto AK, Whittaker J, Siddle K** 1989 Monoclonal antibodies to the insulin receptor mimic metabolic effects of insulin but do not stimulate receptor autophosphorylation in transfected NIH 3T3 fibroblasts. Proceedings of the National Academy of Sciences of the United States of America 86:5217-5221

68. **Slaaby R** 2015 Specific insulin/IGF1 hybrid receptor activation assay reveals IGF1 as a more potent ligand than insulin. Sci Rep 5:7911

69. **Slaaby R, Schaffer L, Lautrup-Larsen I, Andersen AS, Shaw AC, Mathiasen IS, Brandt J** 2006 Hybrid receptors formed by insulin receptor (IR) and insulin-like growth factor I receptor (IGF-IR) have low insulin and high IGF-1 affinity irrespective of the IR splice variant. The Journal of biological chemistry 281:25869-25874

70. **Bailyes EM, Nave BT, Soos MA, Orr SR, Hayward AC, Siddle K** 1997 Insulin receptor/IGF-I receptor hybrids are widely distributed in mammalian tissues: quantification of individual receptor species by selective immunoprecipitation and immunoblotting. Biochem J 327 (Pt 1):209-215

71. **Oh Y, Muller HL, Lee DY, Fielder PJ, Rosenfeld RG** 1993 Characterization of the affinities of insulin-like growth factor (IGF)-binding proteins 1-4 for IGF-I, IGF-II, IGF-I/insulin hybrid, and IGF-I analogs. Endocrinology 132:1337-1344

72. **Wright RJ, Holly JM, Galea R, Brincat M, Mason HD** 2002 Insulin-like growth factor (IGF)-independent effects of IGF binding protein-4 on human granulosa cell steroidogenesis. Biology of reproduction 67:776-781

73. **Poretsky L, Cataldo NA, Rosenwaks Z, Giudice LC** 1999 The insulin-related ovarian regulatory system in health and disease. Endocr Rev 20:535-582

74. **Conover CA, Oxvig C, Overgaard MT, Christiansen M, Giudice LC** 1999 Evidence that the insulin-like growth factor binding protein-4 protease in human ovarian follicular fluid is pregnancy associated plasma protein-A. The Journal of clinical endocrinology and metabolism 84:4742-4745

75. **Lawrence JB, Oxvig C, Overgaard MT, Sottrup-Jensen L, Gleich GJ, Hays LG, Yates JR, 3rd, Conover CA** 1999 The insulin-like growth factor (IGF)-dependent IGF binding protein-4 protease secreted by human fibroblasts is pregnancy-associated plasma protein-A. Proceedings of the National Academy of Sciences of the United States of America 96:3149-3153

76. **Hernandez ER, Roberts CT, Jr., LeRoith D, Adashi EY** 1989 Rat ovarian insulin-like growth factor I (IGF-I) gene expression is granulosa cell-selective: 5'-untranslated mRNA variant representation and hormonal regulation. Endocrinology 125:572-574

77. **Oliver JE, Aitman TJ, Powell JF, Wilson CA, Clayton RN** 1989 Insulin-like growth factor I gene expression in the rat ovary is confined to the granulosa cells of developing follicles. Endocrinology 124:2671-2679

78. **Wandji SA, Wood TL, Crawford J, Levison SW, Hammond JM** 1998 Expression of mouse ovarian insulin growth factor system components during follicular development and atresia. Endocrinology 139:5205-5214

79. **el-Roeiy A, Chen X, Roberts VJ, LeRoith D, Roberts CT, Jr., Yen SS** 1993 Expression of insulin-like growth factor-I (IGF-I) and IGF-II and the IGF-I, IGF-II, and insulin receptor genes and localization of the gene products in the human ovary. The Journal of clinical endocrinology and metabolism 77:1411-1418

80. **Geisthovel F, Moretti-Rojas I, Asch RH, Rojas FJ** 1989 Expression of insulin-like growth factor-II (IGF-II) messenger ribonucleic acid (mRNA), but not IGF-I mRNA, in human preovulatory granulosa cells. Hum Reprod 4:899-902

81. **Zhou J, Bondy C** 1993 Anatomy of the human ovarian insulin-like growth factor system. Biology of reproduction 48:467-482

82. **Qu J, Godin PA, Nisolle M, Donnez J** 2000 Expression of receptors for insulin-like growth factor-I and transforming growth factor-beta in human follicles. Molecular human reproduction 6:137-145

83. **Thierry van Dessel HJ, Chandrasekher Y, Yap OW, Lee PD, Hintz RL, Faessen GH, Braat DD, Fauser BC, Giudice LC** 1996 Serum and follicular fluid levels of insulin-like growth factor I (IGF- I), IGF-II, and IGF-binding protein-1 and -3 during the normal menstrual cycle. The Journal of clinical endocrinology and metabolism 81:1224-1231.

84. **Kwon H, Choi DH, Bae JH, Kim JH, Kim YS** 2010 mRNA expression pattern of insulin-like growth factor components of granulosa cells and cumulus cells in women with and without polycystic ovary syndrome according to oocyte maturity. Fertility and sterility 94:2417-2420

85. **Giudice LC** 1999 Growth factor action on ovarian function in polycystic ovary syndrome. Endocrinol Metab Clin North Am 28:325-339, vi

86. **Baker J, Hardy MP, Zhou J, Bondy C, Lupu F, Bellve AR, Efstratiadis A** 1996 Effects of an Igf1 gene null mutation on mouse reproduction. Mol Endocrinol 10:903-918

87. **Hara N, Takizawa I, Isahaya E, Nishiyama T, Hoshii T, Ishizaki F, Takahashi K** 2012 Insulin-like growth factor-1 is associated with regulation of the luteinizing hormone production in men receiving androgen deprivation therapy with gonadotropin-releasing hormone analogues for localized prostate cancer. Urol Oncol 30:596-601

88. **Longo KM, Sun Y, Gore AC** 1998 Insulin-like growth factor-I effects on gonadotropin-releasing hormone biosynthesis in GT1-7 cells. Endocrinology 139:1125-1132

89. **Adashi EY, Resnick CE, Svoboda ME, Van Wyk JJ** 1985 Somatomedin-C enhances induction of luteinizing hormone receptors by follicle-stimulating hormone in cultured rat granulosa cells. Endocrinology 116:2369-2375

90. **Adashi EY, Resnick CE, Svoboda ME, Van Wyk JJ** 1985 Somatomedin-C synergizes with follicle-stimulating hormone in the acquisition of progestin

biosynthetic capacity by cultured rat granulosa cells. Endocrinology 116:2135-2142

91. **Adashi EY, Resnick CE, Brodie AM, Svoboda ME, Van Wyk JJ** 1985 Somatomedin-C-mediated potentiation of follicle-stimulating hormone-induced aromatase activity of cultured rat granulosa cells. Endocrinology 117:2313-2320

92. **Angervo M, Koistinen R, Suikkari AM, Seppala M** 1991 Insulin-like growth factor binding protein-1 inhibits the DNA amplification induced by insulin-like growth factor I in human granulosa-luteal cells. Hum Reprod 6:770-773

93. **Erickson GF, Garzo VG, Magoffin DA** 1989 Insulin-like growth factor-I regulates aromatase activity in human granulosa and granulosa luteal cells. The Journal of clinical endocrinology and metabolism 69:716-724

94. **Erickson GF, Garzo VG, Magoffin DA** 1991 Progesterone production by human granulosa cells cultured in serum free medium: effects of gonadotrophins and insulin-like growth factor I (IGF-I). Hum Reprod 6:1074-1081

95. **Devoto L, Christenson LK, McAllister JM, Makrigiannakis A, Strauss JF, 3rd** 1999 Insulin and insulin-like growth factor-I and -II modulate human granulosa-lutein cell steroidogenesis: enhancement of steroidogenic acute regulatory protein (StAR) expression. Molecular human reproduction 5:1003-1010

96. **Di Blasio AM, Vigano P, Ferrari A** 1994 Insulin-like growth factor-II stimulates human granulosa-luteal cell proliferation in vitro. Fertility and sterility 61:483-487

97. **Nardo LG, Bosch E, Lambalk CB, Gelbaya TA** 2013 Controlled ovarian hyperstimulation regimens: a review of the available evidence for clinical

practice. Produced on behalf of the BFS Policy and Practice Committee. Hum Fertil (Camb) 16:144-150

98. **Ubaldi F, Vaiarelli A, D'Anna R, Rienzi L** 2014 Management of poor responders in IVF: is there anything new? Biomed Res Int 2014:352098

99. **Breckwoldt M, Selvaraj N, Aharoni D, Barash A, Segal I, Insler V, Amsterdam A** 1996 Expression of Ad4-BP/cytochrome P450 side chain cleavage enzyme and induction of cell death in long-term cultures of human granulosa cells. Molecular human reproduction 2:391-400

100. **Makabe S, Naguro T, Stallone T** 2006 Oocyte-follicle cell interactions during ovarian follicle development, as seen by high resolution scanning and transmission electron microscopy in humans. Microscopy research and technique 69:436-449

101. **Scoccia B, Demir H, Kang Y, Fierro MA, Winston NJ** 2012 In vitro fertilization pregnancy rates in levothyroxine-treated women with hypothyroidism compared to women without thyroid dysfunction disorders. Thyroid : official journal of the American Thyroid Association 22:631-636

102. **Hales KH, Diemer T, Ginde S, Shankar BK, Roberts M, Bosmann HB, Hales DB** 2000 Diametric effects of bacterial endotoxin lipopolysaccharide on adrenal and Leydig cell steroidogenic acute regulatory protein. Endocrinology 141:4000-4012

103. **Fan HY, Shimada M, Liu Z, Cahill N, Noma N, Wu Y, Gossen J, Richards JS** 2008 Selective expression of KrasG12D in granulosa cells of the mouse ovary

causes defects in follicle development and ovulation. Development 135:2127-2137

104. **Byers SL, Wiles MV, Dunn SL, Taft RA** 2012 Mouse estrous cycle identification tool and images. PloS one 7:e35538

105. **Rice S, Ojha K, Mason H** 2008 Human ovarian biopsies as a viable source of pre-antral follicles. Hum Reprod 23:600-605

106. **Eppig JJ, Chesnel F, Hirao Y, O'Brien MJ, Pendola FL, Watanabe S, Wigglesworth K** 1997 Oocyte control of granulosa cell development: how and why. Hum Reprod 12:127-132

107. **Eppig JJ, Wigglesworth K, Pendola F, Hirao Y** 1997 Murine oocytes suppress expression of luteinizing hormone receptor messenger ribonucleic acid by granulosa cells. Biology of reproduction 56:976-984

108. **Otsuka F, Yamamoto S, Erickson GF, Shimasaki S** 2001 Bone morphogenetic protein-15 inhibits follicle-stimulating hormone (FSH) action by suppressing FSH receptor expression. The Journal of biological chemistry 276:11387-11392

109. **Menon B, Sinden J, Franzo-Romain M, Botta RB, Menon KM** 2013 Regulation of LH Receptor mRNA Binding Protein by miR-122 in Rat Ovaries. Endocrinology 154:4826-4834

110. **Knight PG, Satchell L, Glister C** 2012 Intra-ovarian roles of activins and inhibins. Molecular and cellular endocrinology 359:53-65

111. **Chaves RN, de Matos MH, Buratini J, Jr., de Figueiredo JR** 2012 The fibroblast growth factor family: involvement in the regulation of folliculogenesis. Reprod Fertil Dev 24:905-915

112. **Weenen C, Laven JS, Von Bergh AR, Cranfield M, Groome NP, Visser JA, Kramer P, Fauser BC, Themmen AP** 2004 Anti-Mullerian hormone expression pattern in the human ovary: potential implications for initial and cyclic follicle recruitment. Molecular human reproduction 10:77-83

113. **Sasson R, Rimon E, Dantes A, Cohen T, Shinder V, Land-Bracha A, Amsterdam A** 2004 Gonadotrophin-induced gene regulation in human granulosa cells obtained from IVF patients. Modulation of steroidogenic genes, cytoskeletal genes and genes coding for apoptotic signalling and protein kinases. Molecular human reproduction 10:299-311

114. **Miller WL** 2008 Steroidogenic enzymes. Endocr Dev 13:1-18

115. **Varewijck AJ, Brugts MP, Frystyk J, Goudzwaard JA, Uitterlinden P, Waaijers AM, Feng Y, Dimitrov DS, Lamberts SW, Hofland LJ, Janssen JA** 2013 Circulating insulin-like growth factors may contribute substantially to insulin receptor isoform A and insulin receptor isoform B signalling. Molecular and cellular endocrinology 365:17-24

116. **Ide T, Shimano H, Yahagi N, Matsuzaka T, Nakakuki M, Yamamoto T, Nakagawa Y, Takahashi A, Suzuki H, Sone H, Toyoshima H, Fukamizu A, Yamada N** 2004 SREBPs suppress IRS-2-mediated insulin signalling in the liver. Nat Cell Biol 6:351-357

117. **Yuan W, Giudice LC** 1999 Insulin-like growth factor-II mediates the steroidogenic and growth promoting actions of follicle stimulating hormone on human ovarian pre-antral follicles cultured in vitro. The Journal of clinical endocrinology and metabolism 84:1479-1482

118. **Sasson R, Dantes A, Tajima K, Amsterdam A** 2003 Novel genes modulated by FSH in normal and immortalized FSH-responsive cells: new insights into the mechanism of FSH action. FASEB journal : official publication of the Federation of American Societies for Experimental Biology 17:1256-1266

119. **Leung PC, Armstrong DT** 1980 Interactions of steroids and gonadotropins in the control of steroidogenesis in the ovarian follicle. Annu Rev Physiol 42:71-82

120. **Richards JS, Fitzpatrick SL, Clemens JW, Morris JK, Alliston T, Sirois J** 1995 Ovarian cell differentiation: a cascade of multiple hormones, cellular signals, and regulated genes. Recent Prog Horm Res 50:223-254

121. **Ben-Ze'ev A, Amsterdam A** 1987 In vitro regulation of granulosa cell differentiation. Involvement of cytoskeletal protein expression. The Journal of biological chemistry 262:5366-5376

122. **Amsterdam A, Rotmensch S** 1987 Structure-function relationships during granulosa cell differentiation. Endocr Rev 8:309-337

123. **Chen P, Wang SJ, Wang HB, Ren P, Wang XQ, Liu WG, Gu WL, Li DQ, Zhang TG, Zhou CJ** 2012 The distribution of IGF2 and IMP3 in osteosarcoma and its relationship with angiogenesis. J Mol Histol 43:63-70

124. **Gonzalez IJ, Falender AE, Ochsner S, Firestone GL, Richards JS** 2000 Follicle-Stimulating hormone (FSH) stimulates phosphorylation and activation of protein kinase B (PKB/Akt) and serum and glucocorticoid-Induced kinase (Sgk): evidence for A kinase-independent signaling by FSH in granulosa cells. Mol Endocrinol 14:1283-1300

125. **Baumgarten SC, Convissar SM, Fierro MA, Winston NJ, Scoccia B, Stocco C** 2014 IGF1R signaling is necessary for FSH-induced activation of AKT and differentiation of human Cumulus granulosa cells. The Journal of clinical endocrinology and metabolism 99:2995-3004

126. **Klein NA, Battaglia DE, Woodruff TK, Padmanabhan V, Giudice LC, Bremner WJ, Soules MR** 2000 Ovarian follicular concentrations of activin, follistatin, inhibin, insulin-like growth factor I (IGF-I), IGF-II, IGF-binding protein-2 (IGFBP-2), IGFBP-3, and vascular endothelial growth factor in spontaneous menstrual cycles of normal women of advanced reproductive age. The Journal of clinical endocrinology and metabolism 85:4520-4525

127. **Seifer DB, Giudice LC, Dsupin BA, Haning RV, Jr., Frishman GN, Burger HG** 1995 Follicular fluid insulin-like growth factor-I and insulin-like growth factor-II concentrations vary as a function of day 3 serum follicle stimulating hormone. Hum Reprod 10:804-806

128. **Zeleznik AJ, Little-Ihrig L, Ramasawamy S** 2002 Administration of insulin-like growth factor I to rhesus monkeys does not augment gonadotropin-stimulated ovarian steroidogenesis. The Journal of clinical endocrinology and metabolism 87:5722-5729

129. **Wang TH, Chang CL, Wu HM, Chiu YM, Chen CK, Wang HS** 2006 Insulin-like growth factor-II (IGF-II), IGF-binding protein-3 (IGFBP-3), and IGFBP-4 in follicular fluid are associated with oocyte maturation and embryo development. Fertility and sterility 86:1392-1401

130. **Kamada S, Kubota T, Taguchi M, Ho WR, Sakamoto S, Aso T** 1992 Effects of insulin-like growth factor-II on proliferation and differentiation of ovarian granulosa cells. Hormone research 37:141-149

131. **Mason HD, Willis DS, Holly JM, Franks S** 1994 Insulin preincubation enhances insulin-like growth factor-II (IGF-II) action on steroidogenesis in human granulosa cells. The Journal of clinical endocrinology and metabolism 78:1265-1267

132. **Kubota T, Kamada S, Ohara M, Taguchi M, Sakamoto S, Shimizu Y, Aso T** 1993 Insulin-like growth factor II in follicular fluid of the patients with in vitro fertilization and embryo transfer. Fertility and sterility 59:844-849

133. **Poretsky L, Chun B, Liu HC, Rosenwaks Z** 1996 Insulin-like growth factor II (IGF-II) inhibits insulin-like growth factor binding protein I (IGFBP-1) production in luteinized human granulosa cells with a potency similar to insulin-like growth factor I (IGF-I) and higher than insulin. The Journal of clinical endocrinology and metabolism 81:3412-3414

134. **Martinez JC, Stouffer RL, Hazzard TM, Patton PE, Molskness TA** 2003 Insulin-like growth factors-1 and -2, but not hypoxia, synergize with gonadotropin hormone to promote vascular endothelial growth factor-A secretion by monkey granulosa cells from preovulatory follicles. Biology of reproduction 68:1112-1118

135. **Garcia-Echeverria C, Pearson MA, Marti A, Meyer T, Mestan J, Zimmermann J, Gao J, Brueggen J, Capraro HG, Cozens R, Evans DB, Fabbro D, Furet P, Porta DG, Liebetanz J, Martiny-Baron G, Ruetz S, Hofmann F** 2004 In vivo antitumor activity of NVP-AEW541-A novel, potent, and selective inhibitor of the IGF-IR kinase. Cancer cell 5:231-239

136. **Alam H, Maizels ET, Park Y, Ghaey S, Feiger ZJ, Chandel NS, Hunzicker-Dunn M** 2004 Follicle-stimulating hormone activation of hypoxia-inducible factor-1 by the phosphatidylinositol 3-kinase/AKT/Ras homolog enriched in brain (Rheb)/mammalian target of rapamycin (mTOR) pathway is necessary for induction of select protein markers of follicular differentiation. The Journal of biological chemistry 279:19431-19440

137. **Sun GW, Kobayashi H, Suzuki M, Kanayama N, Terao T** 2003 Follicle-stimulating hormone and insulin-like growth factor I synergistically induce up-regulation of cartilage link protein (Crtl1) via activation of phosphatidylinositol-dependent kinase/Akt in rat granulosa cells. Endocrinology 144:793-801

138. **Uchida K, Kondo M, Takeda S, Osada H, Takahashi T, Nakao A, Takahashi T** 1997 Altered transcriptional regulation of the insulin-like growth factor 2 gene in human hepatocellular carcinoma. Molecular carcinogenesis 18:193-198

139. **Riedemann J, Macaulay VM** 2006 IGF1R signalling and its inhibition. Endocrine-related cancer 13 Suppl 1:S33-43

140. **Penarrubia J, Balasch J, Garcia-Bermudez M, Casamitjana R, Vanrell JA, Hernandez ER** 2000 Growth hormone does not increase the expression of insulin-like growth factors and their receptor genes in the pre-menopausal human ovary. Hum Reprod 15:1241-1246

141. **Voutilainen R, Miller WL** 1987 Coordinate tropic hormone regulation of mRNAs for insulin-like growth factor II and the cholesterol side-chain-cleavage enzyme, P450scc [corrected], in human steroidogenic tissues. Proceedings of the National Academy of Sciences of the United States of America 84:1590-1594

142. **Hsueh AJ, Billig H, Tsafriri A** 1994 Ovarian follicle atresia: a hormonally controlled apoptotic process. Endocr Rev 15:707-724

143. **Bley MA, Simon JC, Estevez AG, de Asua LJ, Baranao JL** 1992 Effect of follicle-stimulating hormone on insulin-like growth factor-I-stimulated rat granulosa cell deoxyribonucleic acid synthesis. Endocrinology 131:1223-1229

144. **Liu JP, Baker J, Perkins AS, Robertson EJ, Efstratiadis A** 1993 Mice carrying null mutations of the genes encoding insulin-like growth factor I (Igf-1) and type 1 IGF receptor (Igf1r). Cell 75:59-72

145. **Lewandoski M, Wassarman KM, Martin GR** 1997 Zp3-cre, a transgenic mouse line for the activation or inactivation of loxP-flanked target genes specifically in the female germ line. Curr Biol 7:148-151

146. **Hamilton BE, Martin JA, Ventura SJ** 2010 Births: preliminary data for 2009. Natl Vital Stat Rep 59:1-19

147. **Sehat B, Tofigh A, Lin Y, Trocme E, Liljedahl U, Lagergren J, Larsson O** 2010 SUMOylation mediates the nuclear translocation and signaling of the IGF-1 receptor. Sci Signal 3:ra10

148. **Deng H, Lin Y, Badin M, Vasilcanu D, Stromberg T, Jernberg-Wiklund H, Sehat B, Larsson O** 2011 Over-accumulation of nuclear IGF-1 receptor in tumor cells requires elevated expression of the receptor and the SUMO-conjugating enzyme Ubc9. Biochem Biophys Res Commun 404:667-671

149. **Zhang J, Huang FF, Wu DS, Li WJ, Zhan HE, Peng MY, Fang P, Cao PF, Zhang MM, Zeng H, Chen FP** 2015 SUMOylation of insulin-like growth factor 1

receptor, promotes proliferation in acute myeloid leukemia. Cancer Lett 357:297-306

150. **Warsito D, Sjostrom S, Andersson S, Larsson O, Sehat B** 2012 Nuclear IGF1R is a transcriptional co-activator of LEF1/TCF. EMBO Rep 13:244-250

151. **Conover CA, Faessen GF, Ilg KE, Chandrasekher YA, Christiansen M, Overgaard MT, Oxvig C, Giudice LC** 2001 Pregnancy-associated plasma protein-a is the insulin-like growth factor binding protein-4 protease secreted by human ovarian granulosa cells and is a marker of dominant follicle selection and the corpus luteum. Endocrinology 142:2155

152. **Louhio H, Hovatta O, Sjoberg J, Tuuri T** 2000 The effects of insulin, and insulin-like growth factors I and II on human ovarian follicles in long-term culture. Molecular human reproduction 6:694-698

153. **Greenseid K, Jindal S, Hurwitz J, Santoro N, Pal L** 2011 Differential granulosa cell gene expression in young women with diminished ovarian reserve. Reproductive sciences 18:892-899

154. **Cataldo NA, Giudice LC** 1992 Follicular fluid insulin-like growth factor binding protein profiles in polycystic ovary syndrome. The Journal of clinical endocrinology and metabolism 74:695-697

155. **Cataldo NA, Giudice LC** 1992 Insulin-like growth factor binding protein profiles in human ovarian follicular fluid correlate with follicular functional status. The Journal of clinical endocrinology and metabolism 74:821-829

156. **Gao W, Gu Y, Li Z, Cai H, Peng Q, Tu M, Kondo Y, Shinjo K, Zhu Y, Zhang J, Sekido Y, Han B, Qian Z, Miao Y** 2015 miR-615-5p is epigenetically inactivated and functions as a tumor suppressor in pancreatic ductal adenocarcinoma. Oncogene 34:1629-1640

157. **Baumgarten SC, Convissar SM, Zamah AM, Fierro MA, Winston NJ, Scoccia B, Stocco C** 2015 FSH Regulates IGF-2 Expression in Human Granulosa Cells in an AKT-Dependent Manner. J Clin Endocrinol Metab 100:E1046-1055

XII. VITAE

Sarah Baumgarten
MD/PhD Candidate
Email: sbaumg3@uic.edu

Department of Physiology and Biophysics
University of Illinois at Chicago, College of Medicine

Education

2009-present Medical Scientist Training Program, M.D./Ph.D. Student, Department of Physiology and Biophysics, University of Illinois at Chicago College of Medicine

2005-2009 B.A., Molecular and Cellular Biology, Vanderbilt University, *summa cum laude*, High Honors in Biological Sciences

Teaching Experience

2016-2017 Essentials of Clinical Medicine Tutor, University of Illinois at Chicago College of Medicine

2013, 2014 Reproductive Endocrinology Lectures, Physiology Course for the Summer Pre-matriculation Program (SPP) at University of Illinois at Chicago College of Medicine

2007-2009 Tutor for Department of Biological Sciences, Vanderbilt University

2005-2009 Vanderbilt Student Volunteers for Science: teaching science lessons to children in 3rd-8th grade in the Metro Nashville Public School System

Leadership Experience

2014 Chair, Trainee Committee, 6th annual Illinois Symposium on Reproductive Science (ISRS)

2013-2015 Student member of the University of Illinois at Chicago Medical Scientist Training Program (MSTP) Admissions Committee

2013-2015 Vice President of the Physiology and Biophysics Graduate Student Association

2013-2014 Organizer of the Reproduction, Endocrinology, and Development (R.E.D.) seminar series

2012 Student Trainee Committee for the Illinois Symposium on Reproductive Science (ISRS)

2011-2012 Executive Board member of UIC MSTP Student Activities Committee

2008-2009 President of Vanderbilt Student Volunteers for Science, the largest student-run volunteer program at Vanderbilt with over 400 student volunteers per semester

Research Experience

2012-2015 Ph.D. Thesis Research
University of Illinois at Chicago, Carlos Stocco, Ph.D.
Role of IGFs in Granulosa Cell Differentiation and Ovarian Follicle Maturation

2011-2012 Ph.D. Thesis Research
University of Illinois at Chicago, Jonna Frasor, Ph.D.
Regulation of Gene Expression by Estrogen Receptor and NFκB in Breast Cancer

2006-2009 Undergraduate Researcher
Vanderbilt University, Gerald Stubbs, D.Phil.
Structure and Function of Potato Virus X and Other Filamentous Plant Viruses

2004-2005 Student Researcher
University of Louisville, William Dean, Ph.D.
Parvalbumin Levels in Wood and Green Frogs

2003-2004 Student Researcher
University of Louisville, Irving G. Joshua, Ph.D.
Cardiovascular Effects of Elevated Glucose Levels

Awards

2011-2015 NIH Pre-doctoral Training Grant, Department of Physiology and Biophysics, University of Illinois at Chicago

2014 Mark R. Lambrecht Award for Scholarship and Commitment, Department of Physiology and Biophysics, University of Illinois at Chicago

2014	Silver Prize in the Graduate, MD/PhD, and combined degree students category, College of Medicine Research Forum, University of Illinois at Chicago
2014	First Place in the Platform Presentation Category, Illinois Symposium on Reproductive Sciences
2014	Larry Ewing Memorial Trainee Travel Fund (LEMTTF) for the Society for the Study of Reproduction
2014, 2015	Chancellor's Graduate Student Fellowship, University of Illinois at Chicago
2014	Provost/Deiss Award for Graduate Research, University of Illinois at Chicago
2013, 2014	Chicago Biomedical Consortium Student Scholar
2013	Kate Barany Award, Department of Physiology and Biophysics, University of Illinois at Chicago
2013	Larry Ewing Memorial Trainee Travel Fund (LEMTTF) for the Society for the Study of Reproduction
2012	Gold First Prize in the Graduate, MD/PhD, and combined degree students category, College of Medicine Research Forum, University of Illinois at Chicago
2007	Vanderbilt Undergraduate Summer Research Program Fellowship

Publications

Convissar SM, Bennett J, **Baumgarten SC**, Lydon JP, DeMayo FJ, Stocco C (2015) GATA4 and GATA6 knockdown during luteinization inhibits progesterone production and gonadotropin responsiveness in the corpus luteum of female mice. *Biol Reprod*, 93(6):133.

Baumgarten SC, Convissar SM, Zamah AM, Fierro MA, Winston NJ, Scoccia B, and Stocco C (2015) FSH regulates IGF-2 expression in human granulosa cells in an AKT dependent manner. *JCEM,* 100(8):1046-1055.

Baumgarten SC, Convissar SM, Fierro MA, Winston NJ, Scoccia B, and Stocco C (2014) IGF1R signaling is necessary for FSH-induced activation of AKT and differentiation of human cumulus granulosa cells. *JCEM,* 99(8):2995-3004

Bennett J, **Baumgarten SC**, and Stocco C (2013) GATA4 and GATA6 Silencing in Ovarian Granulosa Cells Affects Levels of mRNAs Involved in Steroidogenesis, Extracellular Structure Organization, IGF1 Activity, and Apoptosis. *Endocrinology*, 154(12):4845-58.

Wu Y, **Baumgarten SC**, Zhou P, and Stocco C. (2013) Testosterone-Dependent Interaction between Androgen Receptor and Aryl Hydrocarbon Receptor Induces Liver Receptor Homolog 1 Expression in Rat Granulosa Cells. *Mol Cell Biol*, 33(15):2817-28.

Zhou P, **Baumgarten SC**, Wu Y, Bennett J, Winston N, Hirshfeld-Cytron J, and Stocco C. (2013) IGF-I signaling is essential for FSH stimulation of AKT and steroidogenic genes in granulosa cells. *Mol Endocrinol,* 27(3):511-23.

Baumgarten SC and Frasor J. (2012) Minireview: Inflammation: an Instigator of More Aggressive Estrogen Receptor (ER) Positive Breast Cancers. *Mol Endo,* 26(3): 360-71.

Pradhan M, **Baumgarten SC**, Bembinster LA, Frasor J. (2012) CBP Mediates NFκB-Dependent Histone Acetylation and Estrogen Receptor Recruitment to an Estrogen Response Element in the BIRC3 Promoter. *Mol Cell Biol,* 32(2): 569-75.

Pradhan M, Bembinster LA, **Baumgarten SC**, Frasor J. (2010) Pro-inflammatory Cytokines Enhance Estrogen-dependent Expression of the Multidrug Transporter Gene ABCG2 through Estrogen Receptor and NFκB Cooperativity at Adjacent Response Elements. *J Biol Chem*, 285(41): 31100-6.

Kendall A, McDonald M, Bian W, Bowles T, **Baumgarten SC**, Shi J, Stewart PL, Bullitt E, Gore D, Irving TC, Havens WM, Ghabrial SA, Wall JS, Stubbs G. (2008) Structure of Flexible Filamentous Plant Viruses. *J Virol*, 82: 9546-54.

Abstracts

Baumgarten SC, Convissar S, Fierro M, Winston N, Zamah AM, Scoccia B, Stocco C. Follicle Stimulating Hormone (FSH)-regulated *Igf2* Expression is Critical for Human Granulosa Cell Differentiation. 2014 College of Medicine Research Forum, University of Illinois at Chicago, Chicago, IL. ***Poster Presentation; Silver Prize Winner***

Baumgarten SC, Convissar S, Fierro M, Winston N, Zamah AM, Scoccia B, Stocco C. Follicle Stimulating Hormone Differentially Regulates Gene Expression through AKT and ERK1/2 Activation in Human Granulosa Cells. 2014 American Society for Reproductive Medicine, Honolulu, Hawaii. ***Platform Presentation***

Baumgarten SC, Convissar S, Fierro M, Winston N, Zamah AM, Scoccia B, Stocco C. Follicle Stimulating Hormone (FSH)-Regulated *Igf2* Expression is Critical for Human Granulosa Cell Differentiation. 2014 Illinois Symposium on Reproductive Science.

University of Illinois at Chicago, Chicago, IL. ***Platform Presentation; First Place in Oral Presentation Category***

Baumgarten SC, Convissar S, Fierro M, Winston N, Scoccia B, Stocco C. Follicle Stimulating Hormone Regulates Insulin-like Growth Factor 2 Expression in Human Granulosa Cells in an AKT-dependent Manner. 2014 Society for the Study of Reproduction, Grand Rapids, Michigan. ***Platform Presentation***

Baumgarten SC, Convissar S, Fierro M, Winston N, Scoccia B, Stocco C. The Interaction of FSH and IGF-1R on the Activation of AKT is Essential for Granulosa Cell Differentiation in Humans. 2014 Women's Health Research Day, University of Illinois at Chicago, Chicago, IL. *Poster Presentation*

Baumgarten SC, Convissar S, Fierro M, Winston N, Hirshfeld-Cytron J, Scoccia H, Stocco C. Follicle Stimulating Hormone (FSH)-induced human granulosa cell differentiation is dependent on the activity of the IGF-1 receptor. 2013 College of Medicine Research Forum, University of Illinois at Chicago, Chicago, IL. *Poster Presentation*

Baumgarten SC, Convissar S, Fierro M, Winston N, Hirshfeld-Cytron J, Scoccia H, Stocco C. FSH induced expression of key differentiation genes is dependent on the activity of the insulin-like growth factor-1 receptor in human granulosa cells. 2013 Illinois Symposium on Reproductive Sciences, Southern Illinois University, Carbondale, IL. ***Platform Presentation***

Baumgarten SC, Zhou P, Fierro M, Winston N, Hirshfeld-Cytron J, Stocco C. A novel approach to study human granulosa cell differentiation reveals follicle stimulating hormone induction of key differentiation genes depends on the activity of the insulin-like growth factor-1 receptor. 2013 Society for the Study of Reproduction, Montreal, Quebec, Canada. ***Platform Presentation***

Baumgarten SC, Zhou P, Stocco C. Follicle stimulating hormone (FSH)-induced activation of steroidogenic genes is dependent on active IGF-1 receptor (IGF-1R) in a human cumulus cell model of undifferentiated granulosa cells. 2012 College of Medicine Research Forum, University of Illinois at Chicago, Chicago, IL. ***Poster Presentation; Gold Prize Winner***

Baumgarten SC and Frasor J. 17-beta estradiol enhances pro-inflammatory cytokine mediated expression of Ninjurin1 in an estrogen receptor and NF-kappaB dependent manner. 2011 College of Medicine Research Forum, University of Illinois at Chicago, Chicago, IL. *Poster Presentation*